DEPARTMENT OF CIVIL AND STRUCTURAL ENGINEERING
UNIVERSITY OF SHEFFIELD

PERFORMANCE OF ALKALI-ACTIVATED SLAG CONCRETE

by

Saud Al-Otaibi, BSc, MSc

A thesis submitted in fulfilment of the
requirements for the degree of
Doctor of Philosophy

September 2002

To my parents

Abstract

The environmental concerns related to the production of cement in terms of the energy consumption and the emission of CO_2 lead to the search for more environmentally viable alternatives to cement. One of those alternative materials is alkali-activated slag (AAS) where ground granulated blast furnace slag is used not as a partial replacement to cement but as the sole binder in the production of concrete. The performance of alkali-activated slag concrete with sodium silicate (water glass) as an activator was studied.

The scope of the work covered seven mixes: a normal strength OPC control mix, a blended OPC/Slag mix of similar compressive strength but of lower water to binder ratio, a second OPC control mix of a water to binder ratio similar to that of the OPC/Slag mix, and four alkali-activated slag mixes of the same binder content and the same water to binder ratio as those of the second OPC mix. The AAS mixes were prepared with slag as the sole binder, activated with water glass at two dosages, 4% and 6% Na_2O (by weight of slag). Two types of water glass were used, one in a solution form and the other in a solid granules form. The two forms of the activator used were also of different silicate modulus (Ms); 1.65 for the solution form and 1.0 for the granule form. Different curing regimes were used including normal water curing, air dry curing and accelerated autoclave heat curing.

The fresh concrete properties studied were setting time, workability and air content. The engineering properties studied were compressive strength, splitting tensile strength, flexural strength, dynamic modulus of elasticity and ultrasonic pulse velocity and drying shrinkage. The durability potential of alkali-activated slag concrete was investigated by testing for oxygen permeability, chloride penetration resistance, porosity, carbonation, and alkali-silica reaction. The hydration of alkali-activated slag was studied using x-ray diffraction and thermogravimetry techniques.

Alkali-activated slag concrete was found to achieve good workability which was, comparable to that of OPC and OPC/slag concrete. The increase of the Na_2O dosage resulted in a lower workability and the activator with higher silicate modulus

exhibited lower workability. AAS concrete however, sets rapidly if not controlled by the addition of lime.

The main hydration products in the AAS systems were C-S-H (I) and hydrotalcite as observed in the XRD patterns with autoclaving resulting in the formation of a more crystalline C-S-H gel and the possible formation of xonotlite.

The mechanical properties of AAS concrete are highly influenced by the activator's silicate modulus and the Na_2O dosage where strength was found to be higher with the higher modulus and dosage. The AAS concrete is very sensitive to curing and dry curing resulted in a reduction in strength for AAS concrete much more than that for OPC concrete. Accelerated curing (autoclave) increased the initial gain of strength in AAS concrete but eventually gave results close to those of water curing. Using a waterglass activator with Ms = 1.65 and 6% Na_2O resulted in the highest drying shrinkage where as it is lower when the dosage is less and the modulus is lower. Autoclave curing of AAS concrete reduces the drying shrinkage as it causes the formation of more crystalline products of hydration.

The increase of the Na_2O dosage in AAS concrete, where the activator has an M_s = 1.0, results in a decrease in porosity, but in the case of the AAS concrete, with the activator having M_s = 1.65, the porosity increases with the increase of the Na_2O dosage. Dry curing increases the porosity of all the concrete mixes. The porosity test results are influenced by the sample preconditioning prior to testing.

The alkali-silica test results show that replacing 60% OPC by slag reduces the expansion of concrete prisms containing reactive aggregates. They also indicate that AAS concrete has low susceptibility to ASR expansion because of stronger binding of alkalis in the hydration products. The carbonation test results show that OPC/slag concrete undergoes higher carbonation than OPC concrete with the same w/c ratio. AAS concrete with low compressive strength around 40 MPa has higher carbonation compared to OPC concrete of the same grade while the carbonation is lower with higher strength.

Acknowledgements

I would like to express my deepest gratitude and appreciation to my supervisors Dr. Cyril Lynsdale for his valuable assistance, advice, and support throughout the course of this project. I am also grateful to my supervisor Prof. John Sharp for his guidance and encouragement.

I would like to thank my colleagues, Dr. M. I. Khan, Dr. Kusno Sambow, Mr. J Dachtar, Mr. A. H. Lone, and Mr. S. M. Torres for their help in conducting the laboratory tests and lively discussion. Thanks are also expressed to the technical staff at the Civil and Structural Engineering Department, Mr. G Brown, Mr. S. Smith, Mr. A. D. Marshall, Mr. C. Todd, Mr. P. Blackbourn and Mr. R Grace for their support during working in laboratory.

The technical staff at the Engineering Materials Department, Mr. Brian Kelly and Mrs. B. Lane deserve all the gratitude for their assistance with the XRD and TGA tests.

I would like also to thank the Appleby Group for supplying the slag used in this investigation, the Ellis and Everard Company for supplying the alkali-activators and BRE for their assistance in providing the reactive sand for the ASR test.

Finally, I would like to express my thanks to my family for their continuous support and encouragement.

TABLE OF CONTENTS

LIST OF FIGURES

LIST OF TABLES

NOTATION

C_3S	=	Tricalcium Silicate
$\overline{C}\overline{C}$	=	Calcium Carbonate
CH	=	Calcium Hydroxide
C_{ip}	=	Chloride permeability in Coulombs
C-S-H	=	Calcium Silicate Hydrate
E	=	Ettringite
E_d	=	Dynamic Modulus of Elasticity
f_c	=	Compressive Strength
f_t	=	Splitting Tensile Strength
G	=	Gehlenite
HT	=	Hydrotalcite
X	=	Xonotlite
η	=	Frequency of vibration for the Dynamic modulus test
η	=	Viscosity of fluid
θ	=	Diffraction angle for X-ray Diffraction
λ	=	Wave Length for X-ray Diffraction
ρ	=	Density of Specimen for the Dynamic modulus test

LIST OF ABBREVIATIONS

OPC	Ordinary Portland Cement
GGBS	Ground Granulated Blastfurnace Slag
ACI	American Concrete Institute
ASTM	American Society for Testing and Materials
AASHTO	American Association of State Highway and Transportation Officials
BRE	Building Research Establishment
BS	British Standard
XRD	X-ray Diffraction
TGA	Thermogravimetric Analysis
RCPT	Rapid Chloride Permeability Test

1. INTRODUCTION

1.1 Introduction

Although the greenhouse effect is a natural phenomenon, where the gases in the atmosphere trap the earth's radiation maintaining an average temperature of 15 °C, the additional greenhouse effect due to human activity is the big concern because it leads, according to environmental scientists, to global warming where the increase in the earth's temperature might lead to flooding and other climatic changes. The concentration of "greenhouse gases" has been increasing continuously for the last three decades; Among these gases is carbon dioxide CO_2. Representatives from more than 160 governments met in Kyoto, Japan, in December 1997 to draft the Kyoto Protocol that called for developed countries to reduce emissions of greenhouse gases on average by 5.2% below 1990 levels by the years 2008-2012 (*Malin*,1998).

Portland cement clinker is made from calcination of limestone (calcium carbonate) and siliceous material where de-carbonation occurs according to the reaction:

$$CaCO_3 \Rightarrow CaO + CO_2$$

The total emission of CO_2 per kg of cement clinker produced is 0.53 kg from the de-carbonation of calcite, plus 0.33 kg from the burning process plus 0.12 kg from the generation of electrical power required, making a total of 0.98 kg. Therefore, for every ton of cement clinker produced, an approximately equal amount of carbon dioxide is released into the atmosphere (*Davidovits*, 1991). The world cement industry contributes some 7% to the total man-made CO_2 emission (*Malhotra*, 1999).

The cement manufacturing industry consumes a vast amount of energy. A closer look at the economics of the production of Portland cement shows that energy inputs account for 58% of the total cost of production (28% for power, 30% for fuel) (*Lang*,1993).

Cement with lower energy consumption and lower CO_2 emission can be produced by modifying the composition of the Portland cement to achieve calcination at lower temperatures and hence saving energy. This can also be done through the use of blended cements having, in addition to Portland cement, other pozzolans such as slag or fly ash to obtain the required properties at lower energy consumption.

The environmental concerns related to the production of cement in terms of energy consumption and the emission of CO_2 lead to the search for more environmentally viable alternatives to cement. One of those alternative materials is alkali-activated slag (AAS) where ground granulated blast furnace slag is used not as a partial replacement to cement but as a binder by itself in the production of concrete. This project studies the performance of alkali-activated slag concrete using sodium silicate (water glass) as an activator in different dosages (4 and 6% Na_2O). Tests were carried out on properties of fresh and hardened concrete to asses its mechanical properties and its durability. Among the concerns relating to the durability of AAS concrete is the possibility of alkali-aggregate reaction, where the introduction of alkalis to the concrete presents a potential risk. The hydration products of AAS concrete will be investigated.

1.2 Objectives and Scope of Work

Alkali-activated slag is not a widely known and used construction material. Most of the research done has been at the material development stage dealing with paste and mortar specimens to study the material's chemistry and microstructure. Information pertaining to the concrete engineering properties and durability of AAS concrete is limited. Therefore this study is an attempt to add to the knowledge at this level.

The scope of the work covers a normal strength OPC control mix, a blended OPC/Slag mix having similar strength as OPC but with a lower water demand, a second OPC control mix having the same w/c ratio as the OPC/Slag mix, and several alkali-activated slag mixes with the same binder content as the second control mix and the same w/c ratio. These comprise four mixes with slag as the sole binder activated

with two forms of water glass each with a dosage of (4, 6% Na_2O). The two types of water glass consist of one in a solution form and the other in solid granules form. Different curing regimes were used including normal water curing, air dry curing and accelerated autoclave heat curing.

The overall aim of the project was to investigate the potential of alkali-activated slag as the sole binder in structural grade concrete by studying its main properties and performance in comparison with portland cement and portland cement/ slag concrete.

The following objectives are set for the work:

1. Study the properties of alkali-activated slag concrete using sodium silicate (water glass) as an activator including the fresh concrete properties (setting time, workability and air content) and engineering properties (compressive strength, splitting tensile strength, flexural strength, none-destructive tests which include dynamic modulus of elasticity and ultrasonic pulse velocity).

2. Drying shrinkage of AAS concrete will be investigated and factors affecting it will be studied.

3. Study the durability of alkali-activated slag concrete including gas permeability, chloride penetration resistance, porosity, and carbonation and alkali-silica reaction.

4. Monitor the hydration of alkali-activated slag mortars and pastes using XRD and TGA and study the hydration products.

1.3 Thesis Outline

The research work is reported in this thesis in 9 chapters. Following this introductory chapter, the other chapters are organized as follows:

Chapter - 2 presents a review of the literature available on the subject of Alkali-Activated Slag Concrete including definition of the materials and the properties of the concrete.

Chapter - 3 presents the materials and experimental design and covers the mix proportions, and research methodology employed.

Chapter - 4 covers properties of fresh concrete such as workability aspects represented by slump, air content, and setting time.

Chapter – 5 is dedicated to microstructural properties of the concrete with the pore size distribution studied through MIP, and the hydration products examined through X-ray diffraction (XRD) and thermogravimetry (TG).

Chapter – 6 is dedicated to the engineering properties of concrete including compressive strength, splitting tensile strength, flexural strength, none destructive tests which include dynamic modulus of elasticity and ultrasonic pulse velocity and the drying shrinkage behavior of the different mixes and factors affecting it.

Chapter – 7 deals with the permeation related properties of the concrete including porosity, oxygen permeability and rapid chloride permeability.

Chapter – 8 covers the study of carbonation of concrete and the alkali silica reaction with the use of reactive aggregates.

Chapter – 9 presents the main conclusions and recommendations for future research. The list of references is presented at the end of the thesis.

2. REVIEW OF LITERATURE

2.1 Introduction

The purpose of this chapter is to review and discuss the available literature on alkali-activated slag concrete, studying the research done on the different variables related to its application and the constraints to its use. The area of further research is to be looked into to open new avenues to enhance the knowledge on this new construction material.

2.2 Slag

Slags are by-products of the metallurgical industry. They are normally composed of calcium-magnesium aluminosilicate glass. Although the oxides of calcium, magnesium, aluminum and silicon often make up to 95% of slag composition, the precise composition of slag varies according to the raw materials and the industrial process. The cooling process and chemical composition are the two factors that significantly influence the structure and properties of slag. Blastfurnace slag refers in particular to the slag produced from the manufacture of pig iron. If the molten slag is quenched sufficiently rapidly it forms a glassy material called "granulated blastfurnace slag"or ggbs for short.

Slag has latent hydraulic properties. If ggbs is placed in water alone, it dissolves to a small extent, but a protective film deficient in Ca^{2+} is quickly formed, which inhibits further reaction. Reaction continues if the pH is kept sufficiently high. The pore solution of a Portland cement, which is essentially one of alkali hydroxides, is a suitable medium. The supply of K^+ and Na^+ ions is limited, but these ions are only partially taken up by the hydration products, and the presence of solid calcium hydroxide ensures that the supply of OH^- is maintained. The slag can be similarly activated by OH^- ions supplied in other

ways, such as the addition of sodium hydroxide or silicate (*Taylor*, 1997). This shows that slag can be activated by OPC, which is most common, and also by chemical alkalis introducing the concept of alkali-activated slag (AAS). AAS cement is composed of ground slag and an alkali component. The slag may be granulated blastfurnace slag, electrothermal furnace phosphorus slag and steel slag. Granulated blastfurnace slag is the most common type of slag used. The alkali can be alkali hydroxide (MOH), non silicic salts of weak acids (M_2CO_3 , M_2S, MF), and silicic salts of $M_2O.(n)SiO_2$ type as well as combinations of these, where M stands for an alkali metal such as Na, K, Li. Of these alkalis, sodium silicate (Na_2SiO_3) is the most effective activator (*Wang et al.*, 1995).

Alkali-activated slag cements using granulated blastfurnace slags were invented by Glukhovsky and patented in 1958. A review given by *Glukhovsky* (1980) commented that alkali-activated slag cements had been introduced into construction practice in the USSR in 1960 and in Poland in 1972. Alkali-activated slags have been employed on a limited scale as oilwell cements and as a roof support system in mine applications in South Africa and Canada. Industrial experience of precast products utilizing these cements is widespread in Eastern Europe, Finland and France (*Talling and Brandstetr*, 1989). Research in China has confirmed the high strength of these systems (*Wang*, 1991).

2.3 Factors affecting Slag Activation

The factors affecting slag activation can be summarized as:

1. Type of slag
2. Fineness of slag
3. Type of Activator
4. Method of Adding Activator

5. Dosage

6. Modulus of Waterglass

7. Influence of curing

These are discussed in the following sections.

2.3.1 Type of slag

The chemical composition of the slag plays a major role in its hydraulic activity and consequently the microstructure and properties of the hardened concrete produced. Neutral or alkaline (basic) are much preferred over acidic slags. The high alumina content results in high early strength where a greater amount of slag is reacted and quick setting occurs. Therefore the Al_2O_3/SiO_2 ratio is considered to be a quality modulus and slags with 12 to 15% of Al_2O_3 are preferred. Minor constituents in slag, such as P, F, S, Mn and Ti, often have significant influence on slag quality. The increasing content of Fe_2O_3 decreases the reactivity of the slag (*Talling and Brandstetr*, 1989; *Wang et al.*, 1994). As to mineralogical composition the crystalline compounds found in the slag, and how amorphous it is, play an important role in its reactivity. This differs with the slag sources and means of cooling or quenching. The crystalline forms of the slag can be determined by X-ray diffraction techniques (*Talling*, 1989).

2.3.2 Fineness of slag

The reactivity of ground slag depends on the fineness of grinding and more precisely on the particle size distribution and the specific surface area (*Talling and Brandstetr*, 1989). It is known that increasing the fineness of ggbs improves the strength and decreases the setting time of slag mixes. Wang suggests values of slag fineness for alkali-activated slag in the range of 400-550 m^2/kg (Blaine) (*Wang et al.*, 1994).

2.3.3 Type of Activator

The activators used include OPC, NaOH, Na_2SO_4, Na_2CO_3, and Na_2SiO_3 (water glass), which is according to several researchers the best activator (*Glukhovsky*, 1980; *Wang et al.*, 1994; *Malolepszy and Petri*, 1986; *Douglas et al.*, 1991).

2.3.4 Method of Adding Activator

The alkali activator is added to the slag in three ways: in solution, in the solid state ground together with slag, and in the solid state where the alkali activator is added separately as one of the mix constituents. The addition of alkali in the solid state not only results in much lower strengths than the solution form, but also produces much fluctuation in the test results which can be attributed to lower solubility in the mix and availability of alkali for reaction. The solid alkali might absorb moisture during storage, which will inhibit its activating action. Using hydrous waterglass/sodium metasilicate (containing chemically bound water) in the solid form produces very low or even zero strength under normal curing conditions, but, when the same alkali is added in solution, similar levels of activation can be achieved as in the water glass solution. When Na_2CO_3 is used some results show that grinding Na_2CO_3 together with slag gives high strengths similar to the addition in solution form. When steam/autoclave curing is used the variation in strength with the method of adding the alkali is somewhat reduced. NaOH as an activator works in both ways, solution and solid due to its high solubility (*Wang et al.*, 1994). It can be said in general that adding the alkali in solution is better from the strength point of view but other criteria such as setting time and workability must be considered, as discussed in detail later.

2.3.5 Dosage

Different researchers attempted to arrive at an optimum dosage of alkali but the results are inconsistent. *Isozaki et al.* (1986) reported an NaOH dosage in the range of 1-10% (by slag weight) while *Parameswaran and Chatterji* (1986) arrived at a dosage of 2-5%. All agree that the higher the dosage the better the strength, although *Metso and Kajaus* (1983) showed that the variation of NaOH dosage in the range of 3-11% has little effect on strength. Another way of expressing the dosage of the alkali is the Na_2O content with respect to slag. The more Na_2O used the higher the strength. However, when Na_2O% reaches a certain value (depending on slag, activator and curing condition), the strength no longer increases with higher dosages, but some detrimental properties such as efflorescence and brittleness are increased because of the presence of more free alkali. *Wang et al.* (1994) recommended a dosage of 3.0 - 5.5% Na_2O with waterglass as an activator, where as *Gifford and Gillot* (1996) have used 6.1% Na_2O.

2.3.6 Modulus of Waterglass solution

The modulus of the waterglass solution refers to the molecular ratio SiO_2:Na_2O known as the silica modulus (M_s) where these main components are responsible for the extent of hydration and the strength gain. The alkali activates the slag where the silica SiO_2 forms the silica gel. This means that for a fixed Na_2O content the more silica, the higher the strength. This means the higher modulus gives higher strength, but there are limiting factors where the solid content in the solution has a limit according to the solubility. Therefore for a high modulus more solid is required to achieve a higher dosage of Na_2O. Also waterglass with higher modulus gives rapid setting in alkali activated slag concrete. An optimum modulus is needed. *Talling and Brandstetr* (1989) state that better results for AAS concrete mixes are achieved using waterglass with M_s within the range from 1 to 2, while *Wang et al.* (1994) recommended an M_s in the range from 1 to 1.5.

2.3.7 Influence of curing

Wang et al. (1994) state that the hydration of slag in AAS cement systems is sensitive to curing temperature, where high temperature leads to the formation of some crystalline products, whereas the hydration products of AAS at normal temperature are generally amorphous. In their study they compared accelerated curing of AAS cement with normal cured OPC and concluded the following points:

a) The effectiveness of accelerated curing is more pronounced with acid and neutral slags or weaker alkaline activators. For example, an AAS cement based on phosphorus slag (neutral or acid in nature) and waterglass having a strength of 30 MPa under normal curing can reach 62 MPa after steam curing and 71-76 MPa after autoclave curing, whereas an AAS cement based on granulated blastfurnace slag (ggbs) (basic in nature) and waterglass solution whose strength is 80 MPa under normal curing can only go up to 85-95 MPa after steam or autoclave curing.

b) Using finely ground slag or a strong activator such as NaOH reduces the effectiveness of accelerated curing.

c) Accelerated curing can greatly improve the durability, quality fluctuation and the occurrence of efflorescence of the products.

Kutti et al. (1982) used autoclave curing with NaOH activated slag mortars and found an increase in compressive strength compared to normal water cured mortars.

2.4 Properties of Alkali Activated Slag Concrete

2.4.1 Fresh concrete properties

2.4.1.1 Setting time:

Various reviewed literature presented rapid setting as a practical problem associated with AAS concrete. The retarders, known to be effective with Portland cement, have no effect with alkali-activated slag due to the different chemical composition of the slag cements. *Bakharev et al.* (2000) noted in their work that using a superplasticiser caused a quick set in the concrete. The reason for this, according to the authors, is the polar molecule of the superplasticiser that can be adsorbed rapidly on charged particles. This increases the zeta-potential of the hydrating particles and promotes a quick set.

Wang (1991) stated that alkali activated slag cements will start to set in 15 minutes when producing concrete of > 70 MPa compressive strength without using admixtures. The author cited different sources in the former USSR being unable to solve the problem of too rapid setting for more than 30 years. He also reported that attempts were made in China to retard the setting time of alkali-activated slag cement using surface active agents, dispersants, and water reducers often used in Portland cement but these attempts were not successful.

Talling et al. (1989) recommended slaked (hydrated) lime as the most convenient retarding agent, with the recommended amount of 2-5% $Ca(OH)_2$ of the ground slag in suspension together with the alkali solution. They also pointed out that an increase in water to binder ratio would obviously have a retarding effect.

Quing-Hua and Sarkar (1994) tested waterglass alkali-activated slag pastes and concluded that adding hydrated lime can increase the setting time where the setting time

is less for higher Na_2O dosage . Other researchers (*Douglas et al.*, 1991; *Gifford and Gillot*, 1996;*Collins and Sanjayan*,1999) have also used hydrated lime successfully to control the setting time. *Brough et al.* (2000) used malic acid in their work with AAS mortars as a retarder.

2.4.1.2 Workability:

Since rapid setting is a problem faced with use of AAS concrete, workability will suffer also. The slump decreases with the increase in the dosage of activator or with the use of higher modulus in the case of water glass activated concrete. It can be noted that initial slump might be acceptable due to the mixing action but a quick loss of slump will occur (*Talling and Brandstetr*, 1989). The use of hydrated lime to control setting as explained earlier helps to provide acceptable workability in terms of slump (*Douglas et al.*, 1991, *Gifford and Gillot*, 1996;*Collins and Sanjayan*,1999). *Collins and Sanjayan* (1999) reported that using solid sodium silicate powder provides better workability and minimal slump compared to liquid sodium silicate solution.

2.4.2 Hydration of Alkali -Activated Slag

The hydration products in the alkali-slag system are known to be C-S-H gel with a low Ca/Si ratio, zeolite type minerals and silica gel (*Xu et al.*, 1993). *Wang and Scrivener* (1995) also reported in their study on the hydration of alkali-activated slag pastes that a poorly crystalline C-S-H(I) gel is present and they stated that Al can be incorporated into C-S-H solid solution. They observed that silica gel is formed in the initial stages of hydration of slag activated with waterglass solution. This gel was considered one of the major factors contributing to the rapid setting of the paste of slag activated with waterglass solution. They found that no zeolite phases and no other Na-containing crystalline phases fomed. *Talling and Brandstetr* (1989) commented that it is advantageous in the structure of hardened concretes and mortars to have a certain part of the components in the crystalline structure preferably in the form of needle shaped stable

crystals, acting as micro reinforcement. The prevailing amorphous C-S-H gel structure in AAS systems converts with age into microcrystalline formations, which lead to an increase in compressive strength. *Talling and Brandstetr* (1989) considered this amorphous gel structure as a disadvantage in comparison with Portland cement concretes and they recommend some additives (Portland cement, feldspar, crystalline high-lime slag, etc.) to improve it.

The microstructure of the alkali-activated slag concrete matrices is highly influenced by the type of slag, type of activator, curing regime and temperature.

The heat output of AAS cement is about one third to half that of OPC and is lower than that of low-heat Portland cements. This is due to the overall hydration products having a lower Ca/Si ratio, thus smaller hydration energy than those in OPC (*Wang et al.*, 1994).

2.4.3 Engineering Properties

2.4.3.1 Strength of Alkali-Activated Slag Concrete

High compressive strength can be achieved with AAS concrete using optimum conditions in terms of activator dosages and quality control. Strengths of AAS concrete from 60 MPa to 150 MPa can be achieved without chemical additives. High early strength can be achieved with AAS systems (*Wang et al.* ,1994). The effect of curing on strength development was discussed earlier. *Collins and Sanjayan* (1999) reported achieving higher compressive strength with AAS concrete than OPC concrete for the same water/binder ratio and the same binder content and also higher flexural strengths. *Douglas et al.* (1991) reported a high one day compressive strength, for example 39 MPa after one day reaching 63 MPa in 28 days.

Strength development of AAS concrete is difficult to control compared to OPC concrete. Strength variations occur due to the sensitivity of this type of concrete to different variables that make the control of mix quality difficult and no standard or empirical method of design has been agreed as yet.

2.4.3.2 Drying Shrinkage

Andersson and Gram (1987) noticed that a large number of micro cracks developed in the material and the shrinkage was larger in AAS mortar than for ordinary Portland cement mortar. *Douglas et al* (1992) reported AAS concrete with waterglass activator exhibits shrinkage similar or greater in extent to OPC and can be controlled by curing and controlling mix design. *Wang et al.* (1994) stated that AAS concretes based on NaOH and Na_2CO_3 may exhibit the same amount of shrinkage as OPC concrete, but those based on waterglass solution often undergo greater drying shrinkage due to the formation of silica or silica -rich gel during hydration. This silica-rich gel has a high water content and may dry with water loss. *Collins and Sanjayan* (1999) reported similar results with AAS concrete having higher drying shrinkage than OPC concrete. They also showed the effect of curing on drying shrinkage where sealed samples gave the lowest shrinkage followed by the bath curing for seven days, and the highest shrinkage was associated with the samples left to dry at low humidity from the first day.

Kutti et al. (1992) found that AAS concrete activated by sodium silicate exhibited 2.3 times the drying shrinkage found in OPC concrete at RH > 50%, but they noted that for RH>70% the drying shrinkage of AAS concrete was similar to that of OPC concrete.

2.4.4 Durability of AAS Concrete

Wang (1991) cited some research carried out in China showing AAS mortars to be very impermeable. They also state that the pores in hardened AAS concrete are distinctly

smaller than those in OPC concrete. Alkali-activation ensures long-term alkalinity of AAS concrete, which prevents corrosion.

Deja and Malotepzy (1989) carried out tests on AAS mortars and reported high resistance to sulfates and chlorides. *Roy et al.* (2000) reported very low chloride diffusion in alkali-activated cement pastes.

Researchers *Glukhovsky* (1981) and *Pu et al.* (1991) and *Wu et al.* (1993) showed that the strength of AAS mortars increased after 1 year in 1% - 2% $MgSO_4$ solution and stayed constant for 2 years in dilute acids, HCl and H_2SO_4 , while OPC samples deteriorated in six months. *Byfores* (1989) used an activator (called F-activator) composed of 2.75% NaOH plus 1.0% Na_2CO_3 and reported that for the same w/b ratio AAS concrete showed more carbonation than OPC. They attributed this to the small content of hydrated CaO, which may react with incoming CO_2 and also to the microcracking in their F-concrete. *Neville* (1995) stated that blended cement with high replacement levels of slag exhibits high carbonation rate. But since carbonation and pore structure are interrelated, good curing, which resulted in a more compact structure, helped to reduce carbonation. This also means the higher the strength, the lower the carbonation.

Douglas et al. (1992) reported AAS concrete having good resistance to chloride ion penetration with ion penetration ranging from 1311 to 2547 coulombs for 28 days curing and from 676 to 1831 coulombs at 91 days.

Shi (1996) presented rapid chloride permeability test (RCPT) results for AAS mortars using water-glass as an activator. These results were very high for the early ages 20000 coulombs at 3 days reducing to 12000 coulombs at 7 days and further to a value around 5000 coulombs at 28 and 90 days.

Wang et al. (1994) reported that AAS concrete performs better under freeze-thaw cycles than OPC concrete.

Heavy efflorescence might occur in AAS concrete, where alkali salts are deposited on the surface of concrete when dry after being wet. This depends on the type of activator used and its solubility. Moist cured concrete suffers less efflorescence (*Wang et al.* ,1994).

Although the hydration of OPC/ slag blended and AAS in concrete produces low $Ca(OH)_2$, which is responsible for carbonation in OPC concrete, some researchers had reported higher carbonation with AAS concrete especially with low grade concretes in comparison with OPC concrete. This might be due to carbonation of the C-S-H.(*Wang, et al.*1994 ;*Bakarev*,2001)

Alkali-Aggregate reaction (AAR)

The guidlines given in the *BRE digest* (1988) to control AAR recommend keeping the level of equivalent Na_2O below 0.6% and a total alkali level in the concrete less than 3.0 kg/m^3 . It recommends using slag as a cement replacement to reduce the alkali level. *Hobbs* (1982) also attributes the effect of slag to the dilution of alkali but suggested lowering the 3.0 kg/m^3 limit to 2.5 kg/m^3 for high binder content. The formation of expansive gel in AAR takes place only in the presence of Ca^{++} ions (*Neville*, 1995). Therefore the absence of $Ca(OH)_2$ is desirable to inhibit the alkali-aggregate reaction (AAR). Slag having less $Ca(OH)_2$ explains further its role against AAR in addition to reducing alkali concentration. *Thomas and Innis* (1998) observed a big reduction in expansion due to Alkali-Aggregate reaction when OPC is partially replaced by slag (25-65%) while maintaining Na_2O at 1.25%. The effect in controlling expansion increases with increasing the amount of slag.

Na_2O is usually below 0.8% in OPC while it is typically 3% or more in alkali-activated slag systems. This presents a risk of alkali-aggregate reaction if reactive aggregates are used.

Some researchers report studies made on alkali-aggregate in AAS concrete and observed only slight expansion in the first period and no expansion after 28 days. *Wang et al.* (1994) cited *Krivenko* (1992) stating that AAS concrete suffers no AAR because hydration products bind 80% of the alkali at one year. *Metso and Kajaus* (1983) carried out an AAR study of AAS sand mortar by the measurement of expansion rate and found a maximum expansion for about 8% opal content (reactive aggregate) by total aggregate weight. A similar study reported by Wang (8) indicated that if the content of reactive silica (granulated silica glass in this case) in aggregate is higher than 3% - 4% there is a possibility of alkali-aggregate reaction.

Gifford and Gillot (1996) reported results on alkali-silica reaction (ASR) and alkali-carbonate reaction (ACR) in alkali activated slag concrete. They observed lower ASR induced expansion with AAS concrete compared to OPC while the ACR induced expansion was higher in AAS concrete than OPC where the increased alkalinity lead to increased reaction and expansion which involves dedolomitization.

Bakharev et al. (2001) found evidence of AAR in alkali-activated slag concrete confirmed through SEM images and expansion test for 22 months. The AAS concrete is more susceptible to AAR than OPC concrete of the same grade.

2.5 Conclusions

The following conclusions can be summerised from the literature:

1. The AAS concrete has many advantages in its beneficial use in terms of saving energy and as an environmentally viable alternative to OPC concrete.

2. The best alkali activator is waterglass (Na_2SiO_3) with M_s between 1 and 2 and Na_2O dosage between 3 - 6%.

3. The reviewed literature indicates in general that good strength and durability can be achieved with AAS concrete but the accomplishment of this is affected by different factors. The present work was an attempts to investigate some of those important factors in depth.

4. The literature gives some contradictory results in terms of the alkali aggregate reaction with AAS concrete and this needs to be further investigated. Also the method of adding the activator is argued upon where the solid form provides better workability and the solution form provides higher strength. Some problems may be associated with the use of the solid form in terms of fluctuation and storage life. These factors were taken in consideration with the present investigation

5. Drying shrinkage is higher for AAS concrete compared to OPC but its mechanism is not clear. Some literature associated high drying shrinkage mainly with waterglass activated-slag concretes.

3. MATERIALS AND EXPERIMENTAL DESIGN

3.1 Introduction

This chapter describes the materials used and the experimental work carried out to study the performance of alkali-activated slag concrete mixes with variable Na_2O dosages, in comparison with control OPC concrete and OPC/slag blended concrete.

The properties of materials used in this investigation to produce the different mixes are presented in detail, followed by the mix design, which includes the selection of concrete making ingredients and blending proportions. The mixing procedure and curing regimes used are also presented. The overall experimental programme, which was implemented in the investigation, is given. The specifics of the tests carried out for each property studied are presented in their respective chapters. Finally a description of the means to study the interrelationships between the different variables in the investigation is presented.

3.2 Materials

The same types of ordinary Portland cement, ground granulated blast-furnace slag, lime, alkali activators, fine and coarse aggregates have been used throughout the investigation with one exception when a special reactive fine aggregate was used for the alkali-aggregate reaction test. Details of each material used are given below.

3.2.1 Cement

Ordinary Portland cement, manufactured by Blue Circle Industries PLC (Hope Works), conforming to the requirements of BS 12:1996 class 42.5 N, was used in this investigation. The chemical and physical properties of the cement, as provided by the manufacturer, are given in Table 3.1.

3.2.2 Slag

The ground granulated blast-furnace slag (ggbs) used was obtained from the Appleby Group, Scunthorpe, UK. It complied with BS 6699:1992. Typical chemical and physical properties provided by the manufacturer are shown in Table 3.2.

3.2.3 Lime

Hydrated lime of commercial grade was used in the alkali-activated slag mixtures to control the setting. The lime was added in a slurry form of equal parts (by weight) of lime and water.

3.2.4 Sodium Silicate (Water-glass)

The alkali activator used was a sodium silicate (water-glass). Two forms of the activator were used:

a) A sodium silicate solution was obtained from Ellis and Everard, UK. It has a molecular ratio SiO_2:Na_2O (M_s) = 1.65 with 31.8% SiO_2 and 20.2% Na_2O by weight.

b) A sodium metasilicate Metso520 solid granules from Ellis and Everard, UK, with a molecular ratio SiO_2:Na_2O (M_s) = 1.00.

The two activators are shown in Figure 3.1.

Precaution should be taken when storing of the solid activator. It must be kept away from moisture since it is hygroscopic or it will be coalesced in lumps as shown in Figure 3.2.

3.2.5 Aggregates

Medium graded sand and 20-mm uncrushed gravel complying with BS 882:1992 were used in this investigation. The sieve analysis results for the fine and

coarse aggregates are shown in Figure 3.3. The relative density of the aggregates is shown in Table 3.5.

3.2.6 Water

Yorkshire water, potable tap water available at the laboratory was used throughout the investigation.

3.3 Mix Design Procedure

The proportioning of a concrete mixture is based on determining the quantities of the ingredients which, when mixed together and cured properly will produce reasonably workable concrete that has a good finish and achieves the desired strength when hardened. This involves different variables in terms of water to cement ratio, the desired workability measured by slump and cement content and aggregate proportions.

3.3.1 Designing the Control Mixes

The work started by designing the OPC control mix. This was done using the BRE method targeting a 40 MPa 28 day compressive strength and a slump of 60 mm. Using the values obtained from this method several trial batches were carried out to achieve the target strength with a cohesive workable mix. The w/c ratio for that mix was 0.55. The OPC/Slag blended mix was arrived at in a similar manner with different trials of 50, 60, 80 % cement replacement levels of slag. Since slag has less water requirement than OPC, to obtain a cohesive workable mix less water is used. The mix that satisfied the requirements was an OPC/Slag slag with 60% replacement

level and a w/c ratio of 0.48. To compare the mixes on equal w/c ratio a second OPC control mix was used with the same binder content and same w/c ratio.

3.3.2 Alkali-Activated Slag Mixes

The alkali-activated slag mixes based on the second OPC control mix having the w/c ratio of 0.48. The activator dosages chosen in the recommended Na_2O range were 4% and 6%. The mixture calculations were made to calculate the required amount of activator by weight, which will provide the chosen dosages. The weight of the solids is considered as part of the binder content and the water in the activator is also taken as part of the total mix water. The same approach was followed in the case of the added lime slurry.

3.3.3 Mix Proportions and Mix Notations

Based on the considerations discussed above the details of the different mixes are presented in Table 3.6. The mortar and paste mixtures are designed to have the same mortar or paste fractions of the concrete mixes.

The notation for the mixes is as follows:

CM1: PC control mix with w/c = 0.55

CM2: PC control mix with w/c = 0.48

SLG60: 60% ggbs + 40% OPC mixture with w/c = 0.48

SS4: Sodium silicate alkali-activated slag mixture with Na_2O content of 4% with w/c = 0.48

SS6: Sodium silicate alkali-activated slag mixture with Na_2O content of 6% with w/c = 0.48

MET4: Sodium metasilicate alkali-activated slag mixture with Na_2O content of 4% with w/c = 0.48

MET6: Sodium metasilicate alkali-activated slag mixture with Na_2O content of 6% with w/c = 0.48

3.4 Mixing Procedure

The fine and coarse aggregates were spread out to dry before the mixing day and stored in plastic containers ready for use. The mixing procedure was performed according to the guidelines set out in BS 1881: Part125: 1986.

3.4.1 Paste Mixtures:

The mixing was done in a Hobart mixer having 2-litre capacity.

i. Dry mixing of OPC and slag for 30 seconds.
ii. Half of the mixing water, with the activator dissolved in it, was added during the next 30 seconds.
iii. The lime slurry was added during the next 30 seconds of mixing.
iv. The remainder of the mixing water was added and all the above procedure is carried out at the medium speed of the mixer.
v. Mixing was continued for further 90 seconds at the medium speed.
vi. The mixer was then stopped and the mixture scraped off the sides of the bowl and hand mixed before mixing for additional 2 minutes at high speed setting.
vii. The total mixing time was 5 minutes.

3.4.2 Mortar and Concrete Mixtures:

The mortar was mixed in a horizontal pan mixer having 20-litre capacity. Two horizontal pan mixers of capacities 50 litre and 170 litres were used according to the batch size. The mixing was done as follows:

i. Dry mixing of the material in the order of coarse aggregate (not used with mortar), OPC and or slag, sand for 30 seconds.

ii. Half of the mixing water, with the activator dissolved in it, was added during the next 30 seconds.

iii. The lime slurry was added during the next 30 seconds of mixing.

iv. The remainder of the mixing water was added and the mixing was continued for further 90 seconds.

v. The mixer was then stopped and the mixture scraped off the sides of the pan and hand mixed before mixing for another 2 minutes.

The total mixing time was 5 minutes.

3.5 Casting and Curing

The concrete is cast in pre-oiled moulds in different sizes as required by the tests . It was noticed that alkali-activated slag concrete sticks hard to the moulds (see Figure 3.4). Therefore oiling of the moulds is very important and a proper release agent must be used.

Three curing regimes were used:

1) Curing in water (WC): The moulds were covered after casting with wet burlap and a polyethylene sheet until demoulding the next day. The specimens were stored in water kept at 20 ± 2 °C.

2) Dry curing (DC): The specimens were kept in the moulds and sealed in polyethylene bags for three days before demoulding. The specimens were then stored in a controlled room kept at 20 ± 2 °C and 50% RH.

3) Autoclave curing (AUT): This is a form of accelerated heat curing. The moulds were covered after casting with wet burlap and a polyethylene sheet until demoulding the next day. The specimens were then placed on a steel grid at the bottom of the autoclave, which contained water to a level below the specimens and then was sealed. The heating cycle was started to elevate the temperature from

room temperature of 20 ± 2 °C up to 150 °C at a rate of 30 °C per hour and then maintained at that temperature for 10 hours and then heating was stopped and the temperature was allowed to drop back to room temperature. The autoclave was then opened and the specimens moved to the water-curing tank at a temperature 20 ± 2 °C and kept until the time of testing at the different ages prescribed by the test procedure.

3.6 Research Programme and Techniques used

The research programme has been divided into six phases each phase presents a set of investigations carried out on the properties of concrete.

Phase I

A pilot study was carried on sets of trial mixes of concrete and mortars to study the following:

a) An OPC control mix designed to get a 28 day compressive strength of 40 MPa.

b) Different trials on OPC/Slag blends at 50,60,80 % replacement levels to study the strength development up to 28 days.

c) Different mortar mixes with OPC, OPC/Slag, and alkali-activated slag to study the setting time and means to control it and also to study the compressive strength development up to 28 days.

Phase II

The fresh concrete properties were studied so that alkali-activated slag concrete could be compared to OPC and OPC/slag. This included:

a) Measuring the slump and air content in accordance with BS 1881.

b) Studying workability using the two-point test developed by *Tattersall* (1991).

c) Measuring the setting time in accordance with BS 5075: Part 3.

Phase III

Studying the engineering and durability related properties of alkali activated slag concrete under different curing regimes at various ages. This included the following:

a) Assessing the development of compressive strength of the concrete in accordance with BS 1881.

b) Measuring indirect tensile (splitting cylinder) strength, flexural strength, and dynamic modulus of elasticity and ultrasonic pulse velocity of concrete in accordance with BS 1881.

c) Investigating the absorption/porosity of the concrete in accordance with RILEM CPC-11.3 (1984).

d) Investigating the oxygen permeability using a permeameter developed by Cabrera and Lynsdale (1988).

e) Assessing the rapid chloride permeability of concrete, in accordance with AASHTO T 227 (also adopted as ASTM C 1202 (1991)).

Phase IV

Assessing the durability related properties of alkali activated slag concrete, which included:

a) Investigating the potential for alkali-aggregate reaction by using reactive aggregates. The test is done in accordance with BSI Draft DD218: 1995.

b) Investigating the carbonation depth after 1 year.

Phase V

Studying the hydration of alkali-activated slag concrete which included:

a) Studying the hydration products using X-ray diffraction XRD.
b) Monitoring the extent of hydration using thermogravimetric analysis (TGA) at various ages.

Phase VI

The last phase of the work included:

a) Analysis of the data and studying the correlations between the properties investigated using the experimental results obtained from the different tests carried out on this research study.
b) Thesis write-up, and arriving at the conclusions and recommendations for further research.

3.7 Analytical Method

The analysis of the data involved the correlation between the various investigated properties. Regression analysis of the data has been carried out to investigate the relation between different variables affecting a specific property under study.

Table 3.1 Chemical and Physical Properties of Cement *

Oxide	Percent	Physical Properties
SiO_2	20.7	Specific Surface: 331 m^2/kg
Al_2O_3	5.7	Average particle size: 10μm
Fe_2O_3	2.3	Coarse particles (>45 μm): 11.2%
CaO	64.8	Specific gravity: 3.14
MgO	1.1	Loss on ignition: 0.92%
SO_3	3.21	Colour: Steel grey
Na_2O	0.19	
K_2O	0.6	

* *Provided by the manufacturer*

Table 3.2 Chemical and Physical Properties of ggbs *

Oxide	Percent	Physical Properties
SiO_2	35.84	Specific Surface: 401 m^2/kg
Al_2O_3	13	Specific gravity: 2.91
Fe_2O_3	0.55	Colour: White
CaO	39.53	
MgO	8.28	
SO_3	0.1	
N_2O	0.35	
K_2O	0.5	

* *Provided by the manufacturer*

Table 3.3 The properties of aggregates

Properties	Sand	Gravel	Thames Valley Sand
Relative Density			
- Oven dried	2.59	2.58	2.60
- Saturated and Surface dried (SSD)	2.62	2.61	2.63
- Apparent	2.66	2.65	2.66

Table 3.4 Concrete Mix Proportions

Mix No.	Slag kg/m^3	OPC kg/m^3	Activator (Na_2O %)	Activator kg/m^3	Lime %	Lime Slurry kg/m^3	Water kg/m^3	Total Water kg/m^3	Total Binder kg/m^3	FineAgg. kg/m^3	CoarseAgg. kg/m^3	w/b %
CM1		355					195	201	355	595	1210	0.55
CM2		375					180	186	375	600	1215	0.48
SLG60	225	150					180	186	375	591	1215	0.48
SS4	326.39	0	4	64.63	4	30	133.97	180	375	591	1215	0.48
SS6	305.34	0	6	90.69	6	45	113.96	180	375	591	1215	0.48
MET4	333.15		4	47.93	4	30	144.38	180	375	591	1215	0.48
MET6	314.49		6	67.87	6	45	128.31	180	375	591	1215	0.48

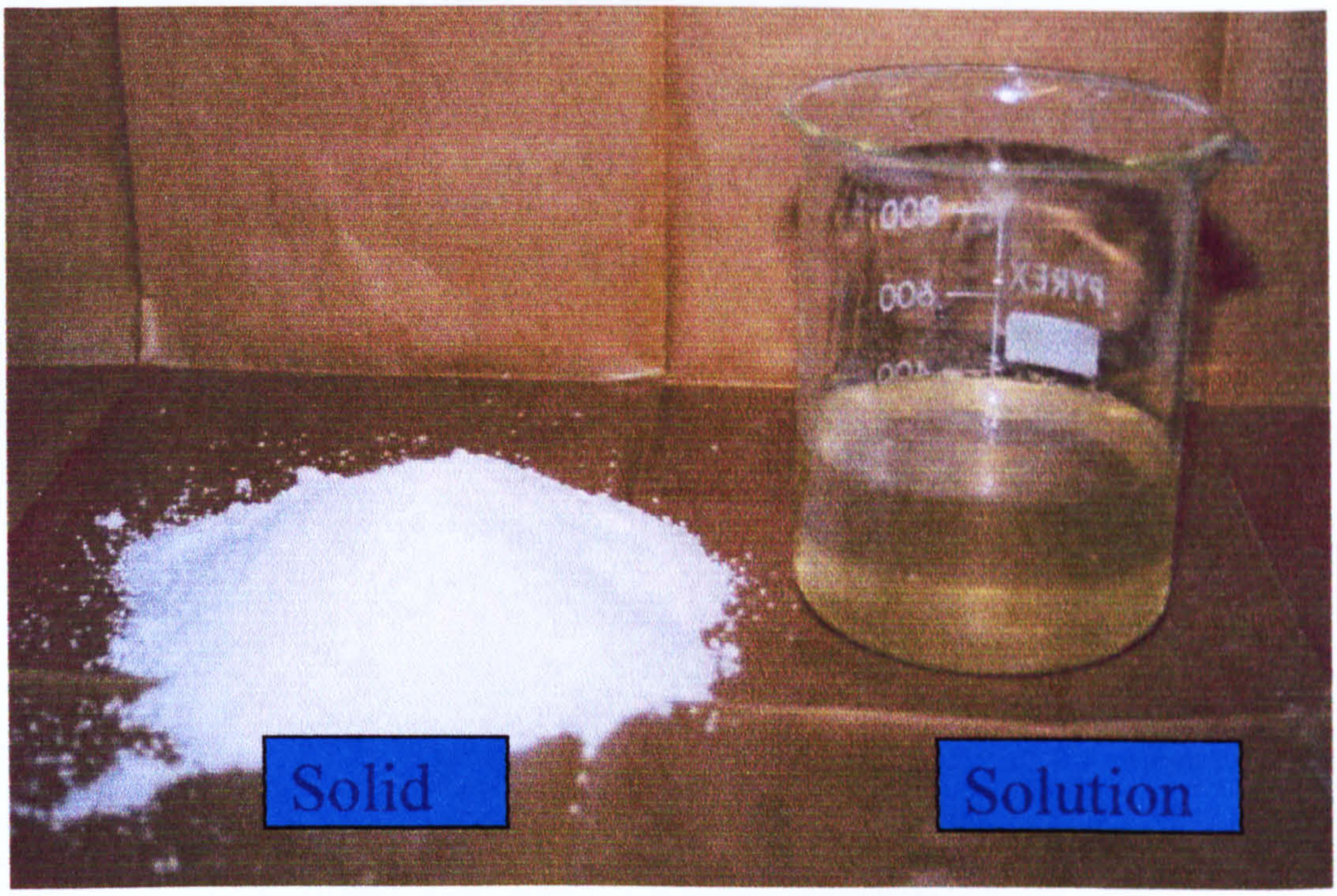

Figure 3.1 The waterglass activators

Figure 3.2 Effect of moisture on the solid granules waterglass activator

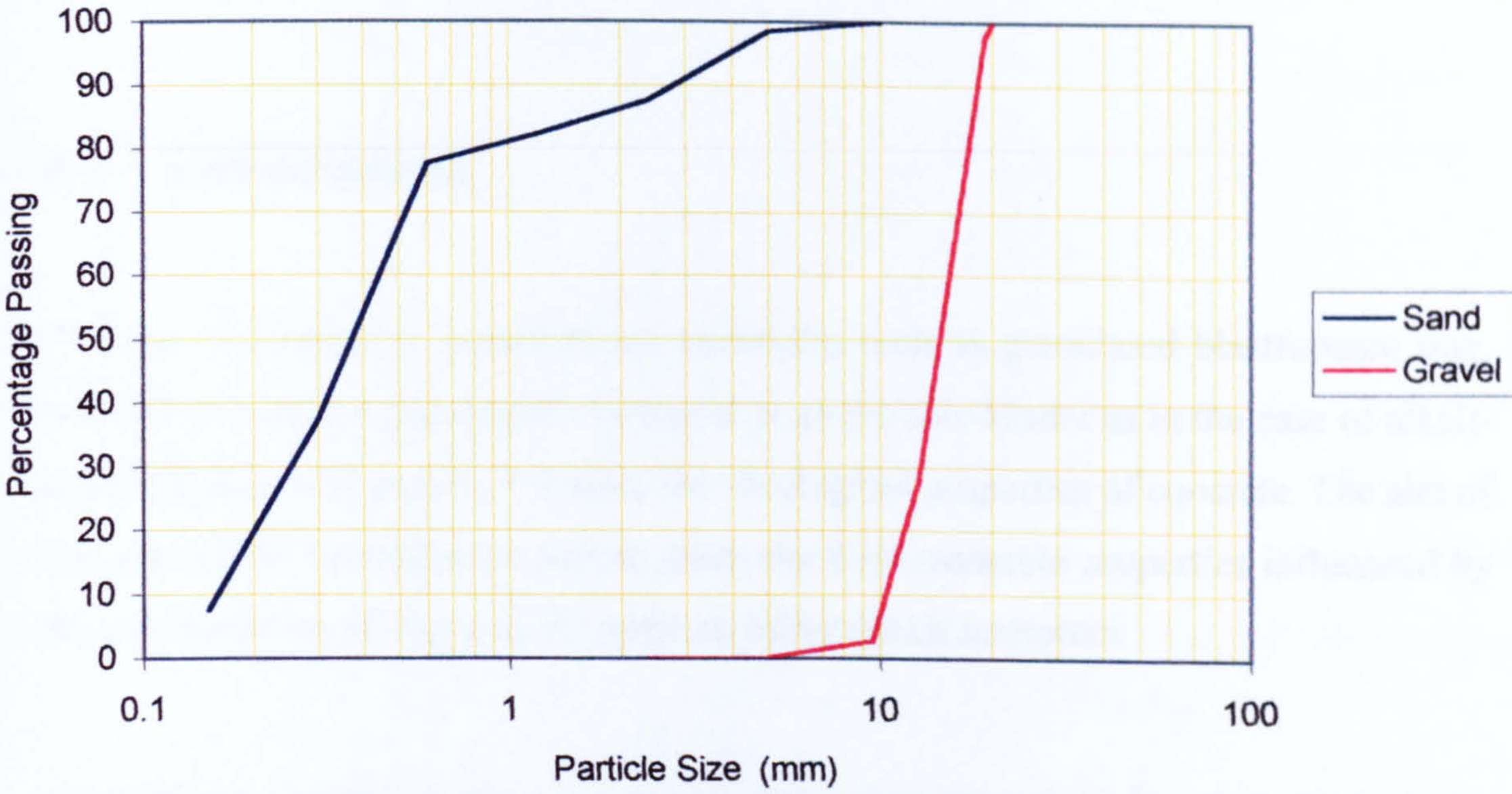

Figure 3.3 Sieve Analysis Results for Aggregates

Figure 3.4 Difficulty in demoulding of AAS concrete

4. PROPERTIES OF THE FRESH CONCRETE

4.1 Introduction

The use of alternative cementitious materials, such as granulated blastfurnace slag, whether in partial replacement of cement or as the sole binder as in the case of alkali-activated slag, will greatly influence the rheological properties of concrete. The aim of this part of the investigation was to study the fresh concrete properties influenced by the incorporation of slag and the addition of the alkali activators.

This chapter reports on the workability of the concrete mixes based on their slump and slump loss with time and workability measure by two point test. Initial and final setting times of standard mortars have been determined to present the different attempts made to control the setting time for alkali-activated slag mortars. Then the setting time results for the concrete mixtures are presented, followed by the air content of the concrete. The chapter concludes with the main points summarizing this investigation.

4.2 Workability

The workability of concrete is one of the most important properties of fresh concrete. It describes the homogeneity and the ease of mixing, handling, placing, compacting and finishing of the concrete (or mortar). The term that has traditionally been used in concrete technology to embrace all these necessary qualities is the workability or rheology of fresh concrete.

According to *Tattersall* (1991), the fresh concrete must be of a suitable composition in terms of quality and quantity of cement, aggregate and admixtures and must also be capable of:

a) Being mixed satisfactorily and transported by one or more of a variety of methods including dumper truck, mixer truck, conveyer belt, and pumping.

b) Flowing into all corners of the mould or formwork to fill it completely, a process that might be difficult with the presence of odd shaped or complex sections or areas of congested reinforcement.

c) Being compacted to expel as much entrapped air as possible, with or without the use of machine methods including extrusion, vibration and pressure.

d) Providing a good surface finish from the formwork, without honeycombing, being finished easily by trowelling or other means of finishing.

4.2.1 Workability tests

There are different tests for the workability of concrete that are adopted in concrete practice. The use of any test is chosen based on the following inter-dependent factors:

- The concrete type; its properties and the desired level of workability, w/c ratio, and use of admixtures.
- The application: whether used in floors or slabs or columns and the formwork used.
- The location of the casting; which affect the means of delivering of concrete whether there is a need for pumping for high altitudes or different equipment.

The tests most commonly used are:

- Slump
- Compacting factor
- Vebe time
- Flow table
- Two-point test

4.2.2 Slump Test

Slump was measured for all concrete mixes in accordance with BS 1881: Part102 (1983).

4.2.2.1 Results and Discussion

The results of the slump tests are presented in Table 4.1. The slump loss with time was also measured for some mixes and presented also in Table 4.1. The results show acceptably workable concrete with the CM2 having the lower slump than CM1 which has a higher w/c ratio. SLG60 had a slump higher than CM2 having the same w/c ratio. The AAS concrete with high Na_2O dosages starts with a high slump and loses the slump more quickly. The phenomenon of thixotropy is clear with AAS concrete, which makes bonds that are breakable by remixing.

4.2.3 Two-point Test

The two-point workability test was carried out on all concrete mixes made with w/c ratio of 0.48 using a MK II apparatus (available in the laboratory) as prescribed by

Tattersall (1991). The experimental set-up is shown in Figure 4.1. The concrete test sample was kept in a cylindrical bowl and was sheared by a suitable impeller, which was driven by an electrical motor operating through an infinitely variable hydraulic transmission and a reduction gear. The pressure developed in the oil in the hydraulic transmission was measured by Budenburg pressure gauge. The pressure produced by concrete shearing was obtained from the total pressure by subtracting the pressure produced by machine idling. The net value may be converted into impeller torque after calibration. The impeller torque T and speed N are found to be related by the linear equation:

$$T = g + hN$$

Where T - is torque (Nm)

N - is speed (rpm)

g - is intercept of the torque axis

h - is reciprocal of the slope of the line.

By measuring the torque produced on an impeller rotating in fresh concrete at various speed settings, the values of g and h can be determined, which therefore define the workability of a particular concrete mix. Different concrete mixes at different workability produce different values of g and h. The resemblance of the equation to the rheological equation of *Bingham* flow is often noted. The theoretical justification that fresh concrete approximates to the *Bingham* model and that the two constants g

and *h* are directly proportional to the *Bingham* constants τ_0 and μ has been provided by *Tattersall* and *Banfill* (1983).

The rheological properties (*g* and *h*) relate to the flowability of the concrete. The lesser value of *g* indicates more flowability of the concrete under its own weight and lower value of *h* depicts less viscosity of the concrete and thus the fast velocity of the flow.

4.2.3.1 Results and discussion

The results of the two point workability test for the OPC, OPC/slag, and AAS mixes were plotted in accordance with the test procedure and presented in Figure 4.2. The values for *g* and *h* for the different mixes are presented in Table 4.2.

Comparing the *g* values for the mixes indicate that the (CM2) mix has the lowest workability and the less flowable, The OPC/slag mix (SLG60) is more flowable compared to CM2, followed by SS6 and the SS4 and MET4 and MET6 have similar workability.

4.3 Setting Time

The setting of cement paste or concrete refers to the change from a fluid to a rigid state. After adding water to cement and mixing them, the workability of cement paste remains unchanged, and this period of time is referred to as the 'dormant period'. At a certain stage, the paste gradually starts to stiffen and becomes solid. The time taken for cement paste or concrete to stiffen is known as setting time. The setting time is classified into two arbitrary stages: initial and final setting times. The cause of setting is due to selective hydration of the anhydrous cement phases. During setting, the temperature of the cement paste changes. The initial set is accompanied by a rapid rise in temperature and the final set corresponds to the peak temperature. The initial setting time represents the length of time in which cement paste or concrete remains plastic and workable. The final setting time corresponds to the time required for the

matrix to reach the stage where it may be regarded as a rigid solid and starts to gain mechanical strength. During the time between the initial set and final set, the concrete is stiff and cannot be re-shaped.

4.3.1 Test Procedure

The setting times were determined using a hand held penetrometer, manufactured by *ELE International*. The apparatus consists of a penetration plunger that is supported by a spring and has a tip area of 32.26 mm^2. The plunger is steadily pushed into the sample to a depth of 25.4 mm, and the penetration resistance can be noted from a scale attached to the shaft of the penetrometer.

Determination of the initial setting and final setting time was carried out for mortar mixtures prepared to overcome the quick set of alkali-activated slag systems. They were eventually carried out on mortar sieved from the concrete mixes.

The initial and final setting time reported correspond to 500 kPa and 3500 kPa respectively, in accordance with BS 5075: Part 1 (1985). The penetration resistance was determined in 30 minute intervals after casting until the final setting time was reached. In order to prevent moisture loss the specimens were covered with polyethylene sheets during the test.

4.3.2 Results and Discussion

4.3.2.1 Controlling the setting time

An initial study was carried out on standard mortars of ratio cement: sand 1:3 to evaluate the means of controlling the quick setting time of alkali activated slag concrete. Conventional retarding agents were tested without any success.

The effect of hydrated lime in controlling the setting time is reported and adopted by several researchers reported earlier in the literature review. Hydrated lime was used to retard the setting or extend the setting time. The relation between the mortars setting time and the % lime for the two activators is shown in Figure 4.3. Figure 4.3 (a) shows the effect of adding lime on the setting time using a sodium silicate solution activator at a w/b ratio of 0.48. Without lime both for 4% Na_2O and 6% Na_2O mortar set very quickly. The addition of lime at 4% of slag weight increased the setting time for the 4% Na_2O mortar to over 4 hours while it did not affect the mortar with 6% Na_2O. Increasing lime to 6% raised the setting time for the 6% Na_2O to almost 3 hours while it decreased it for the 4% Na_2O mortar. It is therefore not useful to increase the lime in this latter case. A similar trend is observed for the mortar with a higher w/b ratio with slightly higher setting time without the addition of lime (Figure 4.3 (b)).

Figure 4.3 (c) shows that there is no need to add lime for metasilicate activated slag mortars with Na_2O content of 4%, while 4% lime addition is adequate to increase the setting time for the 6%Na_2O mortars.

4.3.2.2 Results for the concrete mixes

After deciding on the best dosage of lime needed, this finding was utilised in the concrete mixes. The initial and final setting results for the concrete mixes are presented in Figures 4.4 and 4.5. The results show that the OPC mix with higher w/c ratio had longer setting time compared to the other OPC control mix. Among the mixes of the similar w/c ratio and binder content the addition of slag prolongs the setting time. Alkali-ctivated slag mixes had acceptable setting times through the use of hydrated lime with the mortars having higher the Na_2O dosage which has shorter setting time otherwise. The silicate modulus of the activator is also a factor. The sodium silicate activator (M_s=1.65) in the mixes SS4 and SS6 gave shorter setting times than those for the Metasilicate activator (M_s=1) in the mixes MET4 and MET6.

4.4 Air Content

The air content of concrete has great importance since the presence of voids in concrete greatly reduces its strength: 5 % of voids can lower strength by as much as 30%, and even 2 % voids can result in a drop of strength of more than 10% (*Neville* 1995). Nevertheless it might be required in severe environmental conditions with the risk of freezing to have a higher volume of voids to allow water more space to expand without causing damage.In the present investigation air entraining agents were not used.

4.4.1 Test Procedure

The air content was determined in accordance with BS 1881: Part 106 (method B). The test was carried out 30 minutes after mixing, according to the time interval specified in BS 5075: Part3 (1986). The results reported the volume of air as a percentage of the volume of concrete.

4.4.2 Results and Discussion

The air content values are shown in Figure 4.6. The result show values of air content of alkali-activated slag concrete comparable to the control mixes. Since air-entrainment is not required, the air content values measured were acceptable and within the range for normal concrete .

4.5 Conclusions

The main conclusions drawn from the present investigation are summarised as follows:

1) Slag requires less water for the same workability level. Therefore the slag replacement mix SLG60 had higher slump compared with CM2, where both mixes have the same w/c ratio and same binder content.

2) Alkali activated slag concrete has good workability comparable with OPC and OPC/slag concrete.

3) AAS concrete sets rapidly if not controlled by for example adding lime.

4) The higher the dosage of Na_2O, the lower the slump.

5) The higher the silicate modulus of the activator the less workable is the concrete in terms of its slump, and also the setting time is shorter.

6) The air content of all the mixes was acceptable.

Table 4.1 Slump Results for Different Mixes

Time (min).	Slump for the different mixes (mm.)						
	CM1	SLG60	CM2	SS4	SS6	MET4	MET6
5	130	145	80	Collapse	120	Collapse	130
30			60	140	110	140	120
60			40	120	70	125	60
75			-	110	40	115	40
90			25	-	15	90	20
105				40			
120			15	10		15	

Table 4.2 Two-point workability test results

	CM2	SLG60	SS4	SS6	MET4	MET6
g	3.1	2.36	0.6	2	0.7	0.7
h	1.94	2.33	3.4	2.34	3.9	3.0

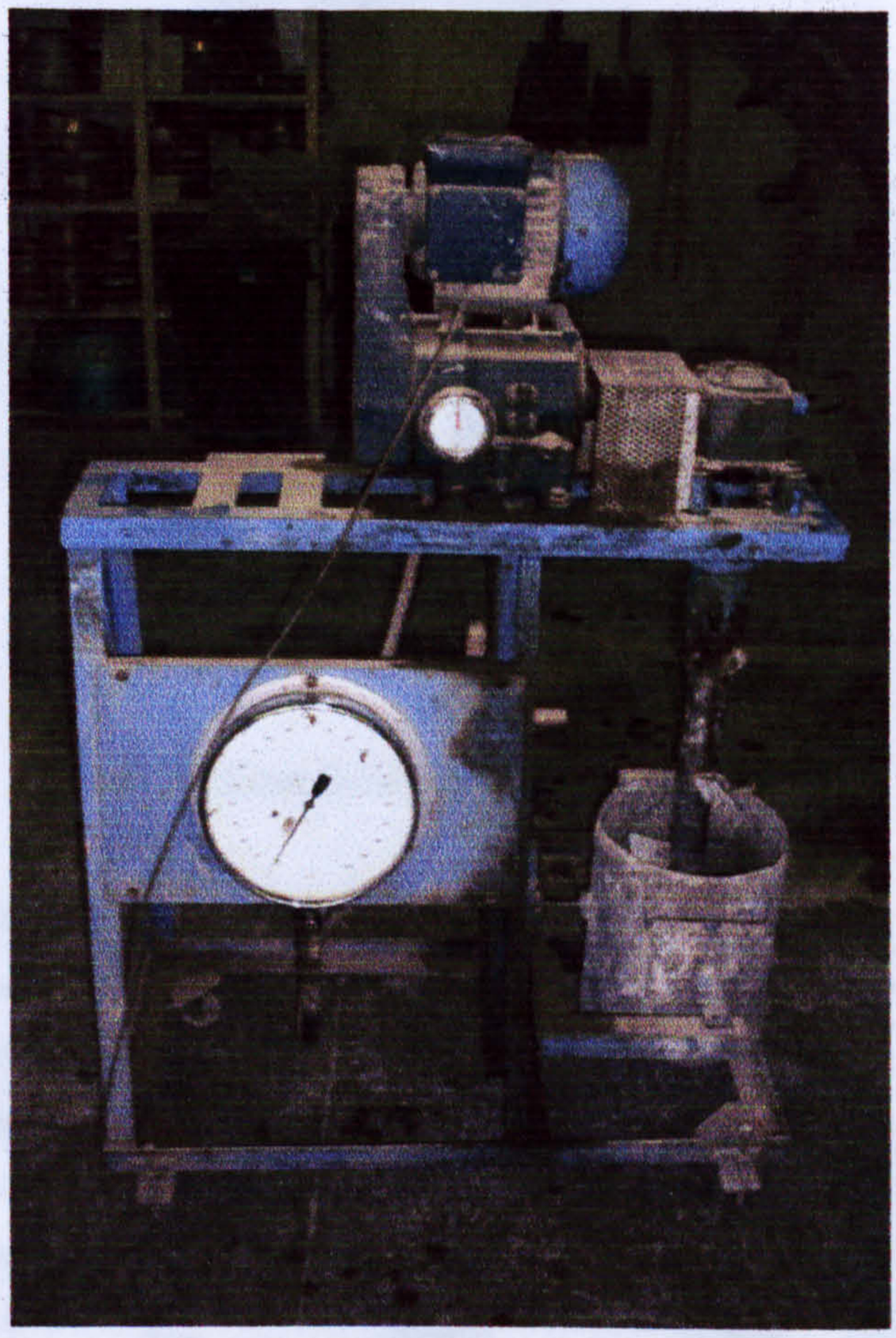

Figure 4.1 The two-point workability test equipment

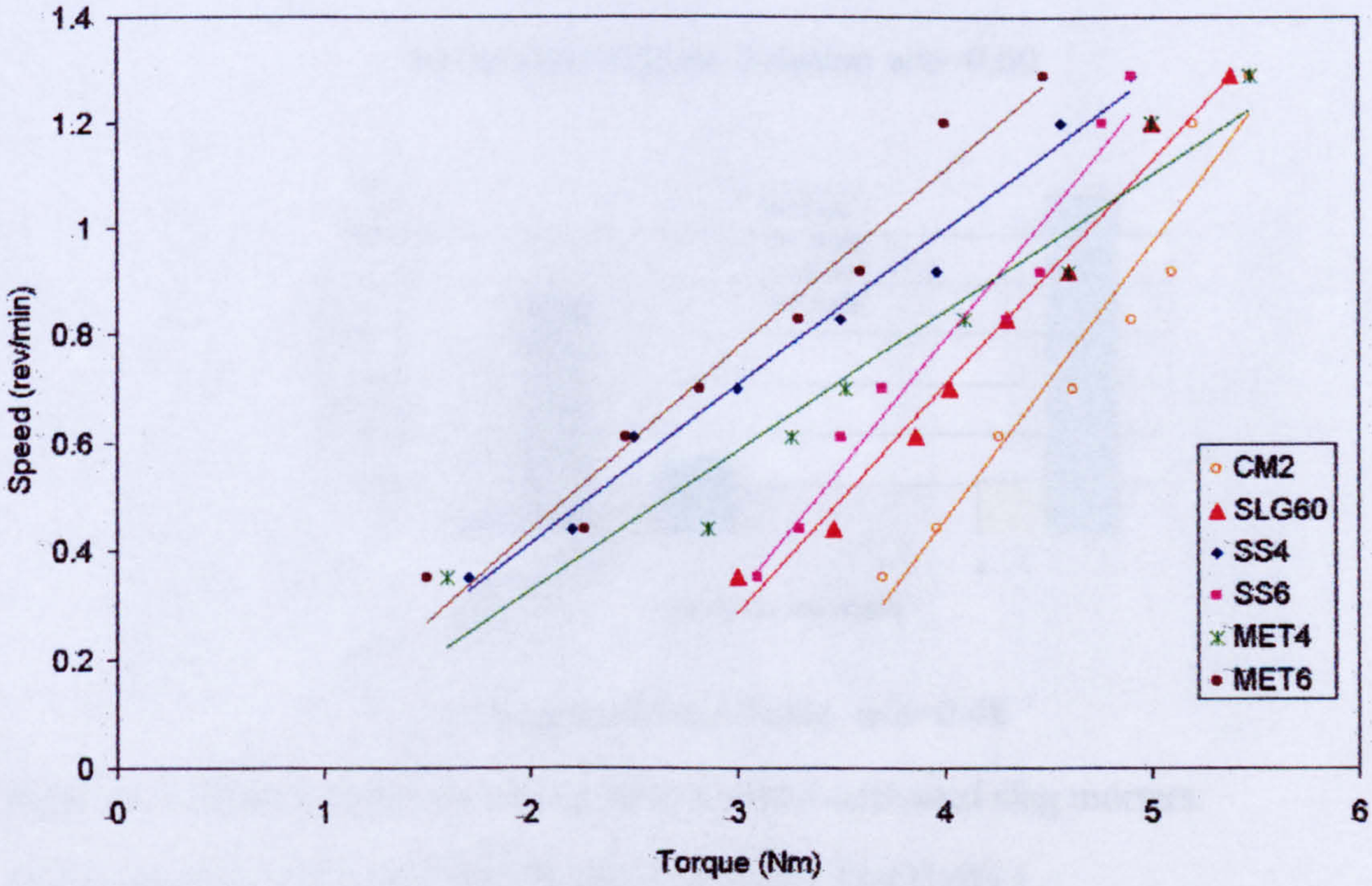

Figure 4.2 Relationship between speed and torque of the different concrete mixes

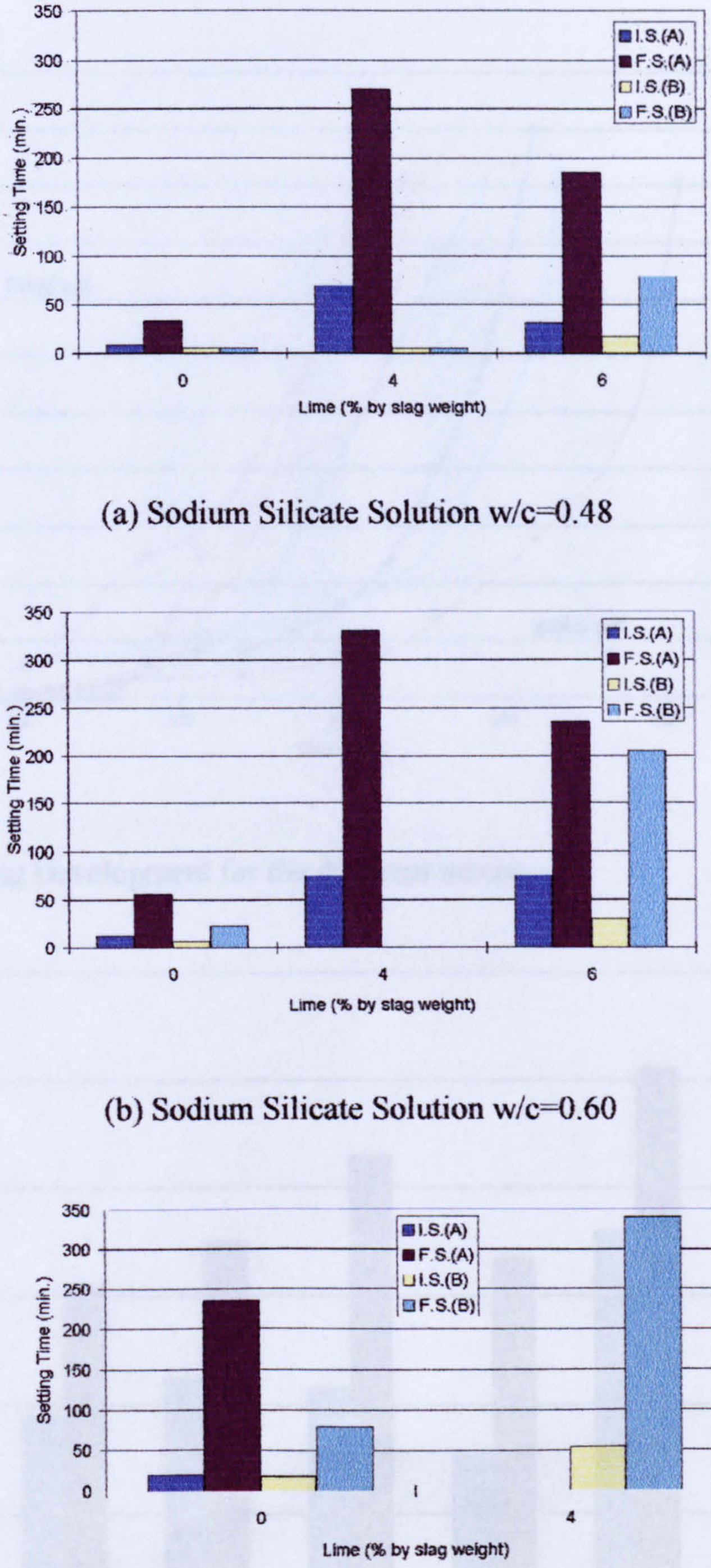

(a) Sodium Silicate Solution w/c=0.48

(b) Sodium Silicate Solution w/c=0.60

(c) Sodium Metasilicate w/c=0.48

Figure 4.3 Effect of lime on setting time of alkali-activated slag mortars.

(I.S: initial set, F.S: final set, (A) Na_2O=4%, (B) Na_2O=6%)

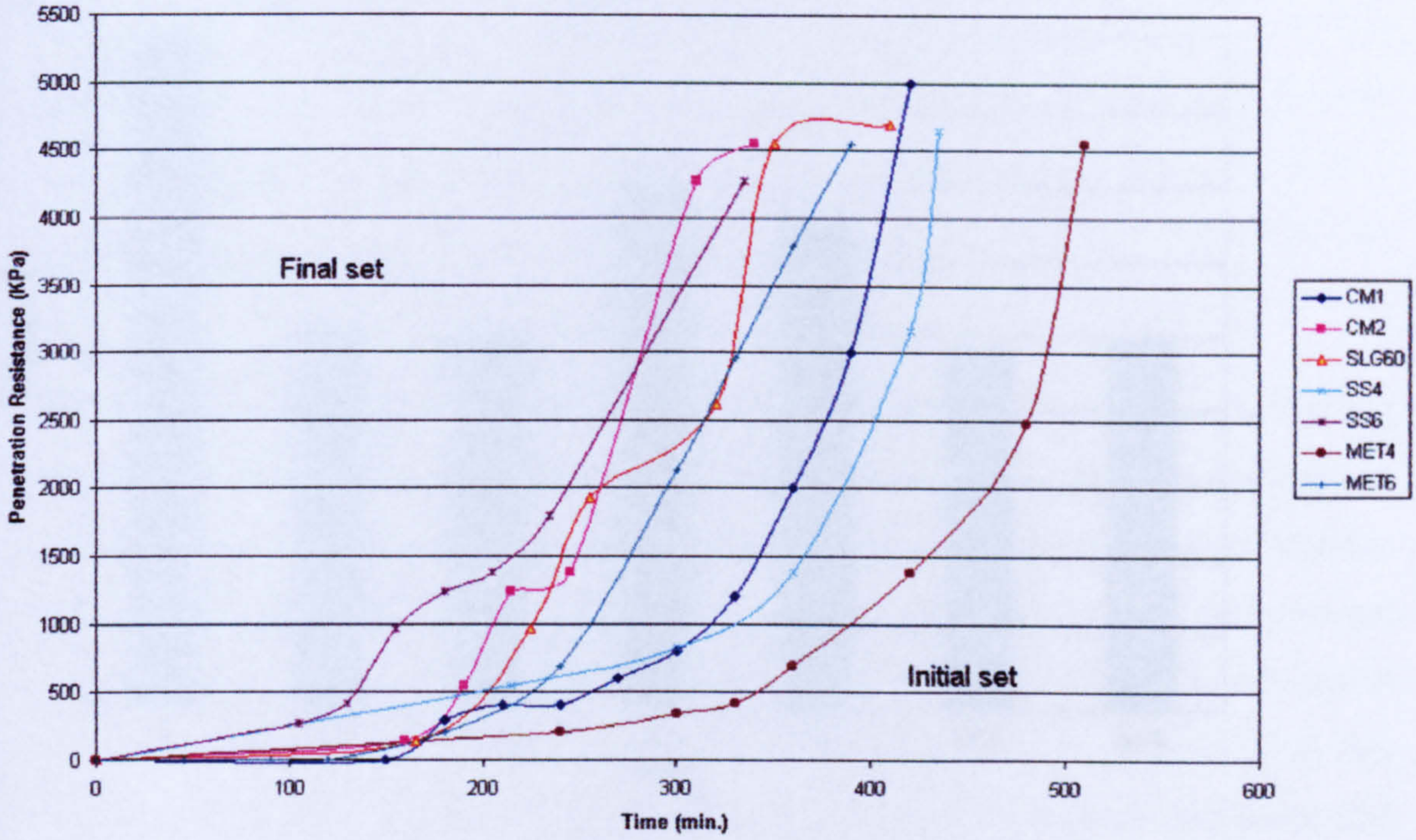

Figure 4.4 Setting Development for the different mixes.

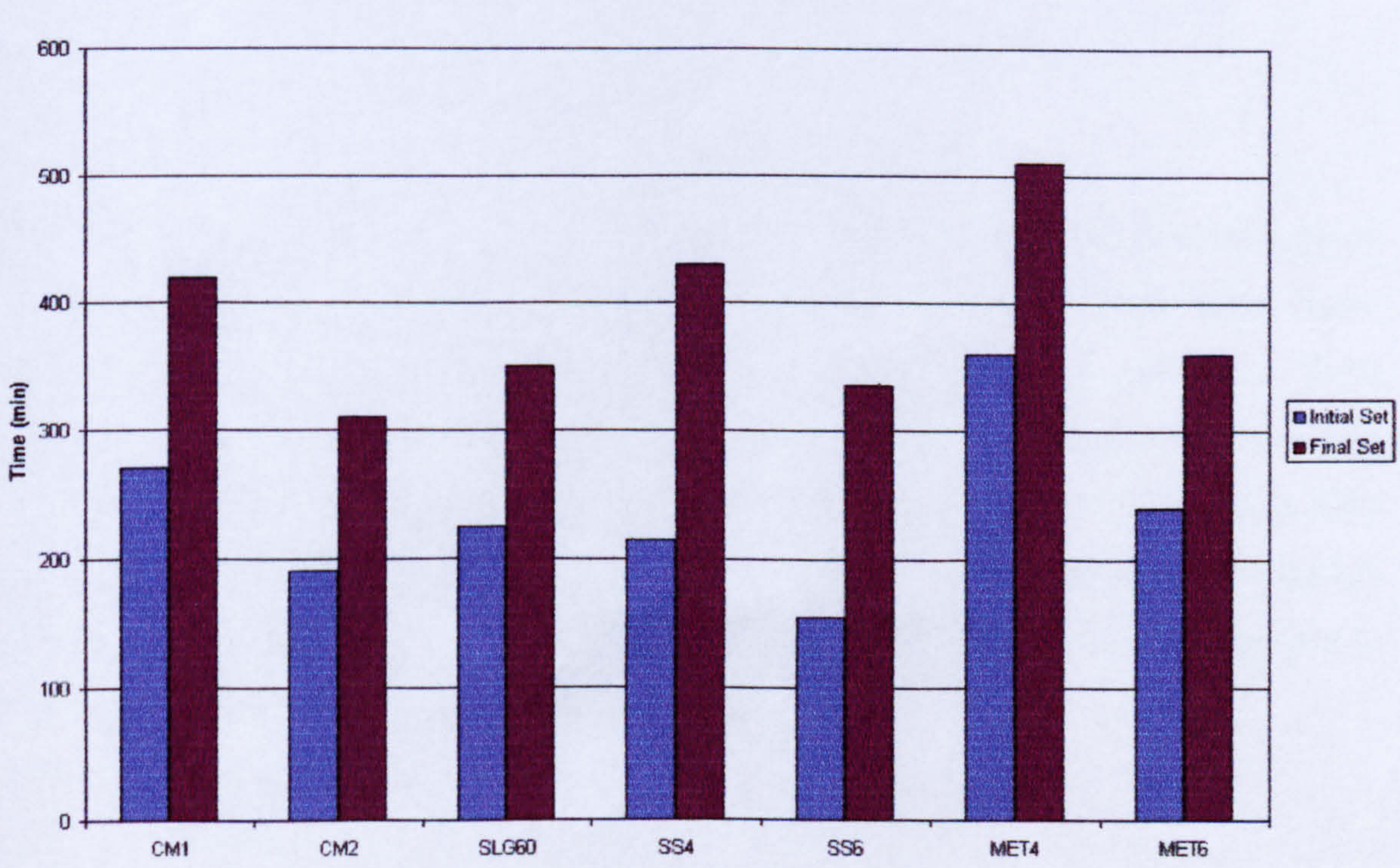

Figure 4.5 Initial and Final Setting Time for the different mixes.

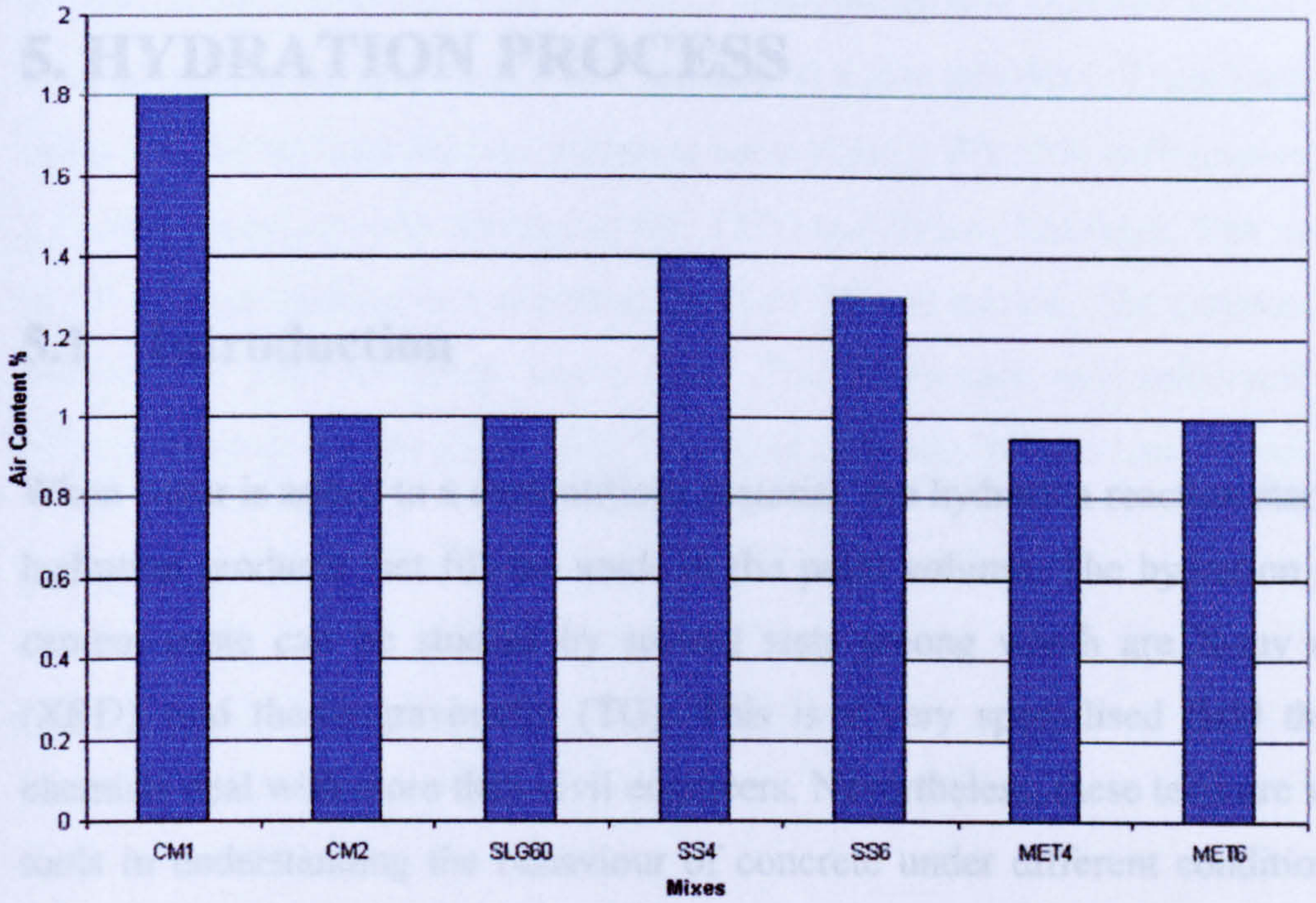

Fig 4.6 Air Content values for the different mixes

5. HYDRATION PROCESS

5.1 Introduction

When water is added to a cementitious material, the hydration reaction starts forming hydration products that fill the voids in the paste volume. The hydration process in cement paste can be studied by several tests among which are X-ray diffraction (XRD), and thermogravimetry (TG). This is a very specialised field that cement chemists deal with more than civil engineers. Nevertheless, these tests are very useful tools in understanding the behaviour of concrete under different conditions. In this chapter, the results of XRD and TG carried out on AAS pastes are presented and discussed.

5.2 Hydration Products

The hydration process results in several hydration products depending on the type of cementitious material and the curing condition at which those products form. X-ray diffraction is a very useful technique for phase analysis of materials. Their characteristic peaks can identify crystalline phases present in a material because each crystalline phase with a specific structure has its own "finger print" characteristic pattern of X-ray diffraction peaks. In this investigation XRD has been used to identify the hydration products formed in OPC, OPC/slag and Alkali-activated slag pastes representative of the concrete mixes studied.

5.2.1 Test Procedure

Paste specimens were cast representative of the concrete mixes studied in this investigation (CM2, SLG60, SS4, SS6, MET4, and MET6). The specimens were cured in water and in addition to that autoclave curing was used for AAS mixtures. At

the testing age specimens were broken to small pieces and kept submerged in acetone. Prior to testing the specimens were crushed to a fine powder (<75μm) and examined using Cu Kα monochromatic radiation on a Philips PW1050 diffractometer (Figure 5.1) in conjunction with Sietronics SIE 122D and Traces Software. The range from 5 to 75° 2θ was scanned at a scanning speed of 2°θ per minute. The computer plots the intensity of the diffracted beam (2θ). The d-spacings are calculated to allow identification of the phases and this is done by utilising Bragg's Law, which is:

$$\lambda = 2d \sin \theta \qquad (5.1)$$

Where: λ = wavelength of copper Kα (1.541838 Å)

d = d-spacing

θ = diffraction angle

Abbreviations have been used to label the X-ray diffraction traces and the following key gives an explanation of those abbreviations.

Key to XRD traces:

CH = Calcium hydroxide ($Ca(OH)_2$)

CC = Calcium carbonate ($CaCO_3$)

E = Ettringite ($Ca_6Al_2(OH)_{12}(SO_4)_3.26H_2O$)

C_3S = Tricalcium silicate (Ca_3SiO_5)

G = Gehlenite ($Ca_2Al_2SiO_7$)

T = Tetracalcium aluminate 13 hydrate (C_4AH_{13}) = $Ca_3Al_2O_6.Ca(OH)_2012H_2O$

CSH(I) = Calcium silicate hydrate ($(CaO)_{0.8\text{-}1.5}SiO_2(H_2O)_x$)

HT = Hydrotalcite ($Mg_6Al_2(CO_3)(OH)_{16}.4H_2O$)

X = Xonotlite = 5 calcium 5 silicate monohydrate ($Ca_6(Si_6O_{17})(OH)_2$ .0.20H_2O)

5.2.2 Results and Discussion

5.2.2.1 OPC pastes

Figure 5.2 shows the XRD traces for OPC paste mixture (CM2) after 28 and 90 days hydration under water curing. The standard OPC hydration products observed were calcium hydroxide (CH), calcium carbonate (CC) and ettringite (E). There was some trace from unhydrated cement indicated by the presence of diffraction peaks from tricalcium silicate (C_3S). Although the XRD test was not used as a quantitative measure for hydration progress it can be noticed by comparing the intensity of the peaks that CH had slightly decreased as CC increased because of carbonation. C_3S decreases with time as expected.

5.2.2.2 OPC/slag pastes

Figure 5.3 shows the XRD traces for OPC/slag paste mixture (SLG60) for 28 and 90 days hydration under water curing. The main phases were: gehlenite (G), calcium carbonate (CC), calcium hydroxide (CH) and ettringite (E). Gehlenite is associated with anhydrous slag. There are some peaks that possibly indicate the presence of tetracalcium aluminate 13 hydrate (C_4AH_{13}) with possibility of carbonated phases. No clear variation can be detected in the intensities with time.

5.2.2.3 AAS pastes

5.2.2.3.1 Normal water curing

It was found that the XRD traces were very similar for all AAS mixes and no clear distinction could be seen with varying the Na_2O dosages or the Ms of the activators. Therefore typical XRD traces for the AAS are shown in Figure 5.4. Peaks indicating poorly crystalline calcium silicate hydrate C-S-H (I) were observed around 3.03 Å, 2.85 Å, and 2.70 Å. Some broad peaks observed around 7.70 Å and 1.90 Å probably indicate the presence of hydrotalcite, which is a magnesium aluminium carbonate hydroxide hydrate. This is due to the high magnesium content of the slag

used, which is around 12%. This observation is in agreement with *Wang and Scrivener* (1995). It is also reported that the hydration products in the alkali-slag system are known to be C-S-H gel with low Ca/Si ratio, zeolite-type minerals and silica gel (*Xu et al.*, 1993). Other researchers reported presence of C-S-H and possibly zeolite phases (*Qing-Hua et al.*, 1992)

5.2.2.3.2 Autoclave curing

The hydration reaction rate is expected to increase under autoclaving and a more crystalline C-S-H is formed (*Taylor*, 1997). The XRD traces for the AAS pastes autoclaved at 150 °C are shown in Figure 5.5. The peaks are similar to the water cured specimens with the possible presence of xonotlite. This cannot be absolutely confirmed since all calcium silicate hydrate phases including C-S-H (I), tobermorite and xonotlite have broad peaks which all have d-spacing very close to each other and overlapping. C-S-H(I) has main peaks at 3.07 Å, 2.81 Å, and 1.83 Å, while tobermorite(14 Å) has peaks around 3.07 Å , 2.81 Å ,and 1.83 Å . Xonotlite has peaks around 3.07 Å , 2.04 Å , and 1.95 Å . Hence these cannot be clearly distinguished with the XRD technique, which has some errors due to shifting in the peaks occurring due to sample preparation and orientation. *Shi et al.* (1991) reported the presence of xonotlite peaks in conjunction with C-S-H(I) for activated ggbs pastes activated with waterglass and cured at 150 °C.

5.3 Progress of Hydration

There are numerous methods of determining the progress of hydration, but all have their limitations. These include the measurement of (a) the amount of $Ca(OH)_2$ present in the paste; (b) the amount of chemically combined water; (c) the heat evolved by hydration; (d) the specific gravity of the paste; (e) the amount of unhydrated cement present (using X-ray quantitative analysis QXDA); and (f) indirectly from the strength of hydrated paste (*Neville* (1995).

The chemically bound or combined water often referred to as the non-evaporable water is usually used to monitor the progress of hydration. Although it is used as an indication of the degree of hydration it is not an absolute measure of the degree of hydration, because neither the composition of the major hydration product (calcium silicate hydrate), nor the stochiometry of the reaction is well defined (*Bye*, 1983).

The technique is essentially heating the sample to release the evaporable water first, then igniting it to 1000°C until constant weight is reached. The percentage of non-evaporable water is then expressed as the ratio of the weight loss to the ignited weight. There is, however, some weight loss due to the decomposition of $CaCO_3$ at around 600-780°C, therefore the total weight loss should be corrected taking this into account (*Keattch and Dollimore*, 1975), although some workers do not make the correction (*Nilsson, 1980*). Nilsson (1980) selected an ignition temperature of 600°C in order to separate the water and the carbon dioxide. However he later found that there is about 10% of water released between 600 and 1000°C. Some other workers (*Fordham and Smally*, 1985; *Qing-Hua et al.*, 1992) used the combined water of the calcium silicate hydrates only as a measure of hydration.

In this investigation only the progress of hydration for AAS pastes will be studied at different ages using thermogravimetric technique by measuring combined water. The OPC and OPC/slag pastes were tested once at an age of 28 days to compare with AAS pastes.

5.3.1 Apparatus and Procedure

The TG test was carried out on a thermobalance (Pyris1 TGA). The instrument consists mainly of an electro-microbalance, a furnace, an operation programmer unit and the data acquisition unit (Figure5.6). A platinum crucible was used. The heating of the specimens was done at a rate of 30°C /min starting from the ambient room temperature up to 1000°C.

Paste specimens were cast representative of the concrete mixes studied in this investigation (CM2, SLG60, SS4, SS6, MET4, and MET6). The specimens were cured in water and in addition to that autoclave curing was used for AAS mixtures. At

the testing age specimens are broken in small pieces and kept submerged in acetone. Prior to testing the specimens were crushed to fine powder and sieved on a 75 μm sieve before loading in the thermobalance in order to improve the uniformity of the sample.

5.3.2 Results and Discussion

Figures 5.7 – 5.9 show typical TG plots for the OPC and OPC/Slag and AAS pastes respectively. They show three peaks on the derivative plot indicating the C-S-H and hydrates, calcium hydroxide, and calcium carbonate. The peaks give a rough estimate of the range of temperature at which each of these products dehydrate and the decarbonation in the case of calcium carbonate. Figure 5.7 shows a peak around 180°C corresponding to C-S-H, another peak around 500°C corresponding to calcium hydroxide and the calcium carbonate peak around 770°C. The peaks for SLG60 mix presented in Figure 5.8 lie around the same temperatures but the calcium hydroxide and calcium carbonate peaks are smaller which indicates that calcium hydroxide is less in OPC/slag pastes as it is consumed in the pozzolanic reaction. The hydration progress with age was not studied for CM2 and SLG60 pastes.

A typical TG plot for AAS pastes is shown in Figure 5.9. The first peak represent C-S-H and other hydrates including hydrotalcite. The other peaks are for calcium hydroxide and calcium carbonate.

The difference in mass between the temperatures 105-320°C as a percentage of the original mass of the specimen was calculated. This percentage mass loss was used as a measure of the combined water in the C-S-H and other hydrates. This mass loss was calculated for all the AAS mixes as a measure of the progress of hydration at ages 7, 14, 28, and 91 days. The effect of autoclave curing is also investigated.

The progress of hydration for all AAS pastes under water curing is illustrated in Figure 5.10. There is a clear overall trend of increase of hydration with age more clear with the 6%Na_2O dosage while the progress in the case of 4% Na_2O is not very

significant. This indicates that the availability of alkalis is a factor in the continuaion of hydration for longer periods. The overall amount of combined water ranges from 7 to 12 %. At 91 days SS4 gives a value of 8.22%. SS6 gives 11.44%, MET4 with 9.20 and MET6 had 12% combined water. The increase of the Na_2O dosage increases the hydration while the difference in the activator silica modulus M_s dos not seem to have a clear effect on the value of combined water. Some researchers (*Qing-Hua et al.* ,1992) used thermogravimetry to study AAS paste with waterglass activator having M_s=2.85 with Na_2O dosage of 4.3 and adding 3.4% lime. They reported 9.7% combined water at 28 days.

The progress of hydration for all AAS autoclaved pastes is shown Figure 5.11.The progress with age has similar trend. The overall amount of combined water ranges from 6.4 to 9.32 %. At 91 days SS4 gives a value of 7.24%. SS6 gives 9.32%, MET4 with 7.56 and MET6 had 9.61% combined water. The increase of the Na_2O dosage increases the hydration while the difference in the activator silica modulus Ms has no clear effect in the value of combined water. The heat curing (autoclaving) resulted in lower values of combined water compared to water curing. This can be explained by the fact that high temperature causes higher rate of hydration at early age forming dense crystalline hydration products on the outer surface of the cement or slag particles this dense layer with low porosity reduces the amount of water passing through and slowing the hydration thereafter. It can be found that the amount of unreacted cement is more in the case of heat curing. *Yang and Sharp* (2000) studied the degree of hydration for OPC after heat curing and reported higher degree of hydration at early age with curing at 100°C follwed by normal 20°C water curing compared to normal 20°C water curing, but eventually almost stopping and the hydration at normal temperature curing exceeding the heat cured after 28 days.

5.4 Conclusions

The main conclusions on the hydration of AAS pastes are summerised as follows:

- The main hydration product in AAS systems is C-S-H (I). The hydrotalcite-like peaks observed in the XRD patterns, which can be attributed to the high magnesium content of the slag.

- Autoclaving results in formation of a more crystalline C-S-H gel and the formation possibly of xonotlite.

- The TG peaks for C-S-H and other hydrates are around 180°C, 500°C for calcium hydroxide and 770°C for calcium carbonate.

- The dosage of activator affects the amount of hydration. The higher the dosage the higher the hydration.

- There is a clear overall trend of increase in hydration with age in AAS pastes as measured by the amount of combined water, more clear with the 6%Na_2O dosage while the progress in the case of 4% Na_2O is not very significant. This indicates that the availability of alkalis is a factor in the continuation of hydration for longer periods.

- Autoclave curing results in lower hydration as measured by the combined water in comparison with water curing.

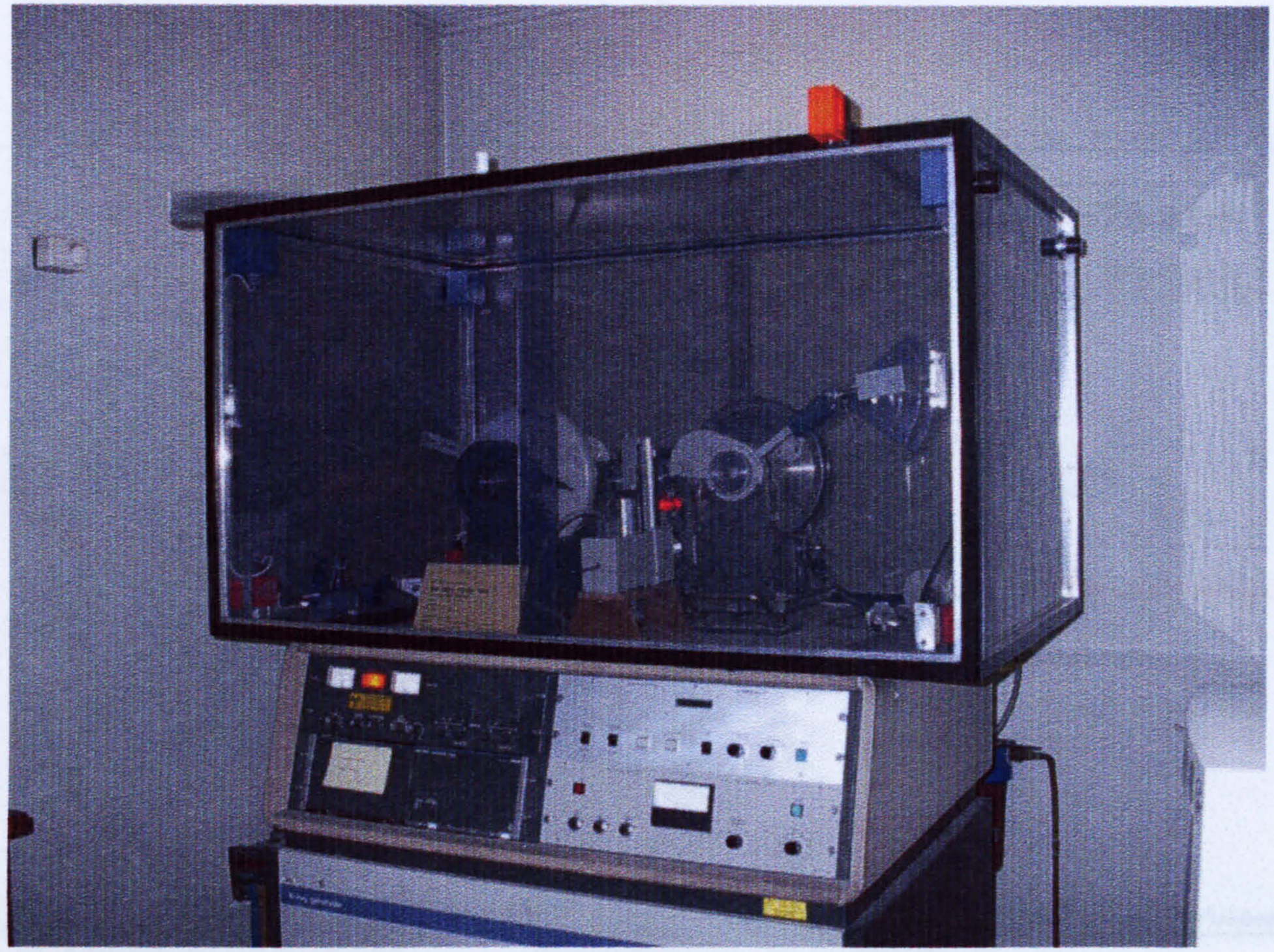

Figure 5.1 X-ray Diffraction Test Equipment

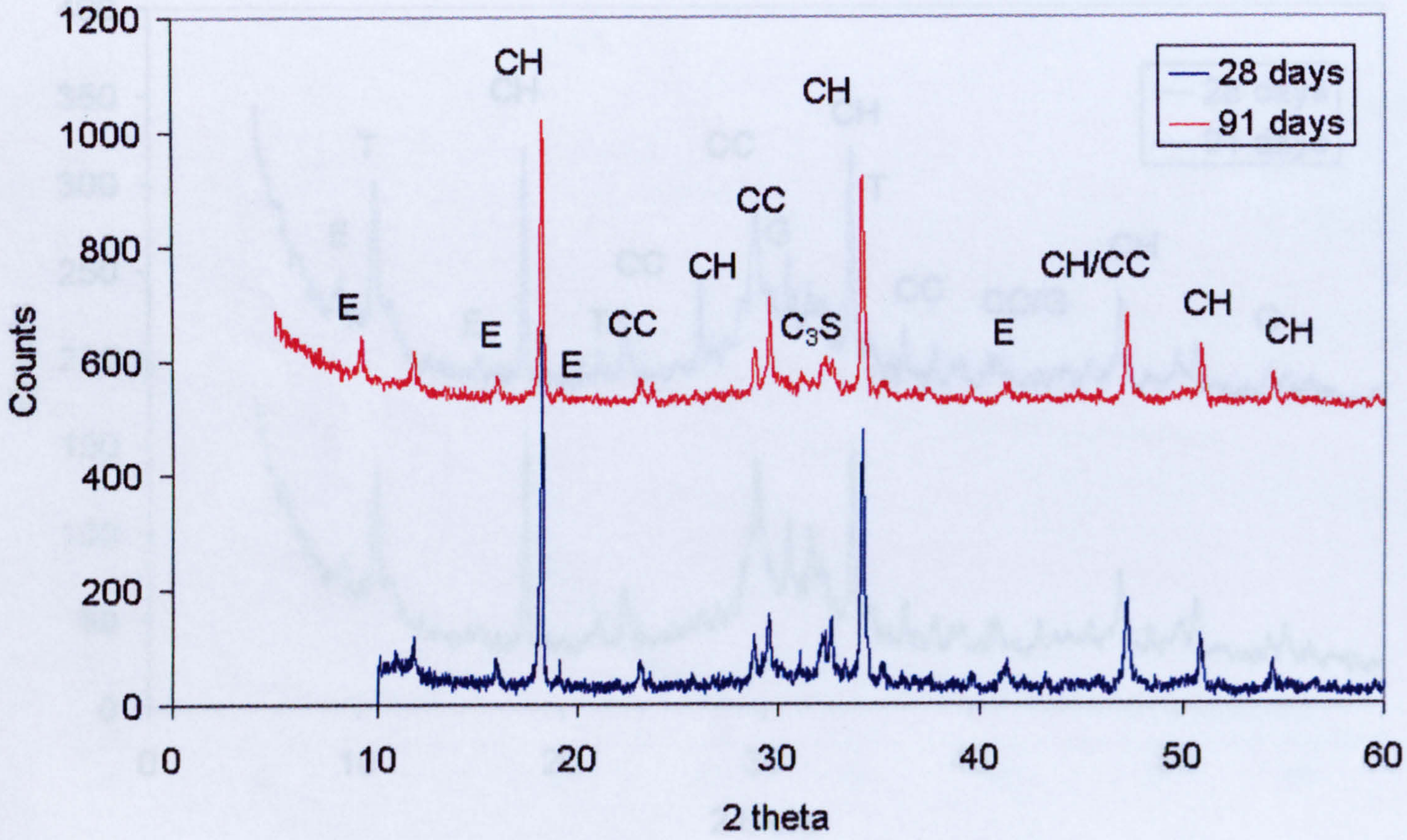

Figure 5.2 XRD patterns for CM2 (WC)

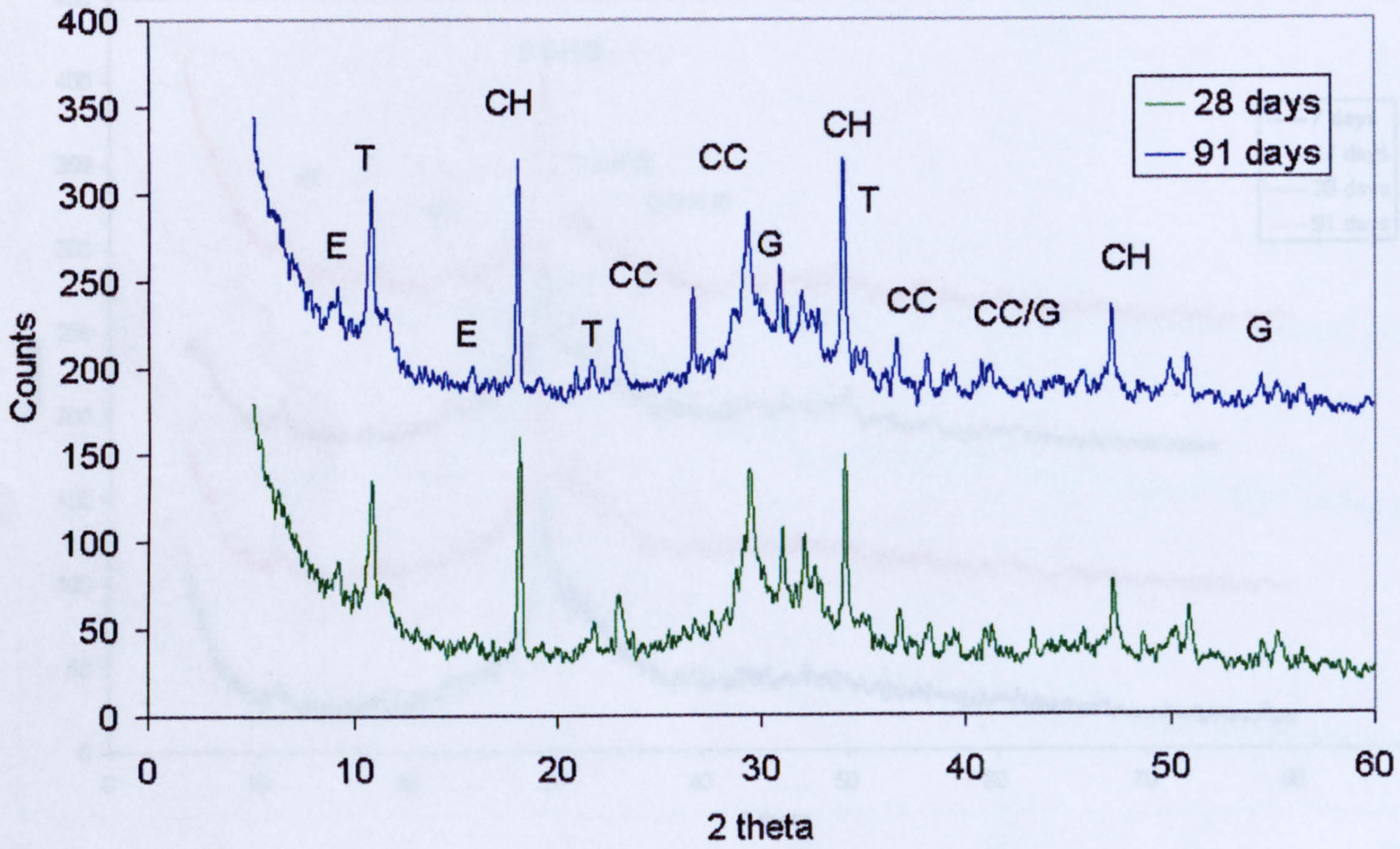

Figure 5.3 XRD patterns for SLG60 (WC)

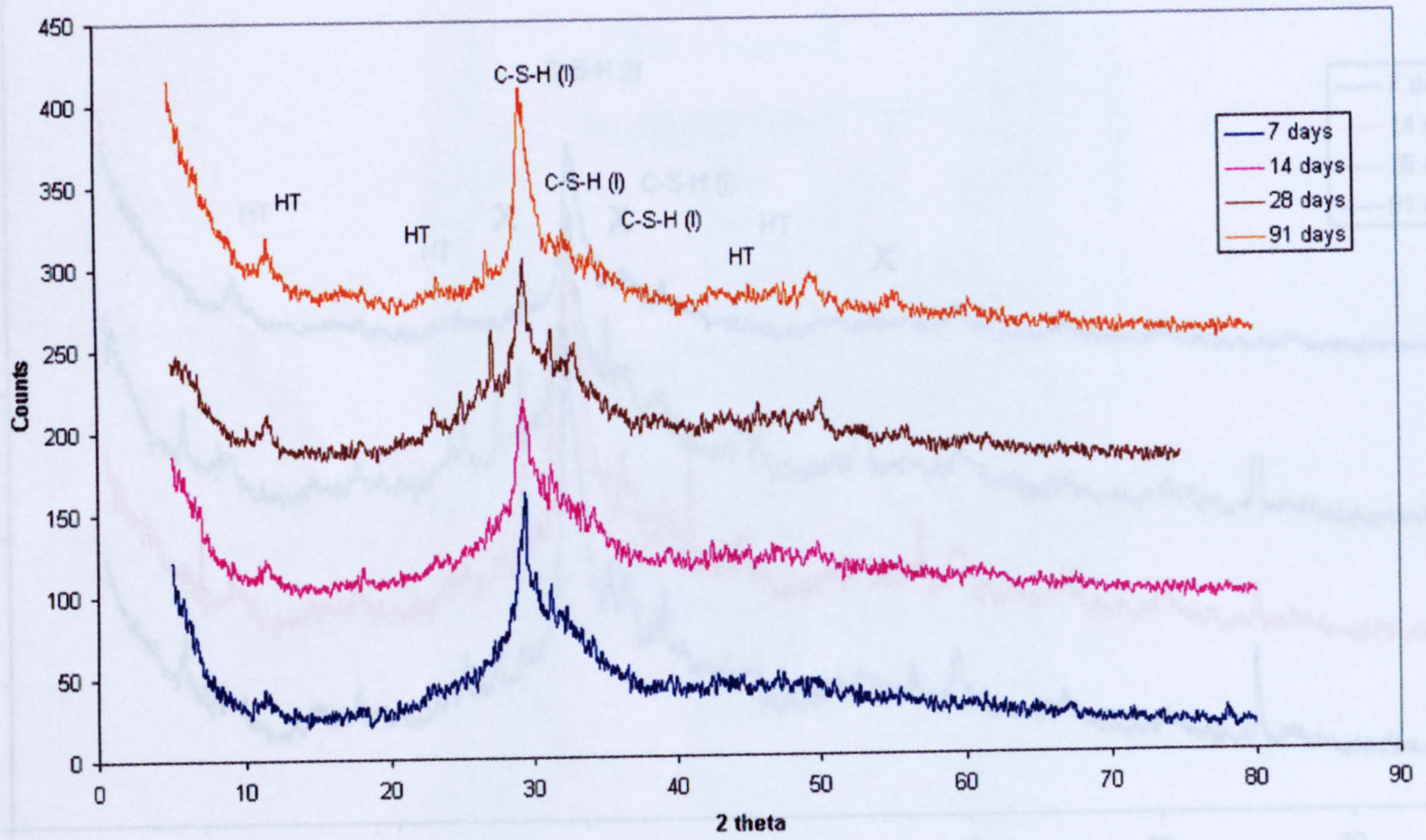

Figure 5.4 XRD patterns for AAS (WC)

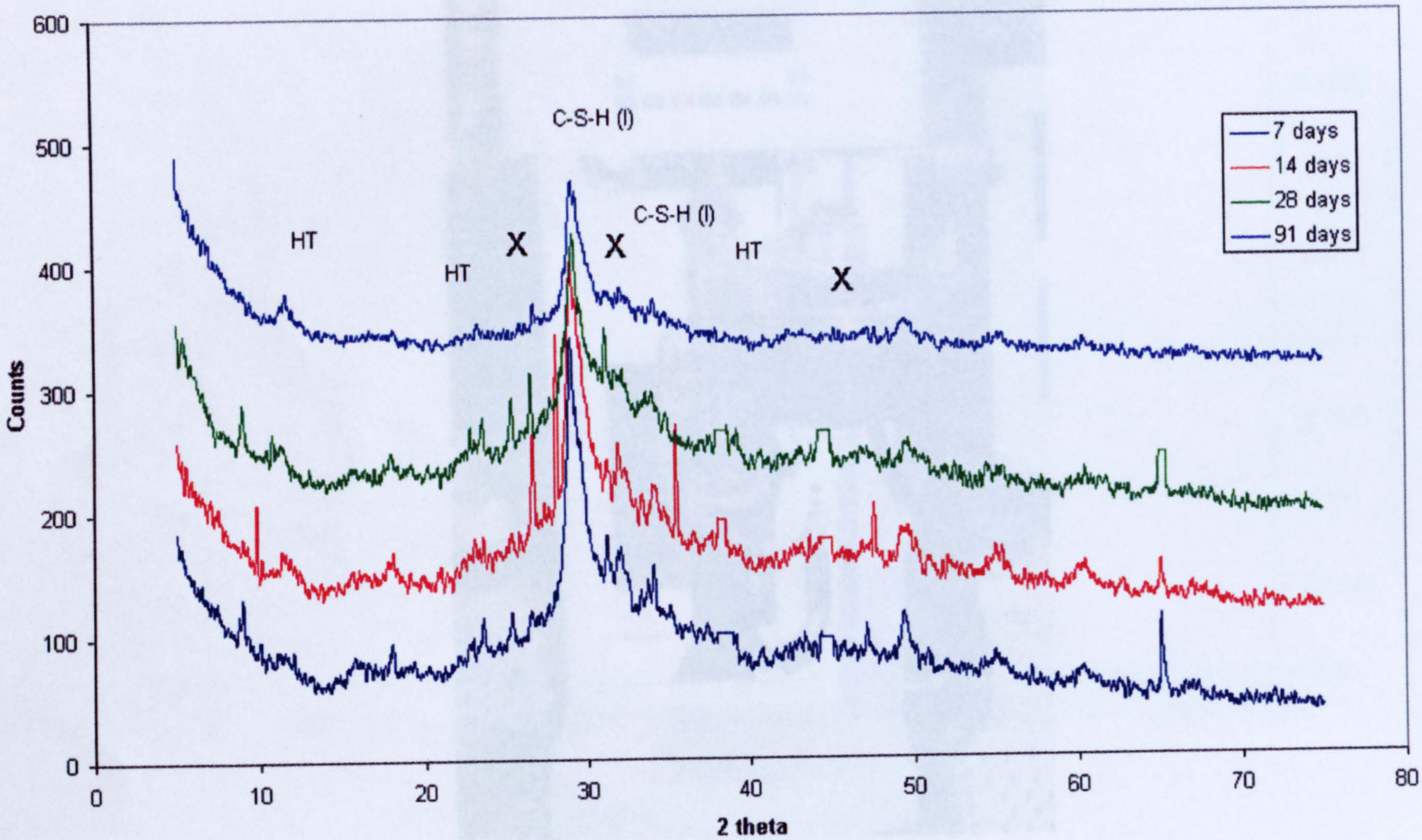

Figure 5.5 XRD patterns for AAS (AUT)

Figure 5.6 TG test equipment

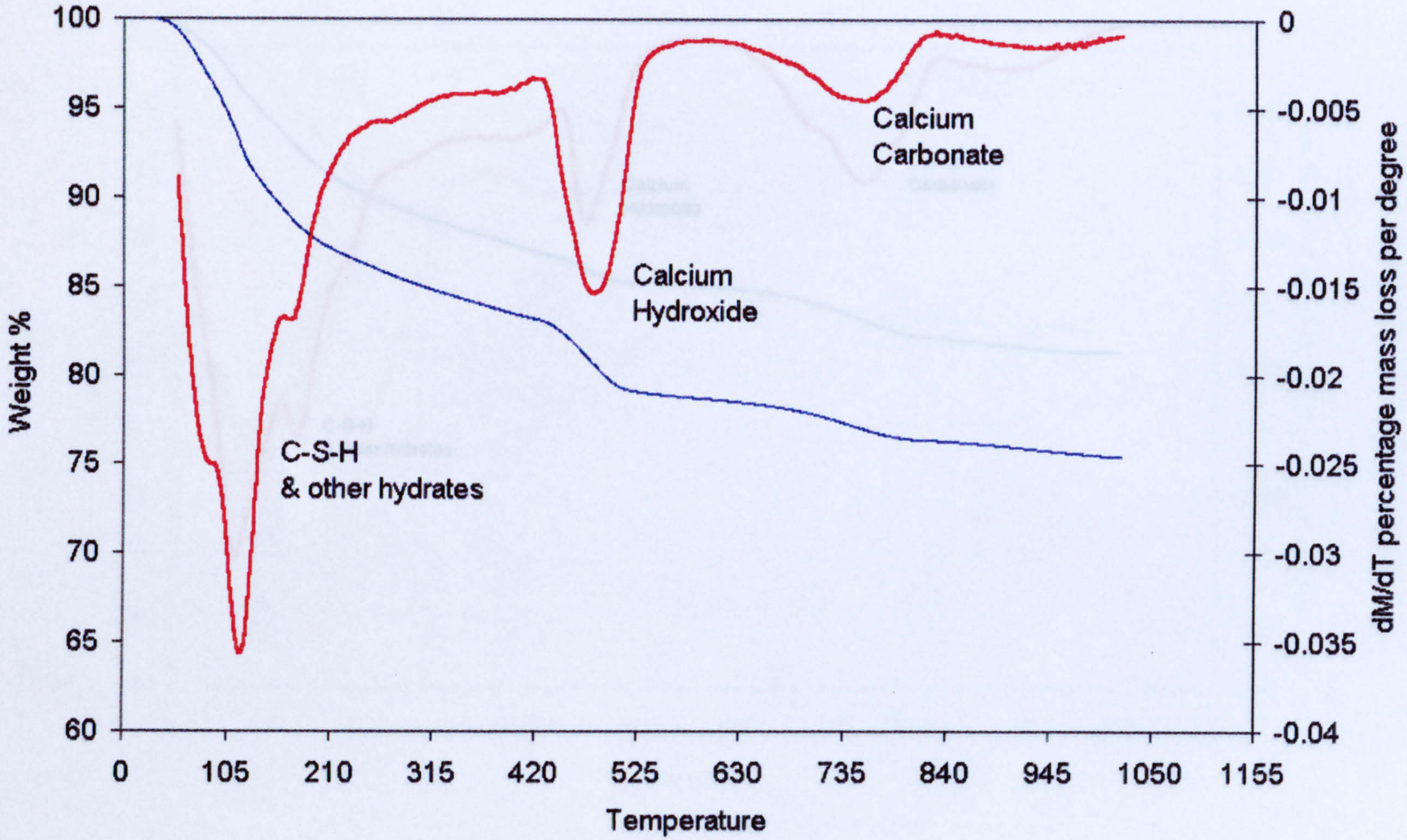

Figure 5.7 TG pattern for CM2 paste

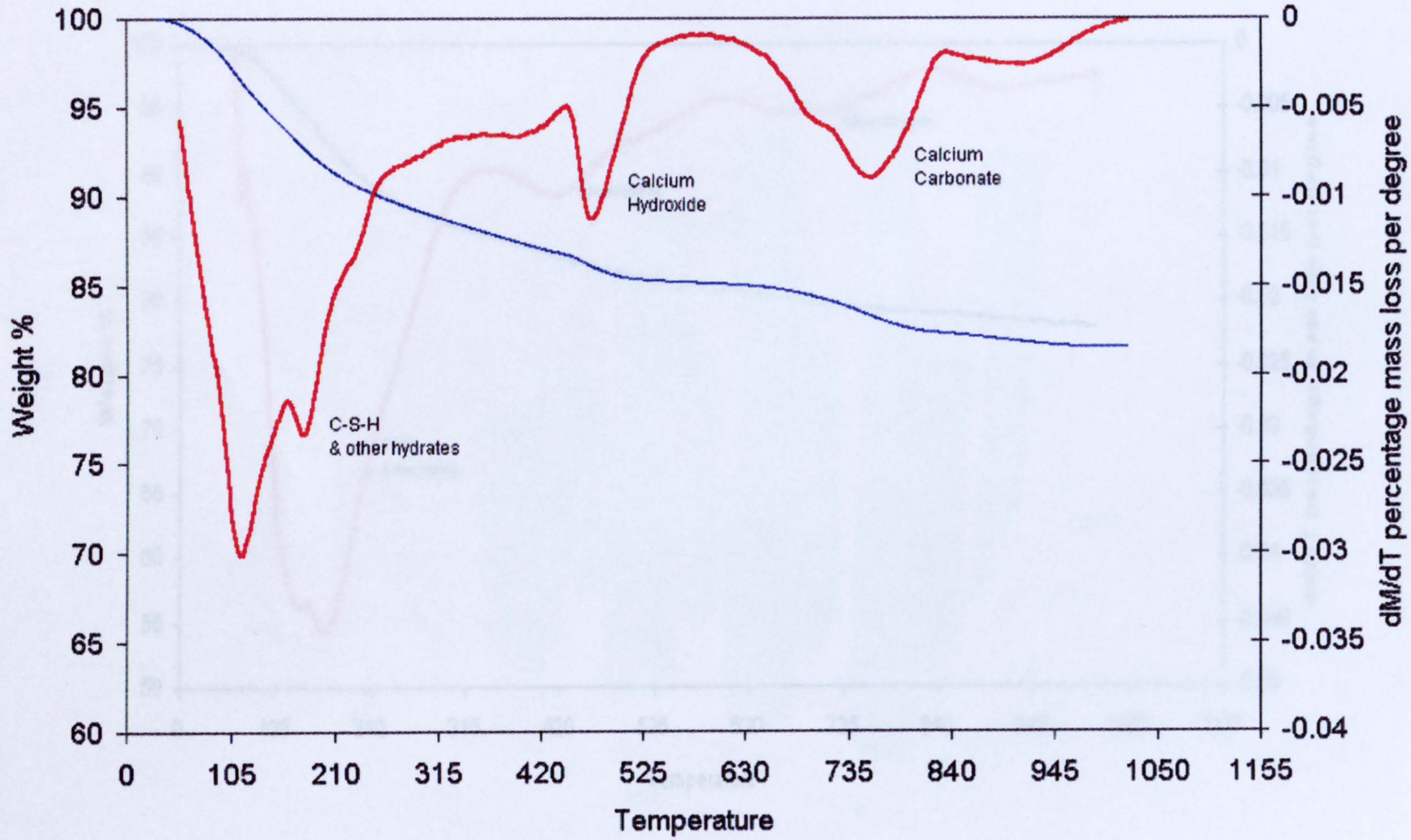

Figure 5.8 TG pattern for SLG60 paste

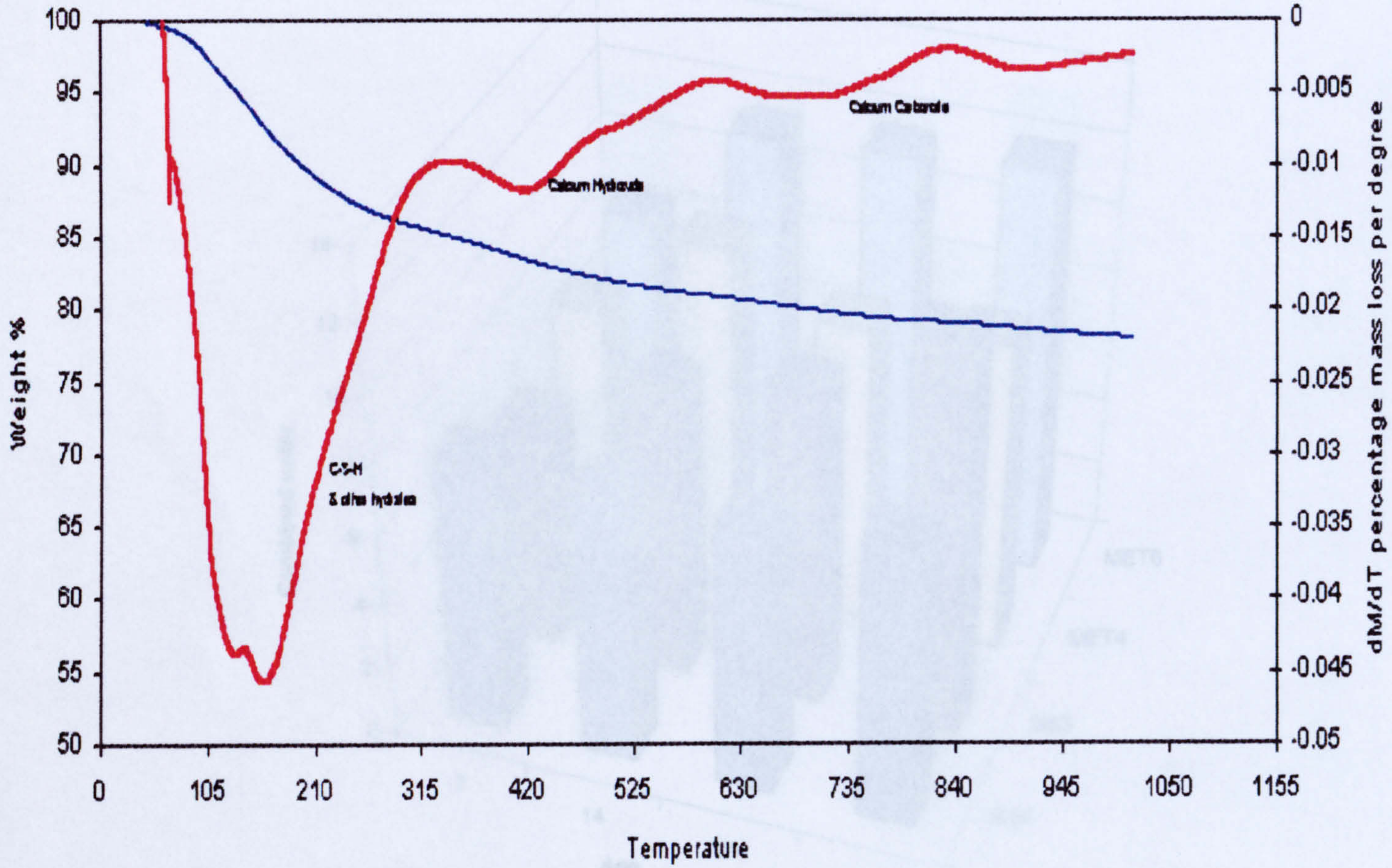

Figure 5.9 Typical TG pattern for AAS paste

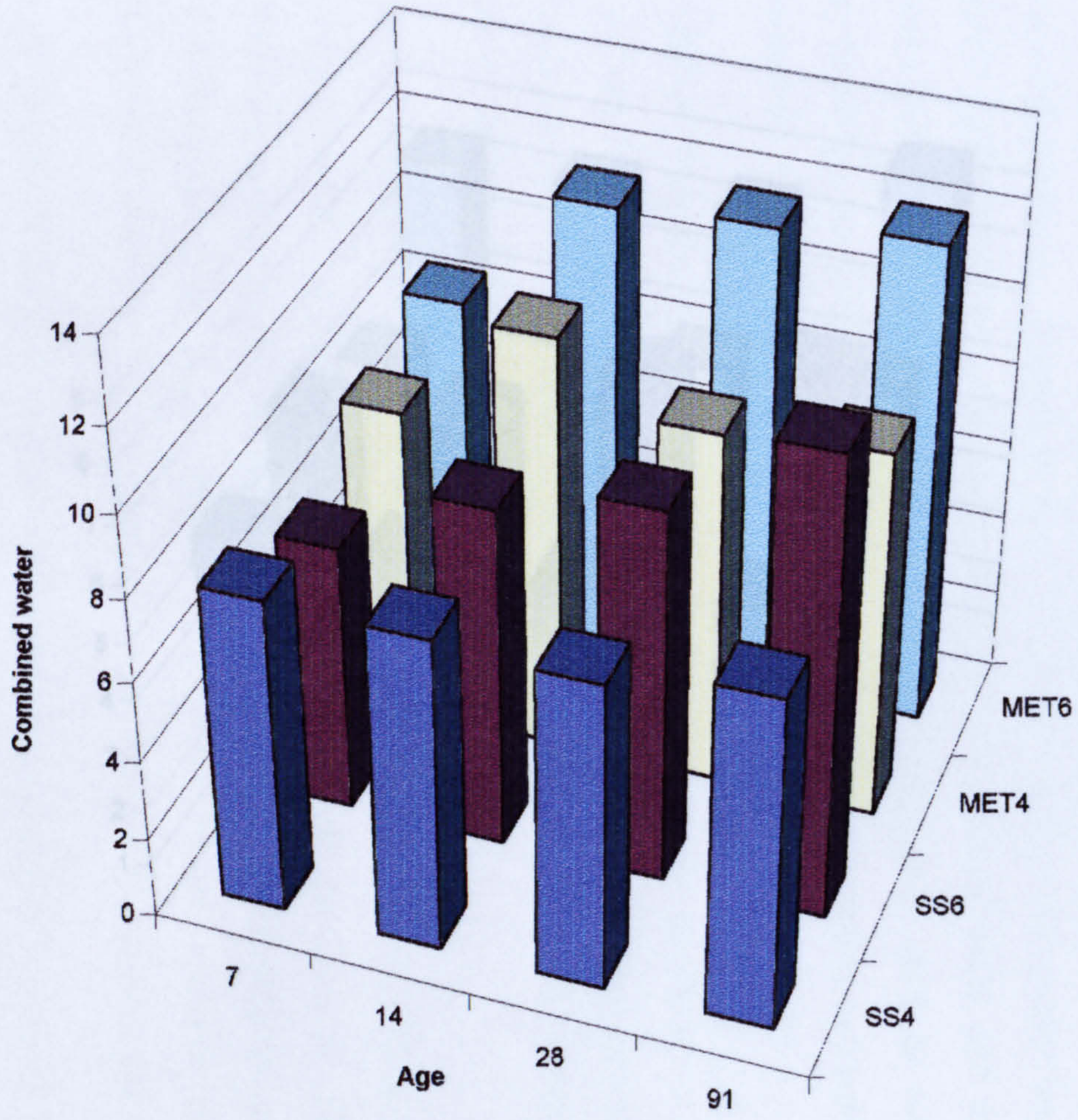

Figure 5.10 Hydration Progress for AAS mixes (water cured)

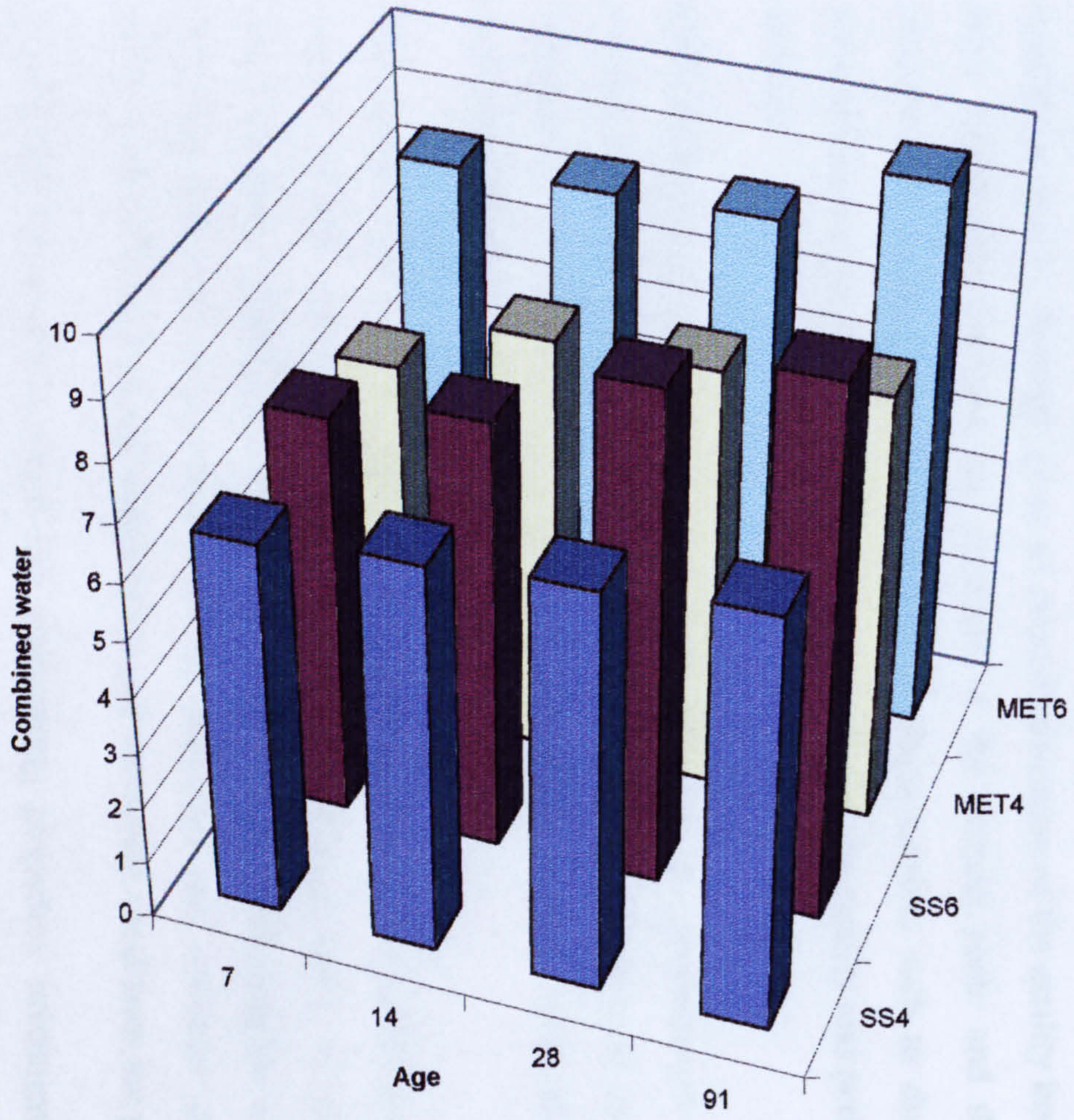

Figure 5.11 Hydration Progress for AAS mixes (autoclave cured)

6. ENGINEERING PROPERTIES

6.1 Introduction

In the field of concrete design and quality control, strength is a generally specified property for the classification of concrete mixtures. Similarly, in construction practice, the strength of cement paste and concrete are commonly considered to be the most valuable properties. Strength gives an overall indication of the quality because of the direct relationship between the structure of the cement paste and the strength. Nevertheless, in many practical cases other characteristics such as durability and permeability may in fact be more critical in assessing the quality and performance of concrete.

Ambient humidity and temperature greatly influence the development of concrete strength from the time it is cast. The knowledge of the effect of environmental condition on the mechanical properties of concrete is essential, to be able to ensure good strength and durability.

This chapter reports on the engineering properties of concrete including compressive strength, tensile strength, flexural strength, dynamic modulus of elasticity and ultrasonic pulse velocity of different concrete mixtures including the control OPC, OPC/Slag and AAS mixes with different activators and activator dosages. The influence of different material composition and the curing conditions are presented.

Correlations developed amongst the engineering properties investigated are also included. Finally, the main conclusions drawn from this investigation are emphasised.

6.2 Compressive Strength

Compressive strength of concrete is the major criterion adopted to evaluate the quality of concrete. It is usually the value that the structural design of a concrete is based on. This section gives details of the investigation carried out to evaluate the compressive strength of OPC, OPC/slag and AAS concrete and the influence of curing on strength development.

6.2.1 Experimental Programme

100x100x100 mm^3 cubes were prepared to determine the compressive strength according to BS 1881:1983. Details of casting and curing were described in section 3.5. The compressive strength is determined by following BS 1881: part 116: 1983. Cubes from the mixtures listed in Table 3.4 were tested in duplicate sets for 1, 3, 7, 28, 90,180 and 365 days, and the average results are reported. All the above-mentioned specimens were cured under water curing (WC) and dry curing (DC), whereas the AAS concrete specimens were cured also by autoclave curing (AUT).

The compressive strength was calculated from the formula bellow:

$$f_c = P/A \qquad (6.1)$$

where:

f_c is compressive strength in N/mm^2 (MPa)

P is maximum load applied to the cube in N

A is the area of concrete surface in mm^2

6.2.2 Results and Discussion

6.2.2.1 Colour of AAS concrete

It was noticed that the crushed slag concrete specimens were initially characterised by a dark green colour, which gradually faded away after being left in air (see Figure 6.1). The colour is attributed to the presence of calcium sulphide in the slag and its slow disappearance is due to oxidation of sulphides in dry air. *Malhotra*, (1983) had previously reported this observation.

6.2.2.2 Early age strength gain

Early strength development is very important in the concrete construction industry. The concern with it arises from economical and practical considerations in terms of formwork removal and progress of work. The early gain of strength depends upon the

concrete temperature, the moisture condition, the mix proportions, and the quality, types and sources of material.

Figure 6.2 and 6.3 show the early strength development under water curing and dry curing respectively for the different mixes. The strength development at early ages is shown numerically in Table 6.1. Analysis of these results is detailed below.

6.2.2.2.1 Effect of slag

It can be noticed from Figure 6.2 that the OPC/ Slag mix SLG60 which incorporates ggbs as replacement for OPC by 60% showed lower gain in strength compared to all the mixes of the same w/c ratio (0.48) and binder content, and is even lower than the OPC mix with the higher w/c ratio (0.55) (CM1). The same can be observed in Figure 6.3. The results in Table 6.1 show that the gain at 7days as a percentage of the 28 days strength as a strength for the SLG60 mix is around 60% while it is 68% for CM1 and 80% for CM2. This slow gain of strength with slag is understandable since slag is a latent reactive material. The overall trend shows potential for gain on the long term due to pozzolanic reaction.

6.2.2.2.2 Effect of the activator dosage

It can be seen in Figure 6.2. that SS6 mix with a dosage of 6% Na_2O achieved higher gain in compressive strength in comparison with all the other mixes. The 28 day compressive strength for SS6 was 79 MPa while it was 51 MPa for CM2 mix and 57.5 MPa for SS4 mix having the dosage of 4% Na_2O. This clearly shows the effect of the Na_2O dosage on the early compressive strength gain. In a similar manner the MET6 mix had higher compressive strength gain (61 MPa at 28 days) in comparison to MET4 (48 MPa at 28 days) which is lower than the control mix CM2. The results in Figure 6.3, representing early strength development under dry curing, show a similar trend and indicate that the AAS mixes having 6% Na_2O gave higher early strength gain than the mixes with 4% Na_2O.

The results in Table 6.1 show the gain in compressive strength at early ages as a percentage of the 28 day strength. Taking 7 day strength gain as an example, these results show CM2 having a gain of 80%, SS6 with 80%, and SS4 with 76% which indicate that the increase in the activator dosage results in an increase in the strength

gain. Similarly MET6 shows a gain at 7 days equal to 88% of the 28 day compressive strength, while MET4 had a gain of 76%.

Wang et al. (1994) Worked on mortars and stated that increasing the dosage within a range between 2-8 Na_2O% increases the strength but they recommended a range of 3-5.5 Na_2O% based on other factors other than strength. The reviewed literature on AAS concrete (*Douglas et al.* 1991; *Gifford and Gillot*, 1996; *Collins and Sanjayan*, 1999) gave variable results with AAS concrete depending on the concrete composition but the compressive strength achieved was comparable to that of OPC control mixes.

6.2.2.2.3 Effect of the activator modulus

Comparing the results of the AAS concrete mixes on the basis of the difference in the silicate modulus of the activator shows that the higher the modulus the higher the compressive strength development. This can be clearly seen from both Figures 6.2 and 6.3. The SS6 achieved higher 28 days strength of 79MPa compared to 61 MPa for MET6 under water curing and 53 MPa, 49.3 MPa respectively under dry curing. Also SS4 achieved 57.5 MPa while MET4 achieved 48 MPa after 28 days of water curing with a similar trend for dry curing.

Wang (1995) had recommended using a waterglass as an activator with a silica modulus M_s in the range 1-1.5 to achieve optimum strength.

The waterglass with low modulus doesn't seem to be widely available which lead some researchers (*Douglas et al.*, 1991; *Collins and Sanjayan*, 1999; *Bakharev et al.*, 2000) to add NaOH to the activator solution to modify the modulus to a lower value.

The effect of the silica modulus comes from the contribution to the strength made by the silica gel. Hence the more silica content the more silica gel but there is a limit dictated by the required alkali content for the activation in relation to the amount of solid fraction of the activator.

6.2.2.3 Long-Term Compressive Strength Development

The long-term strength development of any concrete depends on the continuing presence of moisture for hydration. This is usually achieved by curing to maintain enough moisture for the hydration to progress.

Figure 6.4 presents the long term strength development for the different mixes under water curing conditions which is clearly slower after 28 days. SS6 and MET6 (Na_2O=6%)at later ages achieve the highest strength followed by SS4 and MET4 (Na_2O=4%) and then come CM2 then SLG60 and the lowest strength in CM1. It is worth noting that MET4 and SLG60 concrete strengths started lower than OPC CM2 but they caught up and exceeded the control mix strengths after 90 days. This is attributed to the continuing pozzolanic reaction in slag concrete.

Figure 6.5 shows that under the dry curing condition the strength development at later age slows down and there is even a reduction in strength with time in the case of SS6 and MET6, which clearly shows the detrimental effect of drying on those types of concrete. This will be discussed below.

6.2.2.4 Effect of Dry Curing

It is well known that the lack of curing greatly affects the strength development but the extent of the effect differs among different types of concrete and concreting materials.

Figures 6.6-6.11 clearly show the effect of dry curing on the six mixes having the same w/c ratio of 0.48 and the same binder content. For the AAS mixes the gap is much greater.

Table 6.2 assists in understanding the effect of dry curing where it shows the loss of strength due to dry curing compared to water curing. Taking the 1 year values as an example, it can be seen that while OPC (CM2) and OPC/Slag (SLG60) mixes loose 23% and 27% respectively, the AAS mixes SS4 and SS6 loose 49% and 62% and MET4 and MET6 lose 37%. It seems that the silicate modulus of the sodium silicate activator is a factor in the detrimental effect of drying. AAS concrete with an activator of Ms value of 1.65 are more sensitive to drying than AAS concrete with an activator of Ms value of 1.00.

6.2.2.5 Effect of Accelerated curing (Autoclave)

Some literature reviewed in Chapter 2 recommended accelerated curing for AAS concrete especially with low reactivity solid or waste alkali activators (*Wang*, 1995).

This effect was studied in this investigation by subjecting the AAS concrete mixes to autoclave curing for 16 hours followed by water curing.

Figures 6.8 - 6.11 show that autoclave curing accelerated the strength gain up to 28 days in the case of SS4 and SS6 and then the gain was slower giving very close values to water curing for SS4 and in the case of SS6 mix significantly lower strength. While MET4 and MET6 concrete where the activator used was a dissolved solid with lower M_s, continued to gain strength beyond 180 days for MET4 and beyond 90 days for MET6 eventually giving compressive strength close to the values obtained for water curing.

6.3 Tensile Strength

Concrete in general is known to be weak in tension leading to the use of steel reinforcement in structural concrete. The tensile strength is determined either by a direct tensile test or by indirect tensile tests. The direct tensile strength is difficult to obtain. The indirect tensile strength tests, which are most commonly used, are the splitting cylinder test and the third-point flexural loading test (*Mehta*, 1986). The splitting tensile test will be discussed in this section whilst the flexural test in Section 6.4.

As with compressive strength, the tensile strength of concrete obtained is related to the mix material composition and proportion of ingredients. It is greatly affected by curing conditions.

6.3.1 Experimental Programme

The splitting tensile strength of all mixes was measured using 100 mm Φ x 200 mm long cylinders. The samples were prepared according to BS 1881: part 100: 1983. The curing was done under water curing (WC) and dry curing (DC). The splitting tensile test was performed as described in BS: 1881: part 117: 1983. The specimens were tested in duplicate sets at 7, 28, 90, 180 and 365 days and the average results are reported.

The splitting tensile strength was calculated from the following expression:

$$f_t = 2P/\pi LD \qquad (6.2)$$

where:

f_t is splitting tensile strength (MPa)

P is the failure load in (N)

L is the length of specimen (mm)

D is the diameter of specimen (mm)

6.3.2 Results and Discussion

6.3.2.1 Effect of slag

The results in Figure 6.12 which represent the tensile strength development for the different mixes under the water curing condition, show that the OPC/ Slag mix SLG60 which incorporates ggbs as replacement for OPC by 60% showed lower tensile strength compared to all the mixes of the same w/c ratio (0.48) and binder content, but higher than OPC mix with the higher w/c ratio (0.55) (CM1). This indicates that replacing OPC by 60% with ggbs can produce acceptable value for tensile strength with lower water requirement for the same workability.

6.3.2.2 Effect of activator

The results in Figure 6.12 show that SS6 and MET6 mixes gave the highest values of tensile strength followed by SS4 and CM2 and then MET4 followed by SLG60 and the lowest was CM1.

These results show, as it was also seen from the compressive strength results, that the increase in the activator dosage and the activator modulus in AAS concrete resulted in an increase in tensile strength with continuous water curing.

Figure 6.13 shows that under the dry curing condition the splitting tensile strength development slows and even there is a reduction in strength with time in the case of alkali activated slag mixes. That shows the detrimental effect of drying on those types of concrete.

6.3.2.3 Effect of Dry Curing

It is well known that the lack of curing greatly affects the strength development but the extent of the effect differs among different types of concrete and concreting materials.

Figures 6.14-6.19 clearly show the effect of dry curing on the six mixes having the same w/c ratio of 0.48 and the same binder content. For the AAS mixes the gap is much greater, with the strength decreasing with time.

Table 6.3, which lists all the results, shows the effect of dry curing where it presents the loss of tensile strength due to dry curing compared to water curing. Taking the 1 year values as an example, it can be seen that while OPC (CM2) and OPC/Slag (SLG60) mixes lose 18% and 13% respectively, on the other hand AAS mixes SS4 and SS6 lose 46% and 57% and MET4 and MET6 lose 36% and 44%. This indicates that slag and alkali-activated slag concrete are more sensitive in terms of tensile strength to the type of curing than OPC concrete.

6.4 Flexural Strength

This test programme is included to investigate the flexural strength (Modulus of Rupture / MOR) for AAS concrete in comparison to OPC and OPC/Slag concrete. The effect of curing is also investigated. Details of the test and the results are presented and discussed in this section.

6.4.1 Experimental Programme

The flexural strength of concrete mixes was measured according to BS 1881: Part 118: 1983. 100 mm x 100 mm x 500 mm prisms were used for determining the flexural strength. The prisms that were cast for measuring the dynamic modulus of elasticity were eventually tested for flexural strength at the age of 365 days.

The flexural strength was calculated from the following expression:

$$MOR = PL/(bd^2) \qquad (6.3)$$

where:

MOR Modulus of rupture (MPa)

P maximum total load on beam (N)

L span (mm)

b width of the beam (mm)

d depth of the beam

6.4.2 Results and Discussion

The results presented in Figure 6.20 show that 365-day flexural strength of AAS concrete is comparable to that of OPC concrete. The SS6, MET6 and CM2 give very close values followed by SLG60. MET4, SS4 and CM1 achieving the lowest. The increase in dosage of activator increased the flexural strength this is clear when comparing the results of SS4 to SS6 and MET4 to MET6. While the increase in the silica modulus of the activator, resulted in a slightly lower flexural strength, MET4 had higher flexural strength than SS4 and MET6 had higher flexural strength than SS6.

The Effect of curing is also shown clearly in the test results, where dry curing was more detrimental for AAS concrete.

6.5 Dynamic Modulus of Elasticity

The dynamic modulus of elasticity of concrete is related to the structural stiffness and deformation of concrete, and is highly sensitive to cracking. It is related also to the compressive strength. The results of this test for all the mixes under the WC and DC are presented in this section.

6.5.1 Experimental Programme

The dynamic modulus of elasticity for all mixes was determined according to BS 1881: part 209: 1990. The test was to conduct excitation in the longitudinal mode of vibration on the 100 mm x 100 mm end face of prism with a path length of 500 mm. Duplicate sets of samples were tested at curing ages of 28, 90 180 and 365 days.

The dynamic modulus, E_d (in GPa) of all specimens were calculated based on the following expression:

$$E_d = 4 \eta^2 L^2 \rho 10^{-15} \qquad (6.4)$$

where:

L is the length of the specimen (mm)

η is the fundamental frequency in the longitudinal mode of vibration (Hz)

ρ is the density of the specimen (kg/m^3)

6.5.2 Results and Discussion

6.5.2.1 Effect of Concrete Type

Figure 6.21 shows the results for the dynamic modulus test for all the mixes under the water curing condition, where it shows that SS6 and MET6 achieved the highest values followed by CM2, SLG60, SS4, MET4 and the lowest was for CM1. This shows that replacing OPC by ggbs at the same w/c ratio reduced the dynamic modulus of concrete while it gives higher dynamic modulus when compared with OPC concrete with the same workability level at a higher w/c ratio. The Na_2O content clearly affects the dynamic modulus of AAS concrete as it increases with the increase of the dosage of alkali. The dynamic modulus of all mixes increased with age slightly after 28 days.

6.5.2.2 Effect of Curing

Figures 6.22 and 6.23 show clearly the effect of dry curing in reduction of dynamic modulus of elasticity, which is greater in the case of AAS concrete. This is in agreement with the findings of the strength tests.

6.6 Ultrasonic Pulse Velocity

The velocity of ultrasonic pulses travelling in a solid material depends on the density and elastic properties of that material. Hence this test is performed as a non-destructive test on concrete to study its properties. This test was carried out parallel to the dynamic modulus of elasticity test on the same specimens. The results of this test for all the mixes under the WC and DC are presented in this section.

6.6.1 Experimental Programme

A portable ultrasonic non-destructive indicating test instrument known as PUNDIT was used for the measurement of ultrasonic pulse velocity (UPV) in accordance with BS 1881: part 203: 1986. the measurement was conducted on the 100 mm x 100 mm end face of prism with a length of 500 mm. Duplicate sets of samples were tested at 28, 90 180 and 365 days.

The time taken by the pulsing wave to travel from one longitudinal end of the prism to the other was recorded by means of 54 kHz transducers of 50 mm diameter. The UPV was determined by measuring the time taken for longitudinal vibrations of ultrasonic frequency to travel a known distance through the material and was calculated by the following expression:

$$V = L/T \qquad (6.5)$$

Where:

V is ultrasonic pulse velocity (km/sec)

L is distance travelled by pulse (mm)

T is time taken (μsec).

6.6.2 Results and Discussion

6.6.2.1 Effect of Concrete Type

Figure 6.24 shows the results for the ultrasonic pulse velocity test for all the mixes under water curing condition. The Figure shows that SS6 and MET6 achieved the highest values followed by CM2, SLG60, SS4, MET4 and the lowest is CM1, with the values increasing with age. This shows that replacing OPC by ggbs at the same w/c ratio reduced the UPV of concrete while it gives higher UPV values when compared with OPC concrete with the same workability level at a higher w/c ratio. Increasing Na_2O dosage resulted in an increase in the UPV values.

6.6.2.2 Effect of Curing

Figures 6.25 and 6.26 show clearly the effect of dry curing in on UPV results. This is due to the presence of more voids in dry cured concrete and probable micro cracking due to drying. This test is a good tool to detect cracking and other forms of deterioration in concrete. The effect of dry curing is very clear with AAS concrete with significant reduction in the UPV values obtained by the test.

6.7 Drying Shrinkage

The loss of water from the concrete over time leads to a reduction in volume and is referred to as shrinkage. This shrinkage is represented usually by the length change expressed in microstrains (x 10^{-6}). Drying shrinkage is affected by several factors, among which is the aggregate type and quantity, the w/c ratio, the type of cementitious material, and curing condition prior to drying. This section presents the test carried out and the results obtained for the AAS concrete mixes in comparison with OPC and OPC/Slag mixes. The results are discussed and conclusions derived from the results.

6.7.1 Experimental Programme

Two 75x75x280 mm prisms were prepared for each of the AAS mixes and the control OPC and OPC/Slag mixes. The prisms were cured for 7 days in water in the case of water cured samples. The autoclaved samples were put in water after being removed from the autoclave to complete the 7day curing time. The prisms were then left to dry in the controlled temperature and humidity room described in Chapter 3. The shrinkage was measured using a length comparator in accordance with BS 812: Part 120: 1989. The comparator and a concrete prism are shown in Figure 6.27.

6.7.2 Results and Discussion

The results for drying shrinkage are shown in Figures 6.28 – 6.35. They are presented to show the behaviour of the mixes in terms of drying shrinkage and the effect of the early curing condition on the behaviour of the AAS mixes. Figure 6.28 shows the drying shrinkage cracks in a prism of the SS6 mix that gave the higher drying shrinkage.

6.7.2.1 Drying Shrinkage Development

The development of drying shrinkage with age for the samples cured in water for 7 days prior to drying is shown in Figure 6.29. The replacement of OPC by ggbs gave higher shrinkage compared to the control mix having the same w/c ratio. SLG60 had a shrinkage of 650 microstrain after 182 days compared to 500 micro strain for CM2 control mix in agreement with previous results (*Neville*, 1995). For the AAS concrete mixes increase in the dosage of activator resulted in an increase in drying shrinkage. The SS6 mix exhibited the highest drying shrinkage up to 970 microstrain at 182 days followed by the MET6 mix with 700 micro strain at the same age. The SS4 and MET4 mixes showed the lowest drying shrinkage. The silica modulus for the activator played an effective role in increasing the drying shrinkage of the SS6 mix as the high modulus (M_s =1.65) contributed in the production of larger amounts of the silica or silica rich gel during the hydration process compared to the MET6 with the same Na_2O %.

High shrinkage with AAS concrete has been reported by several researchers, (*Anderson, 1987*), (*Douglas et al., 1992*), (*Kutti et al, 1992*), (*Wang et al., 1995*), (*Collins and Sanjayan*, 1999). All were using one activator at a time and recommended controlling the shrinkage by changes in the mix properties. Looking at some the results as an example; *Wang*, (1991) reported values of shrinkage for AAS concrete around 600 microstrains. *Douglas et al* used an activator with an Ms = 1.47 at 6.8 % Na_2O dosage in AAS concrete with w/c = 0.48 and achieved 980 microstrain at 224 days. *Collins and Sanjayan,(2000)* found a shrinkage of 1700 microstrains after 180 days for AAS concrete using an activator with M_s = 0.75 and 5.4 % Na_2O but they had started drying immediately when demoulded after 24 hours.

The results presented in this investigation show that drying shrinkage can be reduced to a level close to that of OPC with the use of the lower dosage and lower modulus of the alkali activator.

6.7.2.2 Effect of Autoclave Curing

The use of autoclave accelerated curing reduced the drying shrinkage for the AAS mixes. This can be clearly seen in Figures 6.30 and 6.31 especially with the high activator dosage in SS6 and MET6 mixes. Figure 6.32 shows the values of drying shrinkage for the different mixes at 182 days of exposure where the distinction between the several mixes and the effect of curing is shown. The effect of autoclave curing in reduction of drying shrinkage with OPC concrete and paste has been reported by *Soroka.*(1979). In the present investigation it is confirmed to be a useful tool to overcome the problem of drying shrinkage associated with AAS concrete. The effect of autoclave curing on drying shrinkage might be due to the formation of more crystalline products of hydration which undergo less shrinkage when losing moisture.

6.7.2.3 Relation between Drying Shrinkage and Mass Loss

Figures 6.33-6.35 show the relation between the mass loss and drying shrinkage. It is noted that some loss of moisture happens at the start without causing any shrinkage, because the moisture is lost from the capillary pores first, causing little shrinkage. Subsequently when the water starts leaving the gel pores where higher shrinkage occurs. Figure 6.33 demonstrate that CM2 and SLG60 behave similarly in that the slope of the line is slightly higher in the case of SLG60 where the drying shrinkage is

higher. Figure 6.34 indicate that the SS6 mix exhibits higher shrinkage very early and the slope is higher compared to the CM2 mix, whereas the SS4 mix starts drying later than the CM2 and have a lower slope. Figure 6.35 shows that the MET6 mix shows higher shrinkage and the slope is higher compared to CM2 mix, while the MET4 mix starts drying later than the CM2 and have a lower slope.

6.8 Relationship Amongst Engineering Properties

This section presents an attempt made to link engineering properties with each other. The relationships are empirical in nature and have certain limitations because a number of factors including binder type, w/c ratio, age and curing affect the relationships. However, the relationships do provide some idea of development of the properties with age. The detailed descriptions of the relationships developed in this investigation are presented below.

6.8.1 Relationship Between Compressive and Tensile Strength

Compressive and tensile strengths of concrete are closely related but there is no direct proportionality. A number of empirical formulae connecting f_t and f_c have been suggested, many of them of the type:

$$f_t = \mathrm{k}(f_c)^{\mathrm{n}} \qquad (6.6)$$

Where k and n are coefficients. Values of n between 0.5 and 0.75 (*Neville*, 1995)

The regression results are shown in Figures 6.36, 6.37. The formulas reached are as follows:

$$f_t = 0.054\,(f_c)^{1.06} \qquad (\mathrm{OPC}) \qquad (6.7)$$

$R^2 = 0.8761$

$$f_t = 0.45\,(f_c)^{0.52} \qquad (\mathrm{AAS}, (\mathrm{WC})) \qquad (6.8)$$

$R^2 = 0.9377$

$$f_t = 0.76\,(f_c)^{033} \qquad (\text{AAS , (DC)}) \qquad (6.9)$$

$R^2 = 0.17$

It is clear from Figure 6.36 that there is a relationship between compressive strength and the tensile strength as the tensile strength increases with the increase in strength. The relations arrived at are reasonable for water curing but the dry curing causes a lot of variation in results and the equation arrived at has a lower correlation factor.

6.8.2 Relationship Between Compressive Strength and Dynamic Modulus of Elasticity

The modulus of elasticity is dependent on the compressive strength of concrete. It is convenient to be able to estimate the dynamic modulus of a particular type of concrete from the knowledge of its compressive strength. Two basic forms of equations are generally accepted to adequately describe the relationship between dynamic modulus of elasticity and compressive strength.

$$E_d = \mathrm{k}(f_c)^{\mathrm{n}} \qquad (6.10)$$

$$E_d = l + mf_c \qquad (6.11)$$

Where *k*, *l*, *n* and *m* are coefficients.

The dynamic modulus values of concrete mixes have been plotted against their respective compressive strength values as shown in Figures 6.38. The regression equations for these systems are as follows.

$$E_d = 5.3(f_c)^{0.54} \qquad (\text{OPC}) \qquad (6.12)$$

$R^2 = 0.9134$

$$E_d = 28.3(f_c)^{0.11} \qquad \text{(AAS)} \qquad (6.13)$$

$R^2 = 0.6071$

The relation between compressive strength and the dynamic modulus of elasticity is known, as the strength increases the dynamic modulus increases. The equation show reasonably correlation with OPC while it is more variable in case of AAS.

6.8.3 Relationship Between Compressive Strength and Ultrasonic Pulse Velocity

Generally as the compressive strength of concrete increases the UPV increases. The compactness of strong concrete and the lower volume of voids and cracks result in higher pulse velocity. In an attempt to formulate an equation describing this relation ultrasonic pulse velocity values of concrete plotted against compressive strength values at various ages are presented in Figure 6.39. This relation was presented in *Neville* (1995) in a plotting produced based on the work of *Sturrup et al.* (1984). These results were also plotted adjacent to the results of this investigation as a comparison.

The relationship between pulse velocity, V (Km/sec), and compressive strength, f_c (MPa) fitted expressions as follows:

$$V = 2.52(f_c)^{0.15} \qquad \text{(OPC)} \qquad (6.14)$$

$R^2 = 0.3$

$$V = 3.8(f_c)^{0.054} \qquad \text{(AAS (WC))} \qquad (6.15)$$

$R^2 = 0.56$

$$V = 1.076(f_c)^{0.035} \qquad \text{(AAS (DC))} \qquad (6.15)$$

$R^2 = 0.65$

The equations obtained have good correlation with OPC concrete but the correlation coefficient for AAS is lower. The variation between the water cured and dry cured

sets of results is probably due to difference in the condition of the prisms at the time of testing whether dry or moist in agreement with *Sturrup et al.* (1984).

6.8.4 Relationship between compressive strength and Hydration Progress

The study of the hydration process in chapter 5 presented TGA test results for AAS pastes. These results showed an increase in hydration, measured in terms of combined water, with age. The results for the AAS mixes were plotted in conjunction with the compressive strength. The trends are shown in Figure 6.40. The results show comparable trend as the compressive strength increases with age and with the progress in hydration. This as discussed earlier was clearer in the case of the pastes having an activator dosage of 6% Na2O while the pastes with lower dosage showed no significant chang in the amount of combined water in comparison with the increase in compressive strength.

6.9 Conclusions

The main conclusions drawn from the investigation of engineering properties of AAS concrete and OPC and OPC/Slag blended concrete are summarised as follows:

- AAS concrete can achieve high strength in comparison with OPC concrete.
- Increasing the Na_2O content as a percentage of slag results in an increase in strength
- Using a waterglass with higher silica modulus in AAS concrete increases the strength compared with the activator with lower modulus when the Na_2O dosage is similar.
- Accelerated curing (autoclave) increases the initial gain of strength in AAS concrete but eventually giving results close to water curing with long term. It is more effective with the solid activator.

- The AAS concrete results of dynamic modulus of elasticity and ultrasonic pulse velocity are comparable to OPC concrete. They demonstrated similar patterns to compressive strength and are affected by curing in a similar manner
- Replacing OPC by ggbs by 60 % can achieve a 40 MPa compressive strength with a lower water requirement than the OPC concrete of the same grade.
- The slag/OPC mix exhibited higher drying shrinkage in comparison with the OPC mix having the same w/c.
- AAS concrete with 6% Na_2O exhibited high drying shrinkage compared to the OPC concrete and the AAS concrete with 4% Na_2O.
- Using a waterglass activator with Ms = 1.65 and 6% Na2O resulted in the highest drying shrinkage because of the larger amount of silica gel formed in the hydration process.
- Autoclave curing of AAS concrete reduces the drying shrinkage as it causes the formation of products of hydration which are more crystalline.

Table 6.1 Compressive strength development of different mixes at early ages (water cured)

Concrete Mixes	Age days	Compressive Strength MPa	Percentage of 28 day strength
CM1	1	7.40	19.0
	3	17.70	45.40
	7	26.45	67.80
	14	31.40	80.0
CM2	1	11.50	22.60
	3	28.70	56.30
	7	40.80	80.0
	14	45.80	90.0
SLG60	1	4.15	12.0
	3	12.90	34.80
	7	22.45	60.70
	14	30.30	81.90
SS4	1	6.20	10.80
	3	31.25	54.30
	7	43.30	76.20
	14	51.10	88.80
SS6	1	15.90	20
	3	49.30	62.50
	7	63.10	80.0
	14	72.65	92.0
MET4	1	11.05	23.10
	3	29.40	61.40
	7	36.25	75.70
	14	42.30	88.40
MET6	1	11.90	19.60
	3	44.50	73.40
	7	53.30	88.0
	14	56.70	93.50

Table 6.2 Effect of dry curing on compressive strength development of different mixes

Concrete Mixes	Age days	Compressive Strength MPa		Percentage Loss of strength
		WC	DC	
CM2	28	50.90	45.30	11.0
	91	52.35	46.0	12.13
	182	54.30	46.40	14.55
	365	57.50	44.0	23.48
SLG60	28	37.0	30.80	16.76
	91	43.35	32.50	25.03
	182	45.20	33.20	26.55
	365	47.65	34.70	27.18
SS4	28	57.55	45.55	20.85
	91	71.0	46.20	34.93
	182	70.60	41.05	41.86
	365	69.10	35.25	48.99
SS6	28	78.90	52.70	33.21
	91	85.10	43.35	49.06
	182	95.0	42.20	55.58
	365	96.0	36.0	62.5
MET4	28	47.85	41.15	14.0
	91	50.0	41.70	16.60
	182	56.75	42.50	25.11
	365	62.70	39.30	37.32
MET6	28	60.60	49.30	18.65
	91	79.40	58.60	26.20
	182	82.85	53.65	35.24
	365	89.15	56.20	36.96

Table 6.3 Effect of dry curing on tensile strength development of different mixes

Concrete Mixes	Age days	Splitting Tensile Strength MPa		Percentage Loss of strength
		WC	DC	
CM2	7	3.25	2.70	16.92
	14	3.44	2.86	16.86
	28	3.69	2.97	19.51
	91	3.80	3.0	21.05
	182	3.88	3.07	20.88
	365	4.01	3.30	17.71
SLG60	7	2.22	1.99	14.41
	14	2.29	2.10	8.30
	28	2.42	2.11	12.81
	91	2.71	2.23	17.71
	182	2.83	2.10	25.80
	365	3.59	2.70	24.79
SS4	7	3.10	2.76	10.97
	14	3.57	2.93	17.93
	28	3.90	2.96	24.10
	91	4.13	2.42	41.40
	182	4.14	2.35	43.24
	365	4.10	2.20	46.34
SS6	7	3.79	3.71	2.11
	14	4.11	2.71	34.06
	28	4.46	2.70	39.46
	91	4.63	2.51	45.79
	182	5.02	2.51	50.0
	365	5.28	2.28	56.82
MET4	7	2.93	2.70	7.85
	14	3.27	2.86	12.54
	28	3.40	3.02	11.18
	91	3.62	2.89	20.17
	182	3.82	2.83	25.92
	365	3.85	2.45	36.36
MET6	7	3.62	2.90	19.89
	14	3.72	2.99	19.62
	28	3.74	3.08	17.65
	91	3.97	2.77	30.23
	182	4.44	2.57	42.12
	365	4.66	2.60	44.21

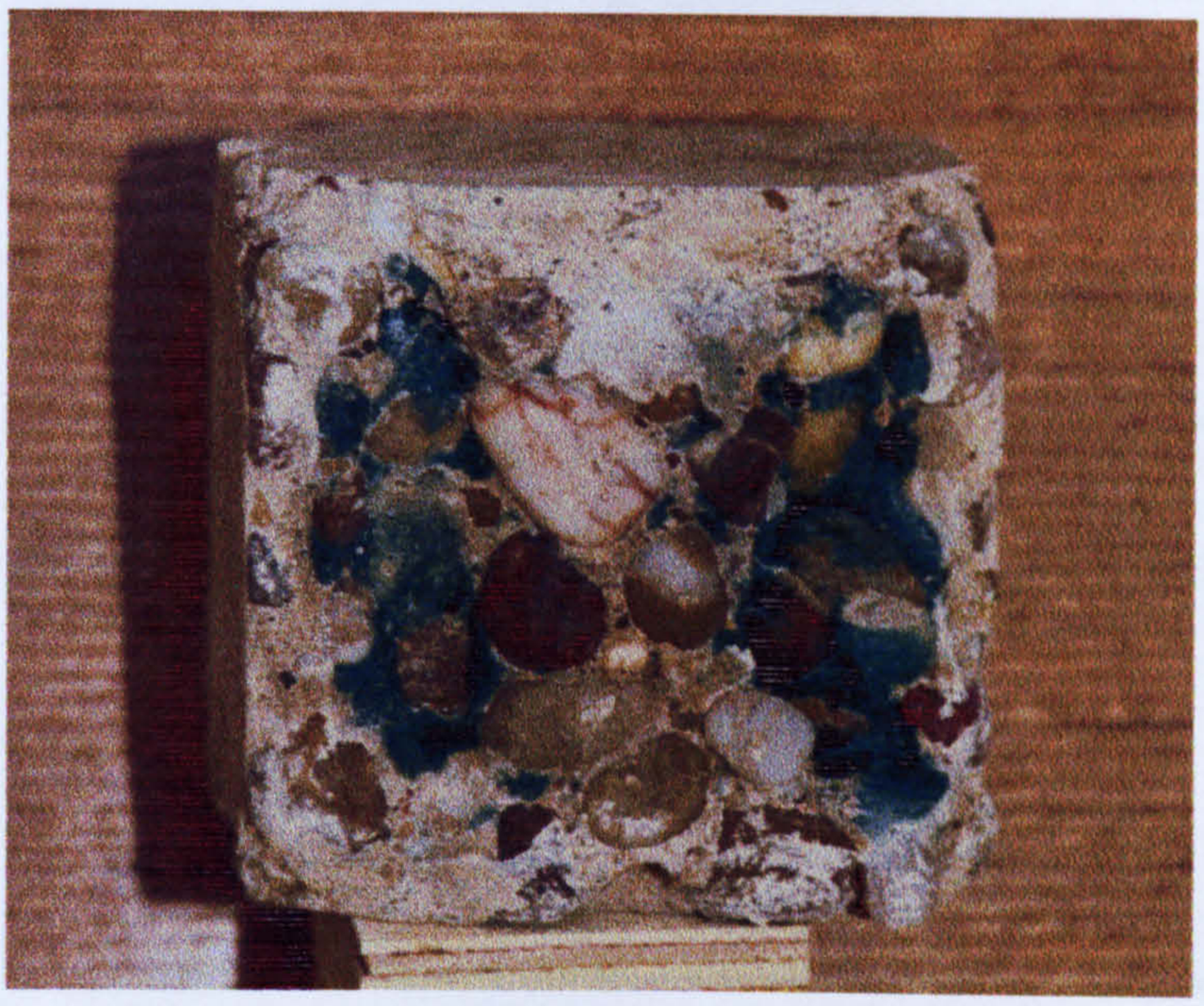

(a)

(b)

Figure 6.1 Colour of AAS Concrete

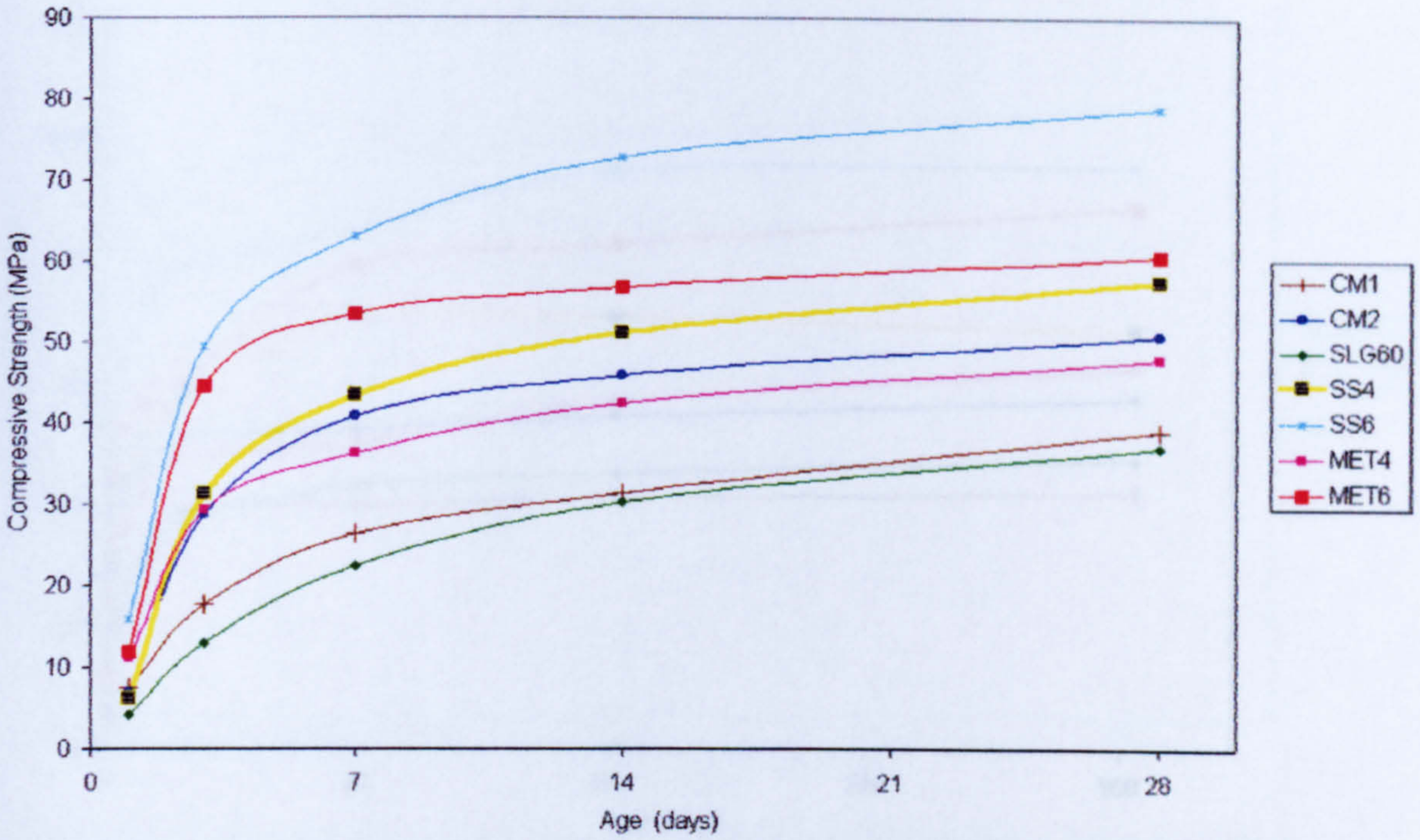

Figure 6.2 Early-Age Compressive Strength Development for the Different Mixes under Water Curing Condition

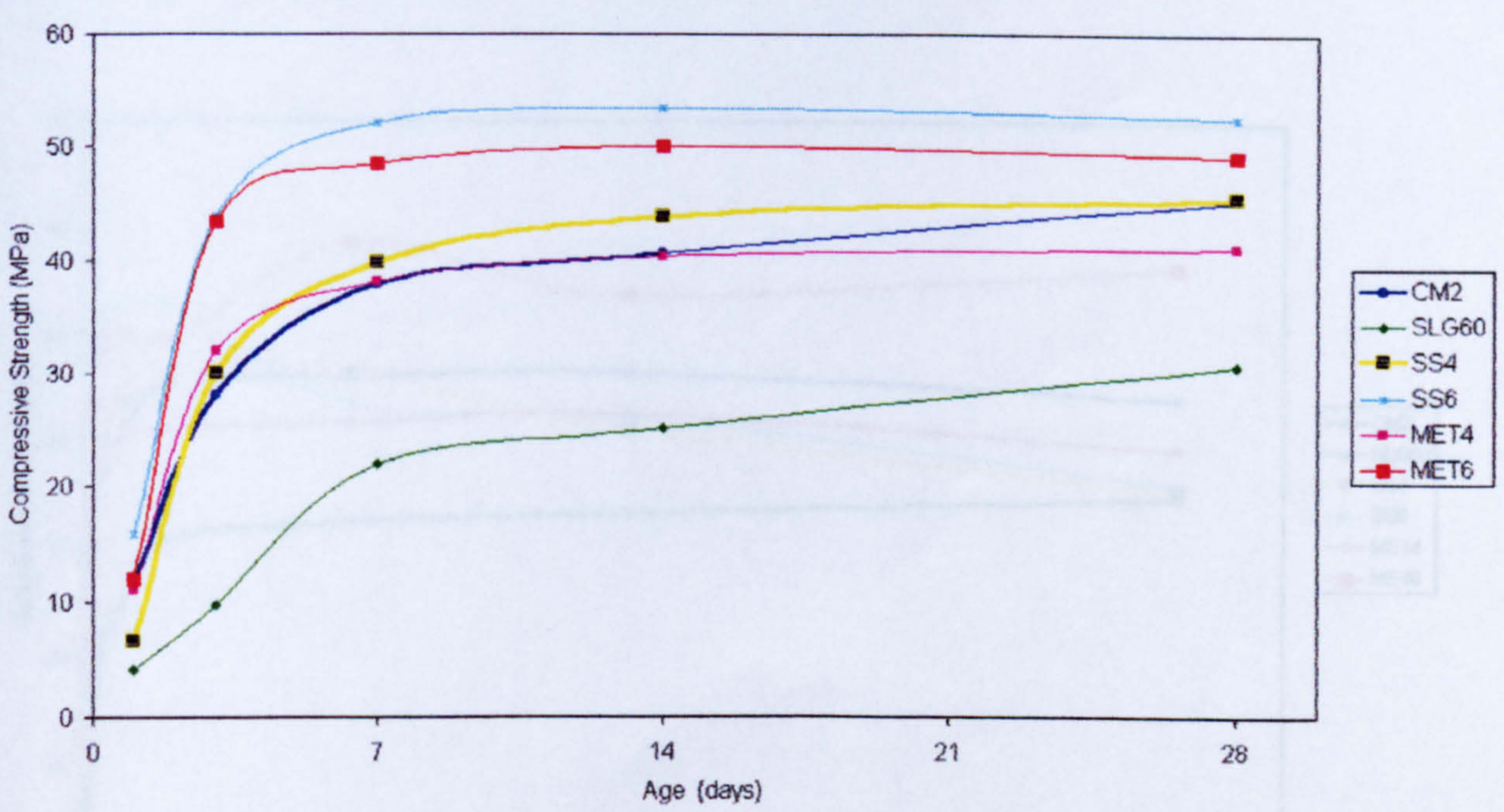

Figure 6.3 Early-Age Compressive Strength Development for the Different Mixes under Dry Curing Condition

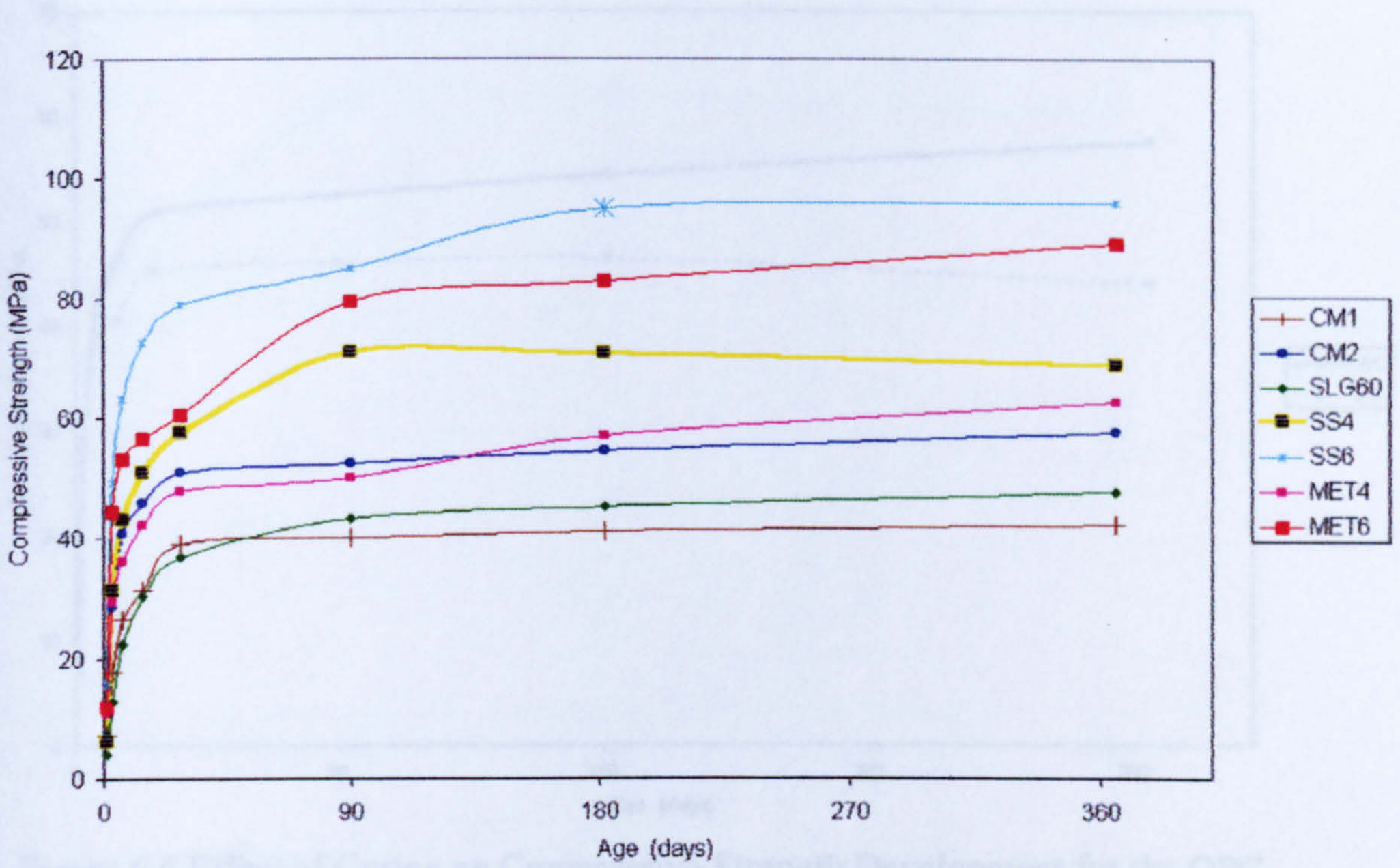

Figure 6.4 Long Term Compressive Strength Development for the Different Mixes under Water Curing Condition

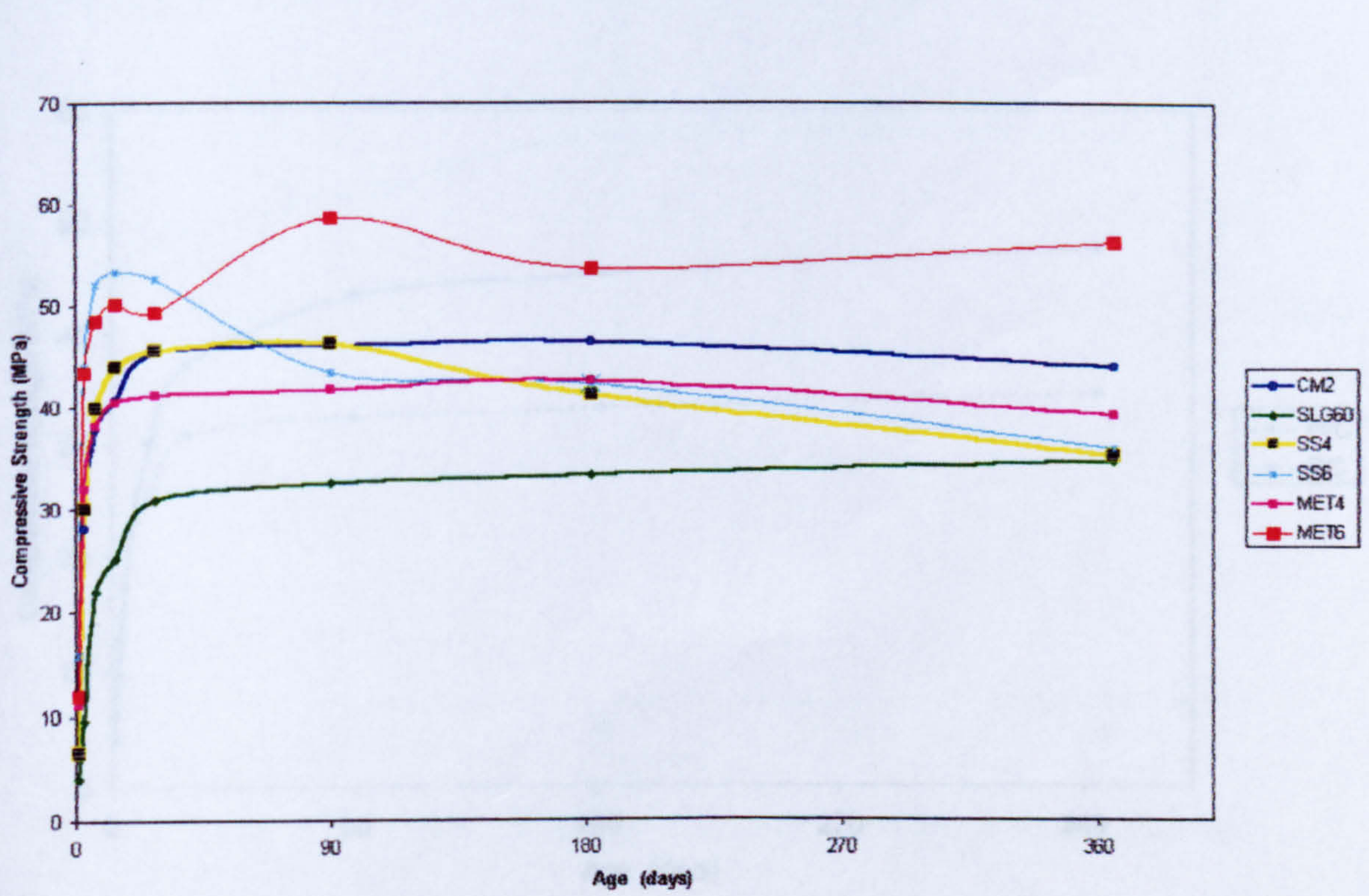

Figure 6.5 Long Term Compressive Strength Development for the Different Mixes under Dry Curing Condition

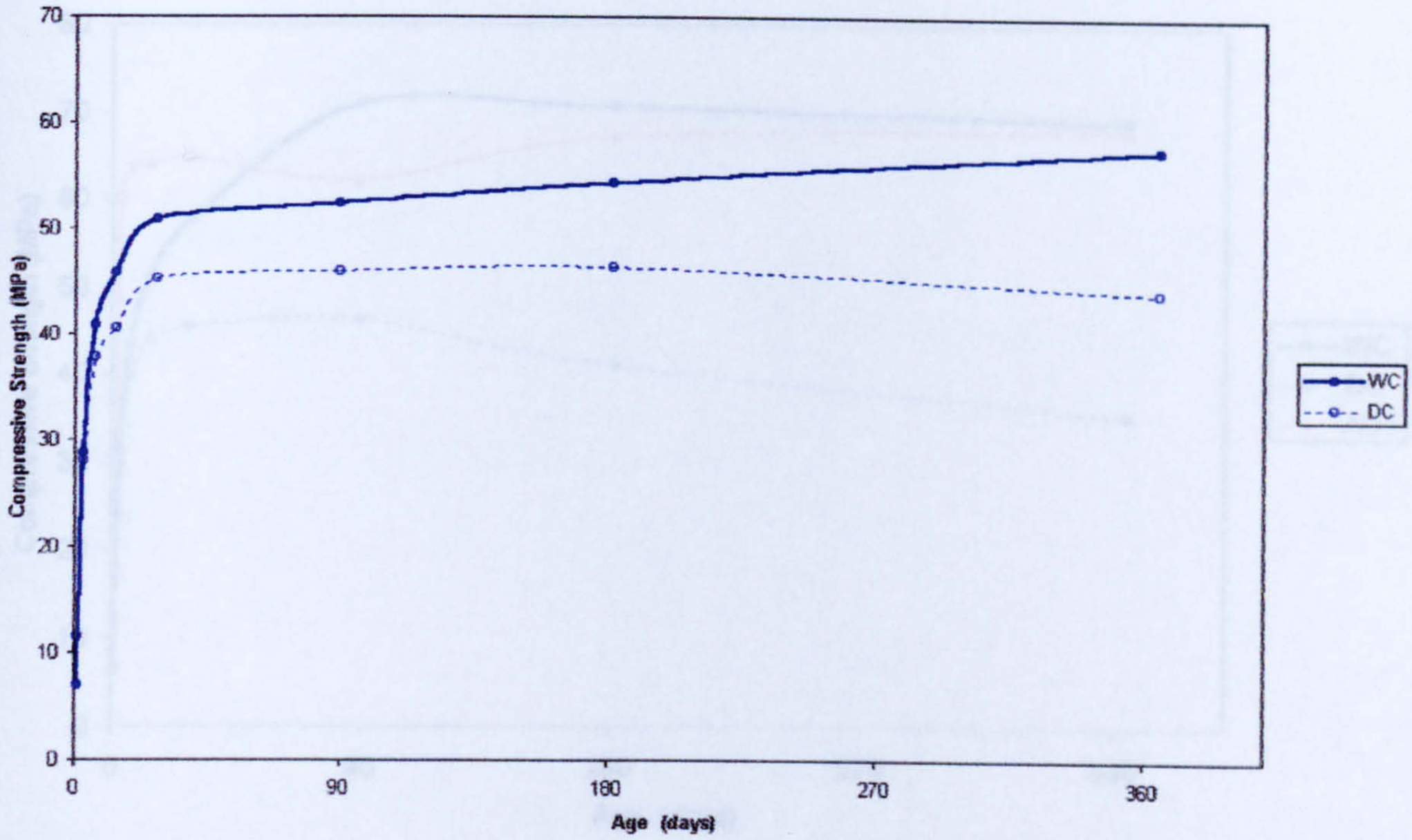

Figure 6.6 Effect of Curing on Compressive Strength Development for the OPC Control Mix (CM2)

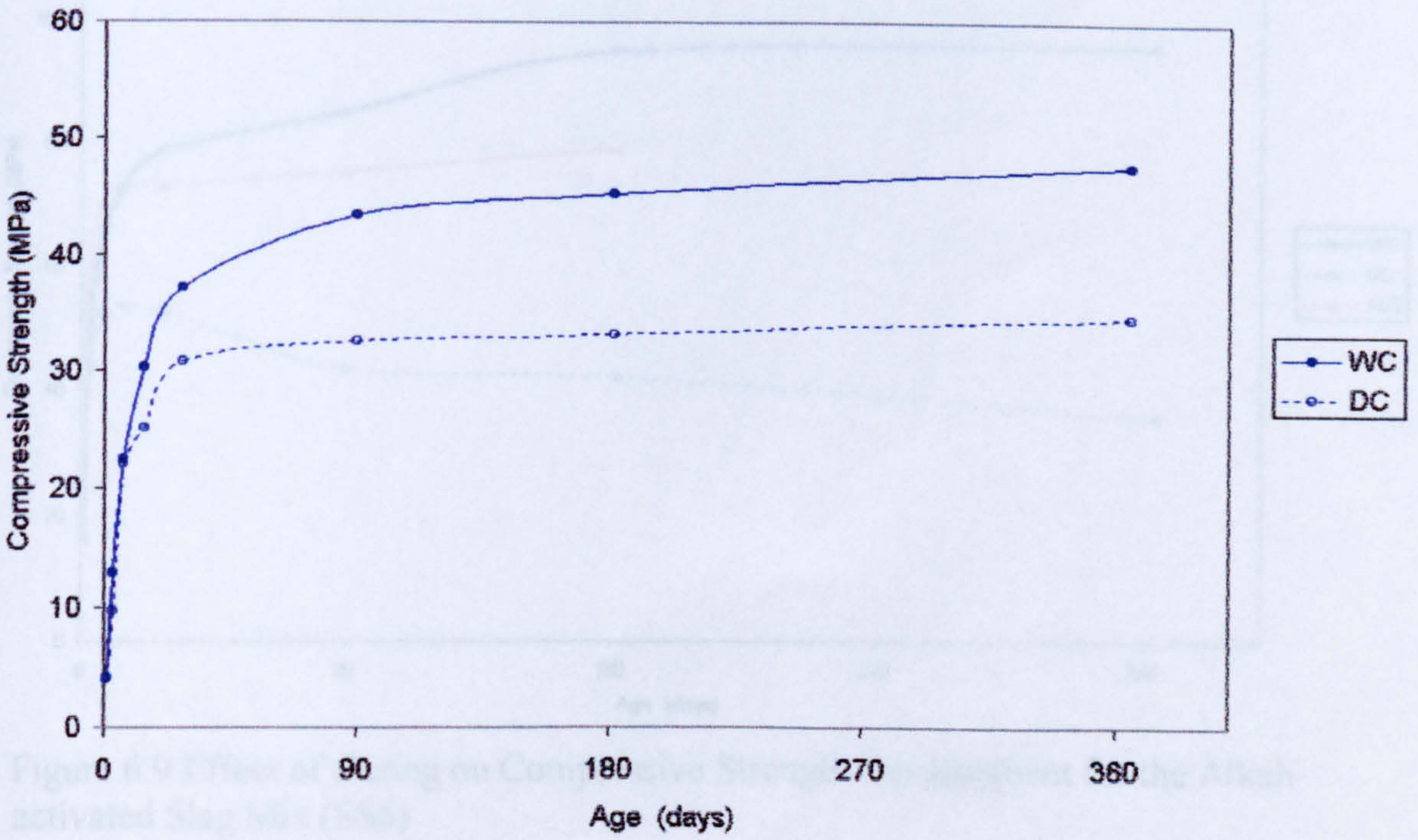

Figure 6.7 Effect of Curing on Compressive Strength Development for the Slag/OPC Mix (SLG60)

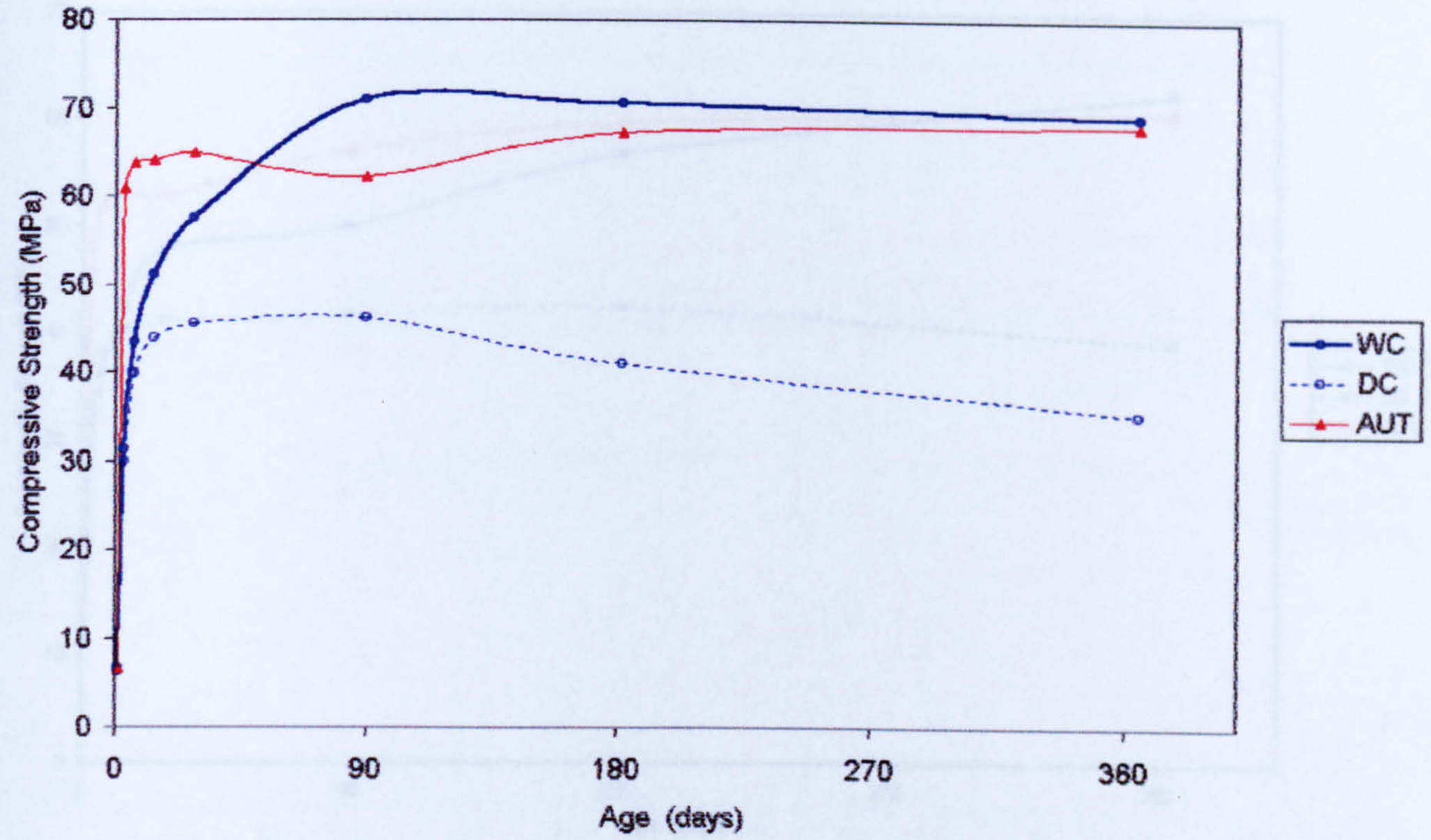

Figure 6.8 Effect of Curing on Compressive Strength Development for the Alkali-activated Slag Mix (SS4)

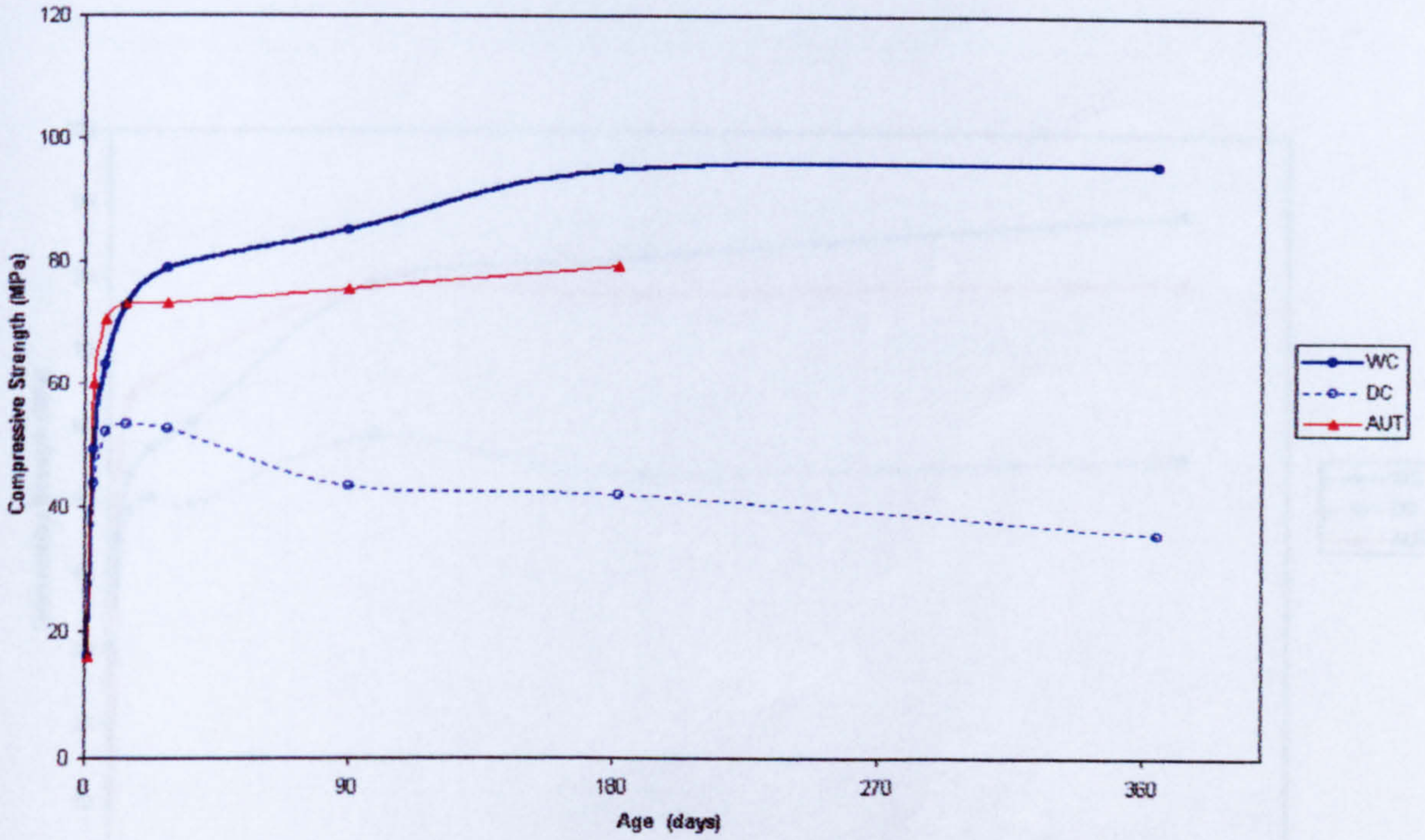

Figure 6.9 Effect of Curing on Compressive Strength Development for the Alkali-activated Slag Mix (SS6)

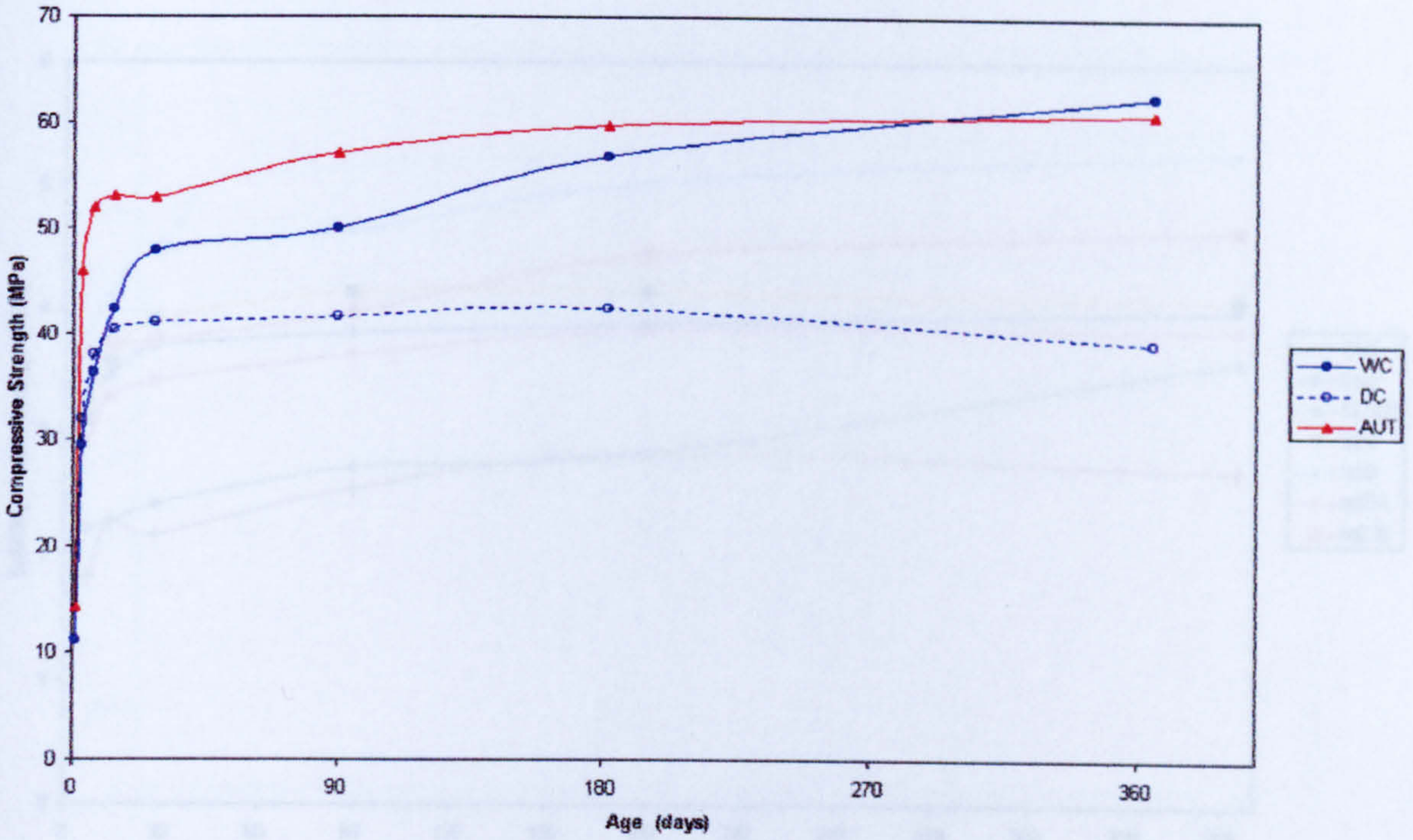

Figure 6.10 Effect of Curing on Compressive Strength Development for the Alkali-activated Slag Mix (MET4)

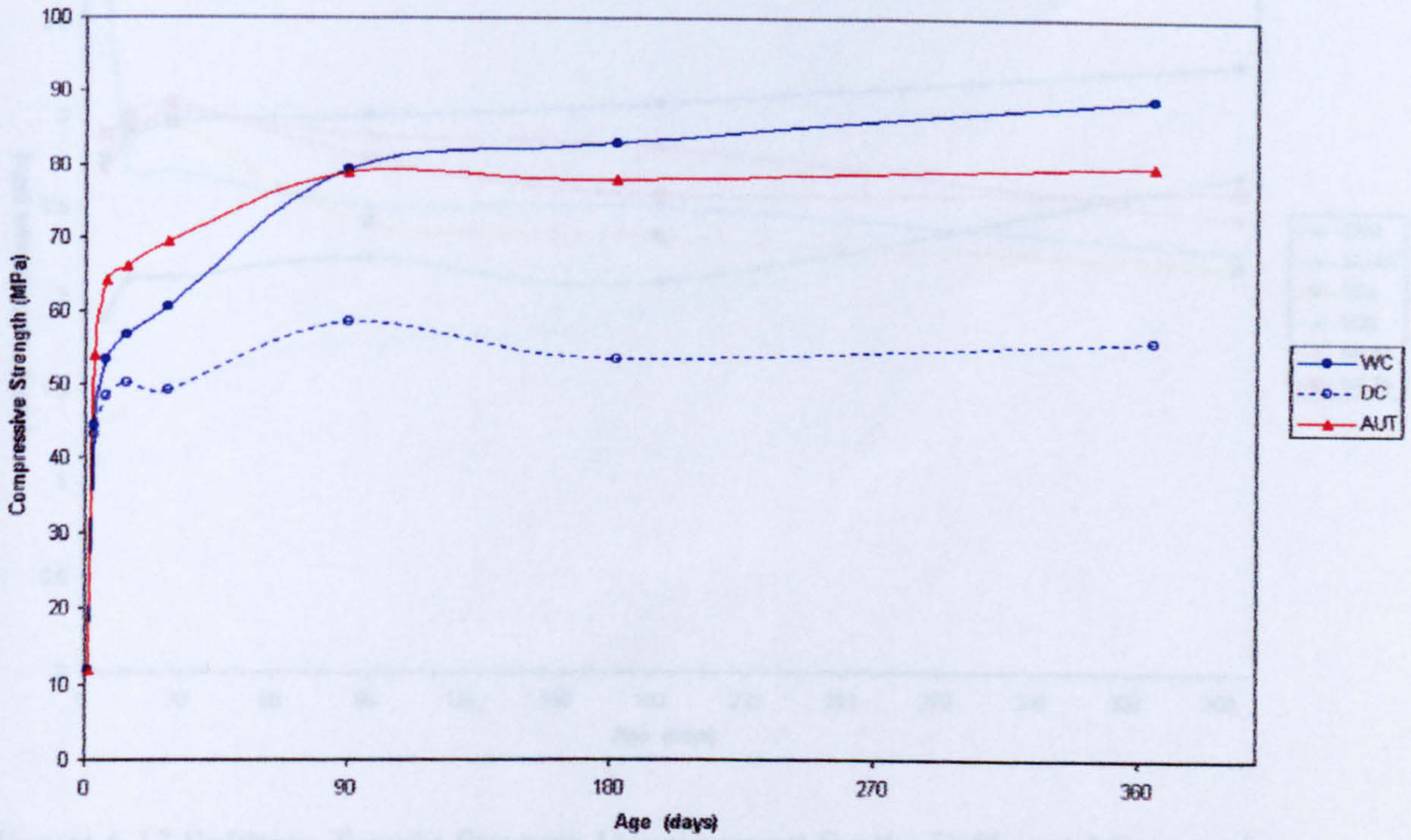

Figure 6.11 Effect of Curing on Compressive Strength Development for the Alkali-activated Slag Mix (MET6)

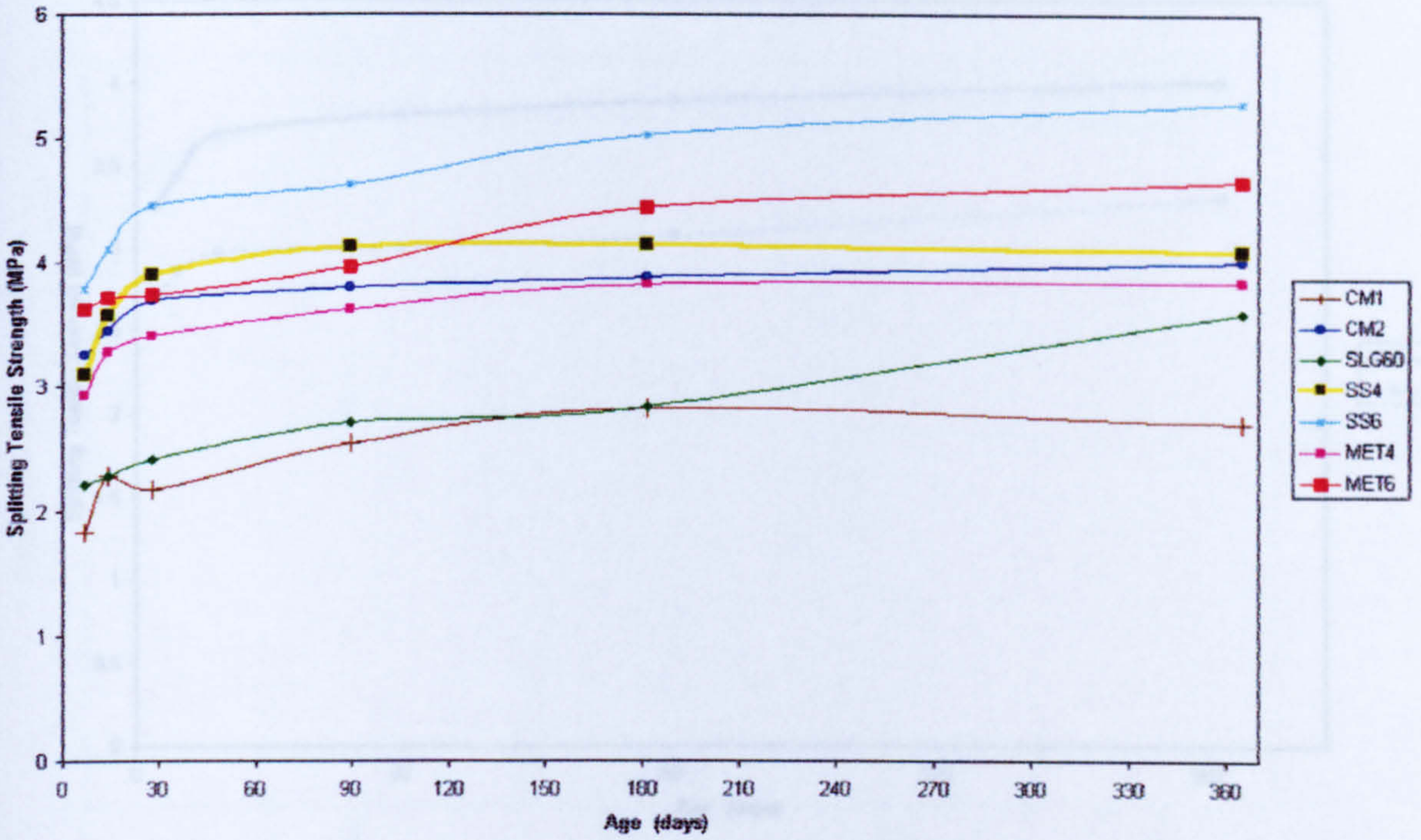

Figure 6.12 Splitting Strength Development for the Different Mixes under Water Curing Condition

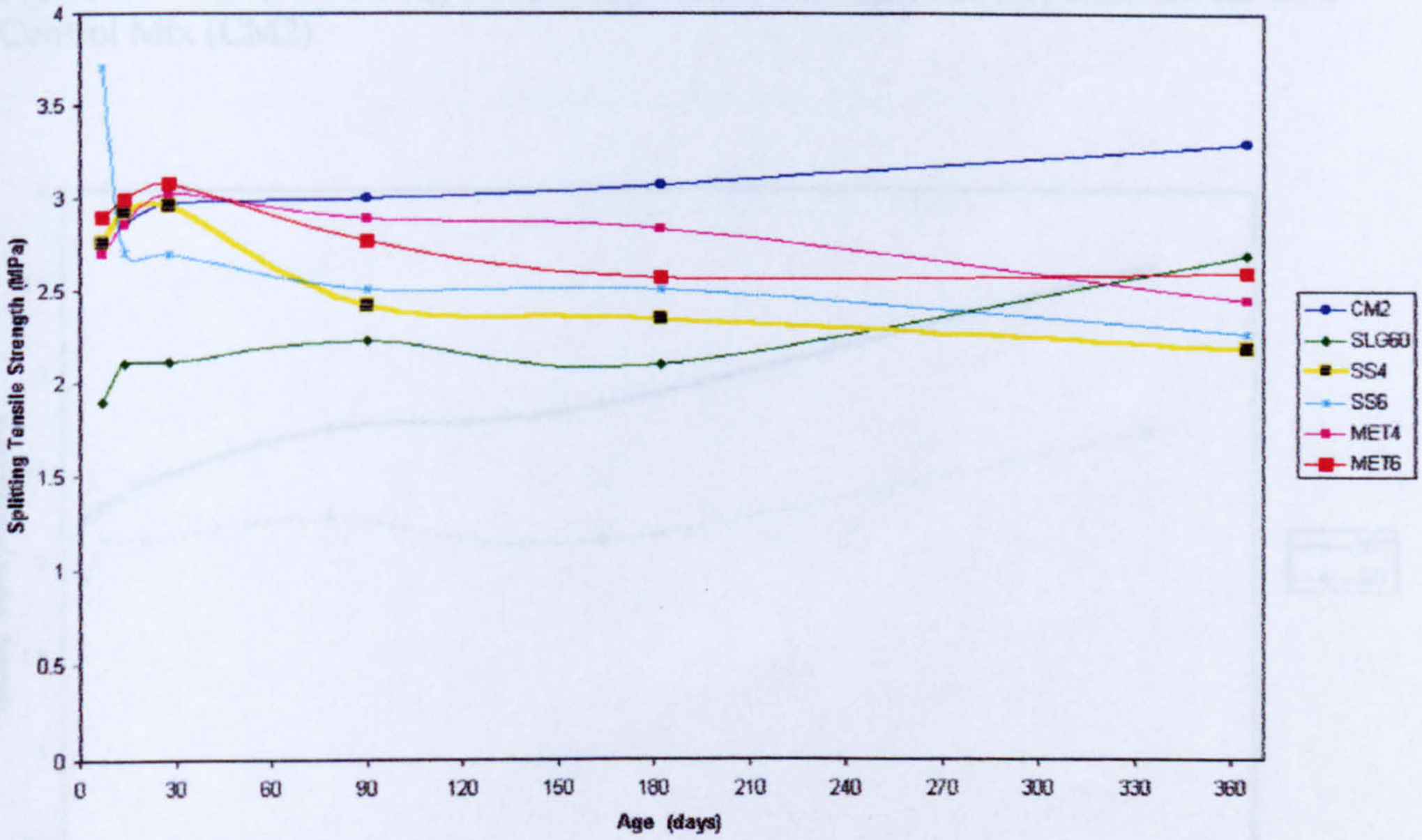

Figure 6.13 Splitting Tensile Strength Development for the Different Mixes under Dry Curing Condition

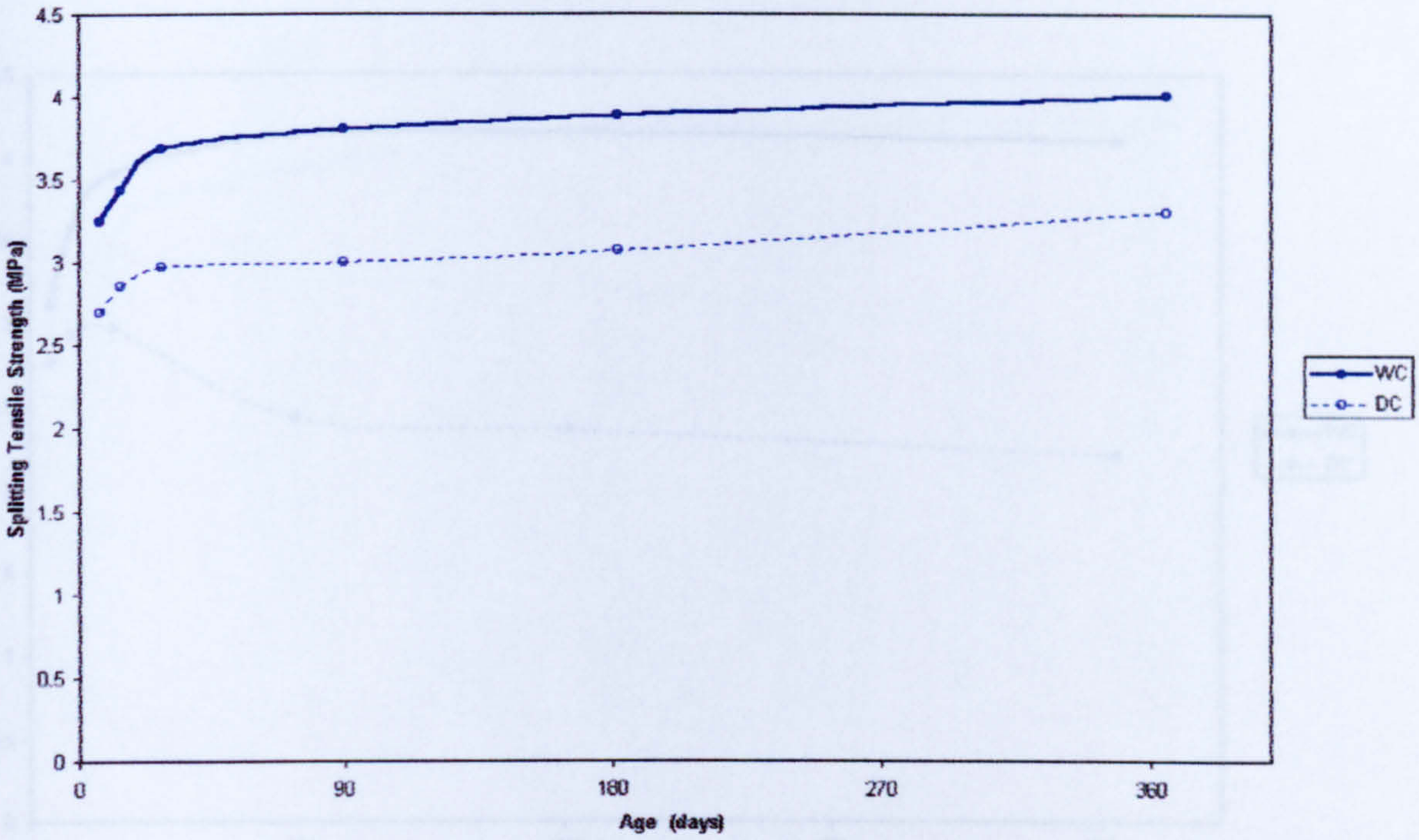

Figure 6.14 Effect of Curing on Splitting Tensile Strength Development for the OPC Control Mix (CM2)

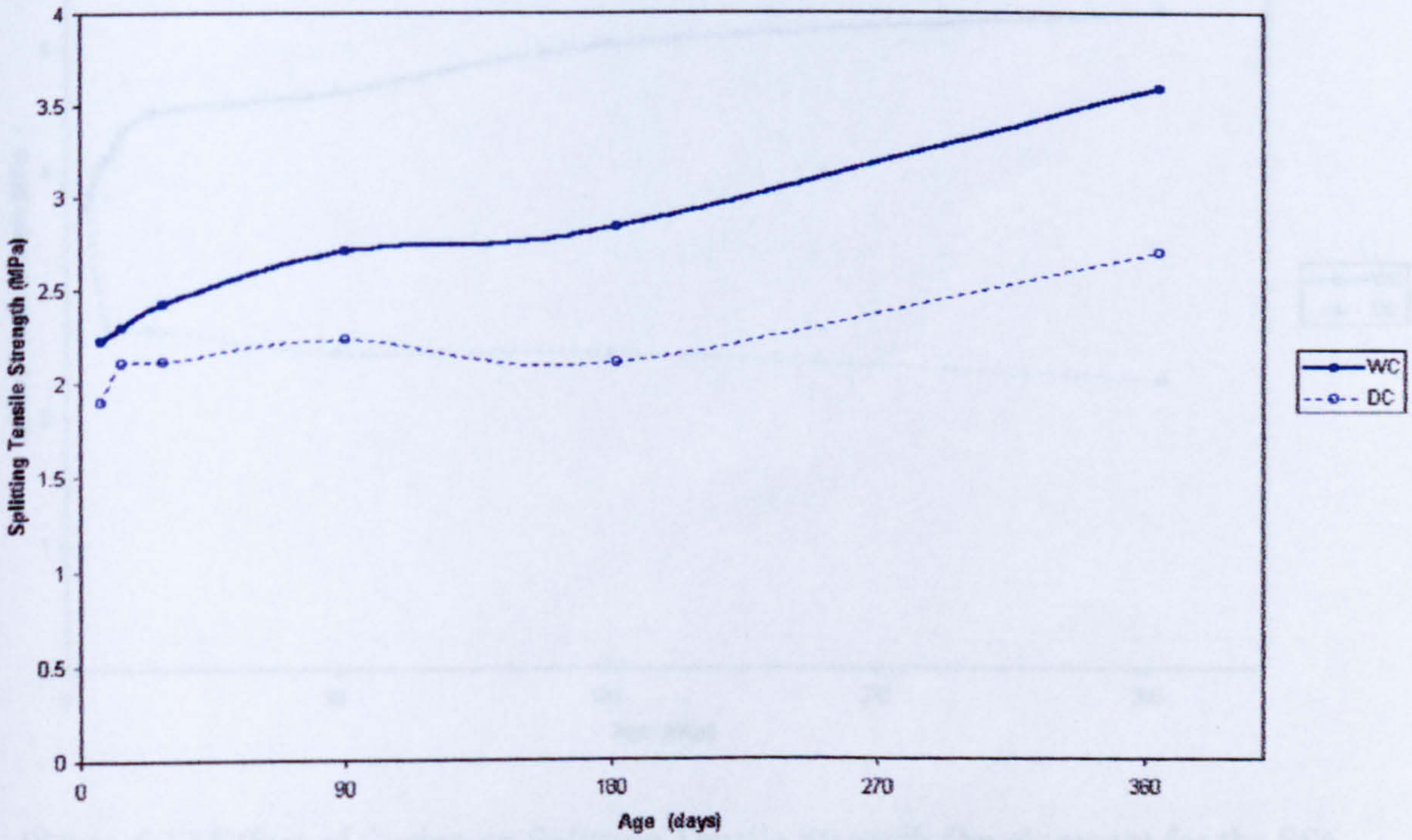

Figure 6.15 Effect of Curing on Splitting Tensile Strength Development for the *SLG60 mix*

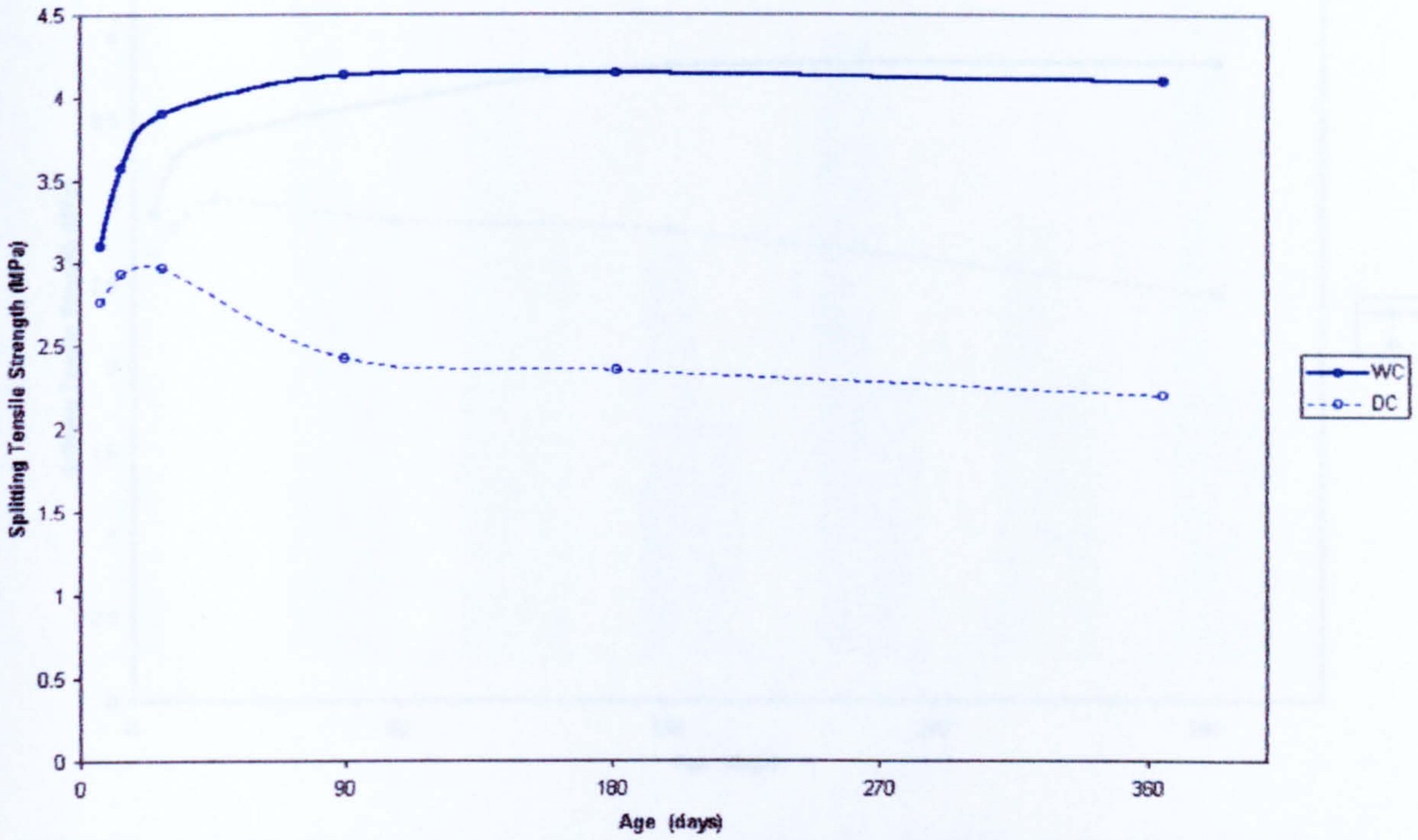

Figure 6.16 Effect of Curing on Splitting Tensile Strength Development for the SS4 mix

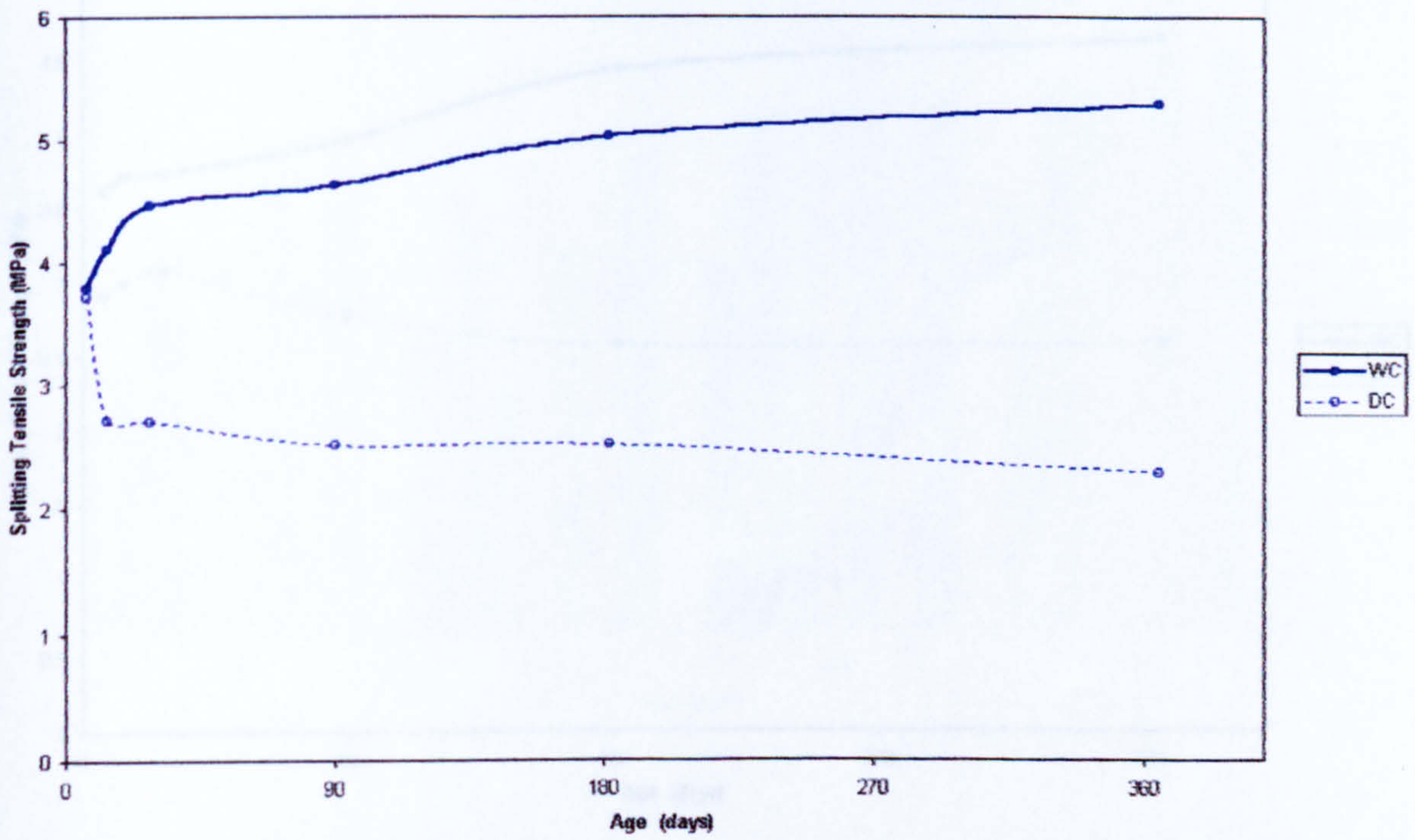

Figure 6.17 Effect of Curing on Splitting Tensile Strength Development for the SS6 mix

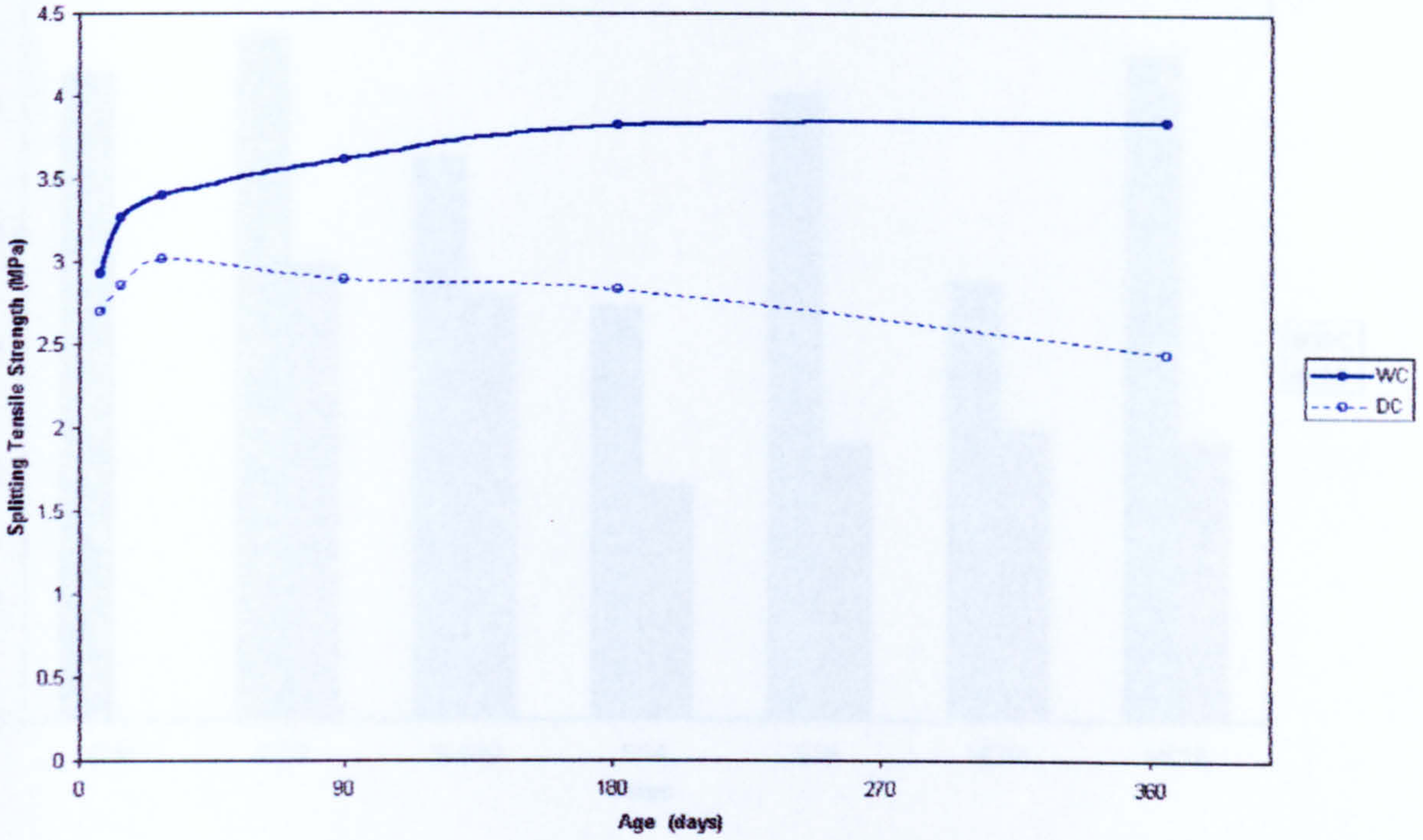

Figure 6.18 Effect of Curing on Splitting Tensile Strength Development for the MET4 mix

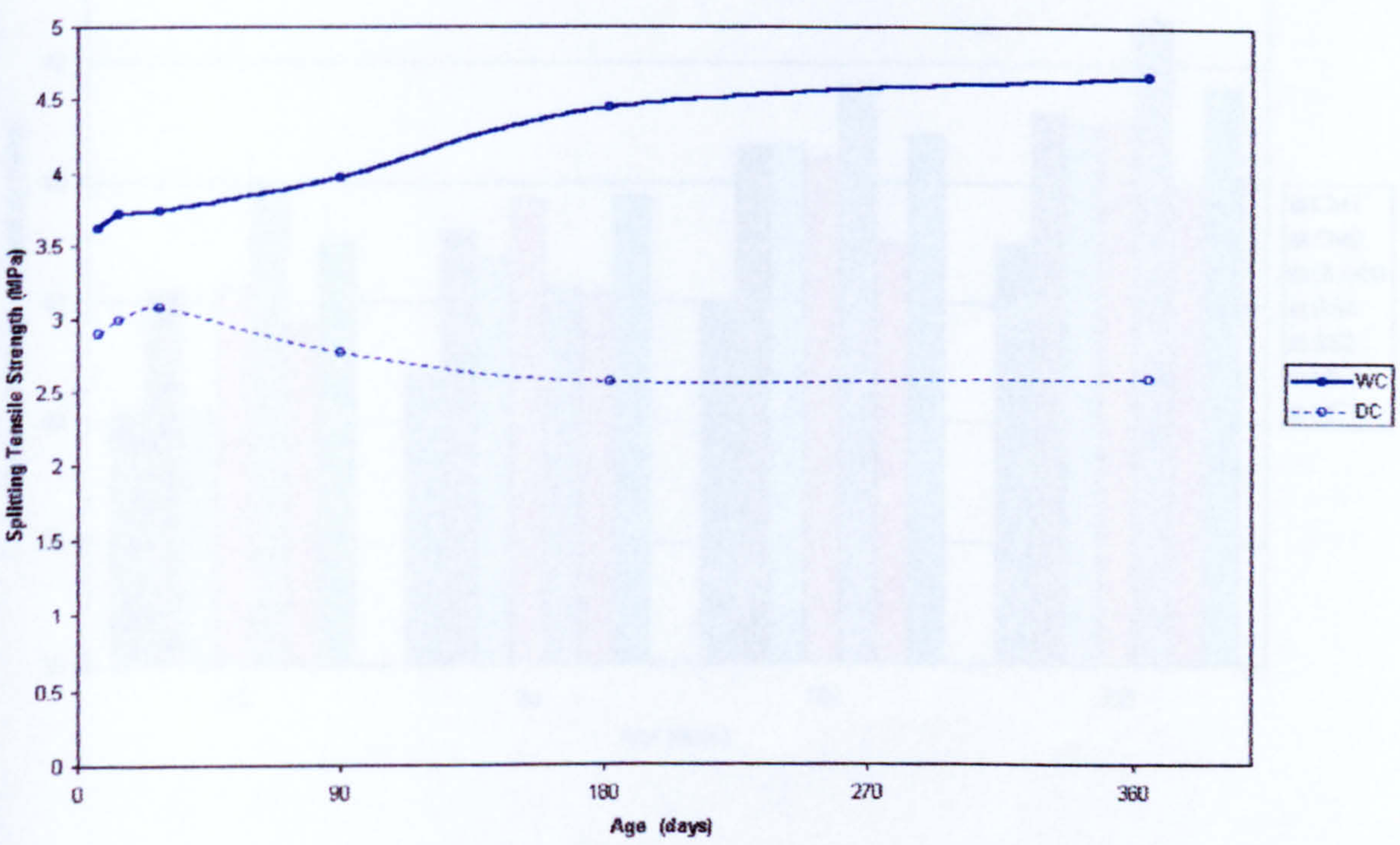

Figure 6.19 Effect of Curing on Splitting Tensile Strength Development for the MET6 mix

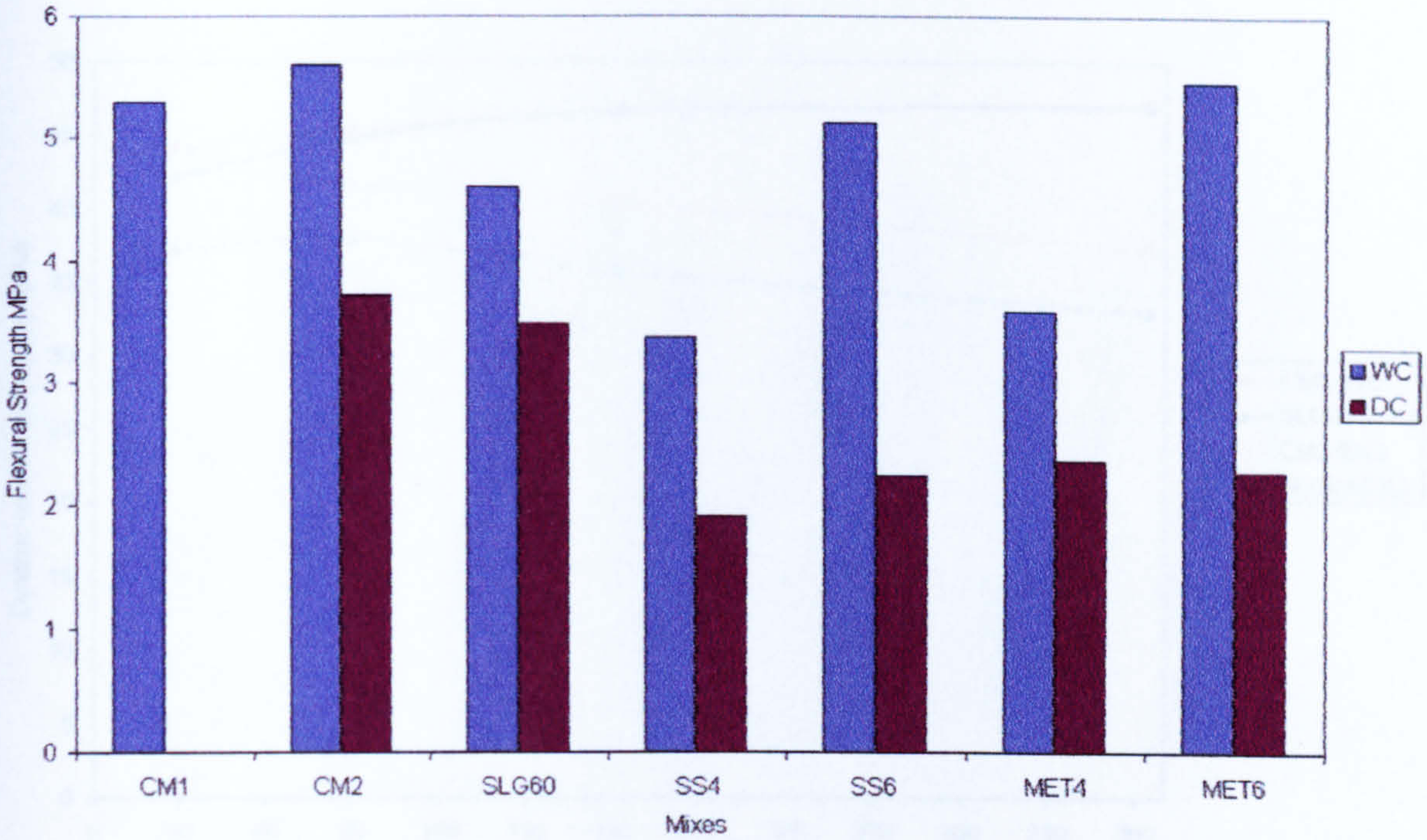

Figure 6.20 Flexural Strength at 365 days for the different mixes under the two curing conditions

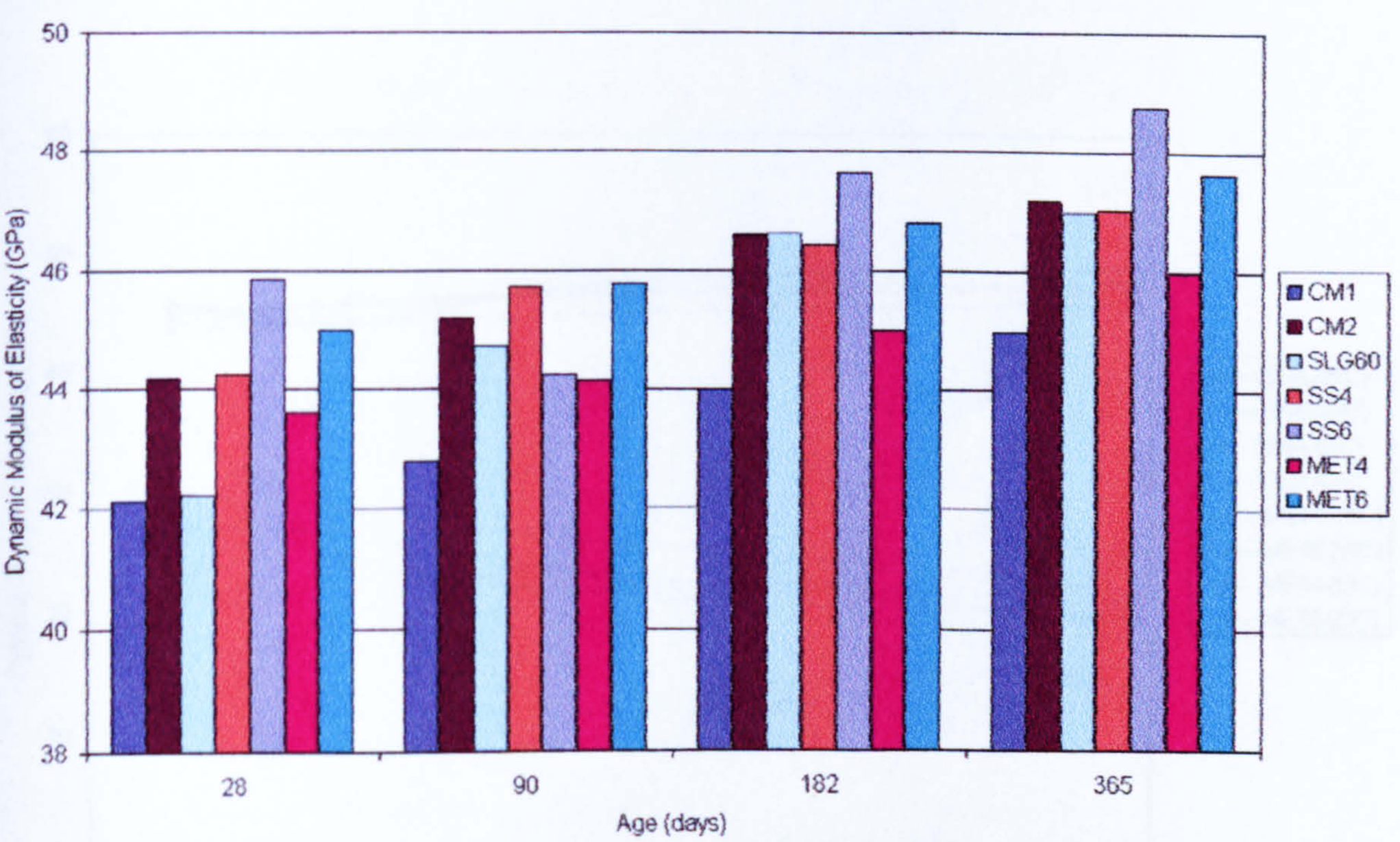

Figure 6.21 Dynamic Modulus of Elasticity for the different mixes under water curing

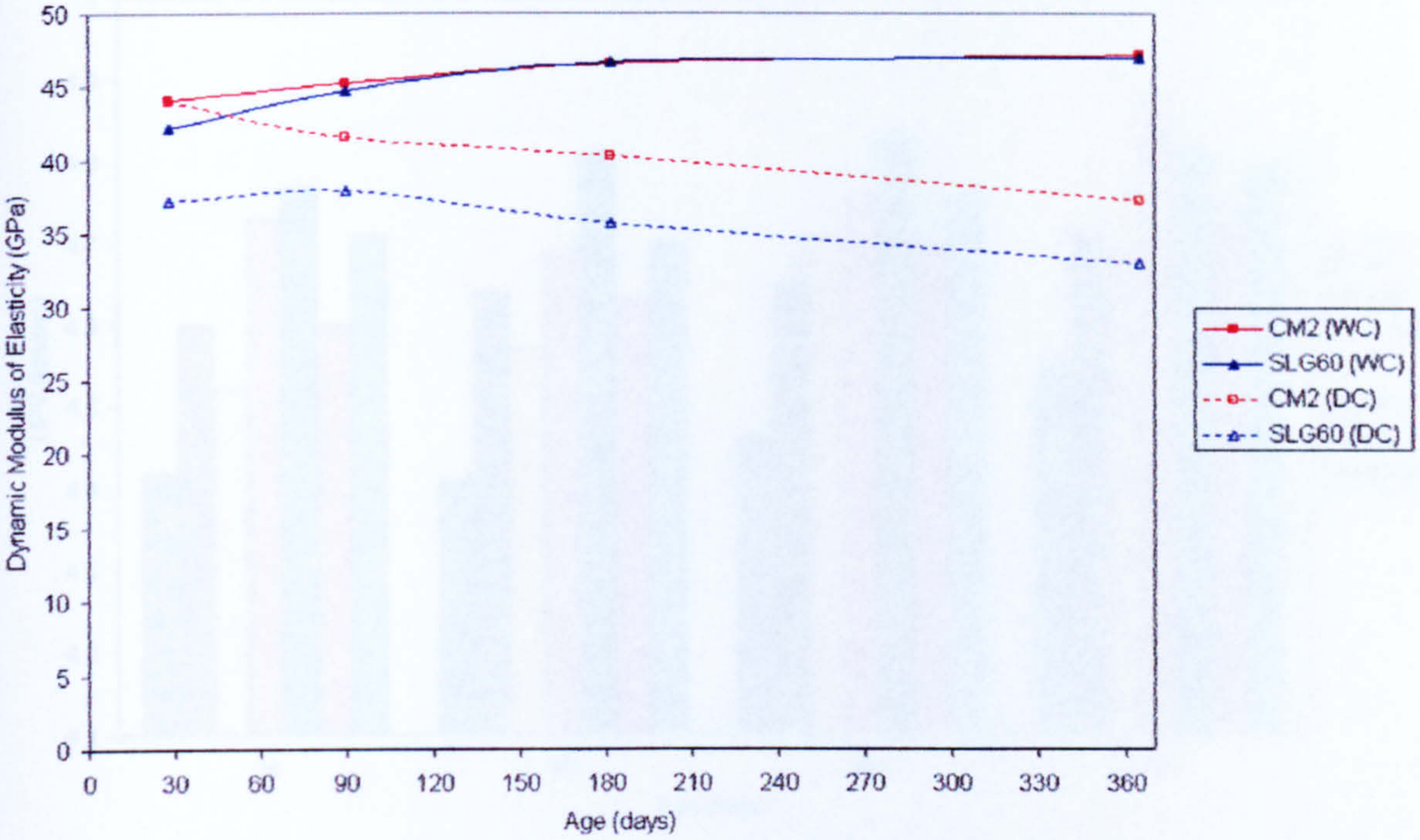

Figure 6.22 Effect of Curing on Dynamic Modulus of Elasticity of CM2 and SLG60 mixes

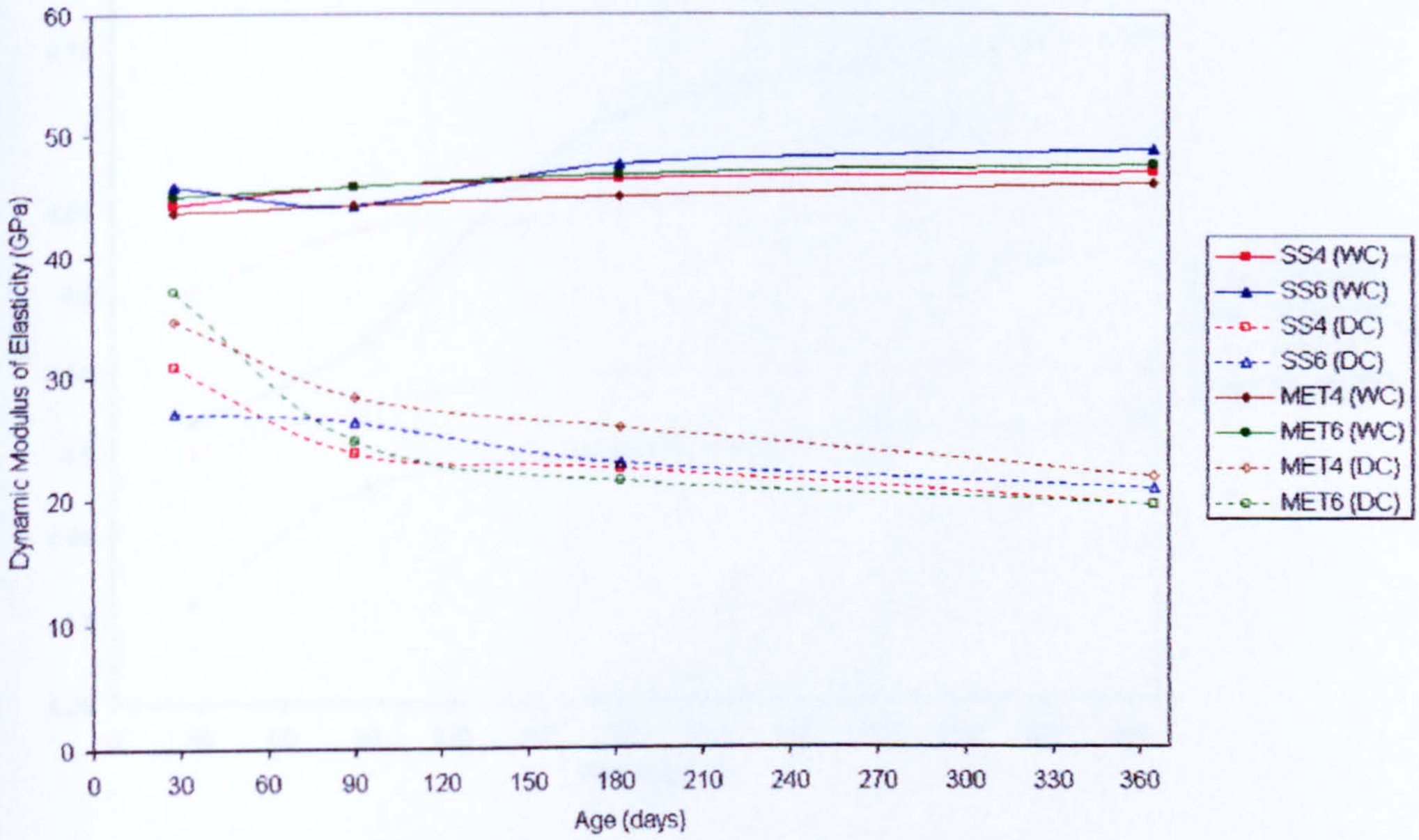

Figure 6.23 Effect of Curing on Dynamic Modulus of Elasticity of AAS mixes

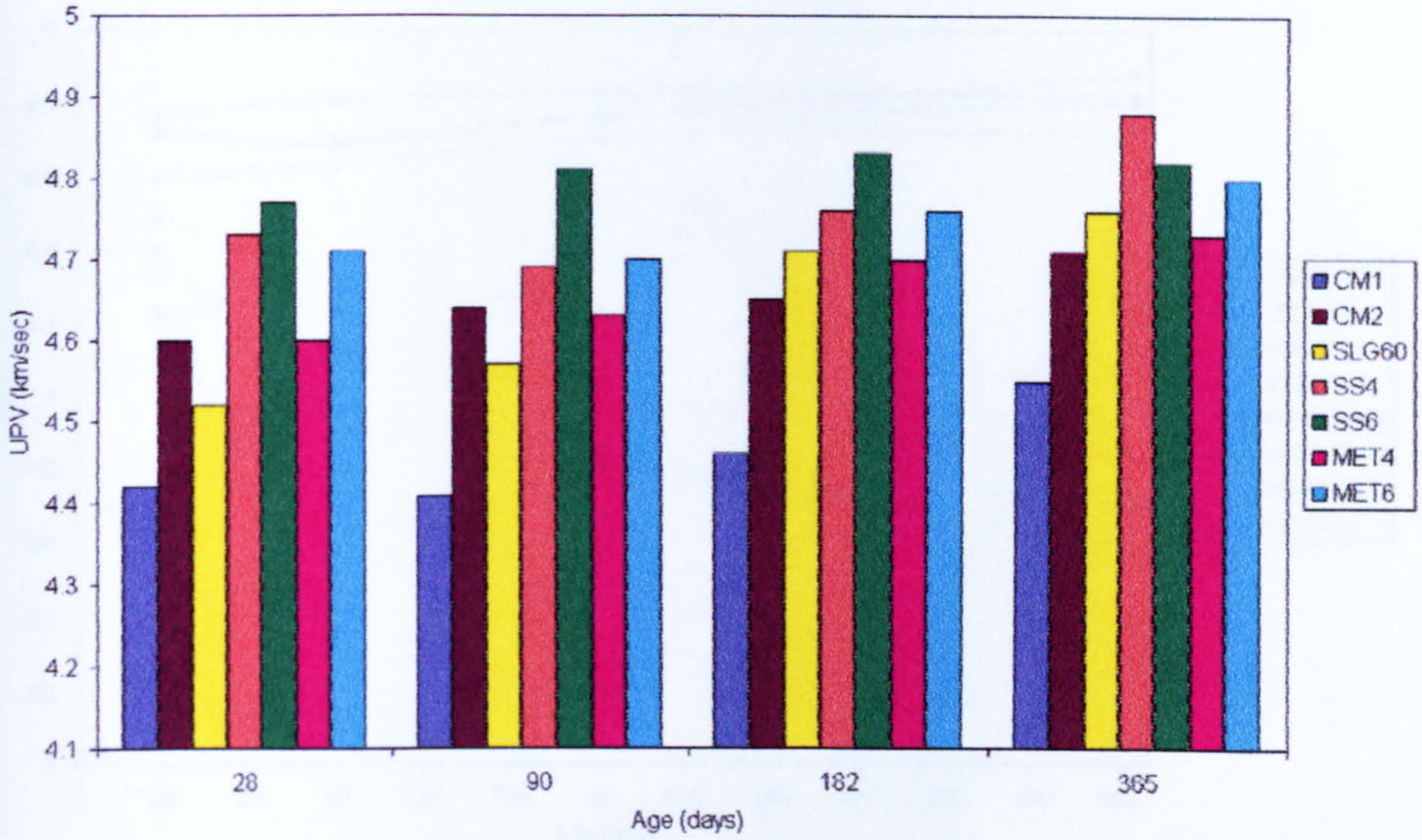

Figure 6.24 Ultrasonic Pulse Velocity for the different mixes under water curing

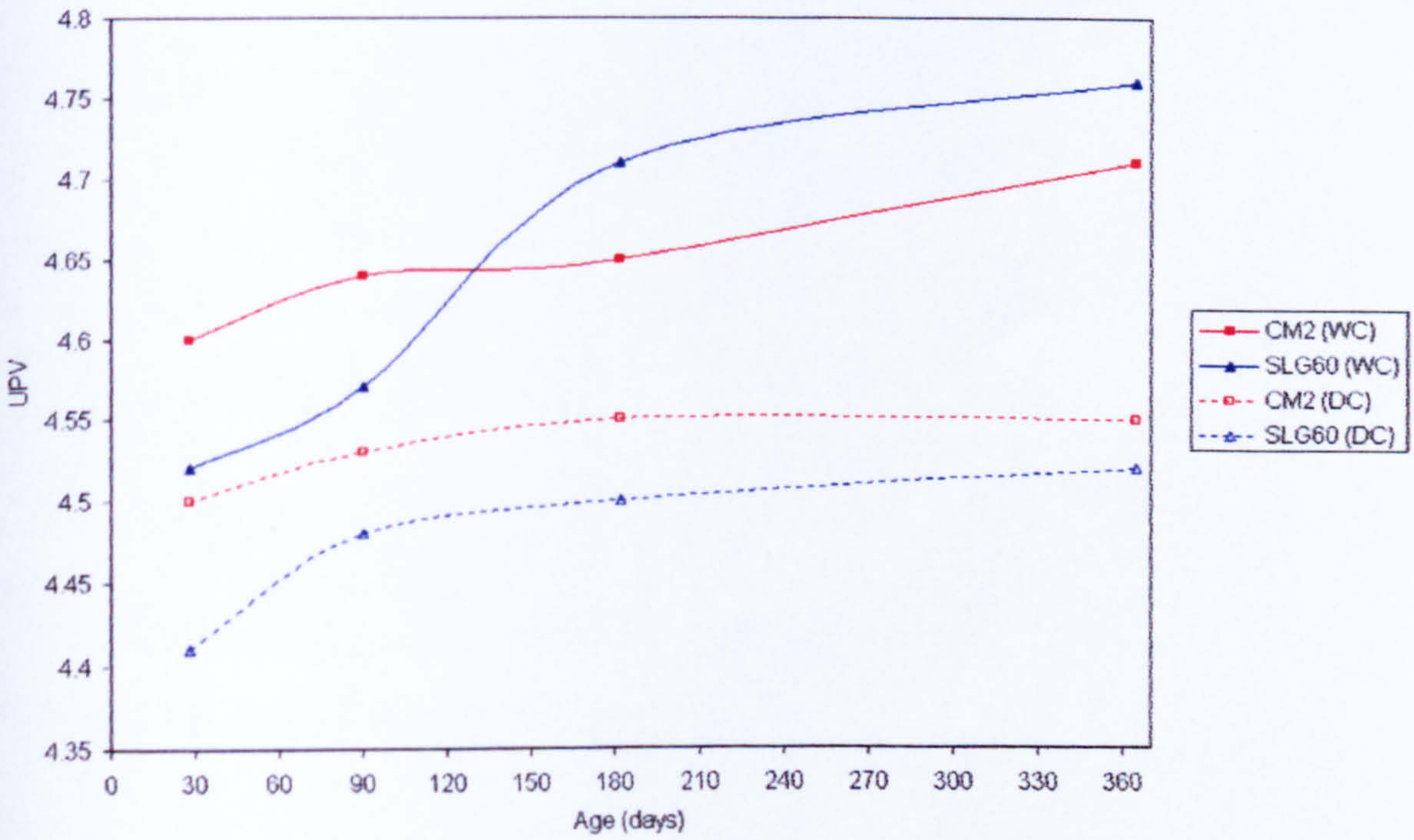

Figure 6.25 Effect of Curing on Ultrasonic Pulse Velocity of CM2 and SLG60 mixes

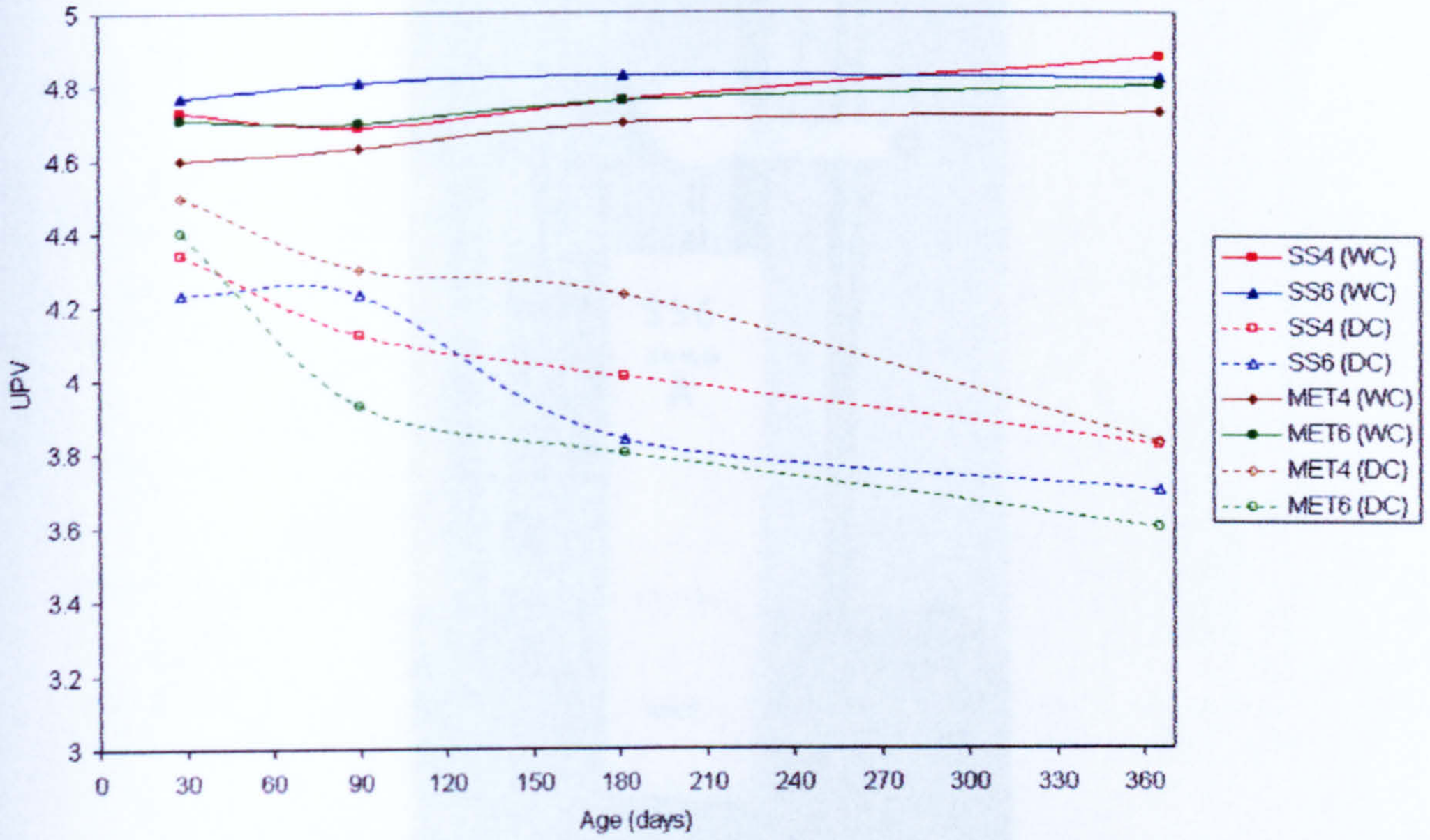

Figure 6.26 Effect of Curing on Ultrasonic Pulse Velocity of AAS mixes

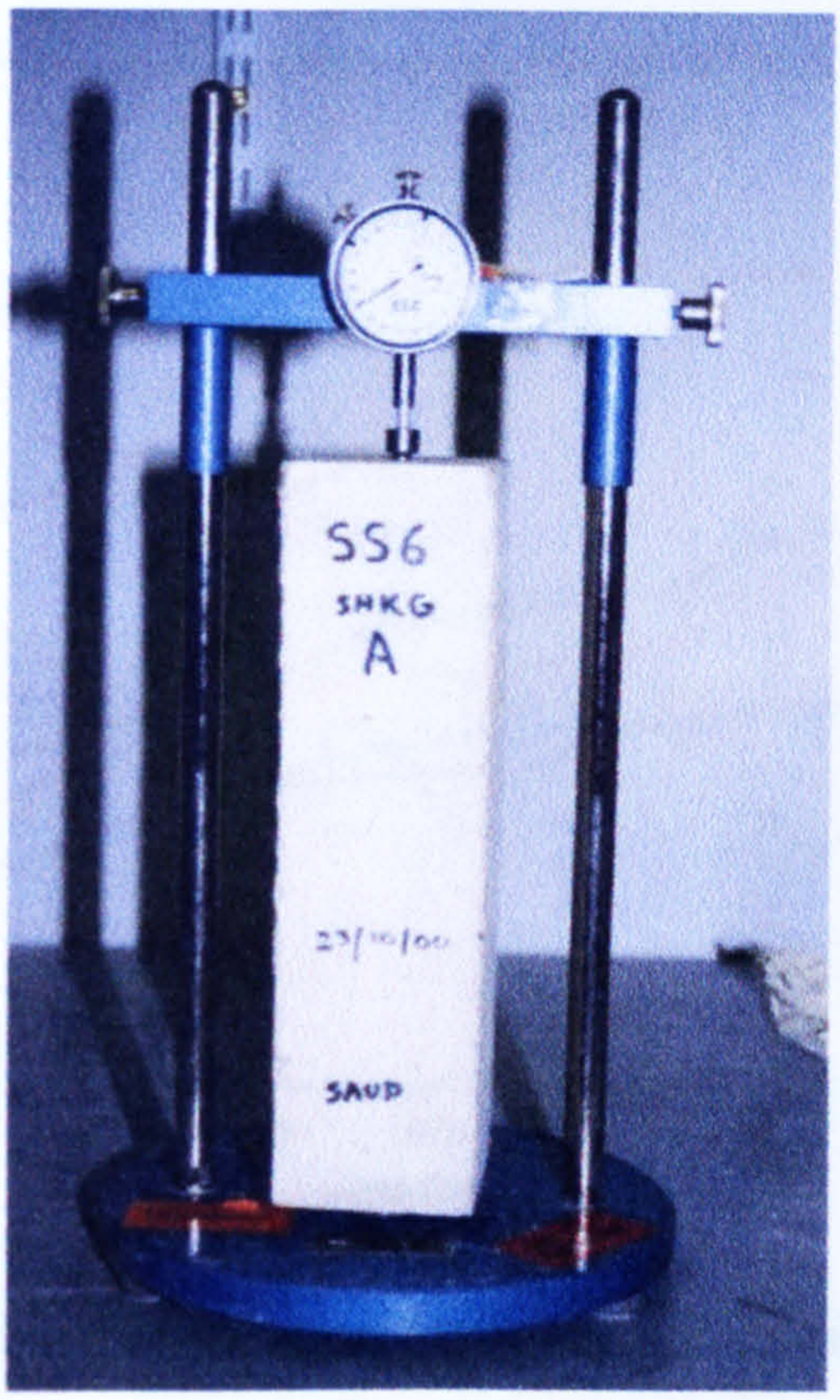

Figure 6.27 Drying Shrinkage testing

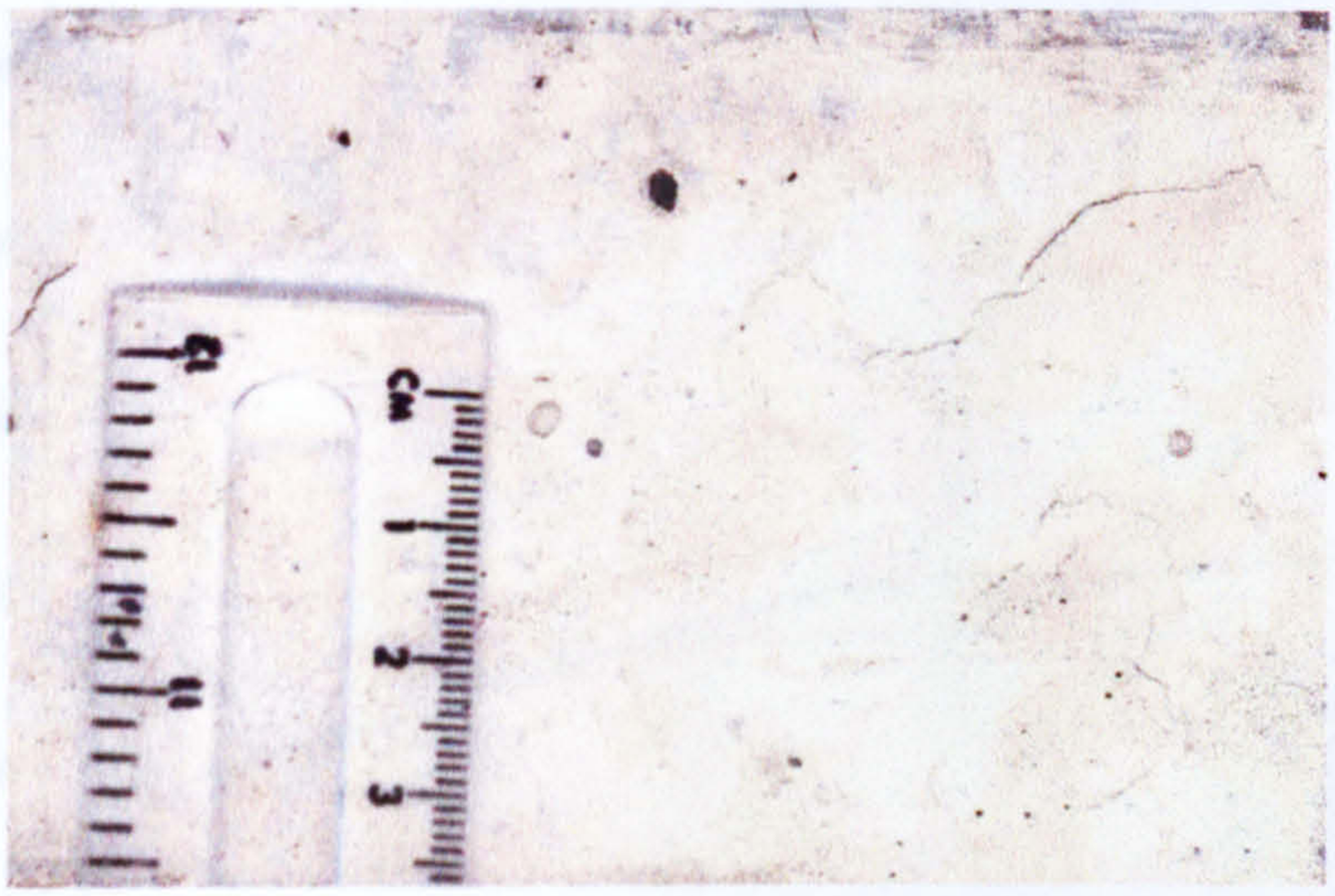

Figure 6.28 Drying Shrinkage Cracks

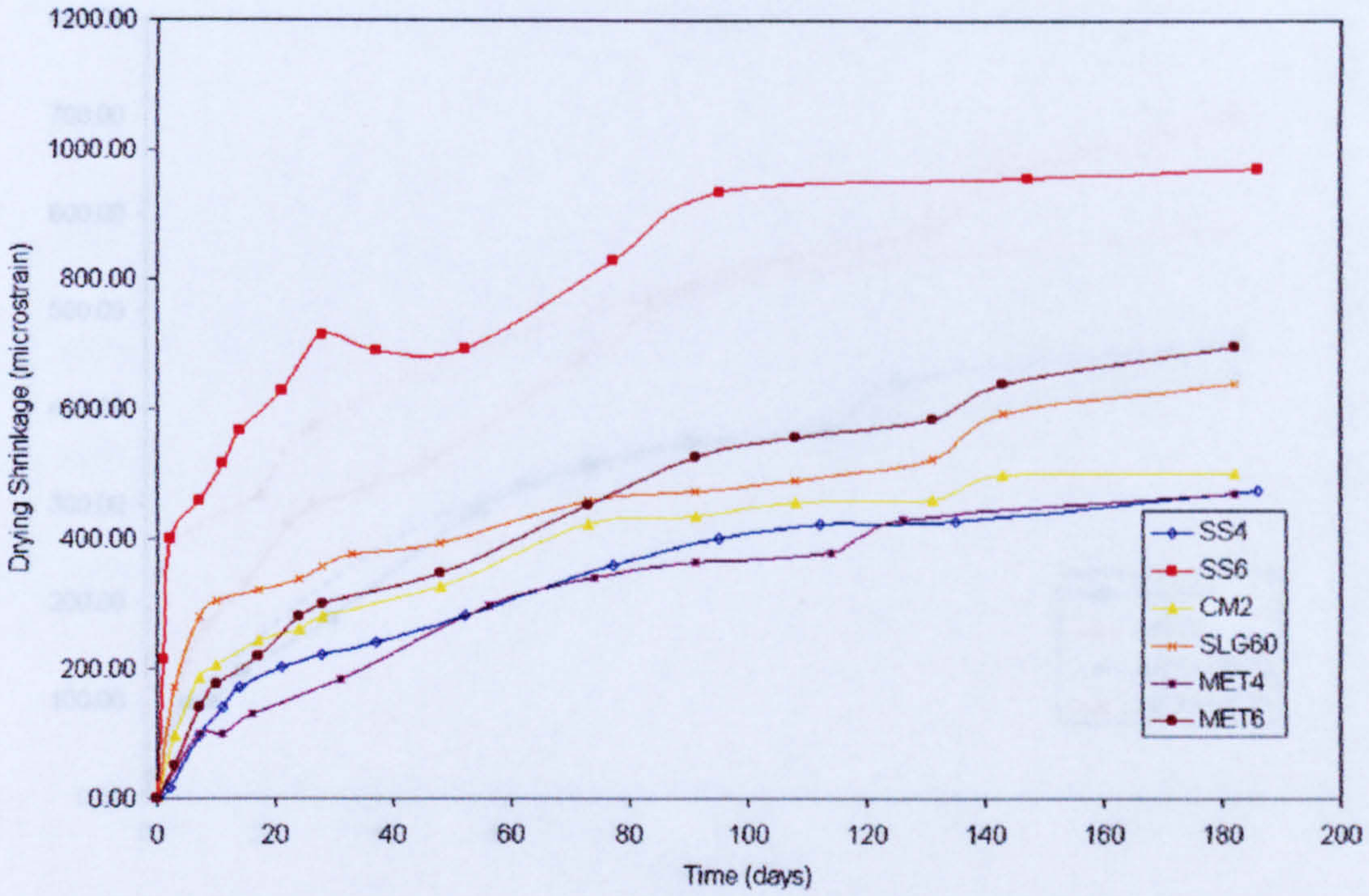

Figure 6.29 Drying Shrinkage development with age for all mixes under water curing

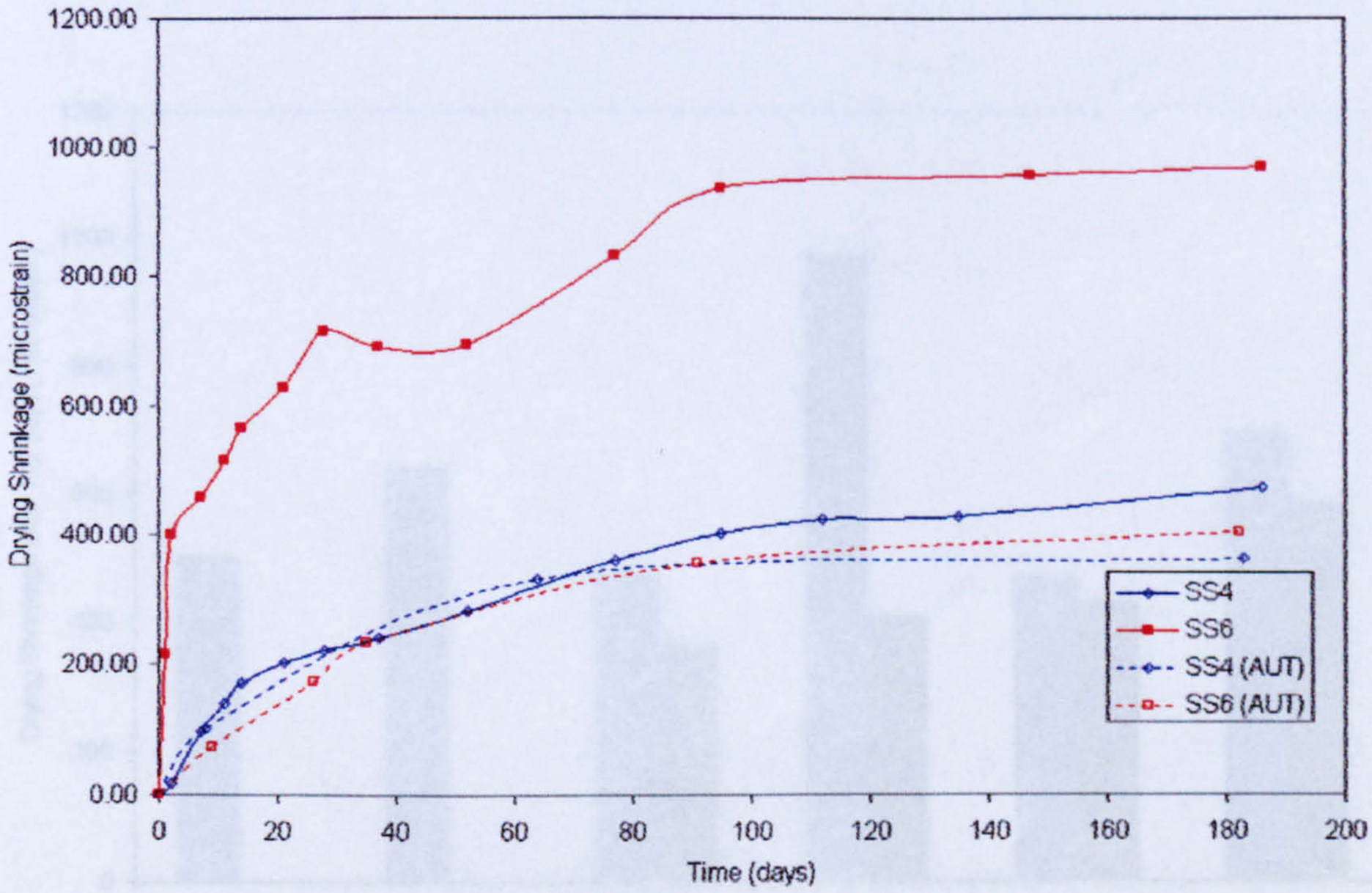

Figure 6.30 Effect of Curing Drying Shrinkage development with age for SS4 and SS6 mixes

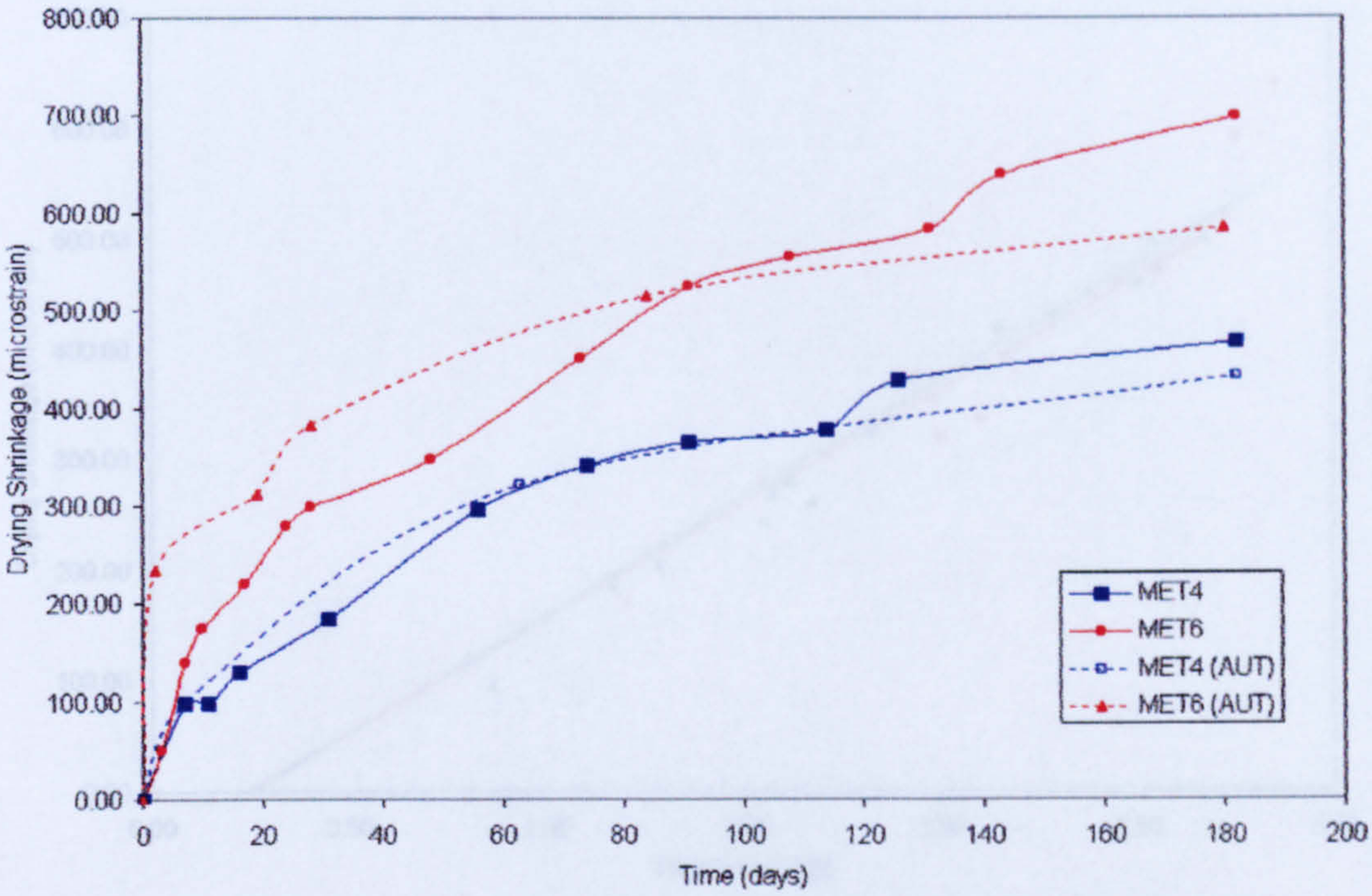

Figure 6.31 Effect of Curing Drying Shrinkage development with age for MET4 and MET6 mixes

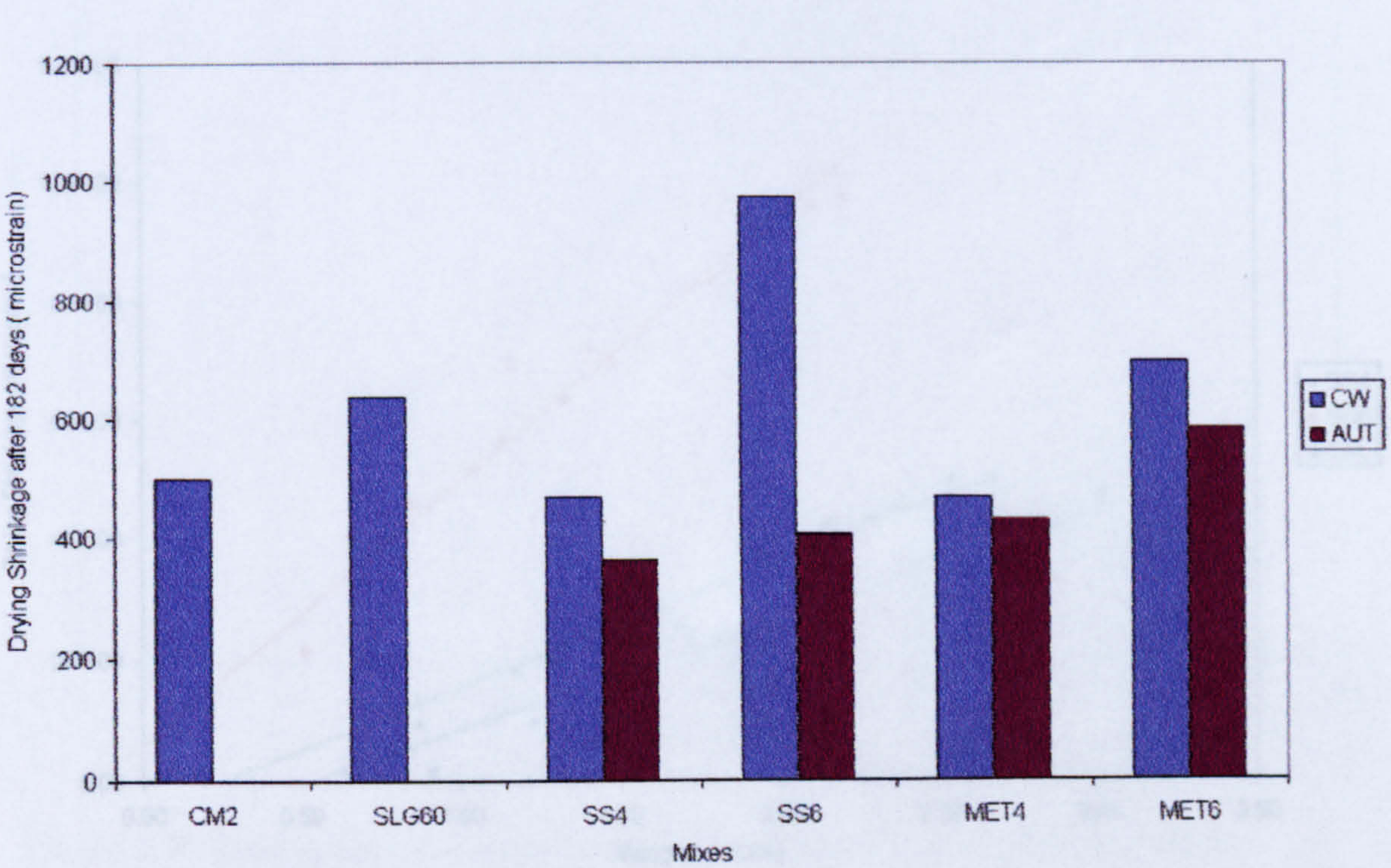

Figure 6.32 Drying Shrinkage after 182 days

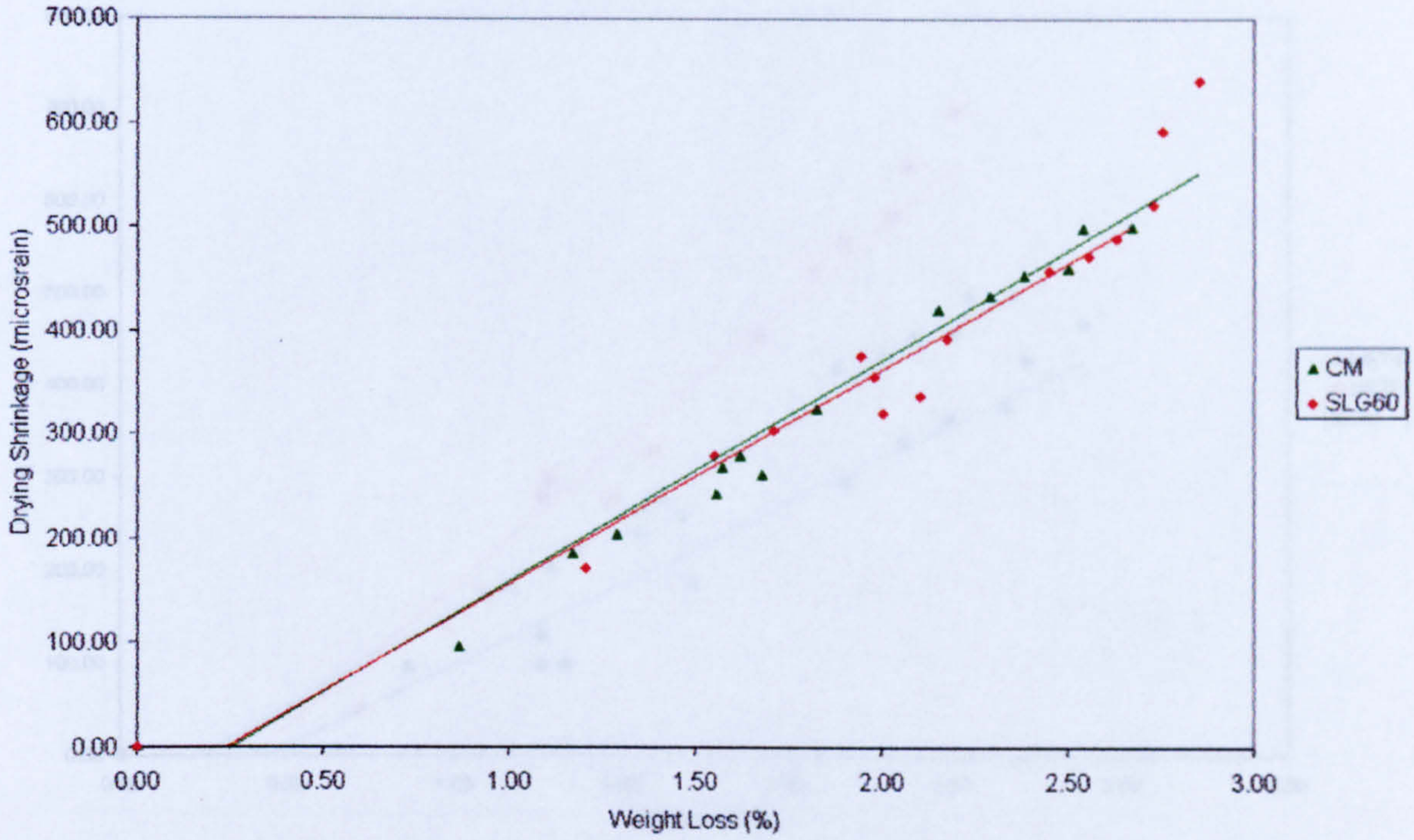

Figure 6.33 Relationship between Drying Shrinkage and Weight Loss for the CM2 and SLG60 mixes

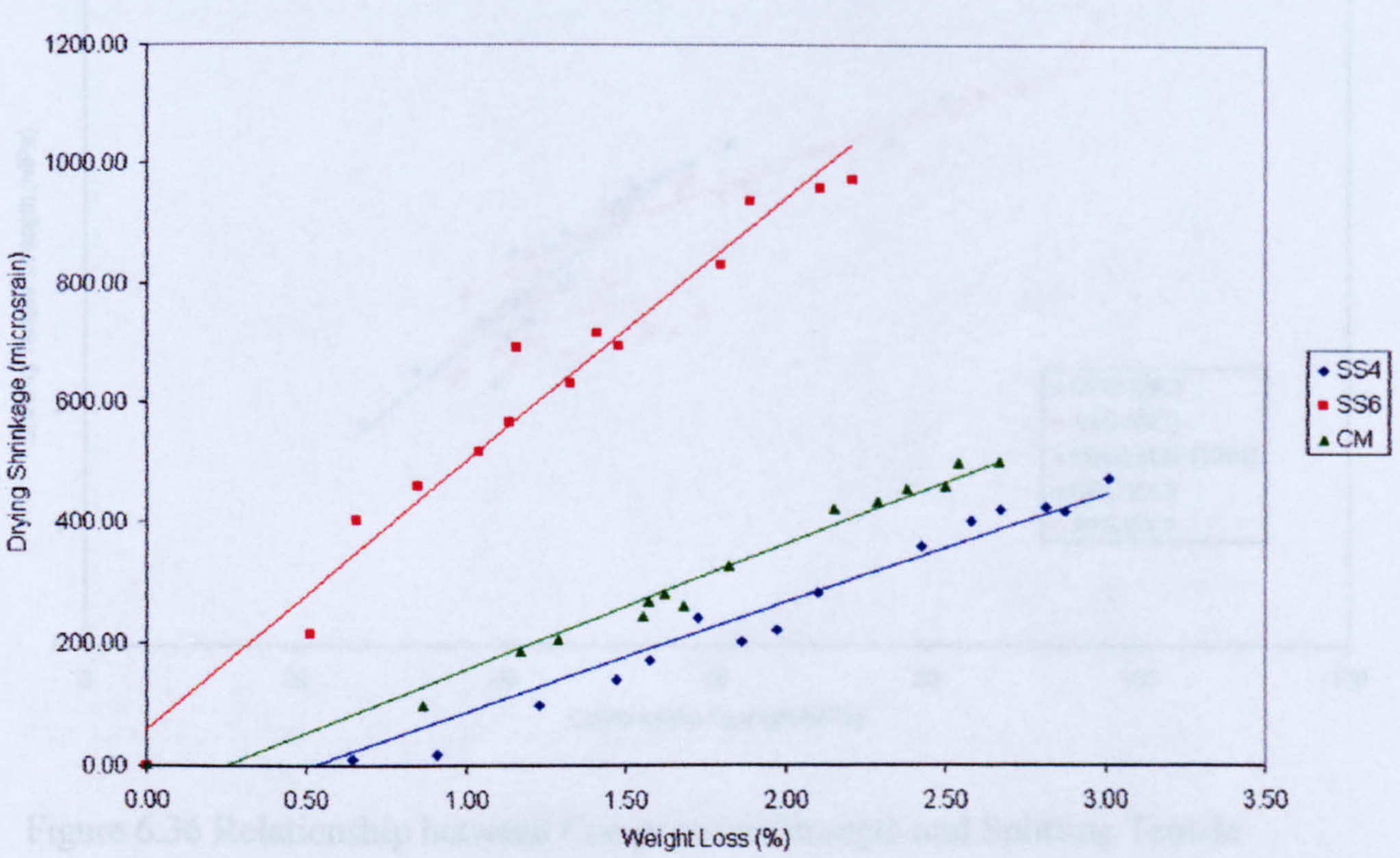

Figure 6.34 Relationship between Drying Shrinkage and Weight Loss for the CM2 , SS4 and SS6 mixes

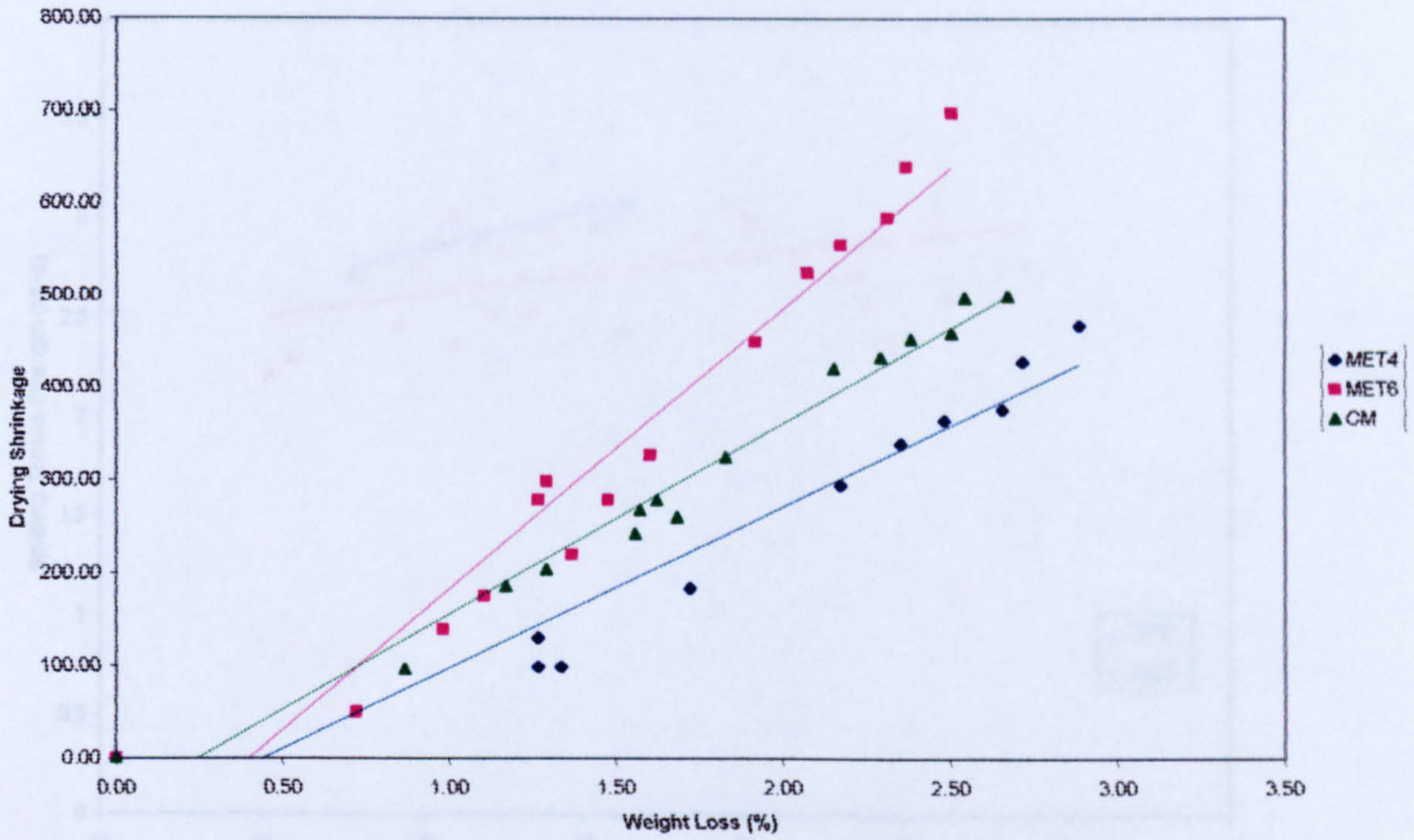

Figure 6.35 Relationship between Drying Shrinkage and Weight Loss for the CM2 , MET4 and MET6 mixes

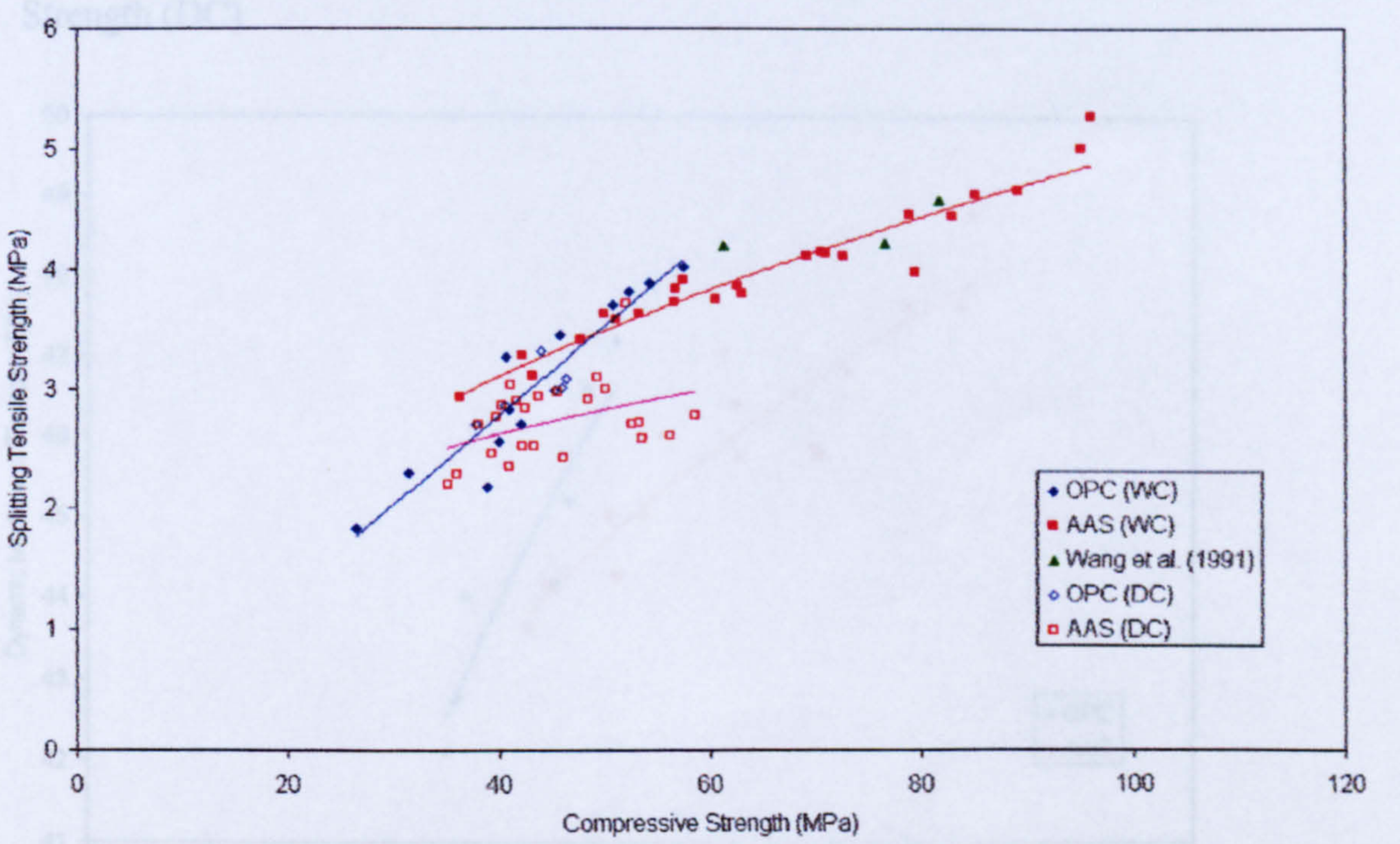

Figure 6.36 Relationship between Compressive Strength and Splitting Tensile Strength (WC)

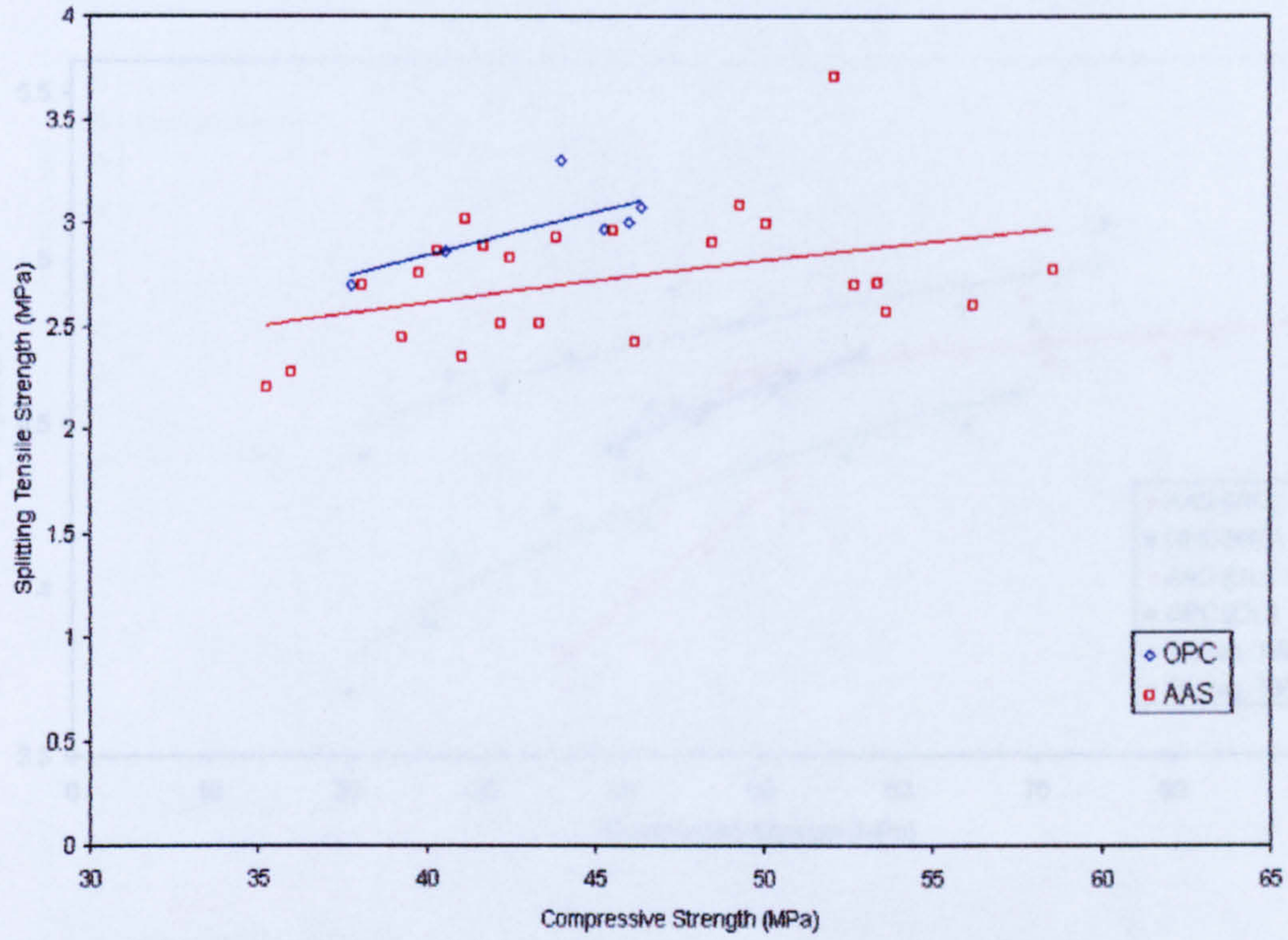

Figure 6.37 Relationship between Compressive Strength and Splitting Tensile Strength (DC)

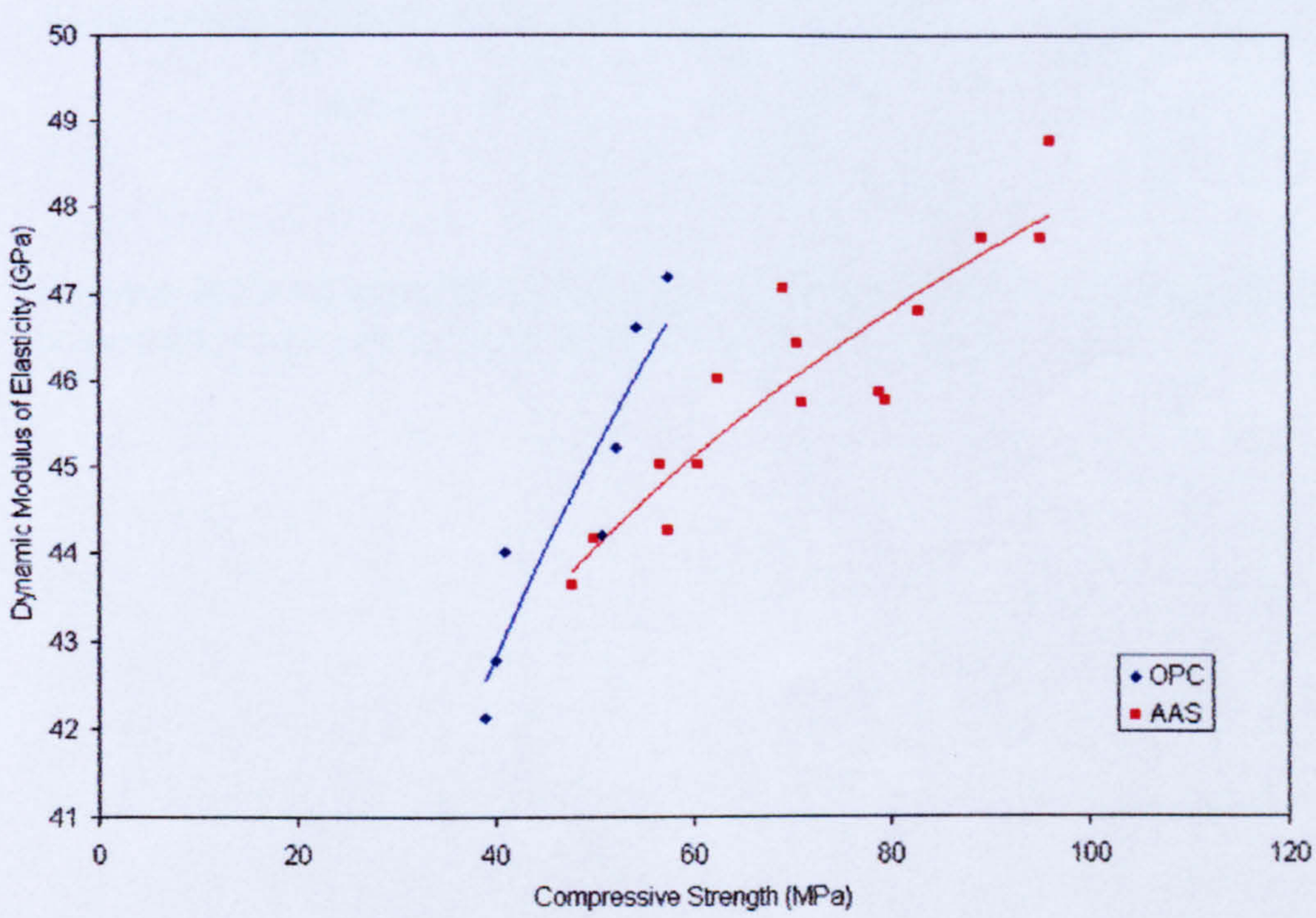

Figure 6.38 Relationship between Compressive Strength and Dynamic Modulus of Elasticity

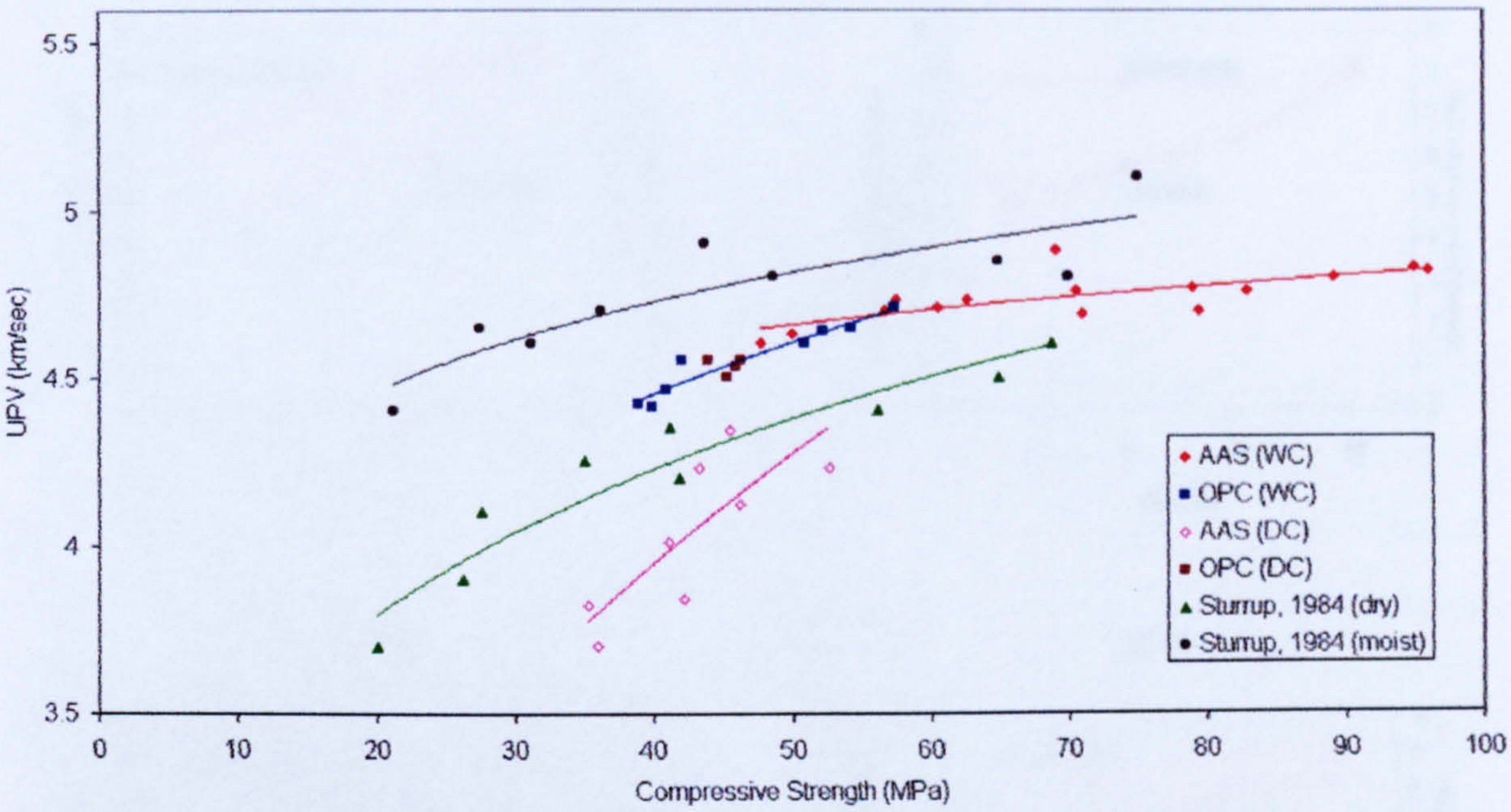

Figure 6.39 Relationship between Compressive Strength and UPV

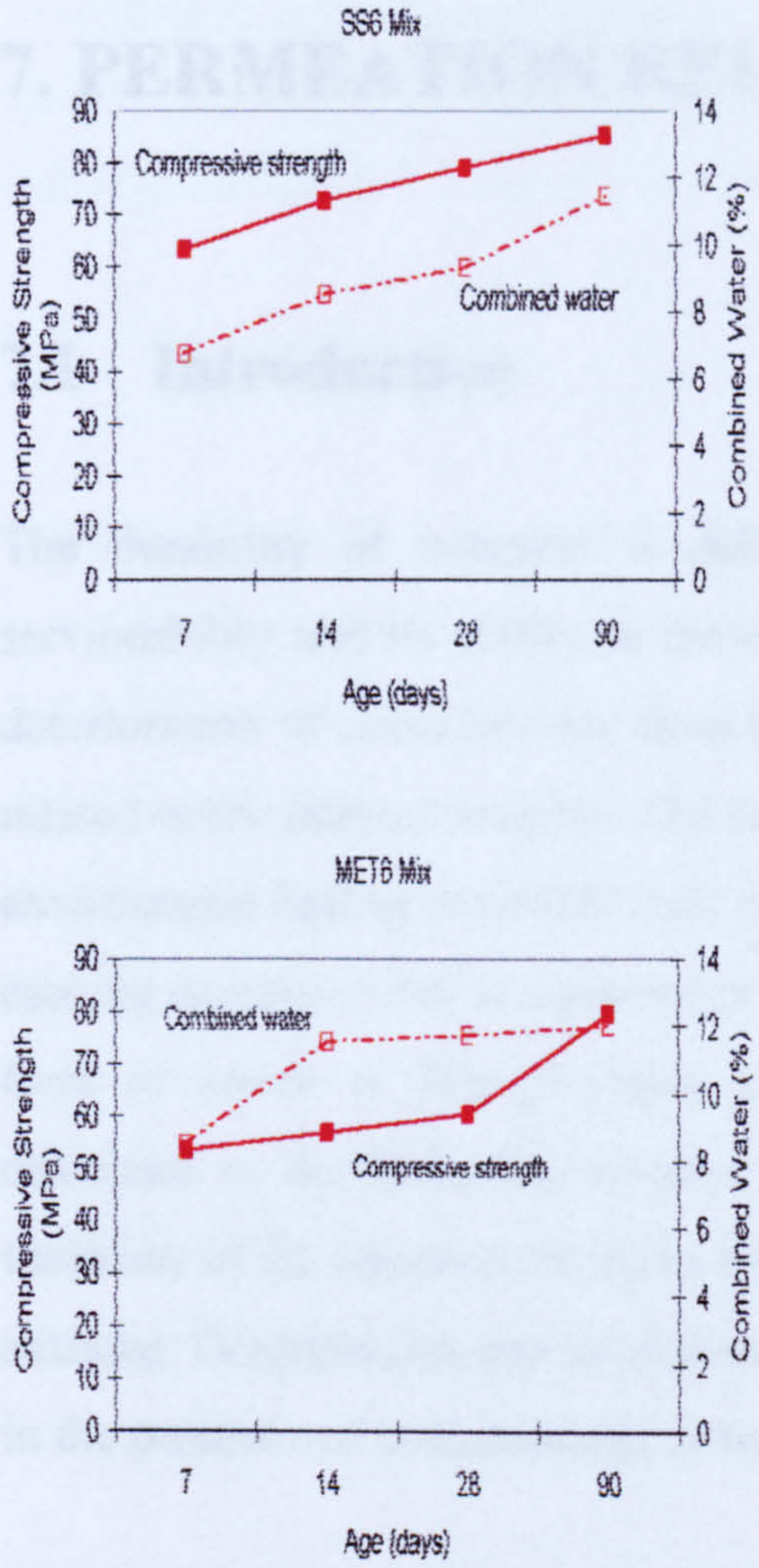

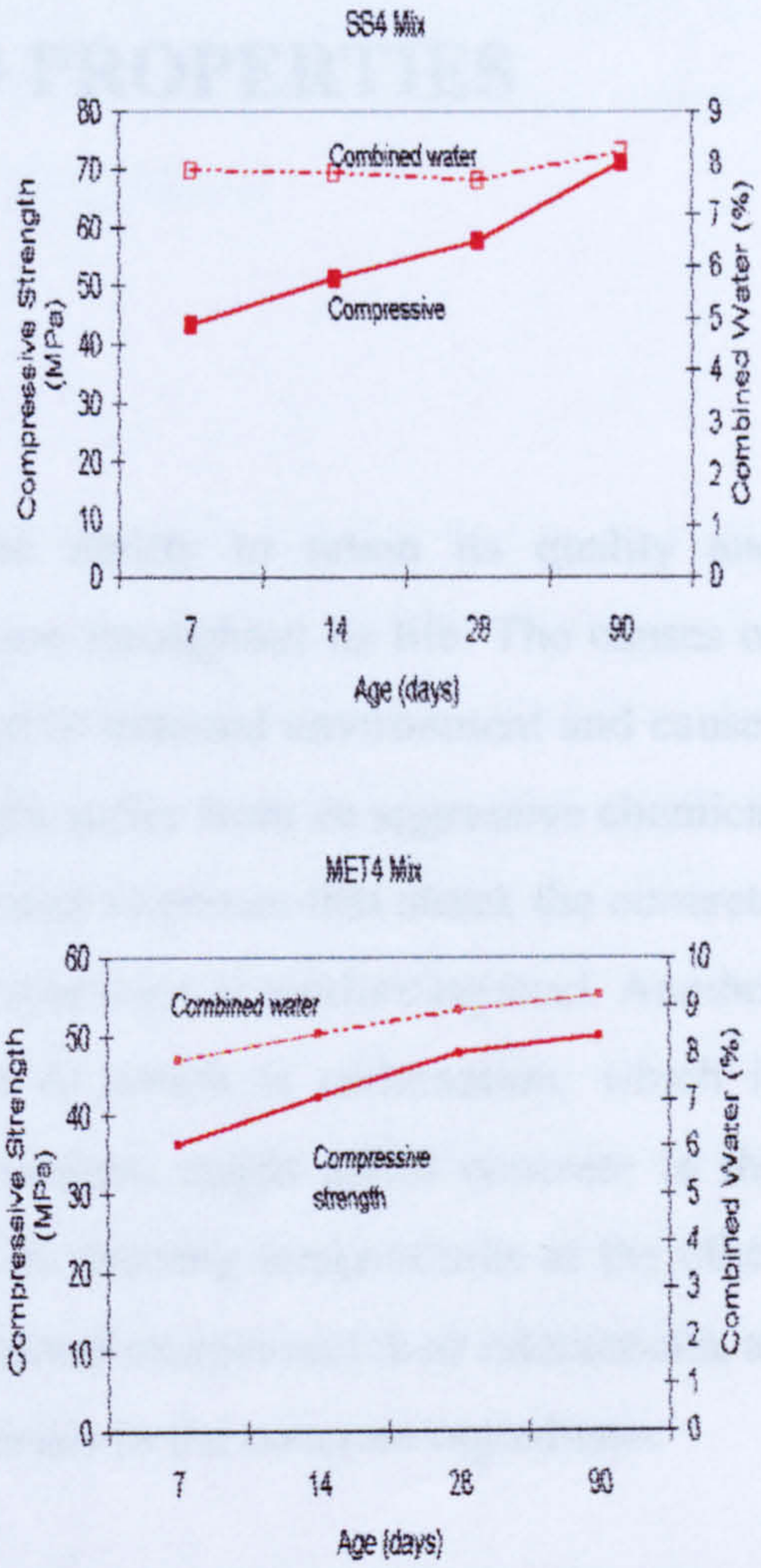

Figure 6.40 Comparison between progress of hydration and development of compressive strength for AAS mixes under water curing

7. PERMEATION RELATED PROPERTIES

7.1 Introduction

The durability of concrete is defined by the ability to retain its quality and serviceability and its ability to resist deterioration throughout its life. The causes of deterioration of concrete vary from those related to external environment and causes related to the internal sources. The concrete might suffer from an aggressive chemical environment having materials such as chlorides and sulphates that attack the concrete causing damage either to concrete or leading to corrosion in reinforcing steel. Another form of attack is through gases, an example of which is carbonation, which is discussed in the following chapter. The environment might affect concrete in the variation of its temperature as in hot climates or freezing temperatures at the other extreme. Deterioration can be also caused by internal sources and their interactions, as in the presence of contaminants or harmful materials in the concrete ingredients.

Among the concrete properties that play a major role in the durability are the porosity of concrete and the permeability. Porosity of a porous material such as concrete is the fraction of the bulk volume of the material occupied by voids. There are three basic transport mechanisms, which can operate in concrete (*Jackson and Dhir,* 1996) namely absorption, permeation and diffusion. Nevertheless, the commonly accepted term 'permeability' will be used here for the overall movement of fluids into and through concrete. Therefore, permeability of concrete is defined as the ease with which external elements such as liquids and gases (fluids) penetrate concrete. Concrete with higher permeability allows faster penetration of gases, liquids and other aggressive materials such as chlorides and sulphates, resulting in rapid corrosion of the reinforcing steel, sulphate attack and other forms of concrete deterioration.

The permeability of concrete is not a simple function of its porosity, but depends on the size, and distribution of the pores (*Neville,* 1995) as illustrated in Figure 7.1.

This chapter presents and discusses the results of porosity, oxygen permeability, and chloride permeability tests carried out to study the performance of AAS concrete mixes in comparison with control OPC and OPC/Slag mixes.

7.2 Porosity

Numerous techniques have been used to study the volume of voids and measure the porosity of concrete, namely helium pycnometry, mercury intrusion porosimetry (MIP) and saturation method. The saturation method can be estimated using methanol (*Feldman,* 1972) or water saturation. The easiest and cheapest technique to measure the porosity of concrete is by water absorption. It can be determined by immersing the sample in water for prolonged periods or by boiling the sample in water for several hours. It is probably the best method of measuring the porosity as it facilitates the real situation encountered by concrete structure. However, *Neville* (1995) reported that it is doubtful that these methods achieve total or full saturation due to the presence of large number of very fine pores (as compared to rocks) and bottlenecks of some of these pores.

In order to reach full saturation, it is necessary to empty the pores first from air and water (by vacuuming) before allowing the water to penetrate them (*Lynsdale*, 1989). *RILEM CPC-11.3* (1984) also recommended a test method based on evacuation of air from the samples then allowing the water to fill in the pores under vacuum to reach total saturation.

This section presents the work carried out to measure the porosity using water absorption.

7.2.1 Apparatus

The porosity for the concrete specimens investigated was determined using a vacuum saturation apparatus (*RILEM CPC-11.3*, 1984), which is shown in Figure 7.2. The apparatus consists of the following components:

1. Vacuum desiccator

2. Three-way valve, connected to the desiccator
3. A 10-liter plastic bottle with tap
4. Vacuum pump
5. Vacuum gauge
6. Tubing

7.2.2 Sample Preparation

Two samples of 100 mm Φ x 50 mm cylinders were tested per curing condition at 7, 28, 90 180, and 365 days. Samples were taken out of the curing environment at required testing age. The samples were then dried in an oven at the temperature of 105±5 °C for approximately 24 hours, until constant weight was reached. Prior to testing of porosity, the samples were kept in a desiccator for cooling for another 24 hours.

7.2.3 Testing Procedure

The procedure for measuring porosity by using the vacuum saturation apparatus is as follows:

- The previously dried and cooled samples were weighed and their weight recorded as (W_{oven}).
- The samples were placed in a desiccator under vacuum for 24 hours before allowing de-ionised de-aired water to fill the desiccator and submerging the samples. Vacuuming was carried out for a further 24 hours to fully saturate the samples.
- The specimens were then left to equilibrate in water, under atmospheric pressure, for a further 24 hours, before weighing in water (W_{sub}). They were then wiped with paper and weighed in air (W_{sat}, saturated surface dry weight in air).
- The porosity is calculated as = 100 x $(W_{sat,} - W_{oven}) / (W_{sat,} - W_{sub})$

7.2.4 Results and discussion

Results of the porosity test are presented in Figures 7.3 – 7.10. Figure 7.3 shows the porosity of the concrete mixes at different ages (7, 14, 28, 90, 180 and 365 days) under water curing condition. CM2 has the lowest value of porosity for all ages. Replacing 60% of the cement by (ggbs) in mix SLG60 resulted in an increase in the porosity of concrete compared to the OPC concrete mix (CM2) with the same w/c of 0.48. But when comparing the slag mix with the OPC control mix having w/c of 0.55 the results show the SLG60 having lower porosity. These results are in agreement with results presented by *Lynsdale and Sit* (1992) where they indicated that 70% slag replacement of OPC resulted in an increase in porosity in the early age up to 28 days. The comparison was done on equal w/c ratio but when the comparison was done on equal slump the slag concrete eventually had lower porosity after 28 days.

On the other hand, looking at the results of the AAS concrete mixes it can be noted that the increase in the Na_2O dosage of the activator from 4 to 6%, that was expected to produce lower porosity, did not do so in the case of the SS4 and SS6 mixes, where the activator has an $M_s = 1.65$, but did so in the case of MET4 and MET6 mixes, with the activator having an $M_s = 1.00$. This discrepancy could probably be caused by the drying of the specimens prior to testing since SS6 showed higher shrinkage in the drying shrinkage test as was discussed in Chapter 5. The porosity of concrete is generally reduced with age as is clearly shown in the results.

The porosity of the concrete mixes under the dry curing condition can be seen in Figure 7.4. At 7 days the CM2 mix shows the lowest porosity around 12%, the slag replacement in mix SLG60 increases the porosity to 14% and the AAS mixes gave a porosity around 13% with only minor differences among them. The values of porosity changed slightly with age.

The effect of curing on the OPC control mix CM2 is shown in Figure 7.5. By comparing the results for water and dry cured specimens it can be seen that water curing reduces porosity with age from 10.5% at 7 days to 8.8% beyond 6 months. Porosity in the case of dry cured samples is 12.1% at 7 days which is clearly higher

than the water cured samples, but the change in porosity is insignificant for the remaining period.

The OPC-slag (SLG60) mix was affected by curing in a manner demonstrated in Figure 7.6. As expected the dry cured specimens have higher porosity than water cured specimens. The porosity decreases with time as the hydration progresses. The gap between the porosity results for water and dry cured samples increases with age and the reduction in porosity is more in the case of water curing which is probably due to the continued hydration of slag with age (or pozzolanic reaction).

Figure 7.7 illustrates the effect of curing on porosity of the SS4 mix. No major effect can be noticed throughout the testing period, an expected higher percentage is shown in the 7 days value of porosity for the dry curing sample and stays higher all the time with a slight change in the difference between the two results.

The porosity results for the alkali-activated slag mix SS6 is presented in Figure 7.8 and shows a reduction in porosity from 12.8% at 7 days to 10.3% after one year under water curing. Under dry curing the porosity drops from 13.3% to around 12.0%. The effect of curing is not clear in these results, but this can be attributed to drying shrinkage cracking, induced by drying prior to the testing which caused the water cured specimens to be more porous.

The effects of curing on the AAS mix (MET4) is clearly emphasized in the difference between porosity results under water and dry curing as can be seen in Figure 7.9. For 7 days the porosity values were 13.2% and 13.0 % under water and dry curing respectively. The porosity decreased to 11 % after 6 months in the case of water curing while it only reached to 12.6% under dry curing indicting slower hydration.

The AAS mix (MET6) behaved in terms of its porosity as shown in Figure 7.10. The 7 day results were 12.4% and 13.2% for water and dry curing respectively. The porosity drops to 9.0% after 6 months under water curing and 11.6% under dry curing. This shows an increase in the gap between the results for the two curing conditions with age.

No results of the water saturation porosity test on AAS concrete were available in the literature to compare with the results of this investigation. Some studies on porosimetry indicate low porosity in the case of AAS mortars compared to OPC (*Wang et. al*, 1995).

7.3 Oxygen Permeability

Gas flow rate in concrete is normally very low, resulting in laminar rather than turbulent flow. Laminar viscous flow is dependent on the properties of fluid (i.e. viscosity and density) as well as characteristic of the porous medium (*Dhir et al.*, 1989). If the fluid used is non-compressible such as water, D'arcy's law can determine the steady state flow of water through concrete as follows:

$$R = \frac{kA\Delta P}{\eta L} \qquad (7.1)$$

Where: k = Intrinsic permeability (m^2)

R = Flow rate (m^3/sec)

η = Viscosity of the fluid (Ns/m^2)

L = Length of the specimen (m)

A = Cross sectional area of the specimen (m^2)

ΔP = Fluid pressure head across the specimen (bar)

However, when a compressible fluid such as oxygen is used, D'arcy's equation should be modified using the expression proposed by Grube and Lawrence (*Grube*

and Lawrence, 1984) which calculates the volume of fluid at the average pressure within the specimen (Cabrera and Lynsdale, 1988) as follows:

$$k = \frac{2P_2 R\eta L}{A(P_1^2 - P_2^2)} \tag{7.2}$$

$$k = \frac{4.04RL * 10^{-16}}{A(P_1^2 - 1)} \tag{7.3}$$

Where: k = Intrinsic oxygen permeability (m^2)

P_1 = Inlet absolute applied (gauge) pressure (bar)

P_2 = Outlet pressure at which the flow rate is measured (usually 1 bar)

Equation 7.3 was used in this work to measure the oxygen permeability for the specimens.

7.3.1 Apparatus

Intrinsic Oxygen Permeability test is performed using the permeability cell developed by the *Cement and Concrete Association* (C&CA). The permeameters used in this investigation are shown in Figure 7.11.

7.3.2 Preparation of Specimens

In this investigation, the specimens that were cast were 100 mm Φ x 50 mm height. They were cured under water curing and dry curing and tested at ages 7, 14, 28, 91, and 182 days. Prior to testing the samples were taken out of the curing environment at the required testing age. The samples were then dried in an oven at 105±5 °C for approximately 24 hours, until constant weight was reached.

7.3.3 Procedure

The rubber inner tube, inflated to a pressure of 5 bars, is used to provide a gas-tight seal between the sample that is mounted in a soft rubber collar and the outer steel ring of the cell. Oxygen gas, under the required pressure, is applied to one side of the specimens through the gas inlet valve and the flow rate at the other side is measured using a bubble flow meter.

Equation 7.3 was used in this work to measure the oxygen permeability for the specimens.

7.3.4 Results and Discussion

The results of oxygen permeability for the different mixes investigated, having a w/c=0.48, are presented in Figures 7.12 and 7.13.

Figure 7.12 shows the results for the water-cured specimens of the different mixes. The CM2 mix had the lowest oxygen permeability results starting from $1x10^{-16}$ m^2 at 7 days decreasing with age to a value around $0.5x10^{-16}$ m^2 at 90 days and did not change significantly onward. The OPC/Slag mix (SLG60) had oxygen permeability higher than CM2 with a value of $2x10^{-16}$ m^2 at 7 days decreasing with age to $1x10^{-16}$ m^2 at 90 days and $0.6x10^{-16}$ after 1 year. This can be attributed to the latent hydration of slag where it continues through the late ages.

It is noticed that the results of oxygen permeability for the AAS mixes are much higher in comparison with OPC and OPC/Slag mixes. The SS4 mix gave a value of $67x10^{-16}$ m^2 at 7 days then decreasing drastically to $14.6x10^{-16}$ m^2 at 90 days and maintaining a value of $13.61x10^{-16}$ m^2 after 6 months. As for the SS6 mix the results were $67x10^{-16}$ m^2 at 7 days decreasing to $8.41x10^{-16}$ m^2 at 90 days reaching $4.90x10^{-16}$ m^2 after 1 year.

MET4 mix gave a value of $31.52x10^{-16}$ m^2 at 7 days then decreasing to $16.57x10^{-16}$ m^2 at 28 days and maintaining a value around $13x10^{-16}$ m^2 after 90 days. As for the MET6 mix the results were $33.7x10^{-16}$ m^2 at 7 days decreasing to $10x10^{-16}$ m^2 at 28 days and maintaining a value around $7x10^{-16}$ m^2 after 90 days.

The effect of curing on oxygen permeability for the OPC and OPC/Slag mixes are shown in Figure 7.13 where it is very clear that the oxygen permeability under dry curing was over 10 times higher compared to water curing. The results for the AAS mixes under dry curing were not measurable by the test. The rate of flow was very high and could not be measured.

The high permeability results for the AAS mixes bring into question the reliability of the test especially with relation to the drying of the specimens prior to testing. This technique received a lot of criticism in the literature related to normal concrete.

The preconditioning treatment carried out in the test has some disadvantages although drying is required to remove moisture, which can influence the result. Usually the temperature of drying affects the permeability result with higher values in the case of higher temperatures (*Lynsdale*, 1989). The 105 °C was widely used with OPC concrete on the thought that it is much representative as all water was assumed to be removed. *Mills* (1985) reports that the differences in permeability due to the type of treatment are ascribed to the transformation of the fine-pore structure into a coarser one due to tensile stresses. *Sanjuan* and *Munoz-Martialay* (1996) stated that the variation in results of air permeability due to preconditioning temperatures (from 20-80 °C) was low in the case of w/c ratios between 0.42 and 0.47 implying that there is no effect on the results for such concretes due to variation in preconditioning temperature. A *RILEM* committee (1999) issued a paper on the gas permeability test recommending setting the preconditioning temperature to 50 °C provided that the preconditioning continue until the calculated loss of water (variation in mass) is attained within a 5 percent level of accuracy. Although the preconditioning at 105 °C was acceptable for control mixes, the high results of oxygen permeability for AAS concrete were probably due to the effect of drying. This is in agreement with *Kumar and Roy* (1986) who suggested that extreme drying could cause micro cracking and

damage in the C-S-H gel. Since the main hydration product for AAS concrete is C-S-H this justification is relevant.

7.4 Chloride Permeability

7.4.1 Experimental Programme

This test followed the ASSHTO T277 or ASTM C 1202, which has been modified so that the result can be monitored and stored automatically by a computer (*Cabrera and Lynsdale*, 1988b). Cylinders of 100 mm Φ x 50 mm long were used to determine the rapid chloride permeability. The rapid chloride permeability test procedure was applied at 7, 14, 28, 90 and 180 days. To create saturated surface dried condition before the sample being tested, they were treated in the same way as the samples for porosity as described previously. To reduce the number of samples in this investigation, after the measurement had been taken for oxygen permeability and porosity, the same samples were tested for rapid chloride permeability.

The procedure and set-up for for measuring the Rapid Chloride Permeability of concrete was described by *Lynsdale* (1989) and is as follows. The experimental set-up used for this investigation is shown in Figure 7.14. The experimental set-up consists of 4 perspex cells where 4 samples are housed, a power supply, a digital voltmeter, and a computer control data acquisition system. The perspex cell consists of two reservoirs each capable of holding 250 ml of chemical solution and a 100 mm diameter copper mesh electrode. The sample is covered by an elastic membrane and fitted between the two reservoirs and properly sealed and tightened. The solutions used were a 3% (by wt.) sodium chloride solution (used as the anode) in one reservoir, the other a 0.3 N sodium hydroxide solution (used as the cathode). The concentrations of these two solution were found to provide equal conductivity (*Whiting*, 1981). Each cell was connected to a power supply, Coutant ASD 1000, capable of delivering 60 Volt dc at 10 Ampere. A digital voltmeter was used for the measurement of potential difference across a shunt. A computer interfaced with an intelligent multi-function instrument, MFI 1010 manufactured by CIL UK, for taking the measurements

controlled the data collection. The MFI unit took two hundred readings from each operational cell every 5 minutes and registered the average as a result. The unit was set to monitor changes in potential across four shunts, one for each cell, the rating of which was such that reading of 0.001 mV across the shunt represented a current of 0.1 mA passing through the sample (*Cabrera and Lynsdale*, 1988b: *Lynsdale*, 1989). A total electric charge passed during 6 hours, in Coulombs, was related to chloride ion penetration and expressed as the chloride permeability index (C_{ip}). A ranking of chloride permeability based on charge passed, in Coulombs, has been reported (*Whiting*, 1981) as can be seen in Table 7.1.

7.4.2 Results and Discussion

The results for rapid chloride permeability test (RCPT) for the OPC, OPC/slag and alkali-activated slag concrete with w/c ratio of 0.48 under water and dry curing conditions at various ages are illustrated in Figures 7.15 – 7.19.

7.4.2.1 Effect of slag replacement

The results shown in Figure 7.15 for the water cured mixes show that CM2 gave higher results than SLG60 in all ages. The RCPT values at 7 days are 2490 and 1650 Coulombs for CM2 and SLG60 respectively, decreasing with age to reach 1811 and 690 Coulombs at 182 days. These values indicate low chloride ion penetrability for CM2 and very low chloride ion penetrability for SLG60 after 28 days according to the AASHTO test classification (Table 7.1).

Similarly the results in Figure 7.16 indicate that SLG60 had lower chloride permeability than CM2 under dry curing condition with values of 1864 Coulombs at 7 days decreasing to 852 Coulombs at 182 days, while the values for CM2 were 2900 at 7 days and decreasing to a value around 2500 after 182 days.

This clearly demonstrates that the incorporation of ggbs as a replacement for OPC leads to a reduction in RCPT values.

7.4.2.2 Effect of Na_2O dosage on RCPT results of AAS concrete

It can be noticed from the results presented in Figure 7.15 that Na_2O dosage of the activator plays a role influencing RCPT values for AAS concrete mixes. Comparing SS4 (with Na_2O = 4%) to SS6 (with Na_2O = 6%) indicate that from 7 to 90 days SS6 gave the higher result with the difference between the values decreasing with age until SS6 gave the lower result at 182 days. Similarly it can be noted that MET6 (with Na_2O = 6%) gave results higher than MET4 (with Na_2O = 4%) decreasing with age until it gave lower results from 90 days onward.

The AAS concrete gave generally lower RCPT results in comparison with the control mix CM2 except for the MET6 mix at the first 28 days.

The increase in RCPT results with the higher Na_2O dosage at the early ages is not an indication of the low quality of the concrete, but it directs attention to a shortcoming in the test itself. The test measures the current passed and not the actual permeability of the concrete. Hence the presence of high concentration of alkalis probably gives misleading results. At later ages the alkalis are supposedly bound in the hydration products and this leads to reduction in their influence on the results in addition the effect of hydration progress on the permeability.

Studying Figure 7.16 indicates the same problem with the test at a larger scale. Some fluctuation in the results was probably due to the availability of unreacted alkalis in variable concentration and the cracking due to drying of the specimens.

7.4.2.3 Effect of Silica Modulus of the activator

It can be noted from the results of Figure 7.15 that with AAS concrete having the same Na_2O dosage, the silica modulus M_s has an effect on the chloride permeability. The higher the M_s the lower the RCPT values, thus the SS4 gave lower values than the MET4 and the SS6 gave lower values than the MET6 at all ages.

The results presented in Figure 7.16 which represent the dry cured samples are somewhat fluctuating and do not follow a clear trend. This is probably due to the

cracking and the availability of free alkalis due to the slow hydration with less amount of alkalis bound to the hydration products.

7.4.2.4 Effect of curing

The effect of curing on the control OPC and OPC/slag mixes is demonstrated in Figure 7.17. The dry curing increases the chloride permeability by approximately 20% for CM2 and 34% for SLG60 at 28 days of curing. This shows the higher sensitivity to curing in the concrete incorporating slag.

Figure 7.18 presents the RCPT results for AAS concrete activated with sodium silicate solution with an $M_s = 1.65$. It can be noted that curing has a great effect on these chloride permeability results. Comparing the 28 days results shows that the dry cured SS4 samples gave 3 times higher values than water cured SS4 samples, while the dry cured SS6 samples gave values 6 times higher. This, as discussed earlier, is an indication of not only a drop-in concrete quality but to a larger extent the abundance of alkalis in the concrete matrix.

The same can be said for the AAS concrete activated by sodium metasilicate ($M_s = 1.0$) where the results in Figure 7.19 show values higher than normal in the early ages for water cured samples. Dry cured samples show an increase in values of chloride permeability and erratic fluctuation in the results.

7.4.2.5 Comparison with Literature and test evaluation

Douglas et Al. (1992) reported RCPT results on AAS concrete mixes with w/c of 0.48, activated with water-glass having an $M_s = 1.47$, and moist cured. Their results indicate good resistance to chloride penetration where RCPT values range from 1311 to 2547 Coulombs at 28 days and from 676 to 1831 Coulombs at 90 days. They noted also that the lower the dosage of activator the lower the RCPT values. They suggested that the reason for that is the effect of silicate-slag ratio on the pore size distribution and even the microstructure of the hardened concrete, but this comes in contradiction with the compressive strength results for the same concretes where the lower dosage

gave lower compressive strength but higher chloride penetration resistance, while the higher dosage gave higher strength but lower chloride penetration resistance. Therefore, the role of alkali in increasing the RCPT values is clear.

Shi (1996) presented RCPT results for AAS mortars using water-glass as an activator. These results were very high for the early ages 20000 Coulombs at 3 days reducing to 12000 Coulombs at 7 days and further to a value around 5000 Coulombs at 28 and 90 days. He arrived at a conclusion that the chemistry of the pore solution contributes more than the pore structure to the rapid chloride permeability test results.

RCPT is widely used despite its empirical approach and it is accepted that it is somehow related to permeability (*Hooton 1989*). On the other hand it has been criticized by many researchers over the years because of its high variability, difficulty in evaluating high-quality concrete due to very low values obtained, difficulty in evaluating low-quality concrete due to excessive heat generation, and mainly because the test measures electrical conductivity through concrete, which is not directly related to diffusion (*Buenfeld and Newman* 1987; *Roy, Malek and Licastro* 1987; *Hooton* 1989; and *Zhang and Gjorv* 1991).

Shane et al. (1999) commented that the technique does not distinguish between chloride and hydroxyl ions as the charge carriers. Furthermore, the high voltage may cause microstructural damage during the test. *Shi et al.* (1996) concluded that the replacement of portland cement with supplementary cementing materials, such as silica fume, can reduce the electrical conductivity of concrete more than 90 percent due to the change in the chemical composition of the pore solution, which has little to do with the transport of chloride ions in concrete. They stated that it is not correct to use the passed charge to evaluate the rapid chloride permeability of concrete with supplementary cementing materials. *Mackechnie and Alexander* (2000) have supported these criticisms when comparing the RCPT, Nordic chloride permeability test and chloride conductivity test. They found that RCPT conducted at early ages could not be expected to fully quantify all the influencing factors.

These criticisms of the test are supported by the results obtained with AAS concrete in this investigation and discussed above. Taking the point raised by *Mackechnie and*

Alexander (2000) regarding the age at testing, the results of the investigation support the proposition that the RCPT can probably be adopted for later ages when most of the alkalis are bound to the hydration products.

7.5 Relationship between Porosity and Compressive Strength

It is generally accepted that there is a relation between compressive strength and porosity. An equation representing that relation was suggested by *Roy and Gouda (1973)* which is in the following form:

$$P - P_0 \exp(-Kf_c) \qquad (7.4)$$

Where: P - is porosity

P_0 - is zero-strength porosity

f_c - is compressive strength

K - is a constant.

The results of porosity and compressive strength obtained in this work on the different mixes having w/c ratio of 0.48 under water curing are plotted in Figure 7.20 . All the mixes show the same overall trend resulting in a set of almost parallel straight lines. The compressive strength increases rapidly with the decrease in porosity.

The equations describing the relation between porosity and compressive strength which were arrived at by regression are as follows:

$$P = 17.2e^{-0.0118 f_{cw}}$$

$R^2 = 0.97$ (Control mix) (7.5)

$$P = 16.18e^{-0.0095 f_{cw}}$$

$R^2 = 0.95$ (SLG60) (7.6)

$$P = 19.59e^{-0.0094 f_{cw}}$$

$R^2 = 0.88$ (SS4) (7.7)

$$P = 20.14e^{-0.0067 f_{cw}}$$

$R^2 = 0.93$ (SS6) (7.8)

$$P = 16.53e^{-0.0067 f_{cw}}$$

$R^2 = 0.92$ (MET4) (7.9)

$$P = 20.52e^{-0.0094 f_{cw}}$$

$R^2 = 0.88$ (MET6) (7.10)

The above equations have reasonable correlations; therefore a relationship exists between compressive strength and porosity. The trend of all the mixes is similar, as the strength increases and porosity reduces as expected.

7.6 Relationship between Chloride Permeability and Compressive Strength

An attempt has been made to arrive at a possible correlation between compressive strength and chloride permeability. The compressive strength results of all concrete mixes with w/c ratio of 0.48 under water curing were plotted against their respective chloride permeability values for all ages investigated as shown in Figure 7.21. Clear bands of results can be distinguished. One presenting the control mix CM2, a second presenting the slag mix SLG60, a third presenting SS4 and MET4 mixes, and a fourth presenting SS6 and MET6 mixes.

Generally the trend is that an increase in the compressive strength is accompanied by a decrease in the chloride permeability values. But it is not possible to have one equation representing all the various concretes. Looking at the results of the MET6 concrete mix, with 6% Na_2O, it is noticed that for a compressive strength of 54 MPa the corresponding chloride permeability value is around 4833 Coulombs while for the same compressive strength the control mix CM2 gave a chloride permeability value of 1811 Coulombs. The MET6 mix ends-up giving lower chloride permeability than the control mix at later ages. The reasoning for this was discussed in a previous section as a misleading result due to the high concentration of alkalis.

Figures 7.22 and 7.23 show the above-mentioned groups of results in a clearer way and the relations arrived at are as follows:

$$C_{lp} = 7776e^{-0.0273 f_{cu}}$$

$R^2 = 0.83$ (Control mix) (7.11)

$$C_{ip} = 3676e^{-0.0369 f_{cu}}$$

$$R^2 = 0.83 \qquad \text{(SLG60 mix)} \qquad (7.12)$$

$$C_{ip} = 14330e^{-0.0469 f_{cu}}$$

$$R^2 = 0.88 \qquad \text{(AAS 4\% } Na_2O\text{)} \qquad (7.13)$$

$$C_{ip} = 75092e^{-0.0535 f_{cu}}$$

$$R^2 = 0.95 \qquad \text{(AAS 6\% } Na_2O\text{)} \qquad (7.14)$$

7.7 Conclusions:

The main conclusions drawn from the present investigation are summarised as follows:

1. Replacing 60% of OPC by ggbs results in an increase in porosity compared to the OPC mix of the same w/c ratio while it results in lower porosity when compared to OPC mix with the same workability level.

2. The increase of the Na_2O dosage in AAS concrete, where the activator has an M_s = 1.0, results in a decrease in porosity. But in the case of the AAS concrete, with the activator having M_s = 1.65, the porosity increases with increase of the Na_2O dosage.

3. The AAS concrete porosity test results are higher at early ages than the control mix due to the drying effect of preconditioning the specimens at 105 °C.

4. Dry curing increases the porosity of all the concrete mixes.

5. OPC/slag mix with 60% replacement has an oxygen permeability slightly higher than that OPC mix having the same w/c ratio at later ages after 365 days.

6. Pre-drying the specimens at 105 °C resulted in an increase in oxygen permeability of AAS concrete to much higher levels than those of OPC and OPC/slag mixes. This is probably due to micro-cracking caused by drying.

7. Dry curing increases the oxygen permeability.

8. Incorporating slag as a replacement of OPC by 60% results in lower chloride permeability compared to the control OPC concrete.

9. The RCPT gives misleading high results for chloride permeability of AAS mixes especially in the case of high Na_2O dosage at the early ages.

10. Dry curing increases the chloride permeability but the results are very high and variable in the AAS concrete probably due to micro-cracking and the presence of alkalis.

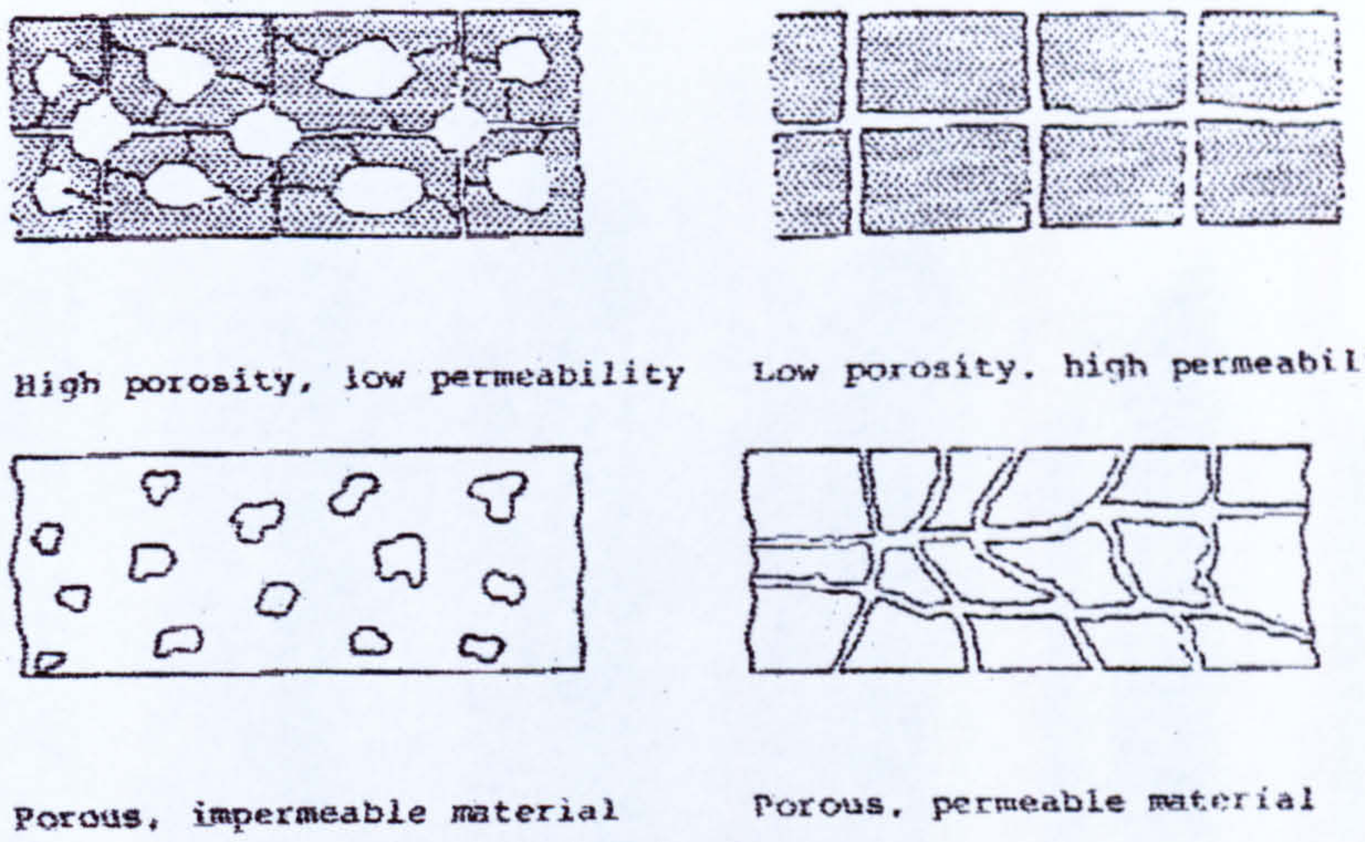

Figure 7.1 Illustration on permeability and porosity (*Bakker*, 1985)

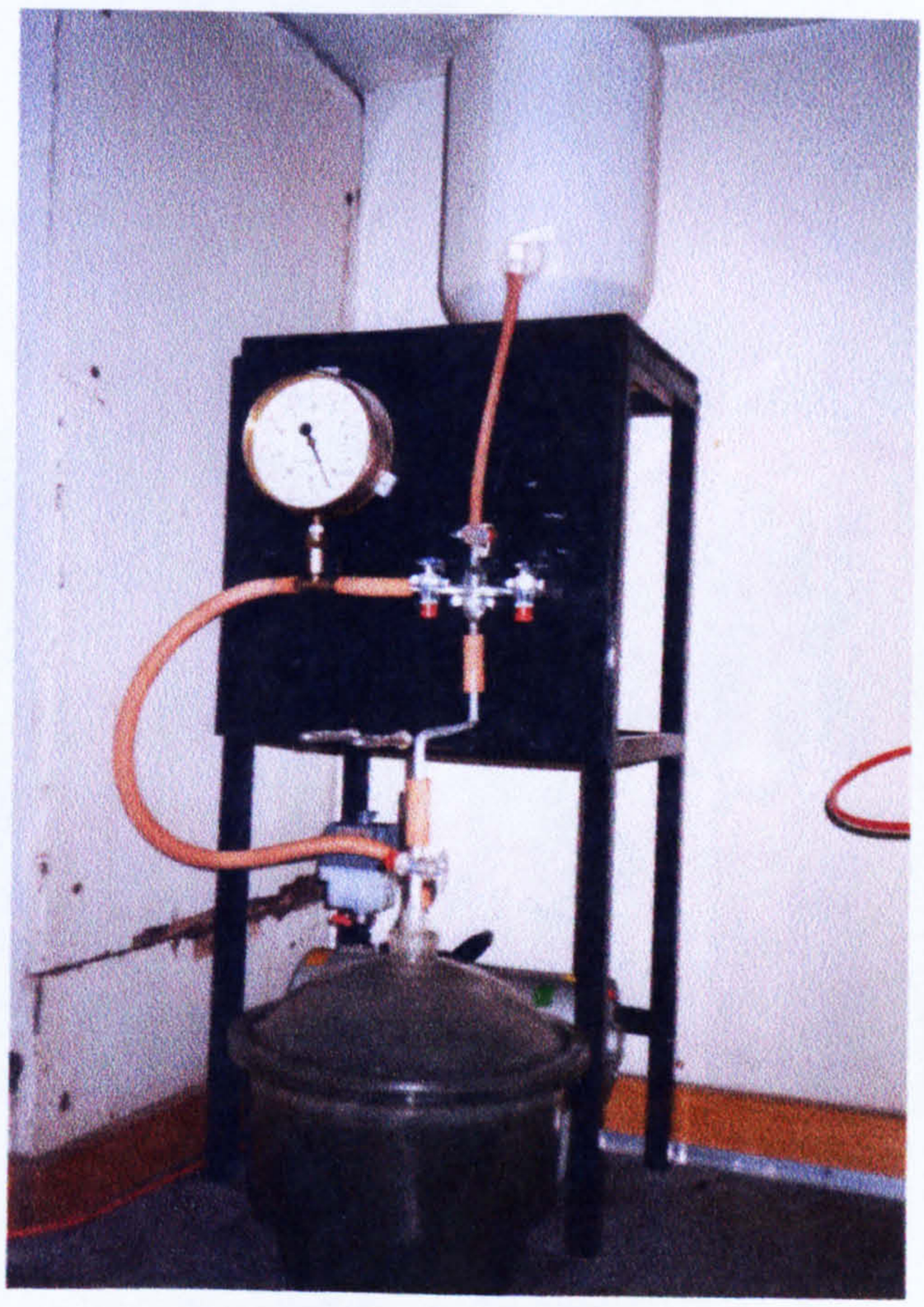

Figure 7.2 Vacuum saturation apparatus used in this investigation

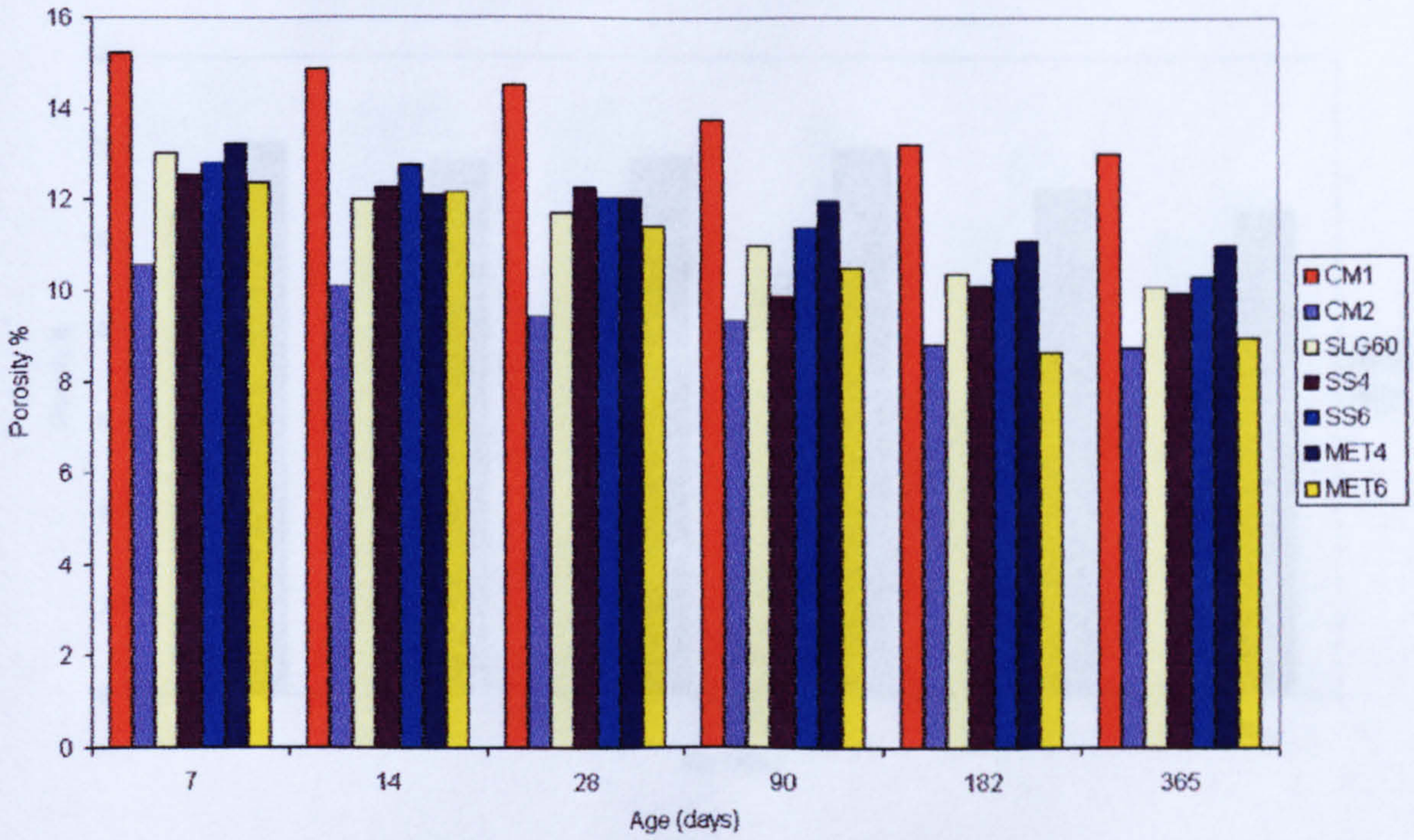

Figure 7.3 Porosity of the different mixes at different ages under water curing condition

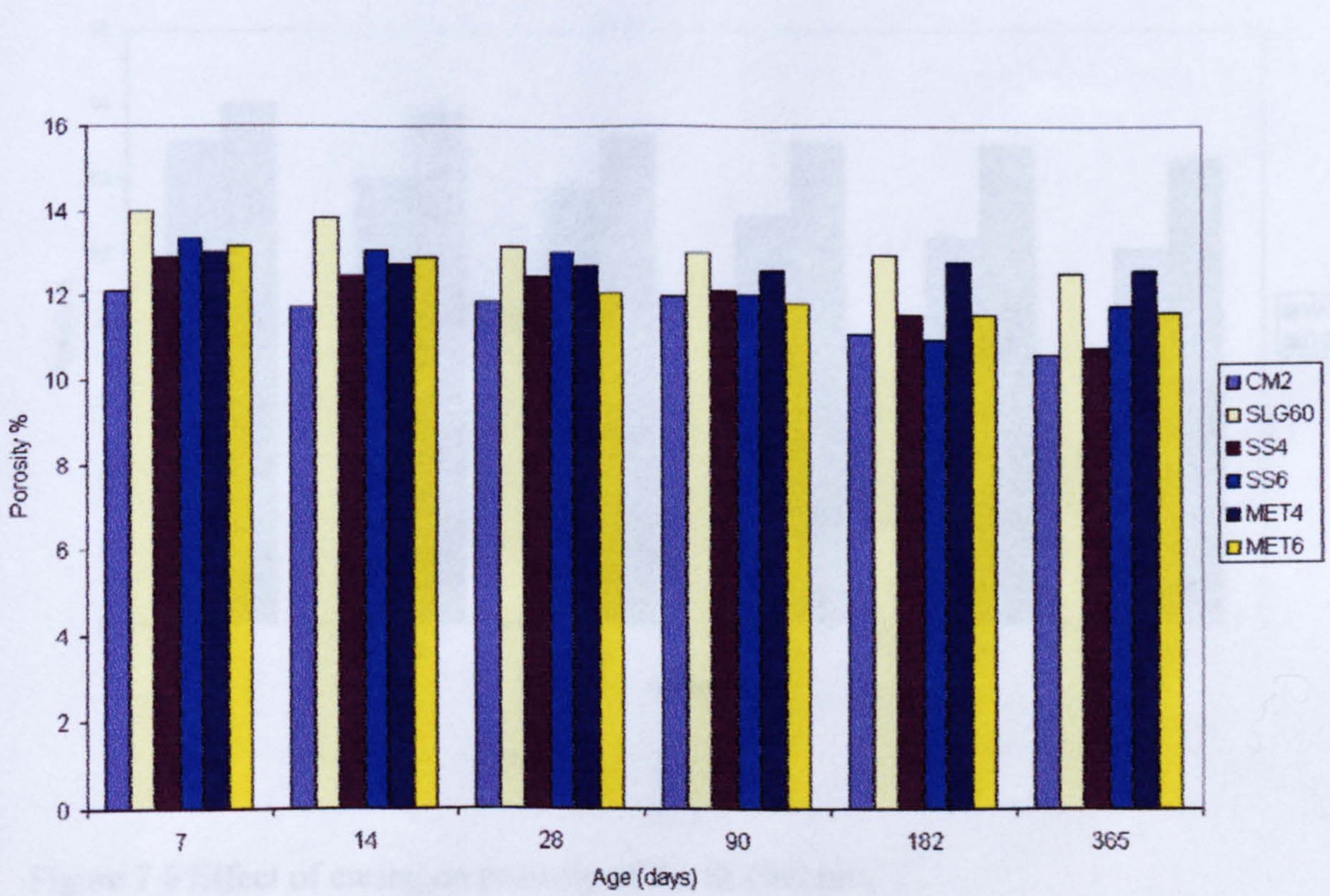

Figure 7.4 Porosity of the different mixes at different ages under dry curing condition

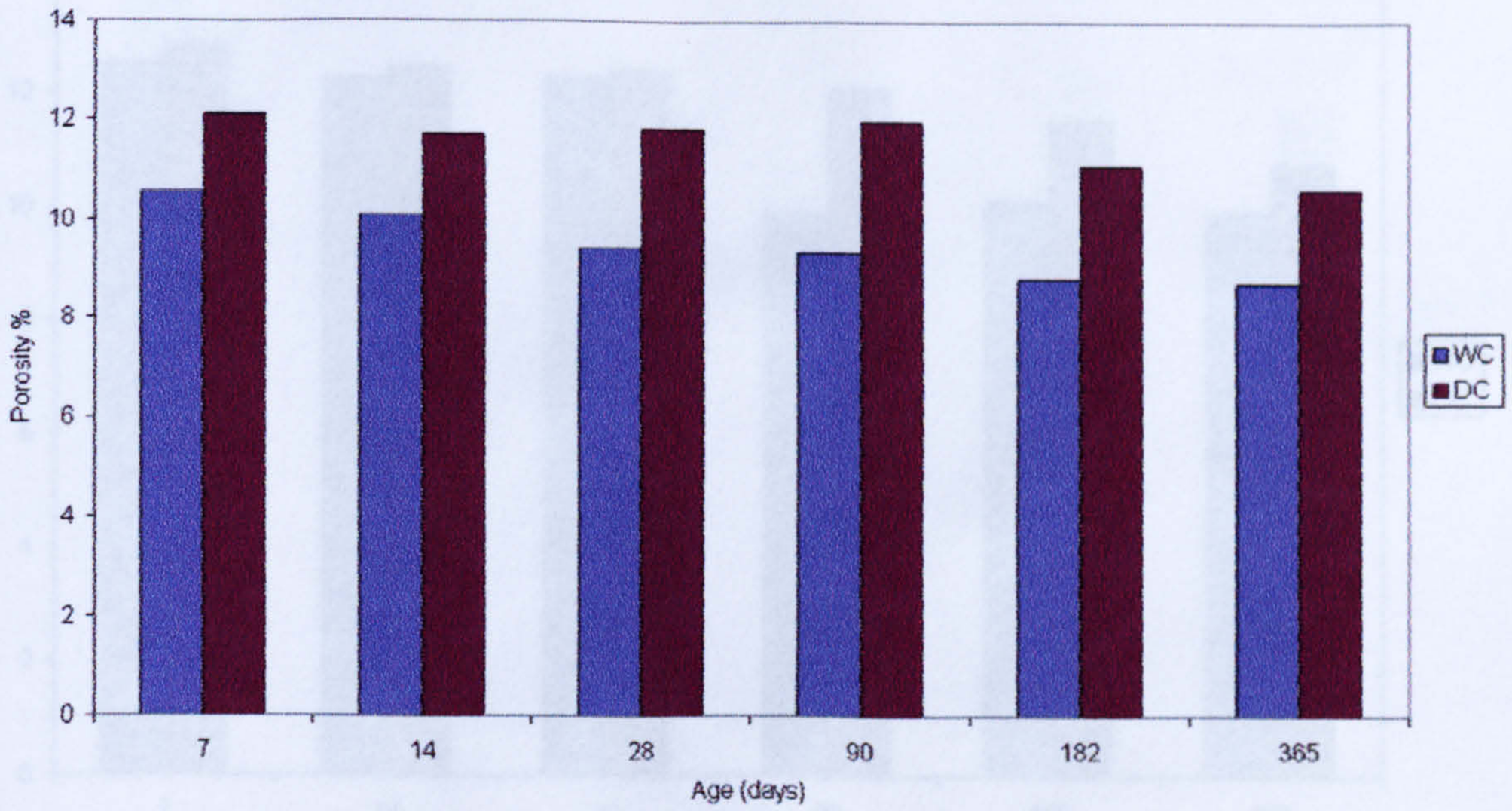

Figure 7.5 Effect of curing on porosity of the CM2 mix

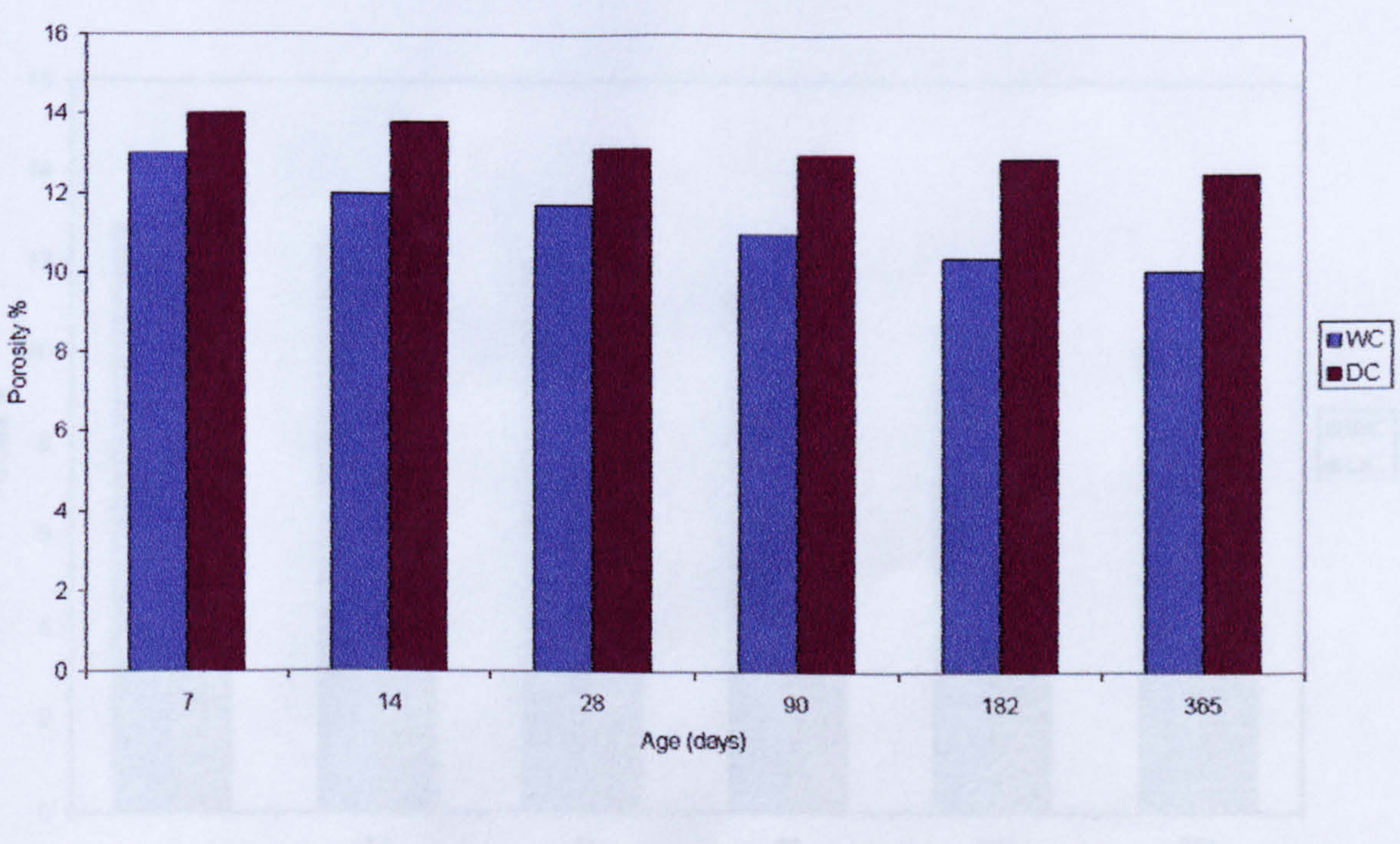

Figure 7.6 Effect of curing on porosity of the SLG60 mix

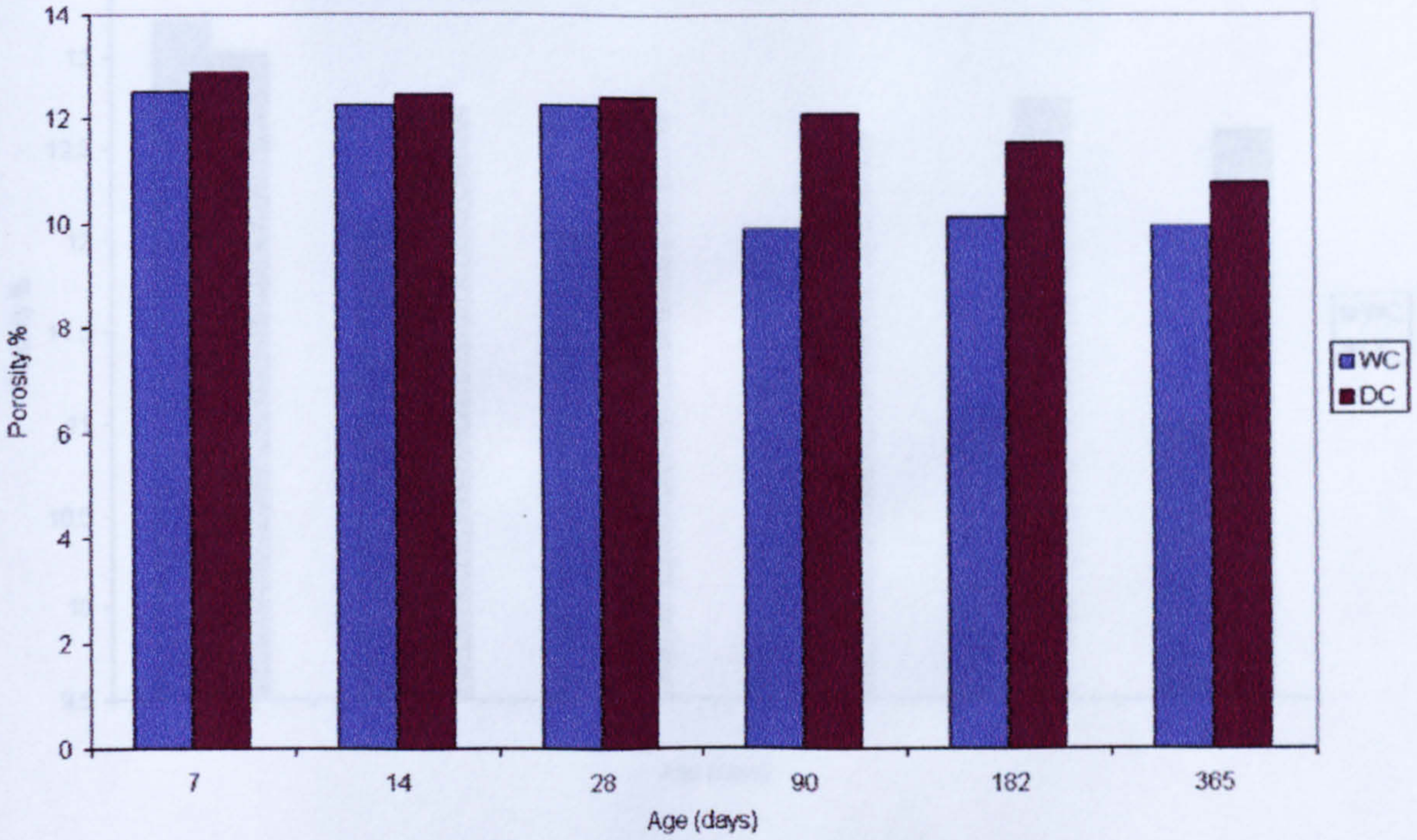

Figure 7.7 Effect of curing on porosity of the SS4 mix

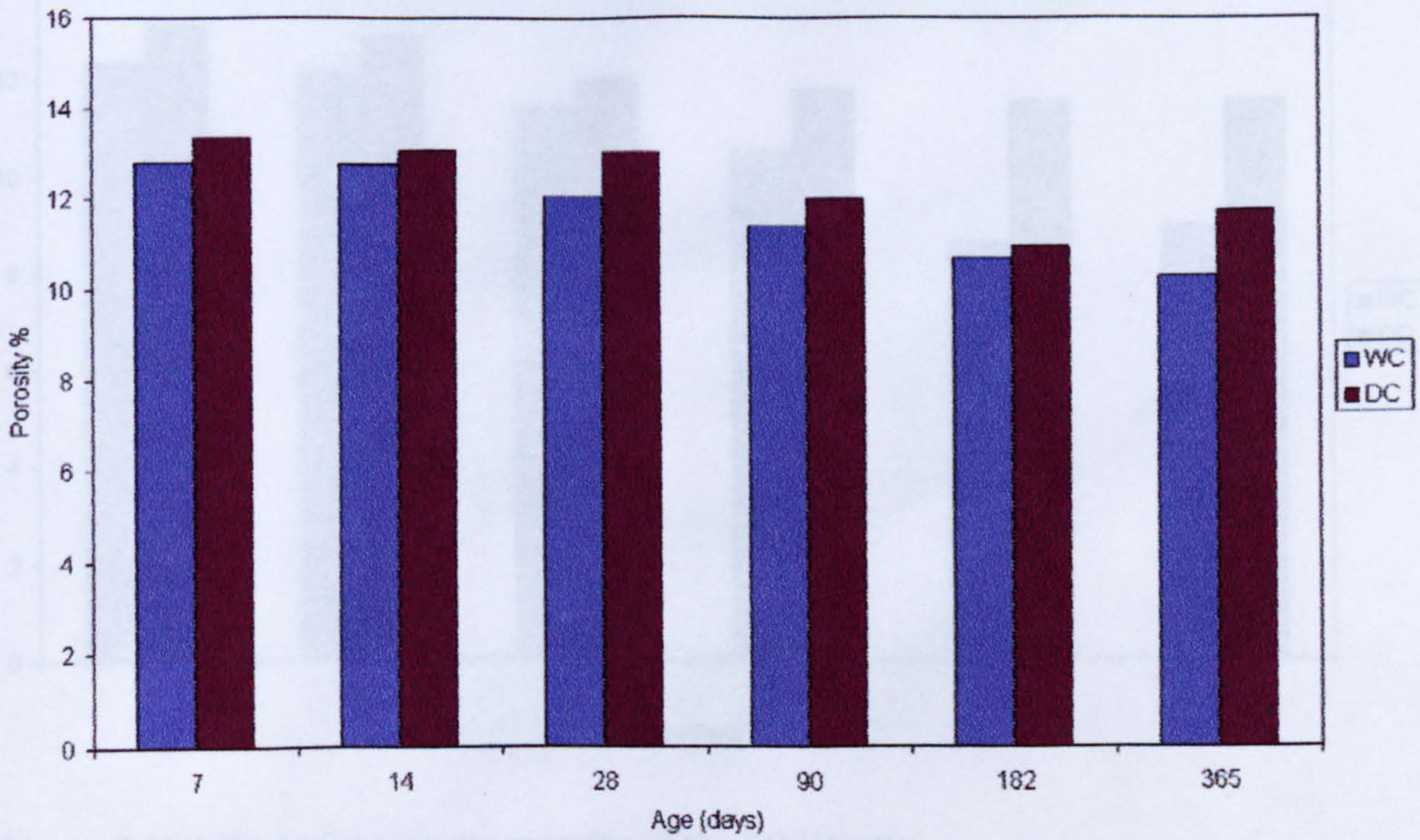

Figure 7.8 Effect of curing on porosity of the SS6 mix

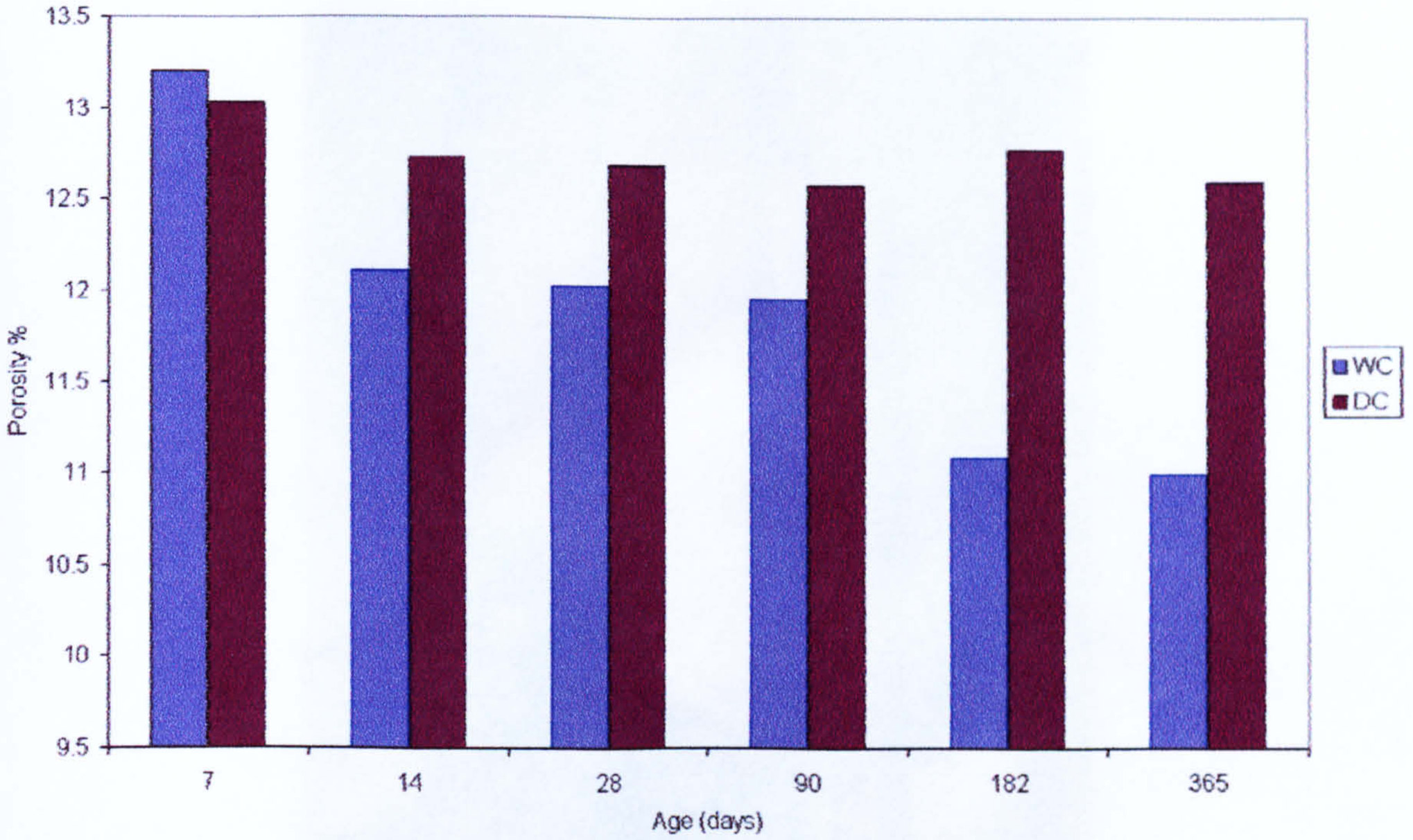

Figure 7.9 Effect of curing on porosity of the MET4 mix

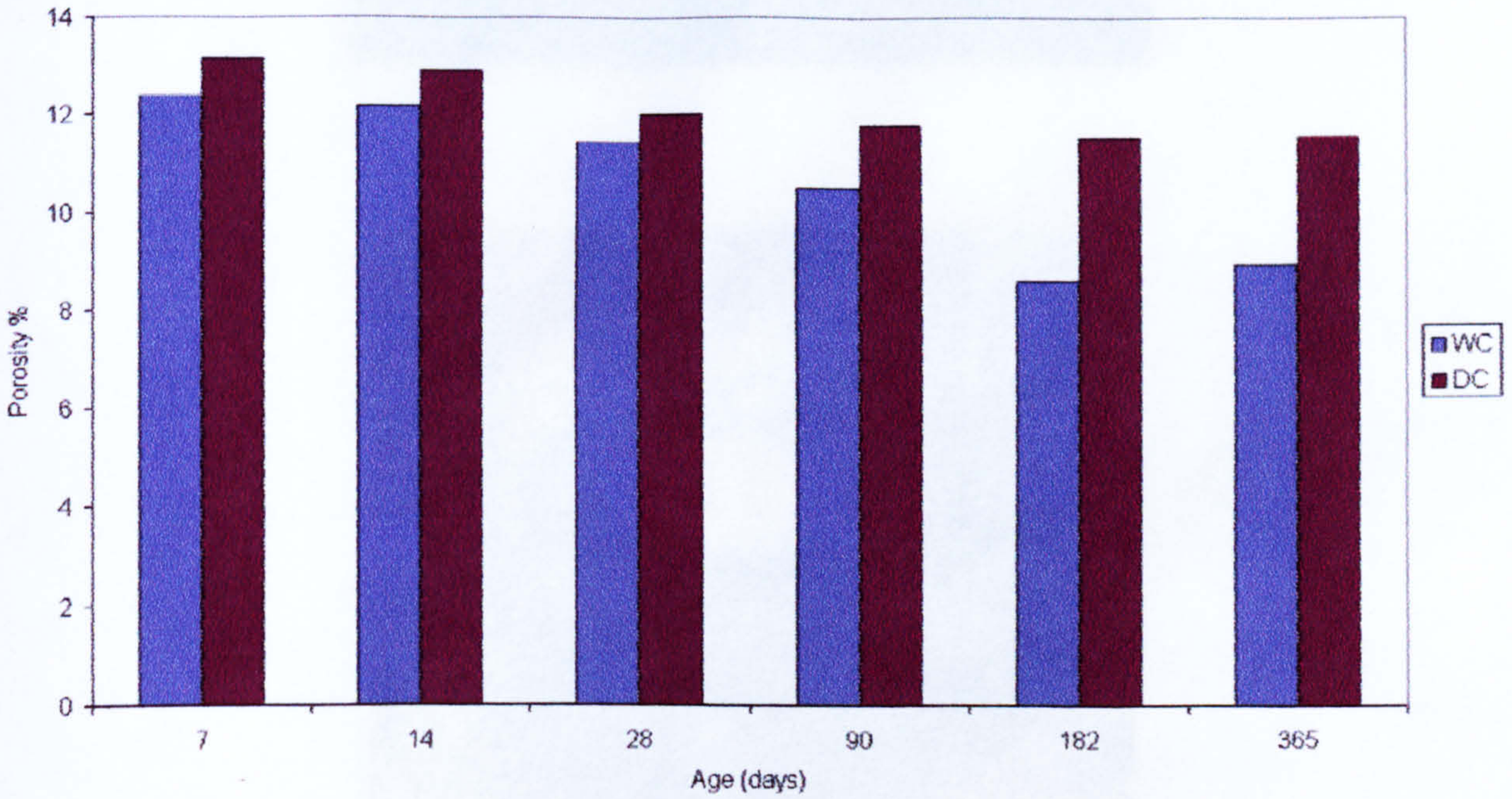

Figure 7.10 Effect of curing on porosity of the MET6 mix

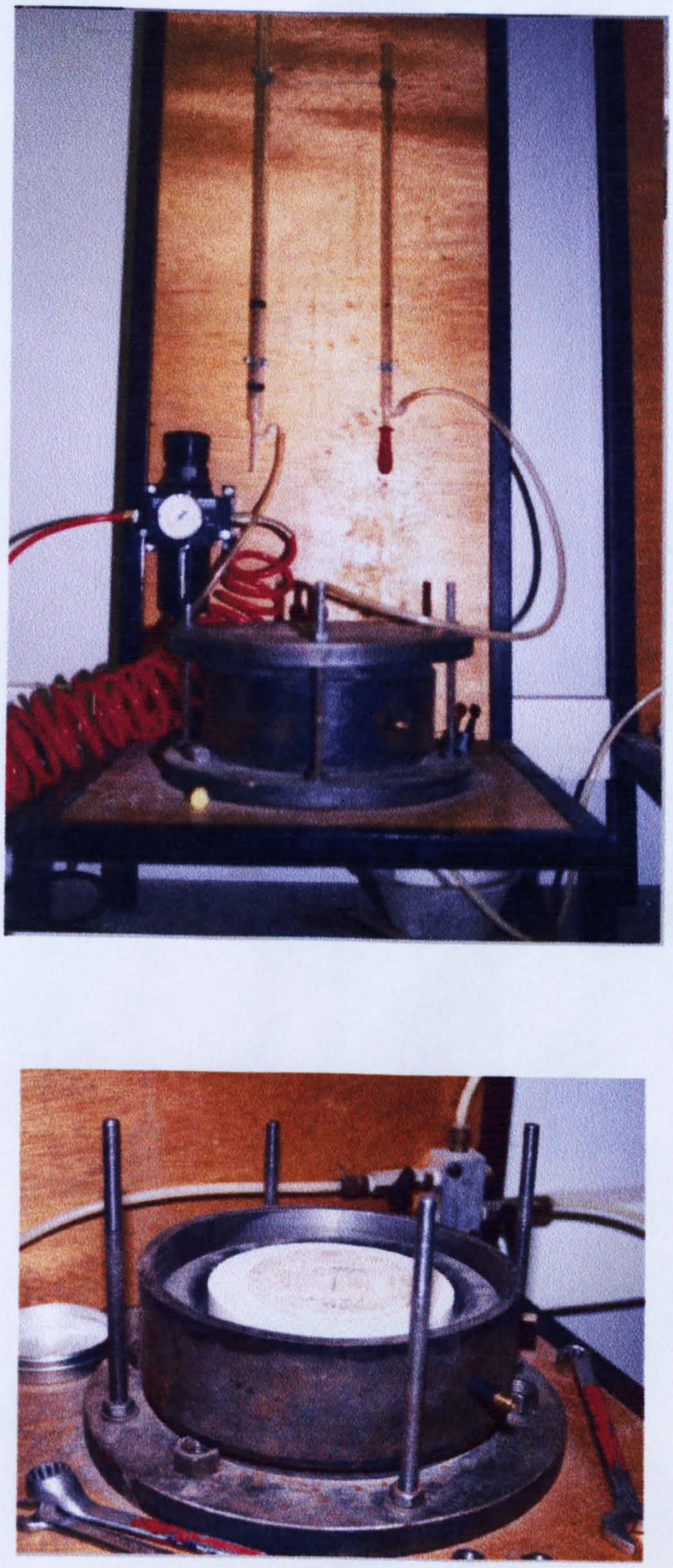

Figure 7.11 Oxygen Permeability Test Set-up

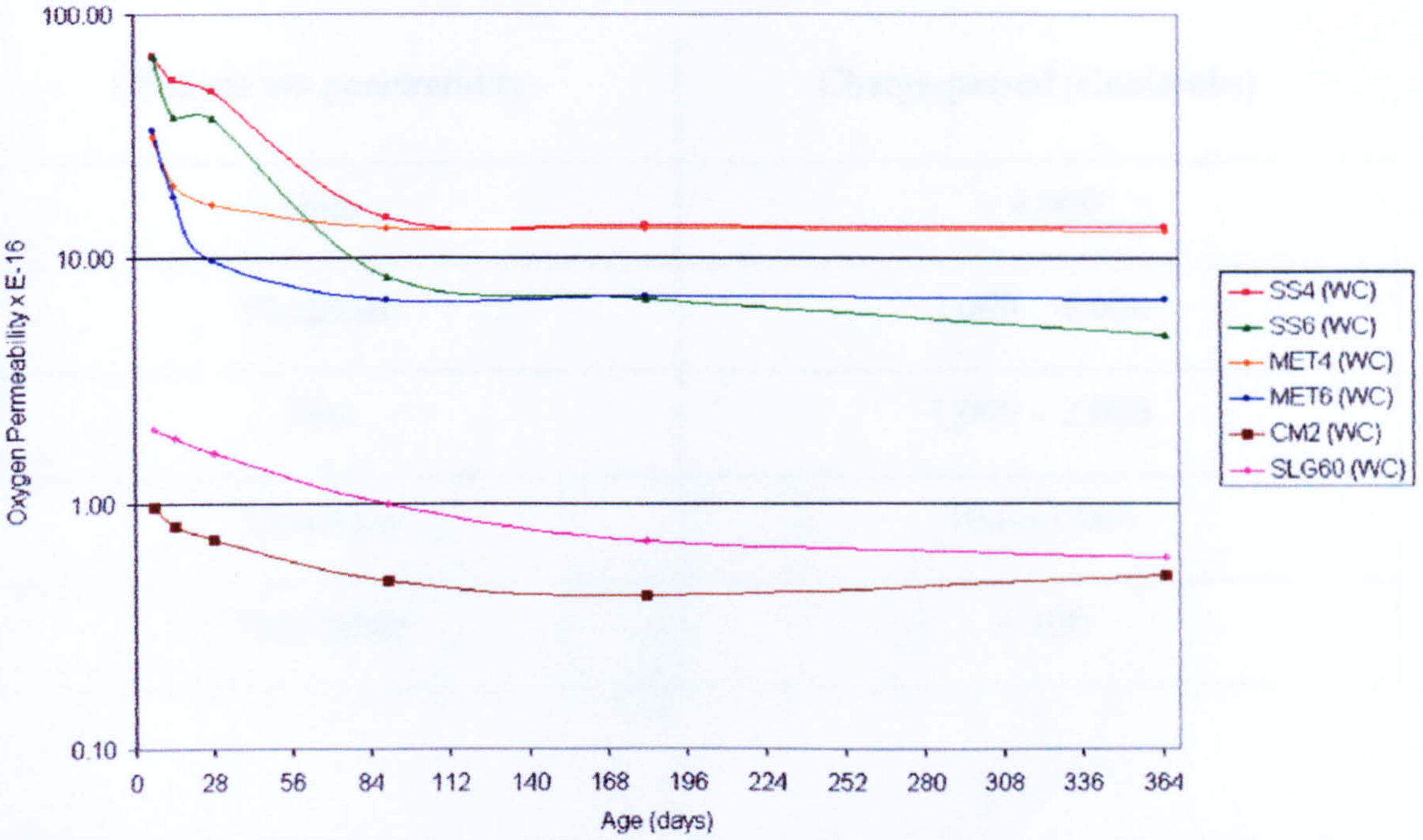

Figure 7.12 Oxygen Permeability of the different mixes under water curing condition

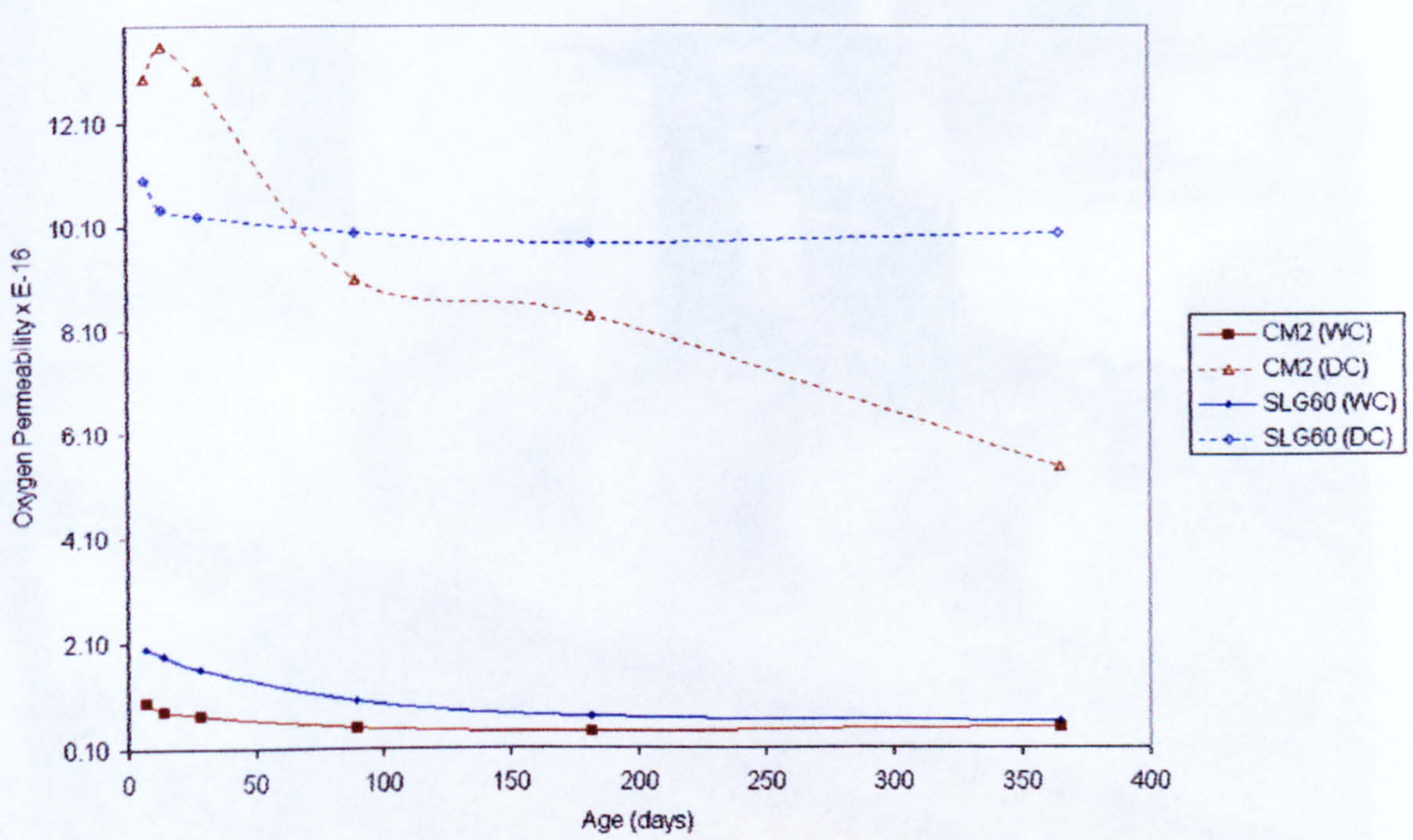

Figure 7.13 Oxygen Permeability of the different mixes under water curing condition

Table 7.1 Chloride ion penetrability in relation to the charge passed (Whiting, 1981)

Chloride ion penetrability	Charge passed (Coulombs)
High	> 4,000
Moderate	2,000 4,000
Low	1,000 – 2,000
Very Low	100 – 1,000
Negligible	< 100

Figure 7.14 Rapid Chloride Permeability Test Set-up

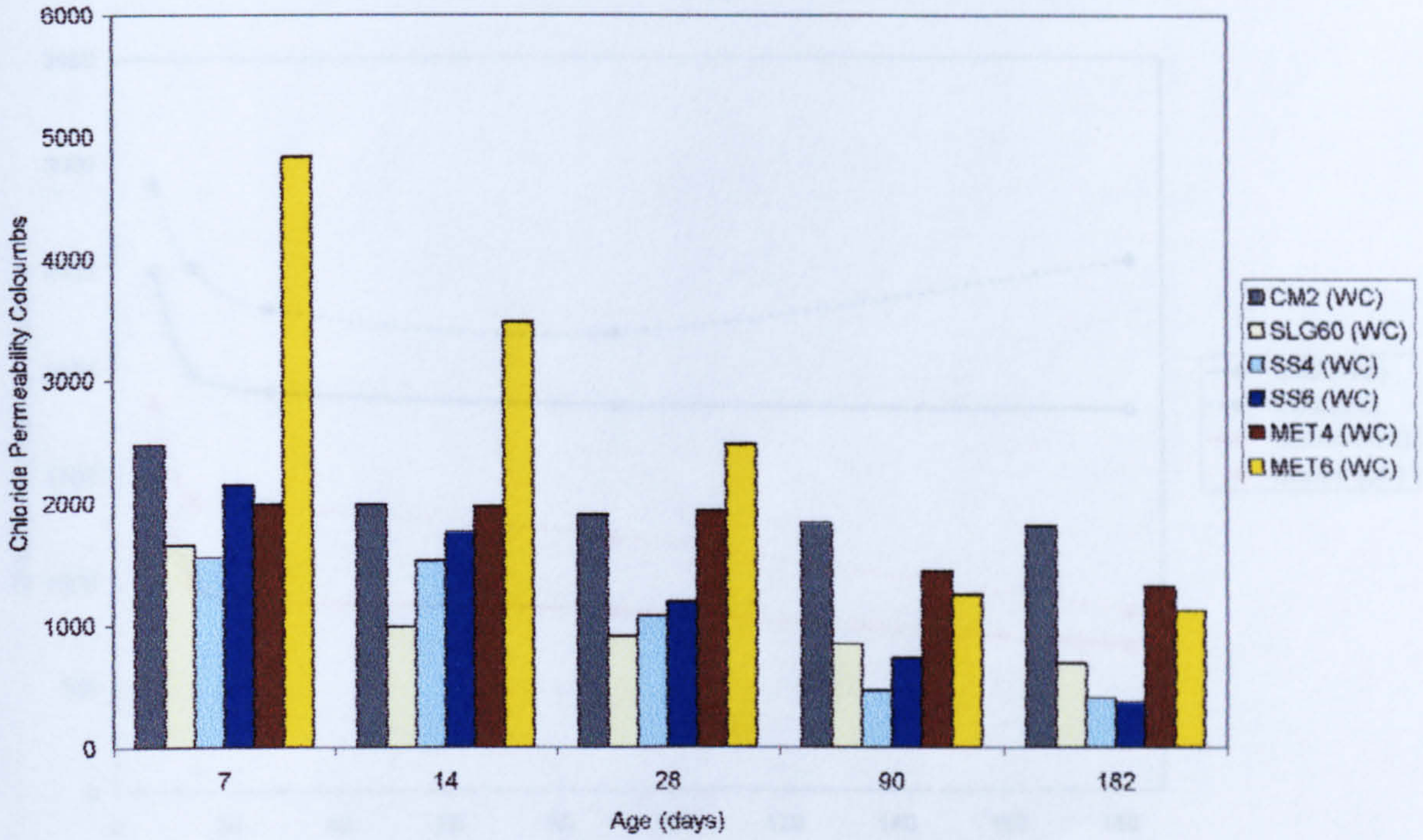

Figure 7.15 Chloride Permeability for the different mixes under water curing

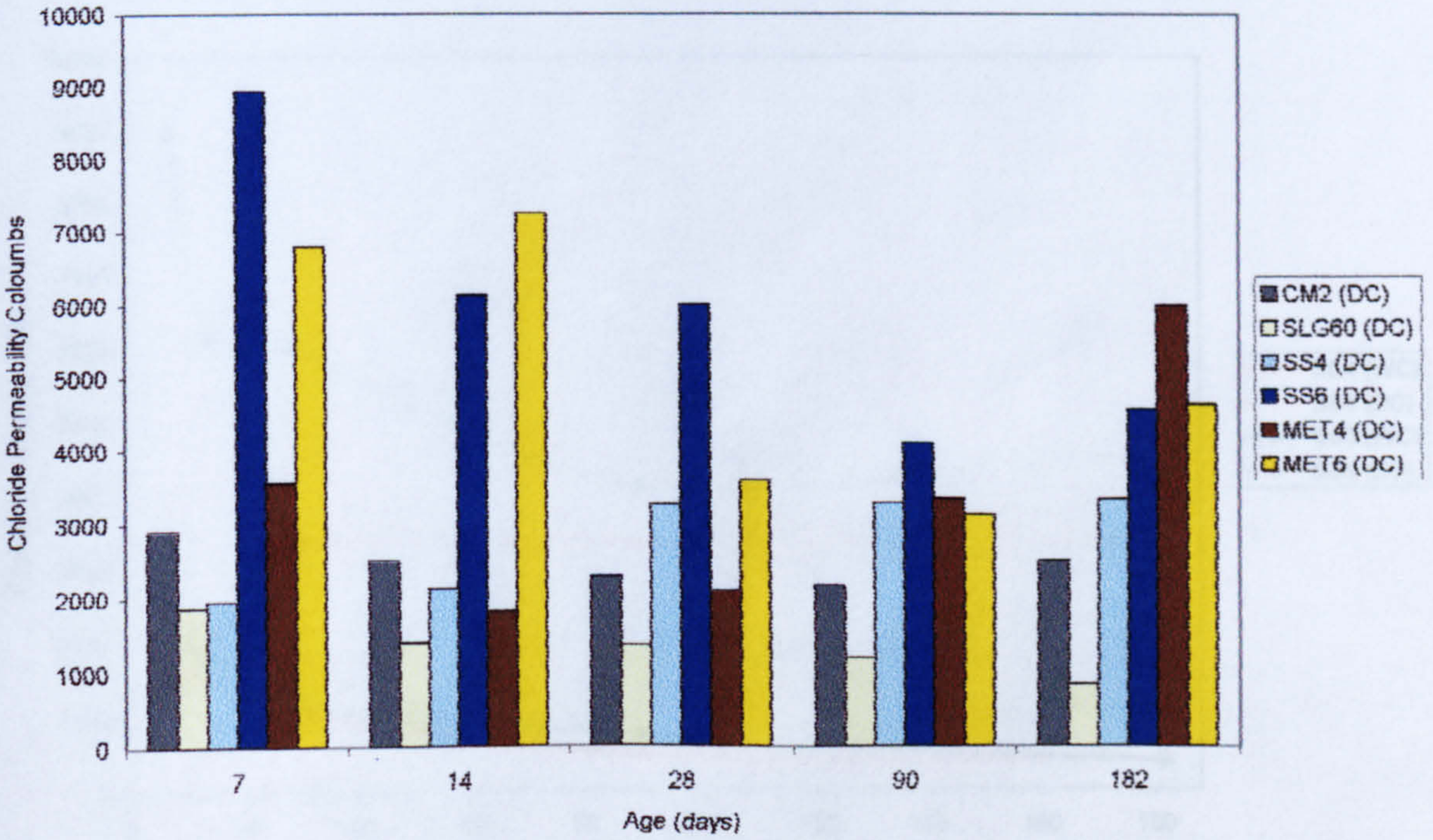

Figure 7.16 Chloride Permeability for the different mixes under dry curing

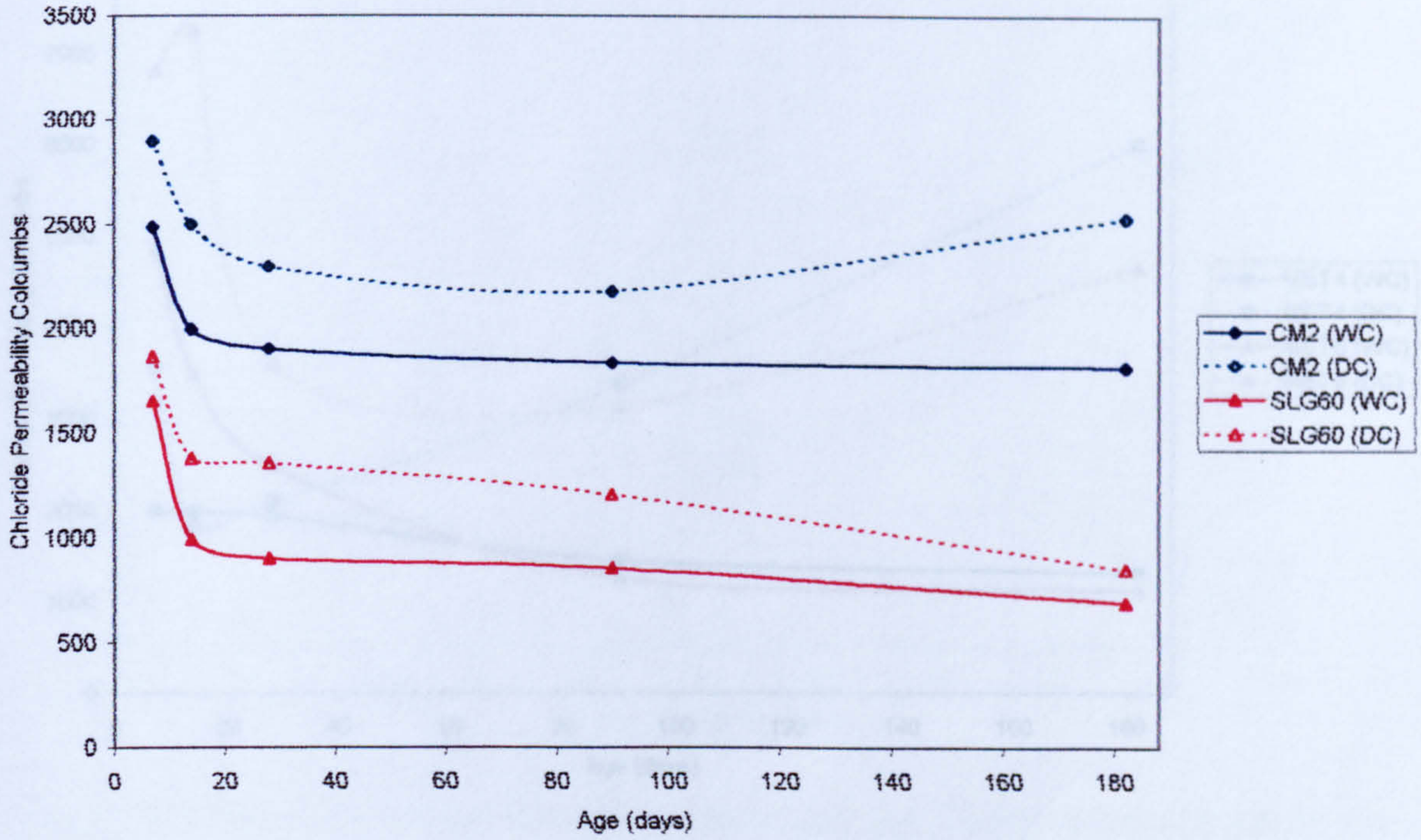

Figure 7.17 Effect of Curing on Chloride Permeability for OPC and OPC/Slag mixes

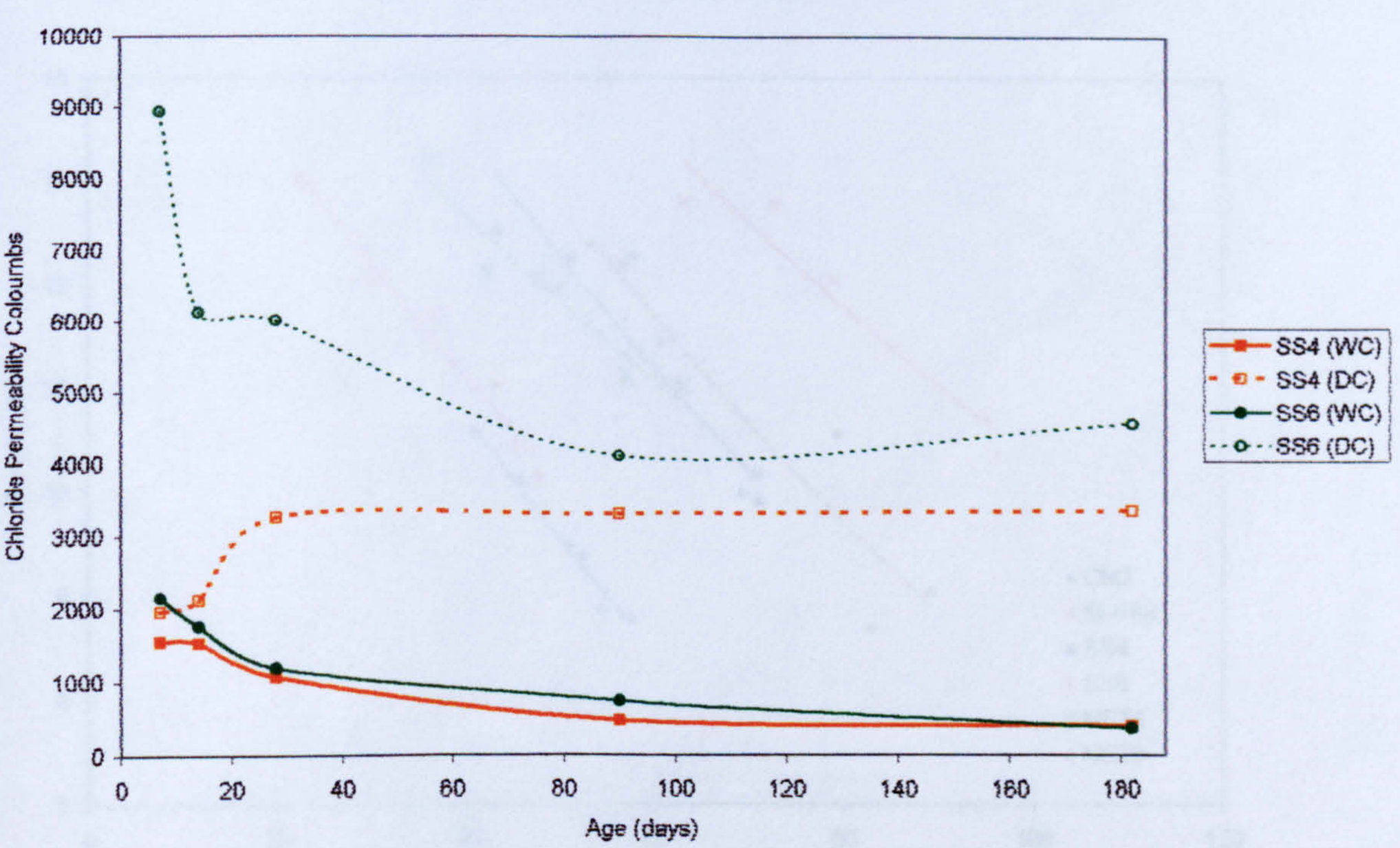

Figure 7.18 Effect of Curing on Chloride Permeability for AAS mixes activated with the water-glass solution activator

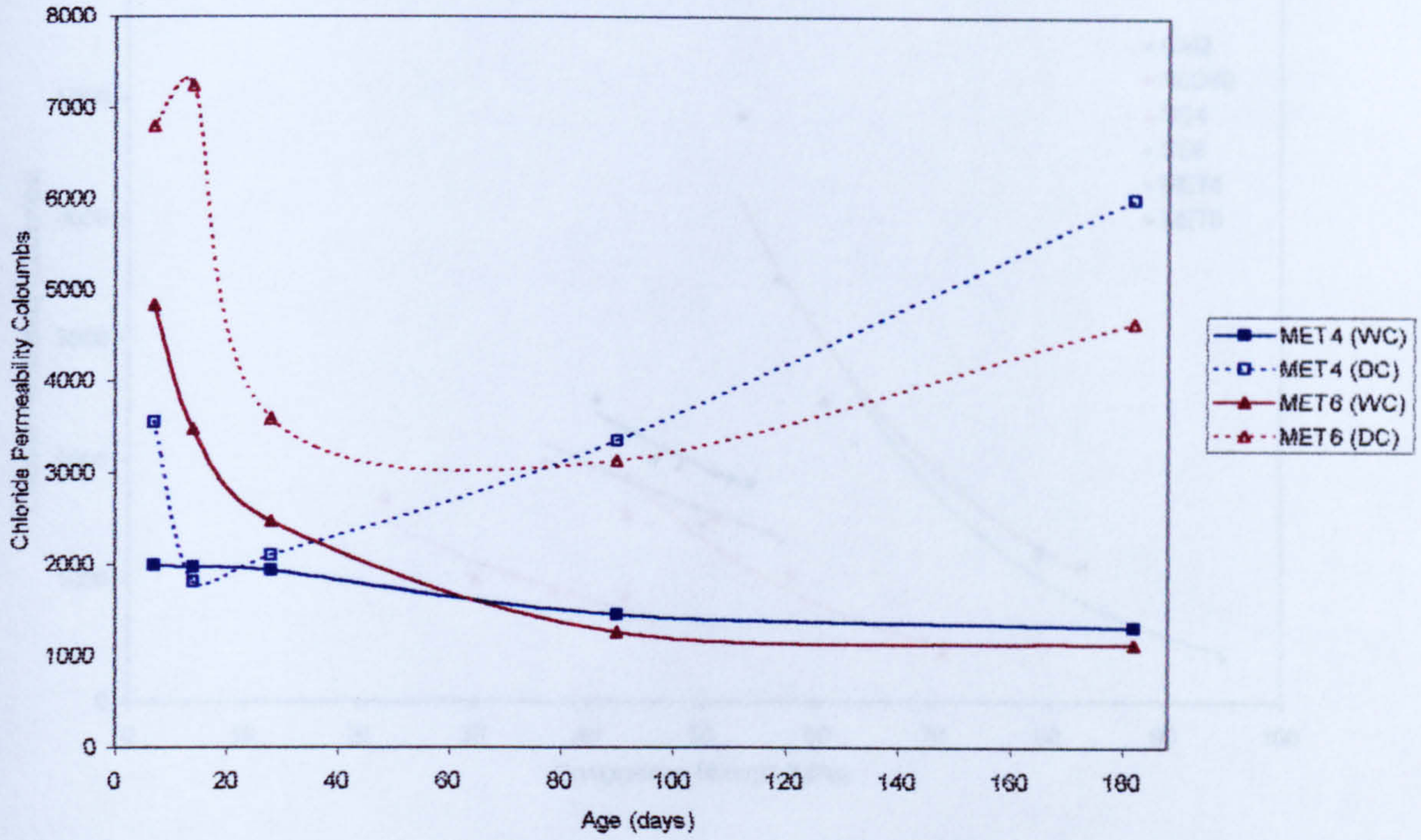

Figure 7.19 Effect of Curing on Chloride Permeability for AAS mixes activated with the water-glass solid activator

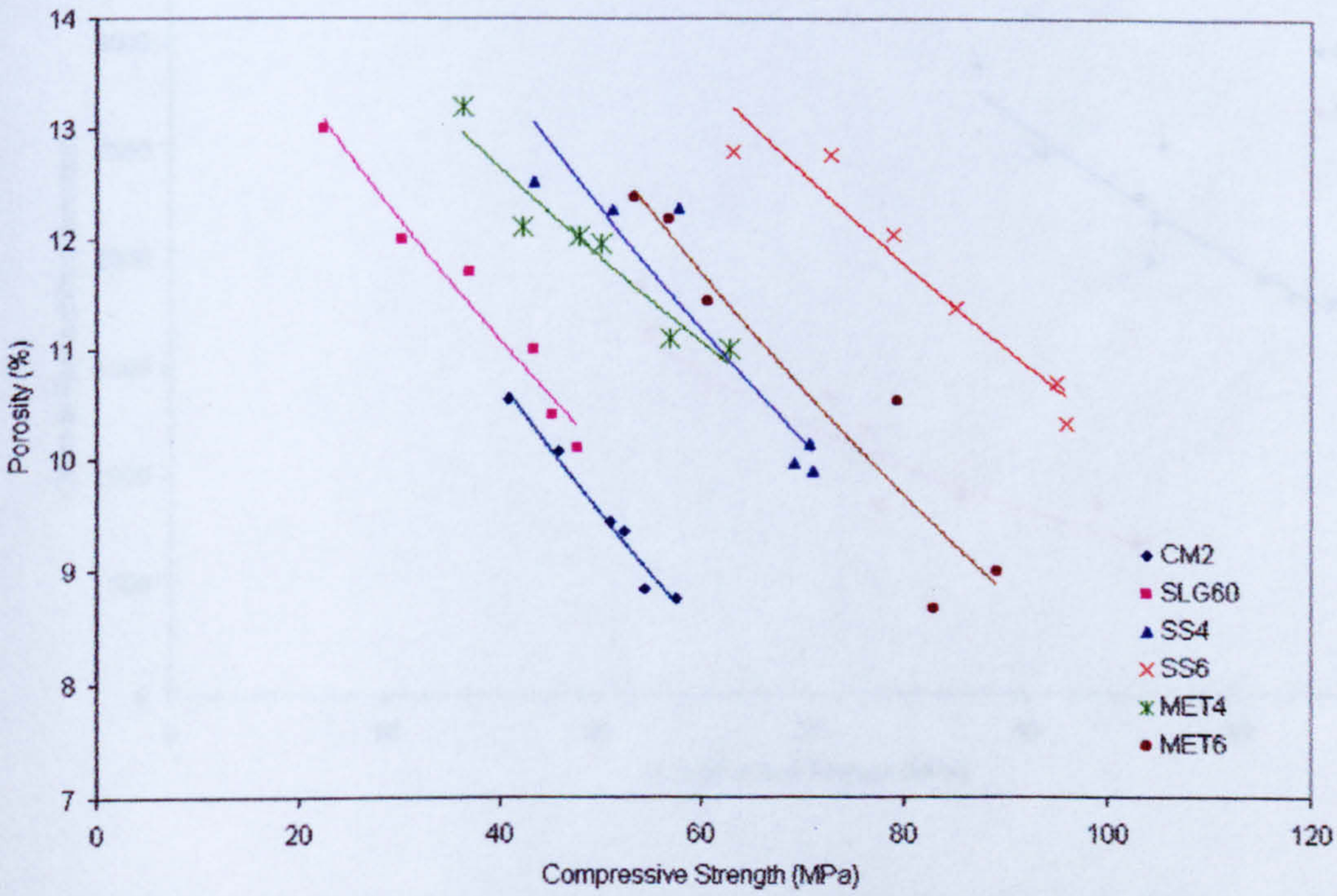

Figure 7.20 Relation between Compressive strength and Porosity

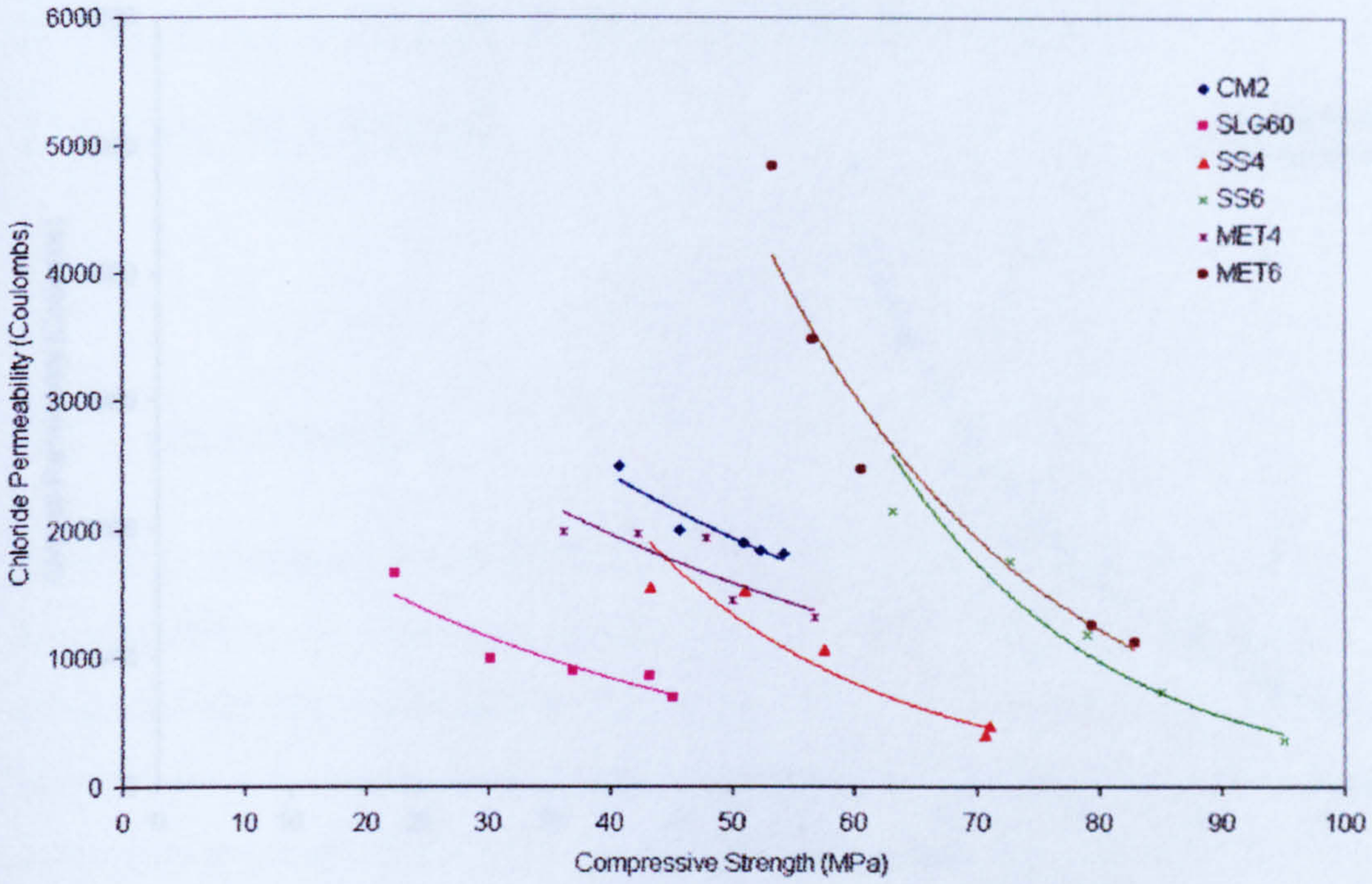

Figure 7.21 Relation between Chloride Permeability and Compressive strength for the different mixes

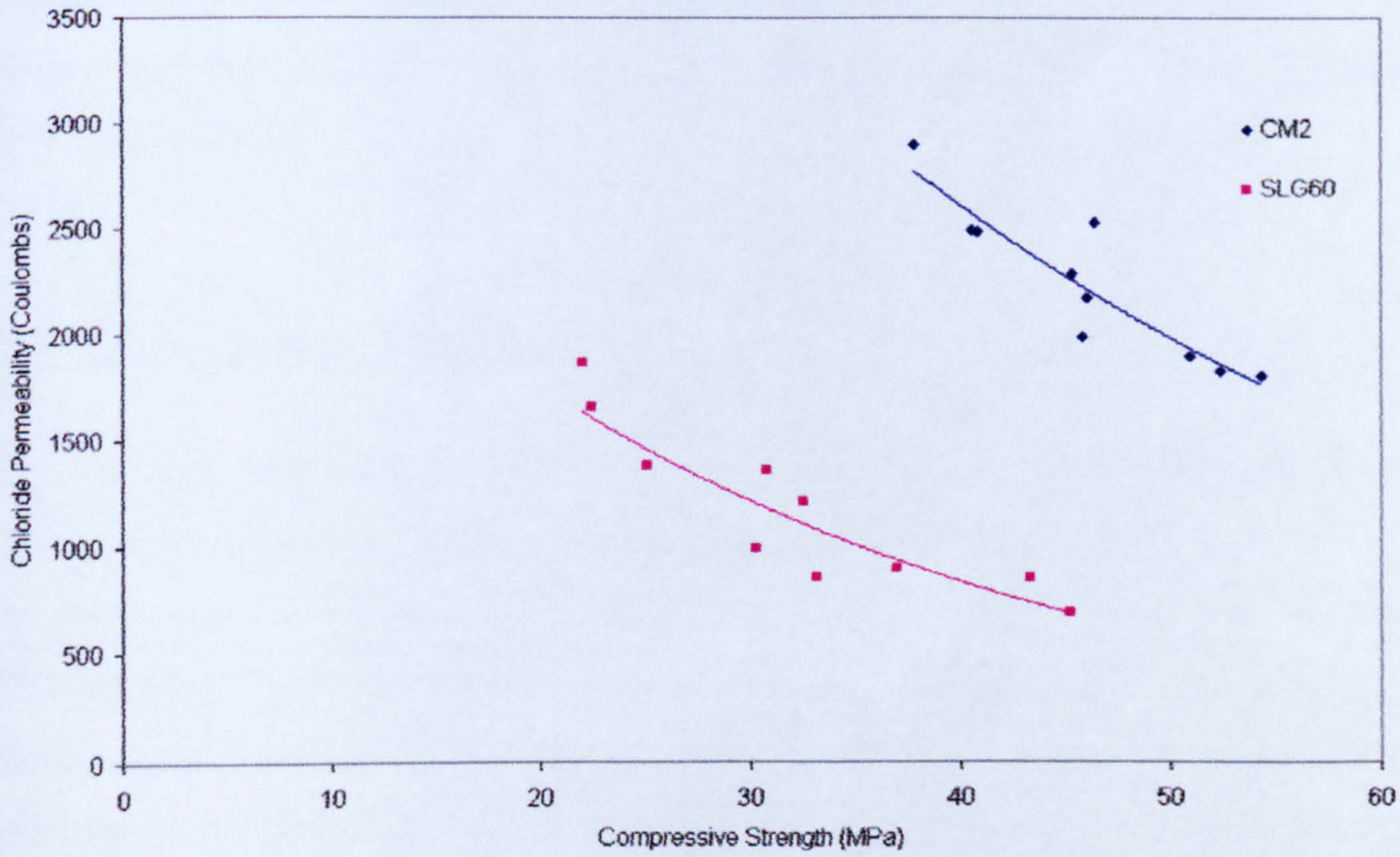

Figure 7.22 Relation between Chloride Permeability and Compressive strength for OPC and OPC/slag mixes

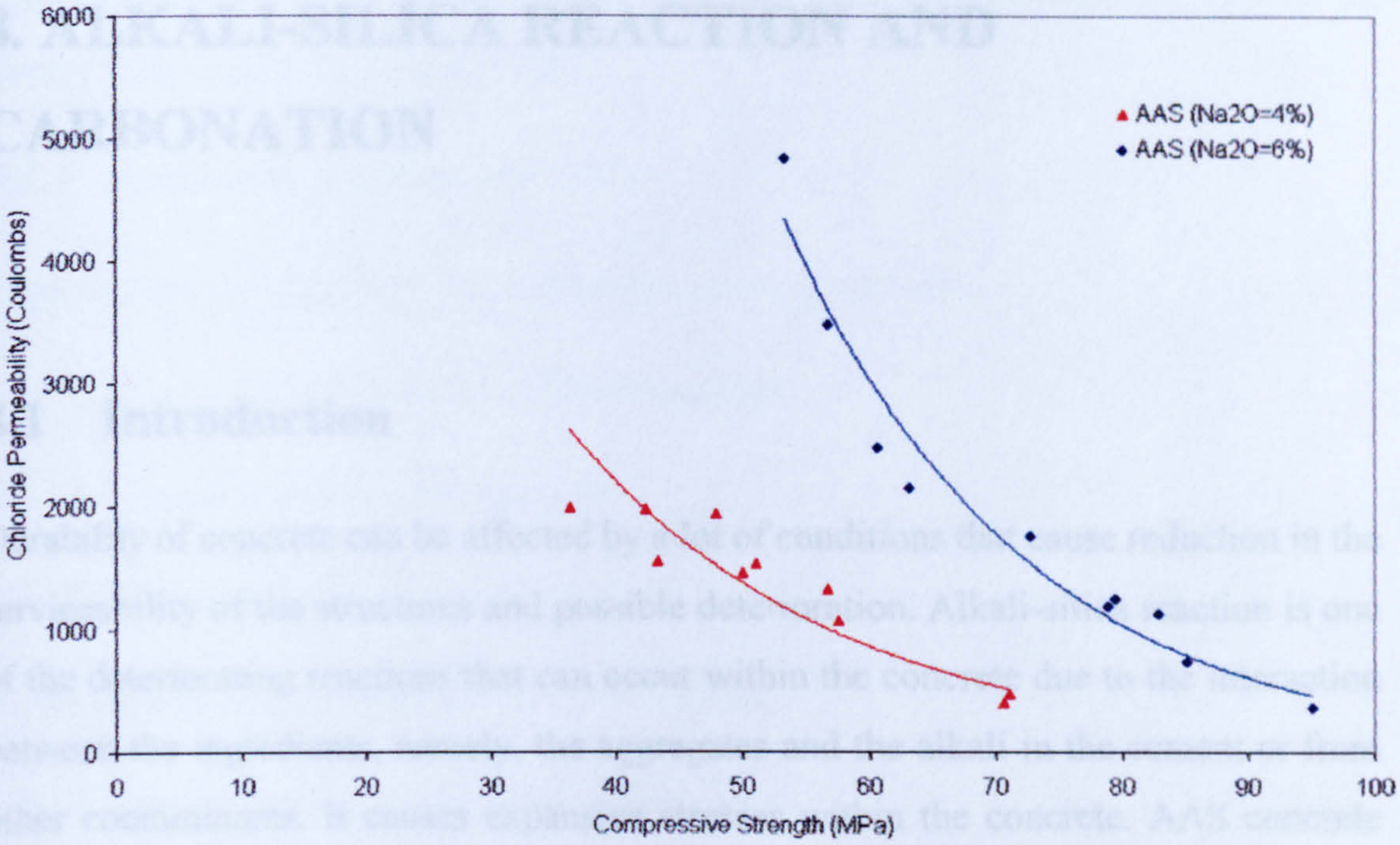

Figure7.23 Relation between Chloride Permeability and Compressive strength for AAS mixes

8. ALKALI-SILICA REACTION AND CARBONATION

8.1 Introduction

Durability of concrete can be affected by a lot of conditions that cause reduction in the serviceability of the structures and possible deterioration. Alkali-silica reaction is one of the deteriorating reactions that can occur within the concrete due to the interaction between the ingredients, namely, the aggregates and the alkali in the cement or from other contaminants. It causes expansive stresses within the concrete. AAS concrete usually incorporates high alkali content, and hence calls for great attention directed at understanding and evaluating the potential for ASR in AAS concrete. Another cause for problems is carbonation, which indirectly affects the protection of steel reinforcement against corrosion. ASR and carbonation are discussed in detail in this chapter and their effect on AAS concrete is investigated compared with OPC and OPC/slag concrete.

8.2 Alkali-Silica Reaction

Concrete can deteriorate as a result of an interaction between alkaline pore fluids (principally originating from the Portland cement and from the activators in AAS concrete) and reactive minerals in certain types of aggregates. The mechanism of deterioration is known as alkali aggregate reaction (AAR); it can occur in a number of forms. Alkali silica reaction (ASR) is the most common form of alkali aggregate reaction. It occurs when there is interaction between the alkaline pore fluid and siliceous minerals in some aggregates forming a calcium alkali silicate gel. This gel takes in water producing a volume expansion, which disrupts the concrete. Other alkali aggregate reactions are the alkali carbonate reaction when the attack is on certain argillaceous dolomitic limestones and and the alkali silicate reaction in which layer silicate minerals are attacked. Alkali carbonate reaction is less common than

ASR worldwide and no harmful alkali carbonate reaction has been observed in the United Kingdom (*BRE Digest*, 1988).

8.2.1 Necessary Factors for ASR

Three factors are necessary for alkali-silica reactivity to occur:

1. Presence of Alkalis in sufficient quantity
2. Reactive silica in the aggregate
3. Water or sufficient moisture.

These factors are discussed below in more detail.

8.2.1.1 Presence of alkalis in sufficient quantity

Usually alklalis are present in the cement coming from the raw material used in its production. In order to assess the total alkalis present in a cement or concrete it has become standard practice to express the alkali content in terms of 'sodium oxide equivalent'. This correlates the sodium and potassum oxides in terms of molecular proportions. The calculation of the sodium oxide equivalent is as follows :

Sodium oxide equivalent = $Na_2O\% + 0.658K_2O\%$

BRE digest (1988) presented limits of the alkali in cement and suggested 3.0 kg of Na_2O equivalent per cubic metre of concrete. It also stated that a portland cement with an alkali level of 1.0% equivalent Na_2O can be used with no further protection against ASR provided the cement content of the mix does not exceed 300 kg/m^3. With an alkali level 0.60% Na_2O in cement; up to 500 kg/m^3 of the cement could be used without further consideration of ASR.

8.2.1.2 Reactive silica in the aggregate

Some rock materials used as aggregate for concrete contain some form of reactive silica, which is an essential component for alkali silica concrete to take place. The reactivity of the aggregate depends on the silica crystalline structure and other conditions to form the expansive silica gel that causes tensile stresses within the concrete matrix. *Coull* (1981) has listed the minerals and rocks that are potentially reactive with high alkali cement, which is shown in Table 8.1.

8.2.1.3 Water or sufficient moisture

The alkali gel may form in dry conditions where concrete still retains pore fluids but it will only expand and cause damage when the concrete is subjected to constant or intermittent exposure to moisture (i.e. moisture saturated soil or rain). Expansion and expansive reaction are negligible when humidity is below 70% RH but above 80% RH the expansive effects increase dramatically (*Poole*, 1990).

8.2.2 The Pessimum Content

For reactions to occur which will cause damage by expansion in concrete, alkali, reactive silica and water must all be present. With one factor absent, no expansion will occur. The alkali reactive silica ratio corresponding with the maximum expansion is called the most critical ratio and the reactive silica content producing the maximum expansion is called the pessimum content. In order to find the pessimum content of any reactive aggregate, and in the absence of any standard method to determine this, many parameters must be taken into consideration. Of these parameters, mix proportion, water/cement ratio particle size, cement content, concrete alkalinity, specimen size, curing and time are all important (*Al-Asali*, 1987).

8.2.3 Testing for alkali-silica reactivity of aggregates

The test methods for alkali-aggregate reactivity can be divided into those that determine the potential reactivity of an aggregate (the chemical test and petrographic method) and those that measure expansivity of aggregate in concrete (mortar bar ASTM C227 (*ASTM*, 1990), concrete prism (*BS - DD 218*, 1995) and (*ASTM C 1293*, 1995) (*Swamy et. al.*, 1988). The latter methods are of interest in this investigation because the objective is not only to test the aggregates but to study the effect of high alkali concentrations in AAS concrete. The concrete prism method adopted by BS will be used in this investigation. Although the BS standard does not specify a limit for expansion, the limit adopted in ASTM C 1293-95 was 0.04% at which an aggregate is considered deleteriously expansive.

8.2.4 Experimental Programme

A set of three prisms 75x75x280 mm for each mix were prepared and tested according to BSI Draft DD218: (1995).

8.2.4.1 The concrete mixes

Reactive sand from Greywacke type rock source provided by BRE was used as fine aggregate in the concrete mixes for this test.

Two mixes were designed initially to assess the reactivity of the aggregates. They were intended to promote ASR expansion therefore they had high binder content.

TEST 1: A control mix (CON1) designed exactly according to the standard using specified high alkali cement and added alkalis to the required Na_2O level of 1% of the weight of cement by adding potassium sulphate. The Na_2O equivalent of the cement originally was 0.68%. The purpose of this mix is to cause ASR and accelerate the reaction.

TEST 2: Replacing 60% of the cement in **TEST 1** by ggbs and maintaining the alkali content of the cement at 1% (SLGCON).

The mixes used throughout the investigation for OPC, OPC/Slag, and AAS concrete are tested replacing the sand by the reactive aggregate and they are the following mixes:

CM2: PC control mix with w/c = 0.48

SLG60: 60% ggbs + 40% OPC mixture with w/c = 0.48

SS4: Sodium silicate alkali-activated slag mixture with Na_2O content of 4% with w/c = 0.48

SS6: Sodium silicate alkali-activated slag mixture with Na_2O content of 6% with w/c = 0.48

MET4: Sodium metasilicate alkali-activated slag mixture with Na_2O content of 4% with w/c = 0.48

MET6: Sodium metasilicate alkali-activated slag mixture with Na_2O content of 6% with w/c = 0.48

The details of the mixes are presented in Table 8.2

8.2.4.2 Storage Conditions

The specimens were treated in accordance with the standard . They were wrapped in a cloth and a polyethylene sheet after demoulding after 24 hours. Then they were stored in a humid room (20 ± 2°C) for the next 6 days and then stored in a controlled temperature tank with water at the bottom not touching the specimens (38 ± 2°C). They were not put in separate containers as in the standard specifications of the test but the specimens were well wrapped and the moisture maintained at all times at RH 95% (see Figure 8.1).

8.2.4.3 Expansion Measurement

The expansion was measured using a length comparator in accordance with BSI Draft DD218: 1995. The comparator is shown in Figure 8.2. The measurement was done in the following steps:

The length of each prism was measured after demoulding from several points and an average value recorded.

The initial reading A0 was measured after demoulding. Another reading was measured after removal from the mist room. Subsequent reading were measured at the end of periods 2 weeks, 4 weeks, 13 weeks, 26 weeks, 39 weeks and one year after mixing.

The expansion E_n is calculated by the equation:

$$E_n = \frac{A_n - A_0}{l_a} \times 100 \qquad (8.1)$$

A_n is the comparator measurement of the prism at age n;

A_0 is the initial comparator measurement of the prism;

l_a is the initial length of the prism.

The average of measurement for the three prisms was calculated.

8.2.5 Results and discussion

The results of the alkali-silica reaction expansion test carried out in this investigation on the prisms of the concrete mixes cast and treated in accordance with the relevant standard detailed in previous sections are presented in Figures 8.3-8.4. The results from the prisms are discussed to reach an understanding of the behaviour and potential for ASR to occur in AAS concrete.

8.2.5.1 Reactivity of the Aggregate

The Thames valley sand used in this investigation was identified by *Blackwell et al.* (1992) being of greywacke source as having deleterious expansion attributed to AAR. This finding is confirmed in this investigation. Results shown in Figure 8.3 show that the TEST1 mix exhibited high expansion up to 0.185% after 1 year of exposure. Greywacke some times is the only available source for aggregate for construction. That is the case with certain areas in the UK. The potential reactivity of such aggregates can still be avoided by several means, including controlling the alkali or using cement replacing binders such as fly ash or slag.

8.2.5.2 Effect of Slag on ASR

The results in Figure 8.3 show that the OPC/Slag mix having high binder content and 60% cement replacement by ggbs (TEST2) achieved a reduction in the expansion reaching only 0.027% after 1 year, which is below the 0.04% limit. This result is in agreement with *Hobbs* (1982) who stated that incorporation of ggbs for 50% of OPC in concrete results in a reduction in the expansion of concrete in the presence of reactive aggregate. *Sims* (1983) stated that the addition of slag had a beneficial effect in reducing expansion. Also *Thomas and Innis* (1995) reached similar conclusions to the reduction in expansion in mortar bars and concrete prisms made with alkali-silica reactive aggregates. It can be noted from Figure 8.4 that the OPC/Slag mix SLG60 reached a maximum value of expansion 0.02%, which is lower also than the limit and lower than the TEST2 mix probably because of the high cementitious content and the

alkali content of the latter. The role of slag in reduction of expansion due to ASR in OPC and ggbs blends containing at least 50% slag was attributed by the BRE digest (1988) to the greatly reduced ability of hydroxyl ions to diffuse within the cement paste. *Glasser* (1990) stated that the products of hydration of blended cements have higher binding power for alkalis resulting in less potential for reaction with aggregate.

8.2.5.3 ASR potential in AAS concrete

The results in Figure 8.4 show that AAS concrete had overall a low expansion indicating less susceptibility to ASR. Comparing the mixes based on the Na_2O dosage shows that the higher the Na_2O content the higher the expansion, as SS6 shows higher expansion than SS4, and MET6 shows higher expansion than MET4. On the other hand, comparison based on the M_s of the activator indicates that the higher the M_s, the lower the expansion, when the Na_2O is the same since, the SS4 expansion was lower than that of MET4, and SS6 expansion was lower than that of MET6. The control OPC mix CM2 also showed low values for expansion reaching 0.0165% at 1 year. The available literature is contradictory. Some researchers pointed out there is no susceptibility for ASR with AAS in agreement with what was found in this investigation. Some of those researchers stated that it is not possible for ASR to take place in the activated slag mortar because all, or almost all, the alkalis (more than 80%) are combined in the different hydration products (*Talling and Branstetr*, 1989; *Shi et al.*, 1992; *Krivenko*, 1992). *Gifford and Gillot* (1996) proposed that AAS concrete is less susceptible to ASR because of the pessimum effect, which results in the consumption of the reactive silica during the early period of hardening. On the other hand others reported potential for ASR in AAS mortars and concrete. *Metso* (1983) reported expansion in AAS mortars. Wang (1991) reported some work done in China that found ASR expansion about 0.1 – 0.15% using 3% granulated silica in AAS mortars. *Bakharev et al.* (2001) tested AAS concrete where slag was activated by a mixture of Na_2SiO_3 and NaOH having an Ms = 0.75. They reported high expansion starting from 0.04% at 90 days, increasing to 0.045% after 12 months, reaching 0.1% after 22 months. They recommended that ASR testing with AAS concrete should continue for over 2 years as they noticed slower expansion at early ages where it is mitigated according to the researchers by rapid strength development. This suggestion is probably reasonable as the results of this investigation, shown in

Figure 8.4, show a trend of probable increase in the future for the AAS mixes having 6% Na2O although the expansion is still below the 0.04% limit after 1 year.

Glasser (1990) as mentioned earlier stated that OPC/Slag blends among other blended cements have higher binding power for alkalis in their hydration products, which can also be true for AAS concrete resulting in less potential for ASR. The results of this investigation can be explained following the same logic. The effect of M_s of the activator on the expansion as it decreases with higher M_s can be due to the binding of the alkali fraction to the silicate fraction of the activator in forming part of the hydration products. SS4, having lower alkali and higher M_s showed the lowest expansion.

8.3 Carbonation

Carbonation is the process whereby concrete is attacked by atmospheric carbon dioxide. More specifically, carbonation is a chemical reaction between one of the main hydration products of cement in the concrete, calcium hydroxide ($Ca(OH)_2$), and carbon dioxide (CO_2) from the atmosphere to form calcium carbonate ($CaCO_3$). Additionally, carbon dioxide may react with calcium silicate hydrate (C-S-H), unhydrated dicalcium silicate (C_2S), and tricalcium silicate (C_3S) (*Loo et al.*, 1994; *Lea*, 1970) and also hydrated alumina (*Lea*, 1970).

The known effect of carbonation on cementitious composites is the loss of alkalinity that protects the reinforcement against corrosion by passivation. Carbonation of concrete, as is widely known, can lead to the gradual deterioration of reinforced concrete. In hardened concrete, steel is normally protected from corrosion by a passive layer of oxide. However, the steel may become susceptible to corrosion in the presence of chloride ions or if it becomes depassified when the alkalinity of the concrete at the location of the steel is reduced (pH approx. 8.0) by carbonation. Corrosion may occur if moisture and oxygen can penetrate the concrete to reach the steel. Consequently, the depth of concrete cover to the steel and the ability of the cover to resist the penetration of chloride ions, carbon dioxide, moisture and oxygen largely control the durability of reinforced concrete.

8.3.1 Process of Carbonation

The pH of concrete pore fluids is normally in excess 12.5. Once the concrete has carbonated, this generally drops to around pH 8 and it is evident at this level of alkalinity that conditions are such that corrosion can occur. *Parrot* (1987) and *Richardson* (1988), as reported by *Byars* (1997), suggested that carbonation due to atmospheric carbon dioxide might be divided into three stages.

Step 1, Ingress of carbon dioxide by diffusion

$$H_2O + CO_2 \rightarrow HCO_3^- + H^+$$

Step 2, Reaction with the concrete pore fluids leading to the formation of carbonic acid

$$HCO_3^- \rightarrow CO_3^{2-} + H^+$$

Step 3, Reaction of the carbonic acid with the alkaline constituents of concrete

$$Ca(OH)_2 + 2H^+ + CO_3^{2-} \rightarrow CaCO_3 + 2H_2O$$

It has also been reported, as indicated above, that as the process of carbonation proceeds, decomposition of the hydrate structure may occur (*Loo et al.*, 1994), in the following reaction:

$$3CaO.2SiO_2.3H_2O + 3CO_2 \rightarrow 3CaCO_3 .2SiO_2.3H_2O$$

$$3CaO.SiO_2 + 3CO_2 + uH_2O \rightarrow SiO_2.uH_2O + 3CaCO_3$$

$$2CaO.SiO_2 + 2CO_2 + uH_2O \rightarrow SiO_2.uH_2O + 2CaCO_3$$

8.3.2 Factors Influencing the Rate of Carbonation

8.3.2.1 Properties of Concrete

Strength of concrete has been found to influence the carbonation resistance of the concrete (*Loo et al.*, 1994; *Watkins and Jones*, 1993). However, caution should be exercised in using strength as a prediction of carbonation resistance since in particular concrete, concrete with similar strength may offer different carbonation resistance

(*Dhir et al.*, 1989). Therefore, factors that influence the strength and microstructure of the concrete may also affect the carbonation resistance such us w/b ratio, cement content, including blended cement, degree of hydration, diffusivity, porosity and permeability of the concrete. In addition, it is found that the fundamental factor controlling carbonation is the diffusivity of the hardened cement paste (*Neville*, 1995; *Jiang et al.*, 2000).

8.3.2.2 Environmental Conditions

The progress of carbonation is greatly influenced by the relative humidity of the exposure condition in which the structure is located, the curing history of the concrete, and the carbon dioxide concentration (*Watkins and Jones*, 1993). Apparently, the rate of carbonation is slightly sensitive to temperature, in that a small variation in temperature has only a little effect on carbonation but a high temperature increases the rate of carbonation significantly. *Loo et al.* (1994) reported that the effect of temperature within the range 20 to 40 ° C on the rate of carbonation is not significant. In the case of carbon dioxide concentration, an increase of CO_2 will generally increase the rate of carbonation. According to *Thomas and Matthews* (1992), the reduction in the rate of carbonation becomes more marked at relative humidity above 80 %. However, the highest rate of carbonation occurs at a relative humidity of between 50 and 70 % (*Neville*, 1995).

8.3.3 Experimental Programme

Cubes of 100 mm were prepared for the OPC control mix, OPC/slag mix and the AAS concrete mixes and cured in water for 28 days then moved into the controlled temperature room with temperature 20 ℃ and 60%RH. The dry cured specimens were also examined. Carbonation measurements were carried out for concrete after exposure for 1 year.

8.3.3.1 Test Procedure

Carbonation in concrete results in a drop in pH. A pH indicator can be used to determine the pH of a freshly broken section of concrete. Phenolphthalein is the most commonly used indicator. When sprayed on the broken face of the concrete section, it remains colourless when the pH is below 8.2 but, turns to pink when pH is higher than 8.2.The procedure is prescribed by *RILEM* (1988).

Measurement of the carbonation of concrete specimens was carried out using phenolphthalein in ethanol solution. When the indicator was applied to a freshly broken surface of concrete. The edges of the sample that remain colourless are to be considered carbonated. The depth of carbonation was measured from the edge surface to where the indicator coloured the paste pink. The average thickness of this layer gives the depth of carbonation. An average of 16 measurements is taken for each specimen. A typical set of specimens tested is illustrated in Figure 8.5.

8.3.4 Results and Discussion

Results of carbonation depth measurement after 1 year of age are presented in Figure 8.6. These results show that CM1 mix, which is the OPC mix with w/c=0.55, had higher depth of carbonation equal to 8 mm compared to CM2, which is the OPC mix with w/c=0.48, having a carbonation depth of 4.5 mm. The OPC/slag mix SLG60 had carbonation depth of 6 mm depth grater than CM2 which has similar w/c ratio. This is in agreement with *Neville* (1995). Nevertheless SLG60 had less carbonation than CM1 which has comparable workability and strength.

The AAS mixes differ in their depth of carbonation, as the lowest depth of carbonation was achieved by SS6 with a depth of only 4 mm of carbonation followed by MET6 with depth of 7.5 mm then SS4 which had a carbonation depth of 9 mm and the highest carbonation depth which was with MET4 having 12 mm.

Although hydrated slag blended and AAS concrete produce low $Ca(OH)_2$ which is the main reactant for carbonation in OPC concrete, some researchers have reported higher rate of carbonation with AAS concrete especially with low grade, low strength concretes. This might be due to carbonation of C-S-H.(*Wang, et al.*1995 ; *Bakarev*, 2001). This investigation arrived at a similar finding.

The effect of dry curing in AAS concrete is very drastic. The dry cured specimens exhibited higher carbonation than specimens cured in water for 28 days. The SS6 suffered the most because of the drying shrinkage cracking.

8.3.5 Relation between Carbonation Depth and Compressive Strength at 28 day

The values for carbonation depth were plotted against the corresponding 28 day compressive strength for the mixes, as illustrated in Figure 8.7. The results show a reasonable relationship for all mixes but the relationship for OPC and OPC/Slag mixes cannot be plotted for 3 points only. It can be noted that AAS concrete had greater depth of carbonation compared with the control mix having the same compressive strength.

The relation for AAS concrete arrived at was as follows:

$$k_d = 68.03e^{-0.036 f_c} \qquad (8.2)$$

R2 = 0.9952

8.4 Conclusions:

The main conclusions drawn from the present investigation are summarised as follows:

1. Replacing 60% OPC by slag reduces the expansion of concrete prisms containing reactive aggregates.
2. AAS concrete has low susceptibility to ASR expansion possibly because of stronger binding of alkalis in the hydration products.
3. Slag/OPC concrete showed higher depth of carbonation than OPC concrete with the same w/c ratio.
4. AAS concrete with low compressive strength (around 40 MPa) has higher carbonation compared to OPC concrete of the same grade.

Table 8.1 Minerals, rocks and other substances, which are potentially deleteriously reactive with alkalis in cement (*Coull*, 1981).

Minerals	
Opal Chalcedony Tridymite Cristobalite Cryptocrystalline, microcyrstalline or glassy quartz Coarse-grained quartz which is intensely fractured, granulated and strained internally or filled with submicroscopic inclusions of which illite is one of the most common Vein quartz	
Rocks	
Rock	Reactive component
Igneous rocks Granites Granodiorites Charnokites	More than 30 % quartz as characterised by suturing and undulatory extinction
Pumice Rhyolites Andesites Dacites Latites Perlites Obsidians Volcanic tuff	Silicic to intermediate silica rich volcanic glasses; devitrified glass; tridymite
Basalts	Chalcedony; cristobalite; opal, palagonite; basic volcanic glass
Metamorphic rocks Gneisses Schists	More than 30% strained quartz as characterised by suturing and undulatory extinction
Quartzites	Strained quartz as above; 5% or more chert
Hornfelses Phyilites Argillites	Possibly certain phyllosilicates e.g. vermiculite; strained quartz, cryptocrystalline quartz
Sedimentary rocks Sandstones	Strained quartz ; 5% or more chert, opal
Greywackes	Possibly certain phyllosilicates e.g. vermiculite; strained quartz
Siltstones	Possibly certain phyllosilicates e.g. vermiculite; strained quartz; opal
Shales	Possibly certain phyllosilicates e.g. vermiculite; strained quartz; opal
Chert Flint	Cryptocrystalline quartz; chalcedony; opal
Diatomite	Opal; cryptocrystalline quartz
Carbonates	Phyllosilicates exposed by dedolomitization; opal; chalcedony.

Table 8.2 The concrete mixes tested for ASR

Mix No.	Slag kg/m^3	OPC kg/m^3	Na_2O %	Activator kg/m^3	Lime Slurry %	Lime Slurry kg/m^3	Water kg/m^3	Total Water kg/m^3	Total Binder kg/m^3	Sand kg/m^3	Gravel kg/m^3	w/b
CON1	0	690	1	6.20	0	0	228	228	690	429	990	0.33
SLGCON	414	276	1	6.20	0	0	228	228	690	423	990	0.33
SS4	326	0	4	64.63	4	30	134	180	375	591	1215	0.48
SS6	305	0	6	90.70	6	45	114	180	375	591	1215	0.48
MET4	333	0	4	47.94	4	30	144.4	180	375	591	1215	0.48
MET6	321	0	6	69.32	4	30	135.2	180	375	591	1215	0.48
CM2	0	375	0	0	0	0	180	180	375	591	1215	0.48
SLG60	225	150	0	0	0	0	180	180	375	591	1215	0.48

Figure 8.1 The prisms stored in a controlled temperature tank (38 ± 2°C)

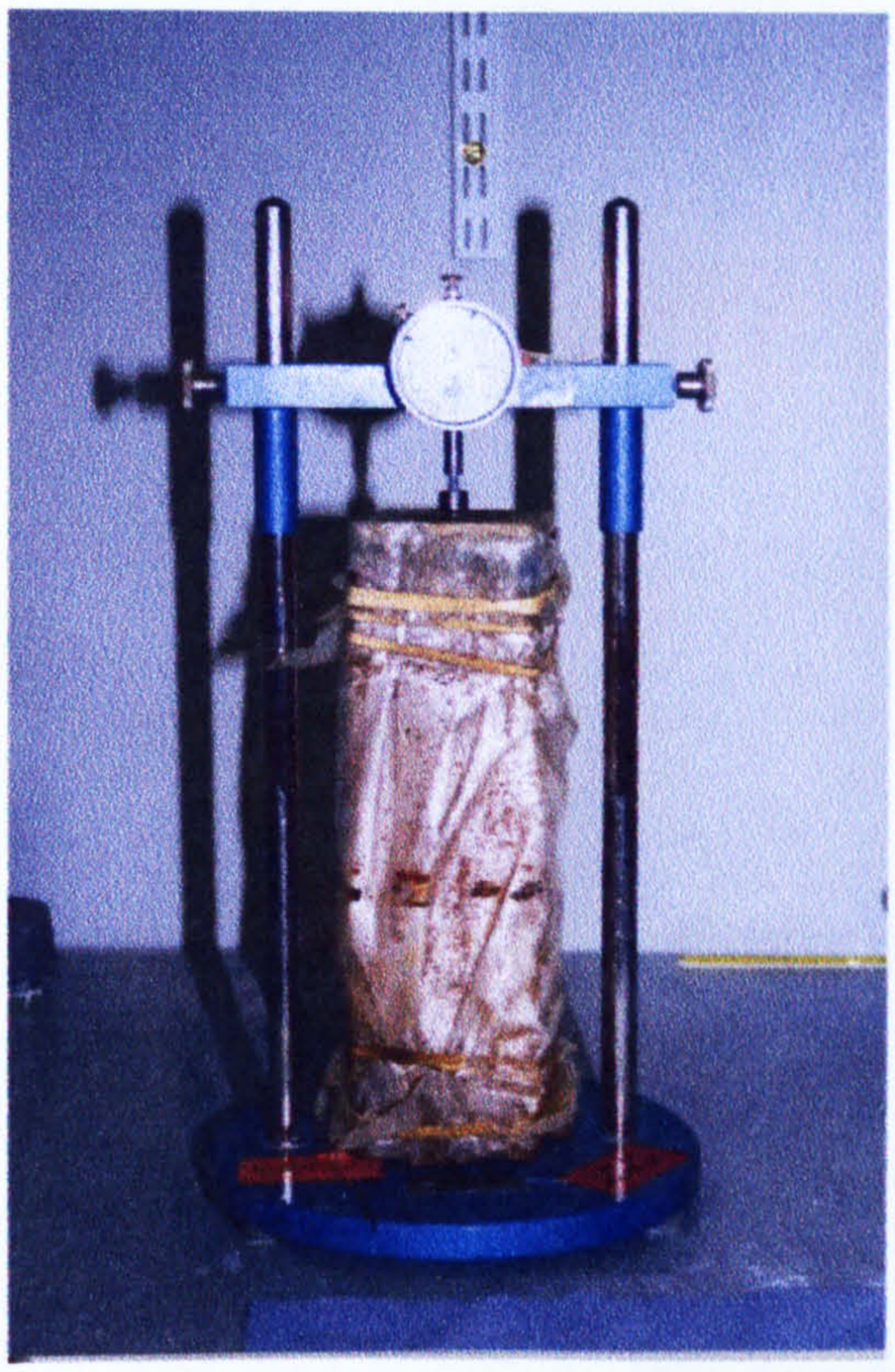

Figure 8.2 The comparator used to measure change in length

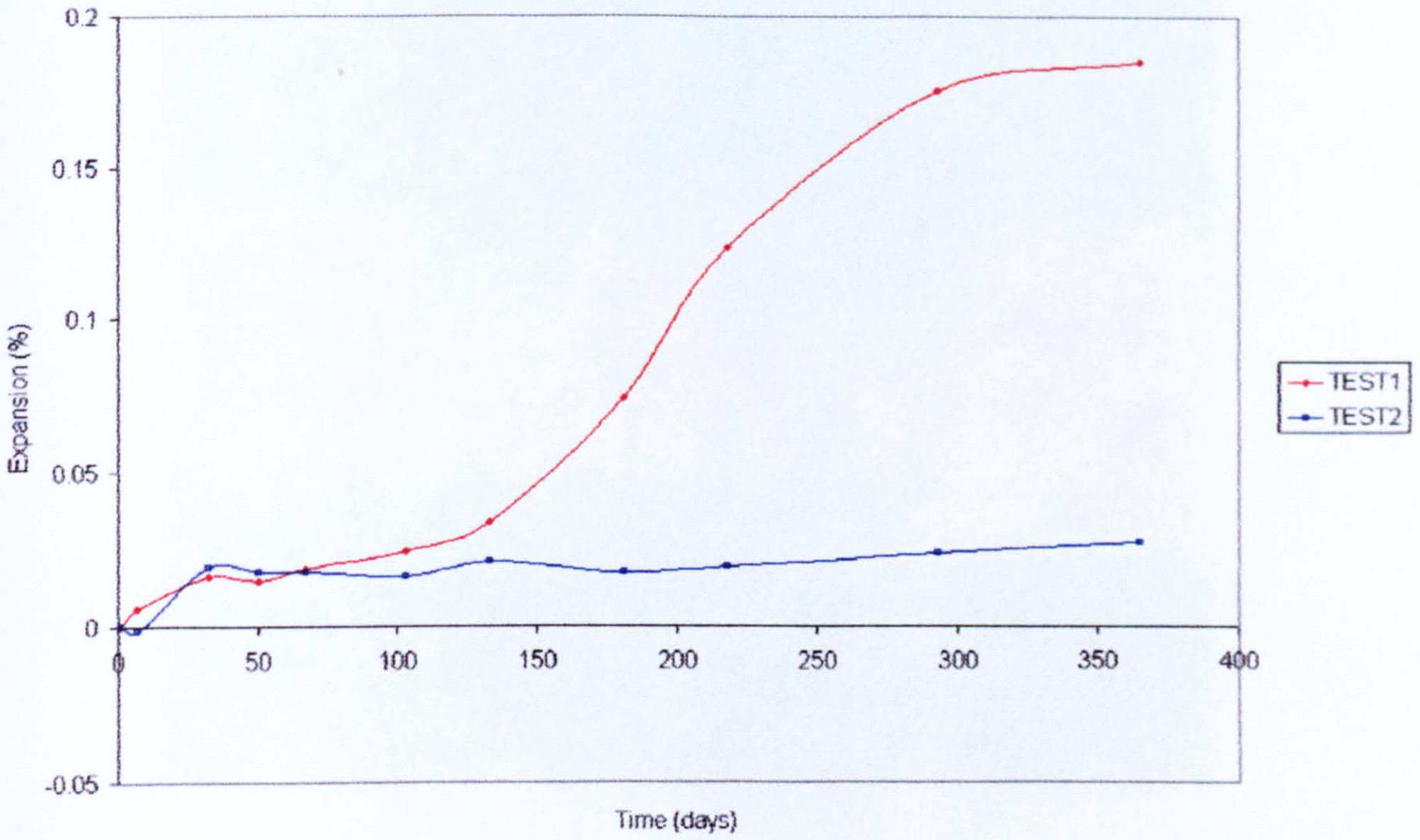

Figure 8.3 Expansion versus for concrete prisms with high alkali cement and slag blended cement

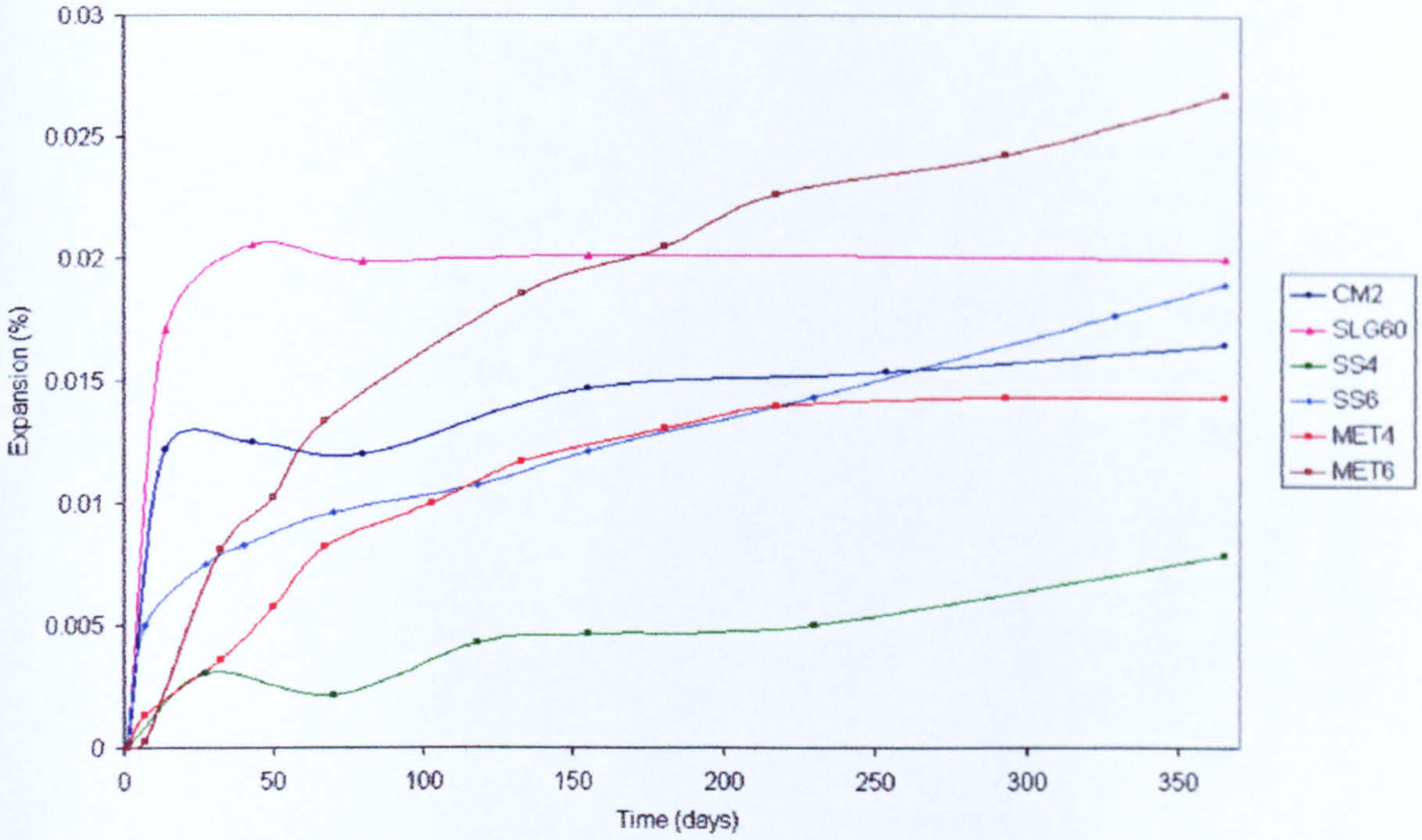

Figure 8.4 Expansion versus for concrete prisms from the different mixes

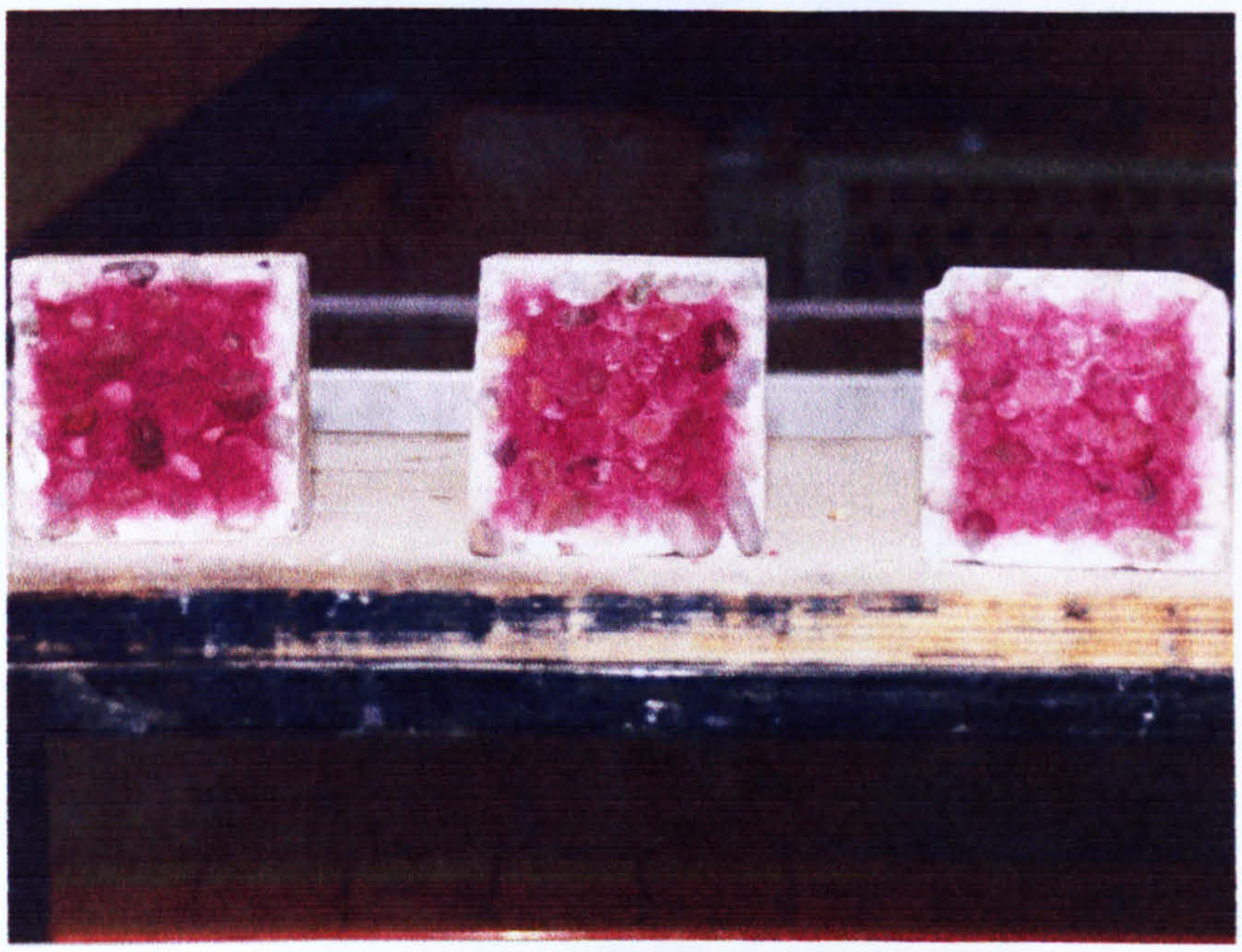

Figure 8.5 Carbonation of AAS concrete specimens

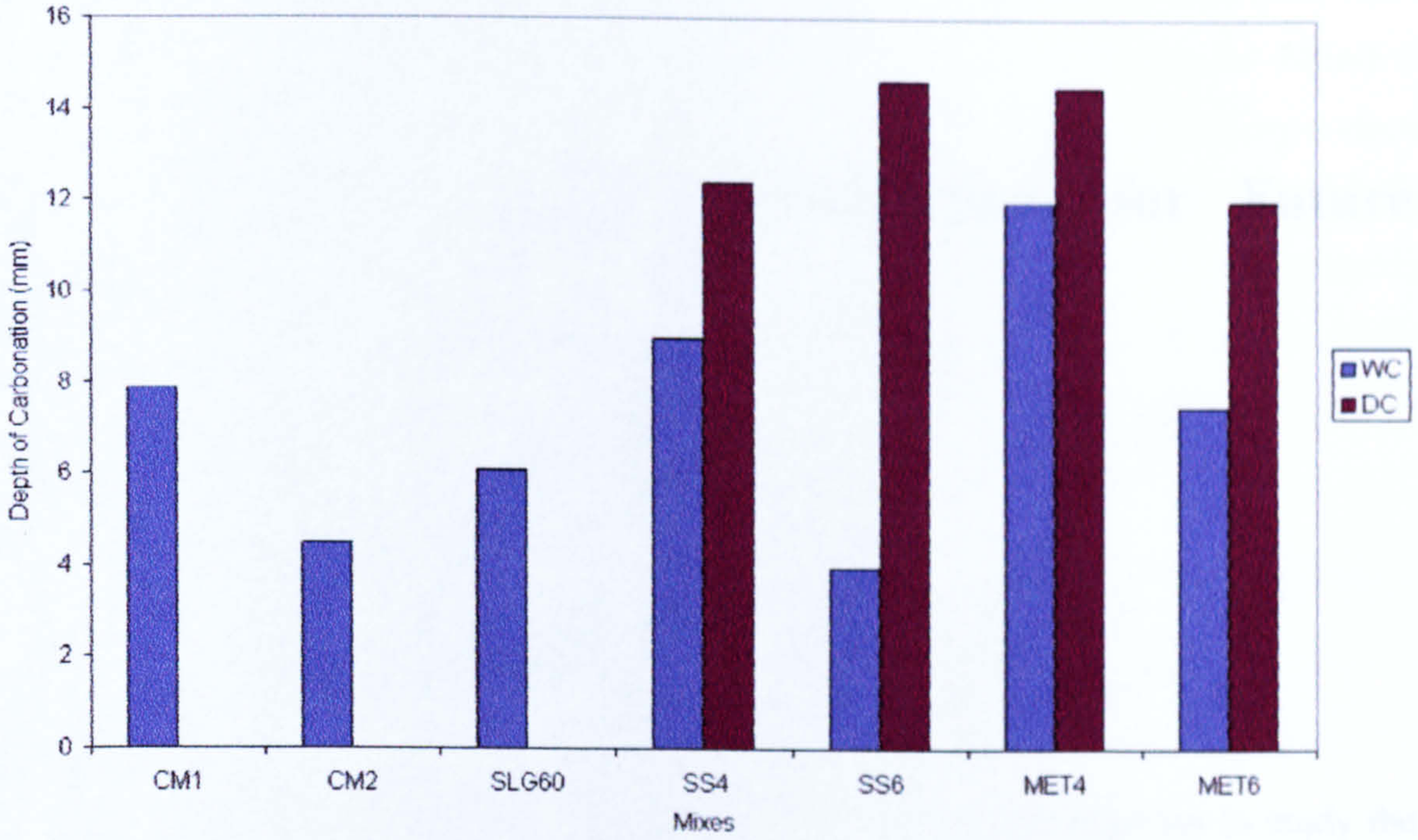

Figure 8.6 Carbonation depths after 1 year for the different mixes showing the effect of dry curing on AAS concrete.

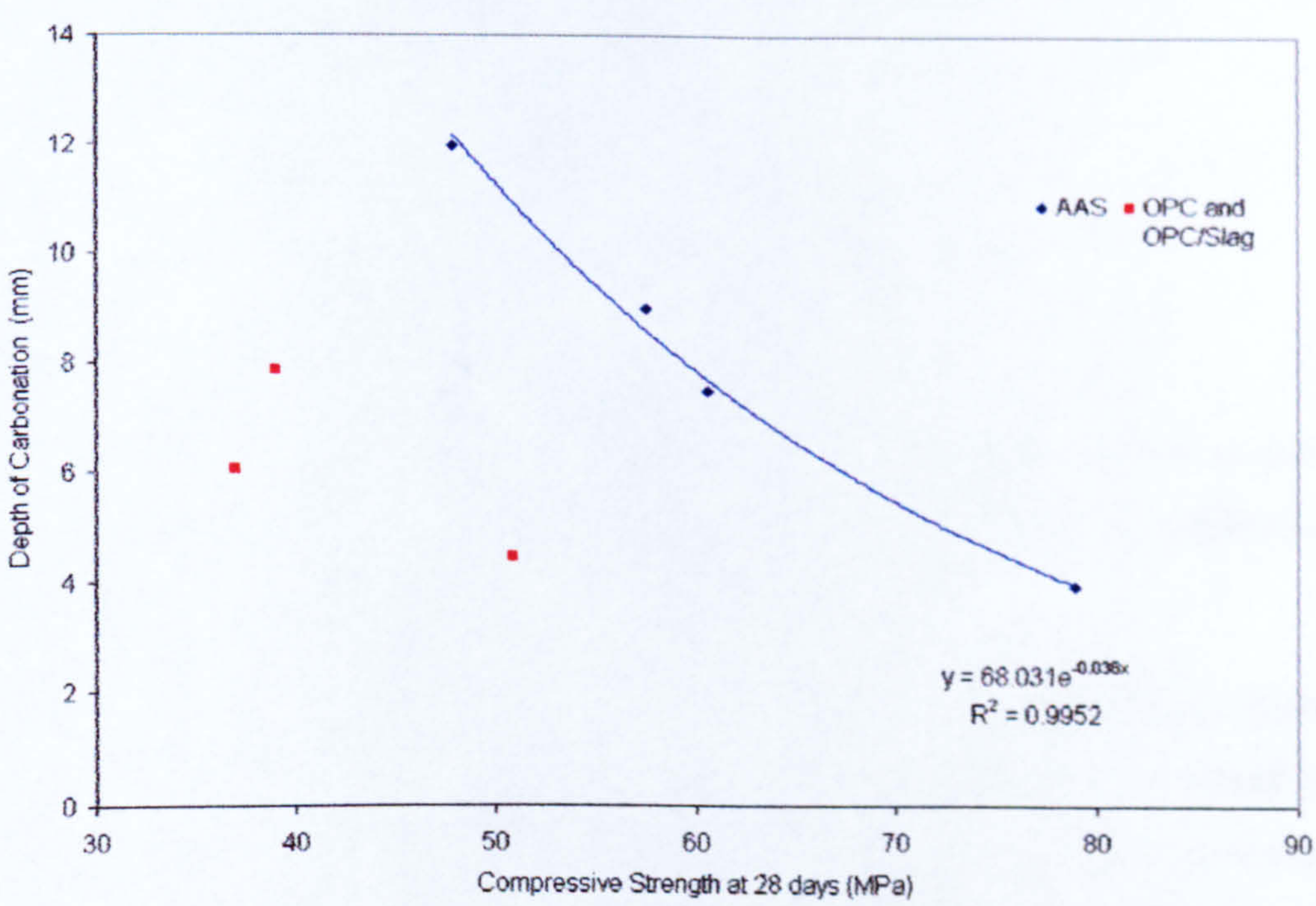

Figure 8.7 Relation between Carbonation depths after 1 year, and 28 day compressive strength for the different mixes

9. Conclusions and Recommendations for Future Research

9.1 Introduction

The objectives of the work were covered throughout this investigation to study the performance of alkali-activated slag concrete in comparison with normal OPC concrete and OPC/slag concrete in terms of its mechanical behaviour and durability.

In this last chapter the main conclusions are stated and some recommendations for further research are suggested.

9.2 Conclusions

Overall it can be concluded that AAS concrete has a great potential and presents a viable alternative to OPC to help decrease the effect on the environment in terms of energy conservation and less CO_2 emission.

Choosing an activator with lower modulus (around 1.0) and a Na_2O dosage (around 4%) is essential to achieve reasonable strength and durability comparable to normal OPC concrete or even surpass it. Due to the unavailability of such activators with the required properties in terms of the low silica modulus care should be taken when choosing the mix proportions to achieve the desired properties. The fresh properties of AAS with high alkali Na_2O dosages of activators with high silica modulus still present some difficulty in terms of shorter setting time and faster loss of workability and they should be avoided if possible.

There were some practical problems with handling the chemicals, which carry some safety risks. In the present work, no attempt was made to change the chemical composition of the activator as was reported in the literature by adding sodium hydroxide to vary the silica modulus because of the inconvenience of handling highly corrosive chemicals and the difficulty to use them in mixing concrete in large batches. Field concrete batching should be much simpler and hence the producers of the construction materials and admixtures should be producing products incorporating alkalis in a solution form that is easily dissolvable and more practical.

The conclusions related to the properties of alkali-activated slag concrete in comparison with OPC, and OPC/ slag concrete are listed below

Fresh Concrete Properties:

1. Slag requires less water for the same workability level. Therefore the slag replacement mix had higher slump compared with an OPC control of the same w/c ratio and same binder content.

2. Alkali-activated slag concrete has good workability, comparable with OPC and OPC/slag concrete. For a given w/c ratio, the higher the dosage of the activator, the lower the slump. The higher is the silicate modulus of the activator the less workable the concrete is in terms of slump.

3. AAS concrete sets rapidly with the higher silicate modulus of the activator and the higher Na_2O dosage resulting in shorter setting time. This rapid setting can be controlled by adding hydrated lime to the mix.

Hydration Process:

1. The main hydration product in AAS systems is C-S-H (I). The hydrotalcite-like peaks observed in the XRD patterns can be attributed to the high magnesium content of the slag.

2. Autoclaving results in formation of a more crystalline C-S-H gel and the formation possibly of xonotlite.

3. The combined water in the hydration products as measured by TGA, for AAS pastes showed an increase with age with the higher Na_2O dosage resulting in higher hydration while no significant increase was noted with the low Na_2O dosage. The autoclave curing resulted in a lower amount of combined water measured in comparison with water curing.

Engineering Properties

1. The choice of the type of activator and dosage is very important in AAS concrete with the higher dosage resulting in higher strength and the higher silicate modulus of the activator resulting in higher strength.

2. The concrete incorporating ggbs as a replacement of OPC develops strength at a slower rate compared to the OPC and AAS mixes with the same w/c ratio.

3. Curing is a very important factor in the engineering properties of concrete in general, but AAS concrete is much more sensitive to curing where the strength of concrete that is dry cured is much lower than that of concrete that is water cured.

4. Accelerated curing (autoclave) increases the initial gain of strength in AAS concrete but eventually gives results close to water curing. It is more effective with the activator having lower silicate modulus.

5. The development of dynamic modulus of elasticity and ultrasonic pulse velocity demonstrated similar trends to those of compressive strength.

6. The slag/OPC mix exhibited higher drying shrinkage in comparison with the OPC mix having the same w/c ratio.

7. AAS concrete with 6% Na_2O exhibited high drying shrinkage compared to the OPC concrete and the AAS concrete with 4% Na_2O.

8. Using a waterglass activator with Ms = 1.65 and 6% Na_2O resulted in the highest drying shrinkage probably because of the larger amount of silica gel formed in the hydration process.

9. Autoclave curing of AAS concrete reduces the drying shrinkage as it causes the formation of more crystalline products of hydration.

Permeation Related Properties

1. Replacing 60% of OPC by ggbs results in an increase in porosity compared to the OPC mix of the same w/c ratio while it results in lower porosity when compared to the OPC mix with the same workability level.

2. The increase of the Na_2O dosage in AAS concrete, where the activator has an M_s = 1.0, results in a decrease in porosity. But in the case of the AAS concrete, with the activator having M_s = 1.65, the porosity increases with the increase of the Na_2O dosage.

3. The AAS concrete porosity test results are higher at early ages than the control mix due to the drying effect of preconditioning the specimens at 105 °C.

4. Dry curing increases the porosity of all the concrete mixes.

5. OPC/slag mix with 60% replacement has oxygen permeability slightly higher than that of the OPC mix having the same w/c ratio at later ages.

6. Pre-drying the specimens at 105 °C resulted in an increase in oxygen permeability of AAS concrete to much higher levels than those of OPC and OPC/slag mixes. This is probably due to micro-cracking caused by drying. Dry curing increased the oxygen permeability.

7. Incorporating slag as a replacement of OPC by 60% results in lower chloride permeability compared to the control OPC concrete.

8. The rapid chloride permeability test gives misleading high results for chloride permeability of AAS mixes especially in the case of high Na_2O dosage at the early ages.

9. Dry curing increases the chloride permeability but the results are very high and fluctuating in the AAS concrete probably due to the micro-cracking and the presence of alkalis.

Alkali Silica Reaction

1. Replacing 60% of the OPC by slag reduces the alkali-silica reaction expansion of concrete prisms containing reactive aggregates.

2. AAS concrete has low susceptibility to ASR expansion possibly because of binding of alkalis in the hydration products.

Carbonation:

1. Slag/OPC concrete undergoes higher carbonation than OPC concrete with the same w/c ratio.

2. AAS concrete with low compressive strength around 40 MPa shows higher carbonation depth compared to OPC concrete of the same grade.

9.3 Recommendations for Future Research

The suggested recommendations for future research in the field of alkali-activated slag concrete are as follows:

1. Attempts should be made to standardise the mix design methods for AAS concrete and specify the activators as a construction material with recommended dosages and properties.

2. There is room for work on finding retarders other than lime for use with AAS concrete especially when using high dosages of the activator and higher modulus.

3. Investigate possibility of blending AAS with pozzolans such as pfa to improve its quality and overcome some of the problems related to workability and setting time.

4. The activation of pozzolans such as pfa can be studied. Also other type of slags and waste materials with some pozzolanic properties carries a good potential to be explored.

5. There is a potential for using accelerated curing including high temperature curing or autoclaving in industrial factory conditions such as precast and

prefabricated concrete products. This field can be investigated for the use of AAS concrete under good quality control conditions.

6. Extensive work is needed on the properties of AAS concrete to create a wider knowledge in terms of its behaviour in different environmental conditions:

   - Freeze-thaw testing
   - Hot climate conditions
   - Aggressive chemical exposure conditions

REFERENCES

AASHTO Designation T277-83 (1993), 'Standard Method of Test for Rapid Determination of the Chloride Permeability of Concrete', American Association of State Highway and Transportation Officials, Washington DC.

Al-Asali, M. (1987), 'The Effect of Alkali-Silica Reaction on Concrete Members and its Control', PhD Thesis, University of Sheffield.

Andersson, Ronny; Gram, Hans-Erik, (1987), 'Properties of alkali activated slag concrete.',Nordic Concrete Research, n 6, p 7-18

ASTM C 1202 (1991), 'Standard Test Method for Electrical Indication of Concrete's Ability to Resist Chloride Ion Penetration', American Society for Testing and Materials, USA.

ASTM C 1293 (1995), 'Standard Test Method for Concrete Aggregates by Determination of Length Change of Concrete Due to Alkali-Silica Reaction', American Society for Testing and Materials, USA.

ASTM C 227 (1990), 'Standard Test Method for Potential Alkali Reactivity of Cement-Aggregate Combinations (Mortar-Bar Method)', American Society for Testing and Materials, USA.

Bakharev, T.; Sanjayan, J. G.; Cheng, Y. –B, (2001). 'Resistance of Alkali-Activated Slag Concrete to Alkali-Aggregate Reaction' Cement and Concrete Research, v 31, n 4, (April 2001), p 1367-1374.

Bakharev, T.; Sanjayan, J. G.; Cheng, Y. -B., (2000) 'Effect of admixtures on properties of alkali-activated slag concrete' Cement and Concrete Research, v 30, n 9, p 1367-1374.

Bakharev., T , Sanjayan, , J. G and Cheng, Y. B.(2001) 'Resistance of Alkali-Activated Slag Concrete to Carbonation', Cement and Concrete Research, v 31, pp. 1277-1283.

Blackwell, B. Q., Thomas, M. D. A., Nixon, P. J. and Pettifer,K (1992) ' The use of Fly Ash to Suppress Deleterious Expansion Due to AAR in Concrete Containing Greywacke Aggregate', The Ninth International Conference on Alkali-Aggregate Reaction in Concrete, London.

Brough, A. R.; Holloway, M.; Sykes, J.; Atkinson, A., (2000) 'Sodium silicate-based alkali-activated slag mortars. Part II. The retarding effect of additions of sodium chloride or malic acid' Cement and Concrete Research, v 30, n 9, p 1375-1379.

BS 12 (1991), 'Specification of Portland Cement', British Standard Institution, London.

BS 1881: Part 102 (1983), 'Methods for Determination of Slump', British Standard Institution, London.

BS 1881: Part 106 (1983), 'Methods for Determination of Air Content and Fresh Concrete', British Standard Institution, London.

BS 1881: Part 108 (1983), 'Methods for Making Test Cubes from Fresh Concrete', British Standard Institution, London.

BS 1881: Part 110 (1983), 'Methods for Making Test Cylinders from Fresh Concrete', British Standard Institution, London.

BS 1881: Part 111 (1983), 'Methods for Normal Curing of Test Specimens (20 °C)', British Standard Institution, London.

BS 1881: Part 115 (1986), 'Specification for Compression Testing Machines for Concrete', British Standard Institution, London.

BS 1881: Part 116 (1986), 'Methods for Determination of Compressive Strength of Concrete Cubes', British Standard Institution, London.

BS 1881: Part 117 (1983), 'Methods for Determination of Splitting Tensile Strength', British Standard Institution, London.

BS 1881: Part 118 (1983), 'Methods for Determination of Flexural Strength', British Standard Institution, London.

BS 1881: Part 125 (1986), 'Methods for Mixing and Sampling Fresh Concrete in the Laboratory', British Standard Institution, London.

BS 1881: part 203: (1986) , 'Recommendations for measurement of velocity of ultrasonic pulses in concrete', British Standard Institution, London.

BS 1881: Part 209 (1990), 'Recommendations for the Measurement of Dynamic Modulus of Elasticity', British Standard Institution, London.

BS 1881: Part 3 (1970), 'Methods for Making and Curing Test Specimens', British Standard Institution, London.

BS 1881: Part 5 (1970), 'Methods for Testing Hardened Concrete for Other than Strength', British Standard Institution, London.

BS 218 (draft) (1995), 'Methods for Determination of Alkali-Silica Reactivity, Concrete Prism Method', British Standard Institution, London.

BS 5075: Part 3 (1986), 'Specification for Superplasticizing Admixtures', British Standard Institution, London.

BS 6699 (1992), 'Specification for ground granulated blastfurnace slag for use with Portland cement', British Standard Institution, London.

BS 812: Part 102 (1989), Testing Aggregates 'Methods of Sampling', British Standard Institution, London.

BS 812: Part 103 (1985), Testing Aggregates 'Methods of Determination of Particle Size Distribution', British Standard Institution, London.

BS 812: Part 120: (1989), 'Testing aggregates. Method for testing and classifying drying shrinkage of aggregates in concrete', British Standard Institution, London.

BS 812: Part 2 (1975), Testing Aggregates 'Methods for Determination of Physical Properties', British Standard Institution, London.

BS 882 (1992), 'Specification for Aggregate from Natural Sources of Concrete', British Standard Institution, London.

Buenfeld, N. R. and Newman, J. B. (1987), 'Examination of Three Methods for Studying on Diffusion in Cement Pastes, Mortars and Concrete', Materials and Structures, Vol. 20, No. 115, pp. 3 – 10.

Byars, E. A. (1997), 'Carbonation, Chloride, Sulphate and Acid Attack', Proceedings of International Conference on Repair of Concrete Structure: Concrete Deterioration Mechanisms, Centre for Cement and Concrete, University of Sheffield, pp 28-44.

Bye, G. C. (1983) 'Portland cement composition, production and properties', Pergamon Press, Materials Engineering Practice Series, pp 149.

Byfores, K., G. Klingstedt, V. Lehtonen 'Durability of Concrete made with Alkali-Activated Slag' Proceedings of the Third International Conference on Fly Ash, Silica Fume, Slag and Natural Pozzolans in Concrete, Trondheim, 2, SP114-70, pp.1428-1466.

Cabrera, J. G. and Lynsdale, C. J. (1988a), 'A New Gas Permeameter for Measuring the Permeability of Mortar and Concrete', Magazine of Concrete Research, Vol. 40, No. 144, pp. 177 - 182.

Cabrera, J. G. and Lynsdale, C. J. (1988b), 'Measurement of Chloride Permeability in Super-Plasticised Ordinary Portland Cement and Pozzolanic Cement Mortars', Proceeding of the International Conference on Measurement and Testing in Civil Engineering - Jullien, J. F. (ed.), Lyon - Villeurbanne, 13 -16 September 1988, pp. 279 - 291.

Collins F.G. and Sanjayan J. G. (1999) , 'Workability and Mechanical Properties of Alkali Activated Slag Concrete',Cement and Concrete Research 29, pp. 455-458.

Collins F.G. and Sanjayan J. G.,(2000), 'Effect of pore size distribution on drying Shrinkage of Alkali-Activated Slag Concrete', Cement and Concrete Research 29,pp. 1401-1406.

Coull ,W. A.(1981) 'Characteristics and Service Record of Commonly Used South African Aggregates' Proceedings of the 5th International Conference on Alkali-Aggregate Reaction in Concrete, Cape Town, South Africa, 30 March-3 April.

Davidovits J., (1991) ' High Alkali Cements for 21 Century Concretes', Proceeding of ACI Conference on Concrete Technology Past, Present and Future, pp.383-397.

Deja J. and Malotepszy , (1989) 'Resistance of Alkali-Activated Slag Mortars to Chloride Solutions', Proceedings of the Third International Conference on Fly Ash, Silica Fume, Slag and Natural Pozzolans in Concrete, Trondheim, 2, SP114-72, pp.1547-1563.

Department of the Environment. Building Research Establishment., (1988) 'Alkali Aggregate Reaction in Concrete', London, H. M. Stationary Office, pp.1-8, BRE Digest 330.

Dhir, R. K. and Jackson, N. (1996), "Concrete in Civil Engineering Materials" Fifth edition, Jackson, N. and Dhir, R. K. (eds.), McMillan Press Ltd, London

Dhir, R. K., Hewlett, P. C., and Chan, Y. N. (1989), 'Near Surface Characteristics of Concrete: Intrinsic Permeability', Magazine of Concrete Research, Vol. 41, No. 147, London, pp. 87 – 97.

Douglas E., Bilodeau A., Brandstetr J. and Malhotra (1991),' Alkali Activated Ground Granulated Blast-Furnace Slag Concrete : Preliminary Investigation' Cement and Concrete Research, Vol. 21, pp. 101-108.

Douglas E., Bilodeau A., Brandstetr J. and Malhotra (1992),' Properties and Durability of Alkali-Activated Slag Concrete' ACI Materials Journal, V89, No.5 pp. 101-108.

Feldman, R. F. (1972), 'Density and Porosity Studies of Hydrated Portland Cement', Cement Technology, Vol. 3, pp. 5 – 14.

Fordham, C. J. and Smalley (1985),'A simple thermogravimetric study of hydrated cement', Cement and Concrete Research, vol 15, pp 141-144.

Gifford P. M. and Gillot J. E. (1996), 'Alkali-Silica Reaction (ASR) and Alkali-Carbonate Reaction (ACR) in Activated Blastfurnace Slag Cement (ABFSC) Concrete', Cement and Concrete Research, Vol.26, No. 1, pp. 21-26.

Gifford P. M. and Gillot J. E. (1996),'Freeze Thaw Durability of Activated Blast Furnace Slag Cement Concrete' ACI Materials Journal, May-Jun, pp242-246.

Glasser,F. P. (1990), 'Chemistry of Alkali Aggregate Reaction', The Alkali-Silica Reaction in Concrete, Editor: Swamy, R. N., Blackie, pp. 30-52.

Glukhovsky V. D. (1980),' High Strength Slag Alkaline Cements', Proc. 7th Int. Congress on the Chemistry of Cement, Paris.

Grube, H. and Lawrence, C. D. (1984), 'Permeability of Concrete to Oxygen', Proceeding of RILEM Seminar on Durability of Concrete Structures under Normal Outdoor Exposure, Hanover, RILEM , pp. 68 – 79.

Hobbs D. W.(1982), 'Influence of Pulverized-Fuel Ash and Granulated Blastfurnace Slag Upon Expansion Caused by the Alkali-Silica Reaction' Magazine of Concrete Research, v 34, n 11, pp 83-94.

Hooton, R. D. (1989), 'What is Needed in Permeability Test for Evaluation of Concrete Quality', Pore Structure and Permeability of Cementitious Materials, Materials Research Society Symposium Proceedings, Vol. 137, L. R. Roberts and J. P. Skalny (eds.), RILEM , pp. 141 – 149.

Isozaki K., Iwamoto S. and Nakagawa K. (1986),' Some Properties of Alkali-Activated Slag Cement', 8th Int. Congress on Chemistry of Cement, Rio de Janeiro, 4, pp.395-399.

Jiang, L., Lin, B., and Cai, Y. (2000), 'A Model for Predicting Carbonation of High Volume Fly Ash Concrete', Cement and Concrete Research, Vol. 30, pp. 699 - 702.

Jiang, L., Lin, B., and Cai, Y. (2000), 'A Model for Predicting Carbonation of High Volume Fly Ash Concrete', Cement and Concrete Research, Vol. 30, Elsevier Science Ltd., New York, pp. 699 - 702.

Keattch,C. J. and Dollimore, D. (1975), 'An introduction to thermogravimetry', Hyden and Son Ltd, Second Edition.

Krivenko P.V. (1992),' Alkaline Cements', Proc. 9th Int. Congr. on the Chemistry of Cement, New Delhi, 4, pp.482-488

Kutti , T., Berntsson, L., Chandra, S.(1992), 'Shrinkage of cements with high content of Blast-Furnace Slag' Malhotra, V. M. (Ed.), Fourth CANMET/ACI Int. Conf. On Fly Ash, Slag, and Natural Pozzolans in Concrete, Istanbul Turkey, pp. 615-625 Supplementary Papers.

Kutti, T., Malinowski, R. and Srebnik, M (1982), 'Investigation of Mechanical Properties and Structure of Alkali Activated Blast-Furnace Slag Mortars' Silicates Industries, pp.149-153.

Lang, T. A. (1993),'Perception of the greenhouse problem and the possibilities in the cement industry for action' IEEE Cement Industry Technical Conference (Paper), p 445-466

Lea, F. M. (1970), 'The Chemistry of Cement and Concrete', Arnold, London

Loo, Y. H. et al. (1994), 'A Carbonation Prediction Model for Accelerated Carbonation Testing of Concrete', Magazine of Concrete Research, Vol. 46. No. 168, pp 191-200

Lynsdale, C. J. (1989), 'The Influence of Superplasticisers on the Engineering Properties and Performance of Concrete', PhD Theses, The University of Leeds, UK.

Lynsdale, C. J. and Sit, W. L. (1992), 'The Influence of Curing on the Early Age Properties of Concrete Incorporating PFA and Slag', An International Workshop on Blended Cements, Singapore, pp. 37 – 42.

Mackechnie, J. R.; Alexander, M. G.(1997), 'Exposure of concrete in different marine environments', Journal of Materials in Civil Engineering, v 9, n 1, pp. 41-45

Malhotra V. M. , (1999) 'Role of Supplementary Cementing Materials in Reducing Greenhouse Gas Emissions', International Conference on Infrastructure Regeneration and Rehabilitation, University of Sheffield, Ed. R. N. Swamy, pp.27-42.

Malhotra, V. M. (1983), 'Strength and Durability Characteristics of Concrete Incorporating a Pelletized Blast Furnace Slag', Publication SP-79 - American Concrete Institute, v 2, , p 891-921

Malin C. B.(1998), 'Kyoto Protocol: A business perspective', Oil and Gas Journal, Vol. 96, No. 3, pp. 33-35.

Malolepszy J. and Petri M.(1986),'High Strength Slag Alkaline Binder', 8th Int. Congress on Chemistry of Cement, Rio de Janeiro, 4, pp. 108-111.

Mehta, P. K. (1986), 'Concrete: Structure, Properties, and Materials', Prentice-Hall Inc., New Jersey.

Metso J. and Kajaus E.(1983),'Activation of Blast Furnace Slag by Some Inorganic Materials.' 1st Int. Conf. on Fly Ash, Silica Fume, Slag and Natural Pozzolans in Concrete, Montbello, Canada, Vol.2, pp.1059-1073.

Mills, R. H.; Markussen, J. B.(1985),'Mass Transfer of Water Vapour through Concrete', Cement and Concrete Research, v 15, n 1, pp. 74-82

Neville, A. M., 'Properties of Concrete', 4th edition, Longman, 1995.

Nilsson, L. (1980), 'Hygroscopic Moisture in Concrete – Drying Measurement and Related Materials Properties', Report TVBM-1003, Lund, Sweden, pp. 162-165.

Parameswaran, P. S. and Chaterji, A.K.(1986), 'Alkali Activation of Indian Blast Furnace Slags', 8th Int. Congress on Chemistry of Cement, Rio de Janeiro, pp.86-91.

Parrott, L. J. (1997), 'A Review of Carbonation in Reinforced Concrete', Cement and Concrete Association and British Research Establishment Report C/1-0987. British Cement Association, 45 pp.

Poole, A. B. (1990), 'Introduction to Alkali Aggregate Reaction in Concrete' ,The Alkali-Silica Reaction in Concrete, Editor: Swamy, R. N., Blackie, pp. 30-52.

Pu X. C. et al.(1991), 'Study on Durability of Alkali-Slag Concrete', Proceedings Int. Symp. on Concrete Engineering, Nanjing, pp. 1144-1149.

Quing-Hua C. and Sarkar S.(1994), ' A Study of Rheological and Mechanical Properties of Mixed Alkali Activated Slag Pastes' Advances in Cement Based Materials, pp.178-184.

RILEM Committee C56 (1988), 'Measurement of Hardened Concrete Carbonation Depth', CPC-18, Material and Structures, Vol. 21, No. 126, pp. 453 – 455.

RILEM Committee CPC 11-3 (1984), 'Absorption of Water by Immersion Under Vacuum', Materials and Structures, Vol. 17, No. 101, pp. 393 – 394.

RILEM TC 116-PCD (1999)' 'Tests for gas permeability of concrete. A. Preconditioning of concrete test specimens for the measurement of gas permeability and capillary absorption of water', Materials and Structures, v 32, n 217, p 174-176

Roy, D. M. and Gouda, G. R. (1973), 'Porosity-Strength Relationship in Cementitious Materials with Very High Strengths', Journal of the American Ceramic Society, Vol. 56, No. 10, pp. 549 – 550.

Roy, D., Malek, R. and Licastro, P. (1987), 'Chloride Permeability of Fly Ash Cement Pastes and Mortars', Concrete Durability, SP-100, J. M. Scanlon (ed.), American Concrete Institute, Farmington Hills, Michigan, pp. 1459 – 1475.

Roy, Della M.; Jiang, Weimin and Silsbee, M. R. (2000) 'Chloride diffusion in ordinary, blended, and alkali-activated cement pastes and its relation to other Properties' Cement and Concrete Research, v 30, n 12, pp. 1879-1884.

Sanjuan, M. A. and Munoz-Martialay, R.(1996), 'Oven-Drying as a Preconditioning Method for Air Permeability Test', Material Letters, v. 27, pp. 283-258.

Shi, C. (1996); 'Strength, Pore Structure and Permeability of Alkali-Activated Slag Mortars' Cement and Concrete Research, v 26, n 12, pp. 1789-11799

Shi, C., Wu, X. and Tang, M. (1991), 'Hydration of Alkali-Slag Cements at 150°C', Cement and Concrete Research, v 21, pp. 91-100.

Sims, I (1983) 'The influence of Ground Granulated Blast Furnace Slag on the Alkali Reactivity of Flint Aggregate Concrete in the United Kingdom' Proceedings of the 6th International Conference on Alkalis in Concrete, Technical University of Denmark, Copenhagen, pp. 69-84..

Soroka.(1979). 'Portland, Cement, Paste and Concrete', Macmillan Press, NY.

Sturrup, V. R., Vehhio, F. J. and Caratin, H. (1984) 'Pulse Velocity as a Measure of Concrete Compressive Strength' In Situ Nondestructive Testing of Concrete, Ed. Malhotra, V. M., ACI SP-82, pp. 201-227.

Swamy, R. N. and Al-Asali, M. M.(1988), 'Expansion of Concrete Due to Alkali-Silica Reaction', ACI Materials Journal, pp. 33-40.

Talling B. (1989)' Effect of Curing Conditions on Alkali-Activated Slags', Proceedings of the Third International Conference on Fly Ash, Silica Fume, Slag and Natural Pozzolans in Concrete, Trondheim, SP114-72, pp.1485-1500.

Talling B. and Brandstetr (1989),' Present State and Future of Alkali Activated Slag Concretes', Proceedings of the Third International Conference on Fly Ash, Silica Fume, Slag and Natural Pozzolans in Concrete, Trondheim, SP114-72, pp.1519-1546.

Tattersall, G. H. (1991), 'Workability and Quality Control of Concrete', E and FN Spon, London.

Tattersall, G. H. and Banfill, P. F. G. (1983), 'The Rheology of Fresh Concrete', Pitman Books Ltd., London.

Taylor H.F.W.(1997), 'Cement Chemistry', 2nd edition, Telford Press, New York.

Teychenne, D. C. et al. (1988), 'Design of Normal Concrete Mixes', British Research Establishment (BRE) Report, Revised Edition, Watford.

Thomas, M. D. A. and Matthews, J. D. (1992), 'Carbonation of Fly Ash Concrete', Magazine of Concrete Research, Vol. 44, No. 160, pp 217-228.

Thomas, M. D. A., and Innis, F.A.(1995), 'Effect of Slag on Expansion Due to Alkali-Aggregate Reaction in Concrete', ACI Materials Journal, November-December, pp. 716-724.

Wang S-D (1991), ' Review of Recent Research on Alkali-Activated Concrete in China' Magazine of Concrete Research, No.154, March, pp.29-35.

Wang S-D, and Scrivener K.L (1995) ' Hydration Products of Alkali Activated Slag Cement', Cement and Concrete Research, Vol. 25, No. 3, , pp. 561-571.

Wang S-D, Pu X., Scrivener K.L. and Pratt P.L.(1995) 'Alkali-Activated Slag Cement and Concrete: a review of properties and problems', Advances in Cement Research, No. 27, pp.93-102.

Wang S-D, Scrivener K.L. and Pratt P.L. (1994), ' Factors Affecting the Strength of Alkali-Activated Slag' Cement and Concrete Research, Vol. 24, No. 6, pp. 1033-1043.

Watkins, R.A.M. and Pitt Jones, A. P. (1993), 'Carbonation: A Durability Model Related to Site Data', Proceedings of Institution of Civil Engineering Structural and Buildings, Vol. 99, pp 155-166.

Watkins, R.A.M. and Pitt Jones, A. P. (1993), 'Carbonation: A Durability Model Related to Site Data', Proceedings of Institution of Civil Engineering Structural and Buildings, Vol. 99, pp 155-166.

Whiting, D. (1981), 'Rapid Determination of the Chloride Permeability of Concrete', FHWA Report FHWA/RD-81/119, Federal Highway Administration, Washington DC, 174 pp.

Wu C. et al. (1993), 'Properties and Application of Alkali-Slag Cement', Journal of Chinese Ceramic Society, 21, No. 2, pp. 176-181.

Xu Z., Deng Y., Wu X. (1993), Tang M. and Beaudoin J.J., 'Influence of Various Hydraulic Binders on Performance of Very Low Porosity Cementitious Systems' Cement and Concrete Research, Vol. 23, pp. 462-470.

Zhang, M. H. and Gjorv, O. E. (1991), 'Permeability of High-Strength Lightweight Concrete', ACI Materials Journal, Vol. 88, No. 5, pp. 463 – 469.

Zia P, Ahmad, S., and Leming, M. (1997), 'High Performance Concretes: A State-of-Art report (1989-1994), Federal Highway Administration, McLean Virginia, Publication No.FHWA-RD-97-030.